RESERVOIR CHARACTERISATION OF THE MESAVERDE FORMATION IN THE WIND RIVER BASIN, WYOMING, U.S.A.

María Josefa Herrero Fernández

Thesis presented in partial fulfilment of the
Degree of Doctor of Phylosophy
August 2000

School of Geography and Geosciences
University of St Andrews

I, María Josefa Herrero Fernández, hereby certify that this thesis, which is approximately 31364 words in length, has been written by me, that it is the record of work carried out by me and that it has not been submitted in any previous application for a higher degree.

Date 4/8/00 Signature of candidate

I was admitted as a research student in June 1997 and as a candidate for the degree of Ph.D. in May 1998; the higher study for which this is a record was carried out in the University of St. Andrews between June 1997 and August 2000.

Date 4/8/00 Signature of candidate.

I hereby certify that the candidate has fulfilled the conditions of the Resolution and Regulations appropriate for the degree of Ph.D. in the University of St. Andrews and that the candidate is qualified to submit this thesis in application for that degree.

Date 4/8/00 Signature of supervisor..

In submitting this thesis to the University of St. Andrews I understand that I am giving permission for it to be made available for use in accordance with the regulations of the University Library for the time being in force, subject to any copyright vested in the work not being affected thereby. I also understand that the title and abstract will be published, and that a copy of the work may be made and supplied to any bona fide library or research worker.

Date 4/8/00 Signature of candidate..

INDEX OF CONTENTS **PAGE**

TABLE OF FIGURES **PAGE**

Chapter 1

Chapter II.

Chapter III.

Chapter V

Index of tables **PAGE**

ABSTRACT

The Mesaverde rocks are prolific oil and gas reservoirs in several basins throughout the Rocky Mountains Region. Numerous studies have accomplished the outcrop analysis of the Mesaverde Formation in the southeastern parts of the Wind River Basin, Wyoming, where mainly marine or marine-influenced deposits occur. In contrast, the northwestern exposures located inside the limits of the Wind River Indian Reservation, have been studied in less detail due to restricted access. These deposits contain a basal marine member overlain by fluvial deposits that form a succession up to 650 metres in thickness. In order to develop a basinwide stratigraphic framework for the Mesaverde Formation, and thus to provide implications and predictions for reservoir characterisation, detailed analysis of the outcrop and subsurface data is necessary.

This study establishes the depositional and stratigraphic framework of the Mesaverde Formation by analysis of 1) outcrop characteristics (facies analysis, architectural arrangements of facies associations, palaeocurrent directions and analyses of sandstone and shale compositions); 2) outcrop gamma-ray profiles of facies successions; and 3) subsurface wireline logs to develop correlations between the northwestern and southeastern areas of the basin.

From the lateral and vertical distribution of facies and the recognition of major bounding surfaces, a stratigraphic framework of six sequences is obtained for the uppermost Cody and Mesaverde Formations; these display very variable stacking patterns and sandstone quality depending on location. Qualitative predictions of reservoir character are inferred. The analyses additionally allow implications for the controls upon sequence architecture to be interpreted.

ACKNOWLEDGMENTS

My thanks go to Tom Brown Inc, for sponsoring the project, and specially to Steve Parks, and Conie Hawkins, whose discussions and ideas have helped to enhance the final product. Also I would like to thank the Shoshone and Arapahoe tribes for giving permission to study the rocks in their land. Not to forget the AAPG, that with their grant showed me their confidence in my work.

Thanks also to the "Zollers" for making my stay in Wyoming as similar to being at home as it can be.

Back here in St Andrews, I would like to thanks first to my supervisors, Tony Prave, Ruth Robinson and Richard Bastes, for their inestimable help during my stay in St Andrews. Not to forget all the help received from all the staff at the department who helped in the various aspects of the project. Many thanks to Colin Cameron, Donald Herd, Angus Calder and Stuart Allison..

Apart from work, my tanks go to Dan (for supporting my "moods"), Scott, Clive, Corina, Amanda,.....and all the friends that were always there whenever I needed, and with whom I shared great moments here in St Andrews, and hopefully will still share more in the future. Special thanks to Mireia, Murielle and Raquel for their help on the critical moment. I will never forget it!. I also would like to thank Miguel for taking care of me when I had my accident and for the good moments we shared while in the rocks.

Finally, I dedicate the final product of my three years work product to my family (parents, grandparents, sister and brothers) who encouraged me in every moment to keep going, and my special dedication and thanks to Jose, who apart from listening to all my stories about the Mesaverde rocks, helped me to work hard by supporting me at every moment, and being very patient during the final countdown.

Chapter I

INTRODUCTION

The purpose of this study is to define the depositional and stratigraphic framework of the Mesaverde Formation in the Wind River Basin in the Rocky Mountains region (Figure I-1) by using outcrop analogues and available subsurface data. The results of the study are applied to the reservoir characterisation of the formation.

The name Mesaverde Formation is applied to sediments of Campanian age consisting predominantly of sandstone, shale, siltstone and coals (Barwin, 1961). Stratigraphically, it overlies the Cody Formation and is overlain by the Lance, Meeteetse and Fort Union Formations (Figure I-2).

The Upper Cretaceous successions of the Rocky Mountains area are characterised by intertonguing marine and nonmarine strata in which each progressively younger regression of the shoreline extended farther eastward into an epicontinental sea (Kauffman, 1977). The Mesaverde Formation is the third of four major Late Cretaceous regressions and, as such, constitutes the last regression prior to complete retreat of the sea from the continent during the Laramide orogeny (Mackenzie, 1975). In the Wind River Basin, its thickness varies from more than 600 metres (2400 ft) in the western part to less than 150 metres (500 ft) in the eastern part; it thins largely by grading laterally into the underlying marine Cody Shale that is termed the Pierre Shale towards the east (Figure I-2). This lateral facies change is not gradual across the basin but occurs as two relatively abrupt wedges, where significant thicknesses of Mesaverde Formation grade into the Cody

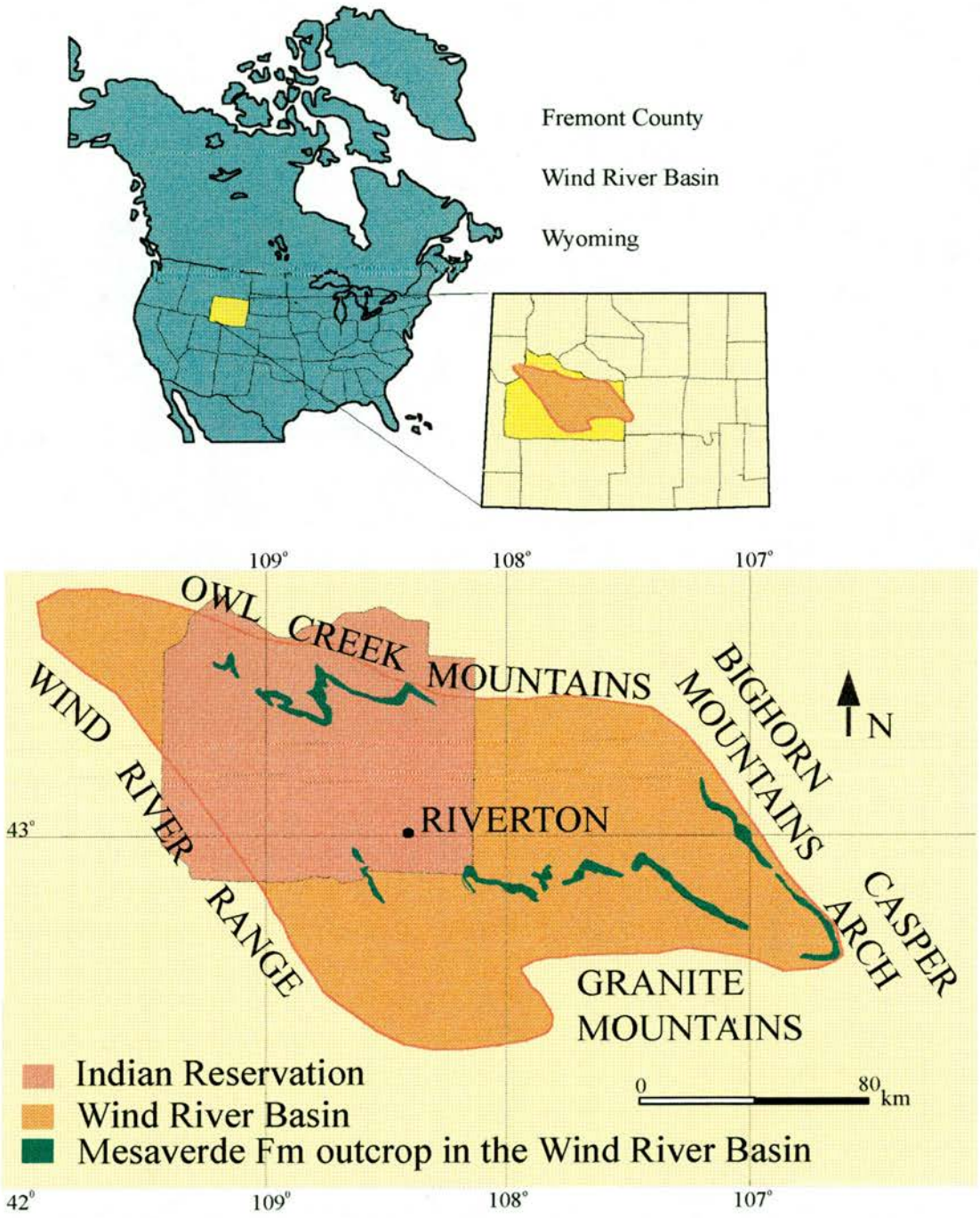

Figure I-1: Location of the Wind River Basin, in Wyoming. Position of the Mesaverde Formation outcrop throughout the Wind River Basin.

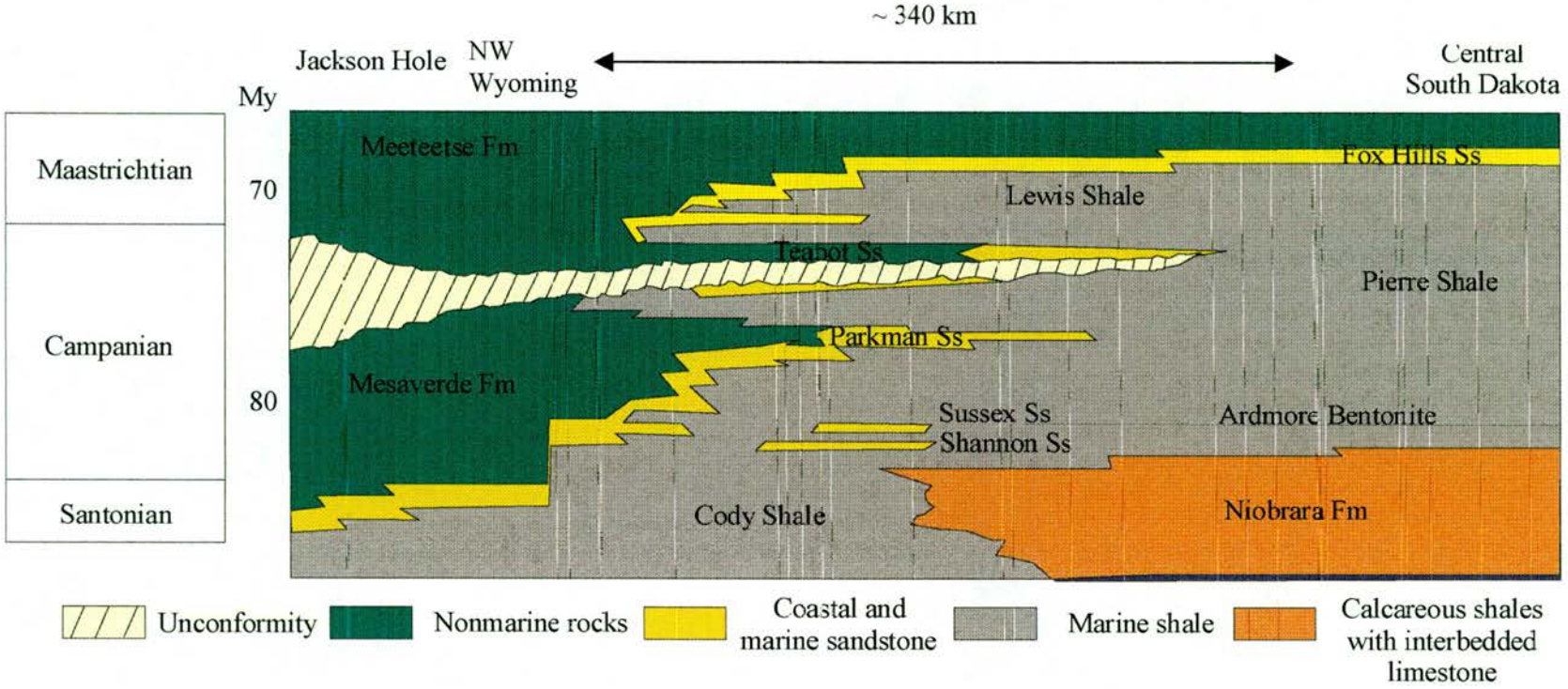

Figure I-2: Generalised time-stratigraphic correlation chart for the Mesaverde Formation from northwestern Wyoming to South Dakota (from Pang, 1994).

Formation over relatively short distances. This indicates that the eastward retreat of the shoreline maintained a relatively fixed position for considerable periods of time. Surface and subsurface studies show several transgressive and regressive pinch-outs within the Mesaverde Formation (Keefer and Rich, 1957). These transgressive-regressive episodes were caused by a combination of tectonic activity, eustatic changes and varying rates of sediment input along the western margin of the basin.

I-1. PURPOSE OF THE STUDY

The Wind River Basin is an example of a "Laramide age" basin that characterises the Rocky Mountain foreland region and was infilled as the Cretaceous Western Interior Seaway retreated across Wyoming. Although the Mesaverde sandstones are a small producer of petroleum relative to other reservoirs in the Wind River Basin (Keefer and Johnson, 1993), future drilling is likely to find significant gas resources based on a history of substantial ongoing production from equivalent rocks in other Rocky Mountain basins. Future development of the gas resources in this formation requires a thorough knowledge of the distribution and characteristics of potential sandstone reservoirs, as well as the overall architecture and geometry of individual and composite sandstone bodies.

The main objectives of this thesis are to: (1) define the stratigraphy of the formation throughout the basin, (2) develop a basinwide depositional framework, and (3) discuss the potential for future exploration of oil and gas. The Mesaverde rocks are considered to have excellent source rock potential because the formation contains coals and associated carbonaceous shales which typically have high TOC values (Johnson et al., 1993).

In order to accomplish these objectives, detailed information of the lithologies, sedimentary features, stratal geometries, contact relations and correlations of the Mesaverde Formation were obtained from 17 detailed measured sections and 40 wireline-logs. Good exposure of the rocks in most of the localities studied provide data of the lateral changes in lithologies and depositional features, such as fluvial channel geometries, in order to construct reservoir analogue models. The stratigraphic studies involve the measurement and description of surface sections of the Mesaverde Formation along its outcrop belt in the Wind River Basin, which includes characterising each facies and facies association, the thickness of depositional packages, sandstone/shale ratios, analysis of palaeocurrents and mineralogical composition of both sandstones and shales. These data were then compared with geophysical logs which were obtained from wells that penetrated the Mesaverde Formation in the subsurface in the basin. Combined, these datasets allow the development of a basinwide depositional framework that permits (1) isopach maps to be constructed for each depositional package and (2) the assessment of the spatial and temporal variability in Mesaverde deposition. This information will provide the basis for the geological evaluation and potential for hydrocarbon production from the Mesaverde Formation in the Wind River Basin.

I-2. LOCATION OF THE STUDY AREA

The Wind River Basin is a northwest-southeast trending intermontane, structural basin in central Wyoming (Figure I-1). The basin is bounded by the Wind River Range on the west, the Casper Arch on the east, the Owl Creek and Big Horn Mountains on the north and the Granite Mountains on the south (Keefer and Van

Lieu, 1966). It was formed by Laramide-style block-uplift. The Wind River Basin in gross form is an arcuate shaped structural depression over 217 km (135 miles) in length and as much as 56 km (35 miles) in width. The Mesaverde Formation is discontinuously exposed along the flanks of northwest-trending anticlines and synclines along the northwestern, southwestern and southeastern margins of the basin (Figure I-1). These folds and associated faults trend N30W to N40W throughout central Wyoming. The northwestern outcrops are located within the Arapahoe-Shoshone Indian Reservation (Figure I-1) and access to these rocks is heavily restricted, thus less is known about this region than other Mesaverde rocks in the rest of Wyoming.

I-3. GEOLOGIC HISTORY OF THE WESTERN INTERIOR SEAWAY

During much of the Palaeozoic, the Cordillera area was a stable tectonic setting. Between Middle Jurassic and Eocene times, the Western Interior of North America became the site of a complex foreland basin, which separated the tectonically active proto-Cordillera from the tectonically quiescent stable craton (Gries, 1983). In early to Middle Jurassic time, the Cordillera was formed by the long-continued motion of the upper North American Plate over an east-dipping subduction zone (Cross, 1986). These features probably reached their fullest development by the Mid Cretaceous, at about the time when plate motions changed to those more characteristic of the Late Cretaceous and Tertiary interval. By early Late Cretaceous time, marine rocks were restricted to the foredeep on the craton to the east (Price 1981). By the end of the Cretaceous, almost the entire Cordillera and flanking regions on the east were uplifted well above sea level.

Analysis of the topography of the basin prior to transgression (Eicher 1967) and of high-resolution stratigraphic shelf to basin transects in the Wyoming portion of the basin (Asquith, 1970), suggest that, at its deepest, the United States portion of the seaway attained depths greater than 600 metres. Asquith (1970) based this interpretation on detailed correlation of clinoform geometry in the Mesaverde Formation in Wyoming. In contrast, Weimer (1983) determined the maximum bathymetry at 300 metres.

The Western Interior Basin was composed of a series of longitudinal tectonic zones which rose or subsided differentially in response to contractional deformation events in the Cordillera and their direct and indirect effects on the crust and mantle beneath the basin. According to Lawton et al. (1994), the pre-thrusting stratigraphic section along the strike of the thrust belt generated differences in its structural style. They showed that the thrust belt is typified by alternation of lobate and broadly arcuate segments associated with the development of anomalously thick pre-existing stratigraphic sections with steep dips of the underlying basement and thinner stratigraphic sections and lower dips of the basement. The differences in dip of the basement produce contrasts in structural styles of adjacent thrust-belt segments which are linked by transverse structural transfer zones that served as conduits for long-term gravel transport to the adjacent foreland basin (Lawton et al., 1994). Therefore, the thrust-belt is formed by segments composed of different number of thrust sheets separated by transfer zones (Figure I-3).

The Wyoming province is characterised by one transfer zone in the north (Monida Zone) and another one in the south (the Salt Lake Zone). The segment in

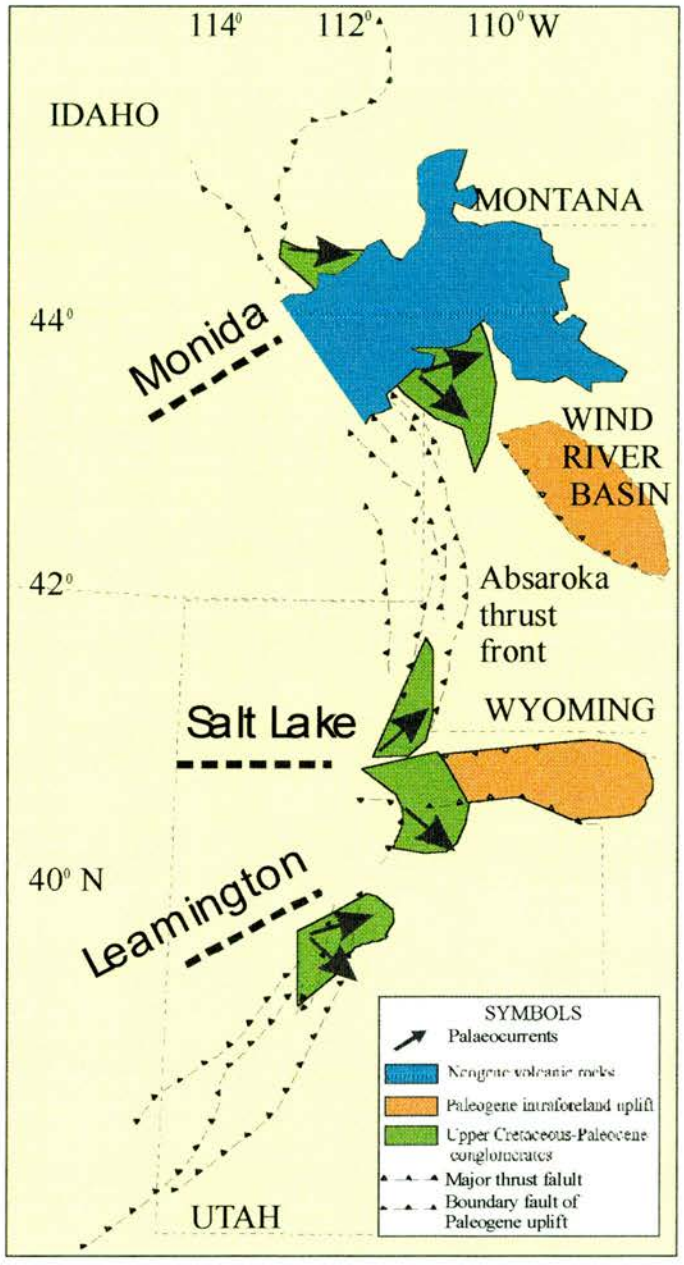

Figure I-3: Map showing part of Late Mesozoic-Early Cenozoic Cordilleran fold thrust belt in the Western Interior of the United States, major lineaments and location of the Wind River Basin (after Lawton et al., 1994).

the middle, the Wyoming salient, (DeCelles, 1994) is composed of 4 main thrust sheets that become more imbricated and folded northward (Lawton et al., 1994). The position of the transfer zones is commonly marked by the location of conglomerates adjacent to the thrust belt. These zones provided easy avenues through the orogen that focused drainages. For the Campanian Mesaverde Formation, the conglomerates complex is the Snake River complex, which includes the Pinyon and Harebell Formations in northwestern Wyoming, derived from thrust sheets in the thrust belt salients (DeCelles, 1994). As the basin evolved, these zones developed identifiable tectono-sedimentologic characteristics and can be distinguished principally by the character of their tectonic movements, the provenance of their clasts and the dominant sediments that accumulated, and the depositional rates and water depths that prevailed within each of them. These criteria define longitudinal tectonostratigraphic sectors in the reconstructed basin of today (Kauffman, 1985). The western foredeep, adjacent to the tectonic front, had the highest sedimentation rates and underwent the greatest subsidence of all tectonostratigraphic sectors. Predominantly coarse-grained, synorogenic, terrigenous clastic sediments accumulated as coastal-plain to shallow marine depositional centres (DeCelles and Giles, 1996). Flanking the narrow foredeep and separating it from the much broader, eastern sectors of the basin, was the forebulge, a discontinuous set of arches along the length of the basin and approximately parallel to the eastern margin of the Cordillera but situated 150-200 km outboard of it (Pang, 1994). In places, the forebulge was underlain by reactivated blocks of Precambrian basement and Lower Palaeozoic supracrustal rocks. These were uplifted at times of active tectonism and

flexure of the lithosphere in response to thrust-loading, resulting in the influx of synorogenic detritus. Coarse-grained sediments were banked against the forebulge and, through time, the forebulge came to separate the coarse-grained, shallow-water sediments characteristic of the foredeep, from the finer-grained, deeper-water sediments typical of the basin farther east (Pang, 1994).

The east-median hinge was another broad tectonostratigraphic sector of the basin. Bounded to the west by a fairly gentle slope rising eastward from the axial or west-median trough, the main part of the hinge zone blended with the essentially flat-lying eastern platform of the basin that overlaid the flank of the craton (Pang, 1994). The broad, low, crustal blocks were separated by localised sub-basins. Generally, sedimentation rates were moderate to low and subsidence varied being lower over the broad, gentle, eastern flank than over the narrower, steeper, western flank of the hinge. Sedimentary sequences that accumulated in this zone commonly varied in facies between those typical of the shallow-water eastern platform in which transgressive systems tracts are highly condensed, and the relatively deep-water west-median trough, in which transgressive system tracts are most completely preserved (Pang, 1994). Lateral shifts of this facies boundary through successive sequences suggest that the basin axis and hinge crest migrated with time, possibly in response to varying rates and magnitude of foreland basin subsidence (Pang, 1994), but also due to accommodation space variations due to sediment supply and eustatic fluctuations.

The eastern platform, which occupied the distal one-third of the basin, was tectonically stable. Subsidence was slow and episodic, leading to thin, commonly

unconformity-bounded sequences of fine-grained terrigenous clastic and pelagic carbonate sediments (Pang, 1994). These were deposited under the low-energy conditions of a broad, shallow-water, marine shelf with little tidal exchange.

In summary, and as discussed below, sedimentation and sequence stratigraphic response in the basin was controlled by four main factors: (1) tectonism which affected the source, supply and depositional site of the predominantly terrigenous clastic sediments (Lawton et al., 1994); (2) eustatic changes, which are recorded in widely correlative transgressive-regressive cyclicity (there are some exceptions as pointed out below) (Kauffman and Caldwell, 1993); (3) watermass dynamics (Slingerland et al., 1996); and (4) climate and sediment flux (Fleming and Jordan, 1989).

I-3.1. EUSTATIC CURVES

During the Cretaceous, rapid plate spreading produced flooding events over several continental areas in the world. As part of this flooding, the North American craton experienced the largest marine incursion since the Palaeozoic and developed a large Western Interior epeiric seaway (Dickinson and Snyder, 1978). This was located between the Cordilleran fold and thrust belt to the west and the drainage divide of the cratonic interior to the east. The maximum length of this sea covered a distance of 5000 km, and reached a width of 1000 km or more in many places. At the end of the Cretaceous the Laramide orogeny broke up the interior seaway by uplift and formation of structural basins (Dickinson and Snyder, 1978). Kauffman (1991) suggested a model for stratigraphic sequences which is based on sequence geometry and facies development across the Western Interior Basin as influenced by

eustatic changes: the western margin of the basin and flanks of the forebulge are characterised by asymmetrical cyclothems consisting of (a) thin, coarse, transgressive lags and little or no preserved transgressive systems tract; (b) a thick, siliciclastic highstand systems tract; and (c) nearshore, fluvial-dominated lowstand facies. More symmetrical cyclothems characterise the median portion of the axial basin. These preserve most of the transgressive systems tract except for those removed by initial ravinement erosion (the main transgressive disconformity or marine flooding surface) and, to a lesser degree, along other transgressive disconformities formed during pulses of rapid sea-level rise and off-shore sediment starvation. In this part of the basin, maximum-flooding surfaces are characterised by sediment condensation and omission of surfaces within pelagic carbonate and clay-rich facies. The regressive phases of the cyclothem sequences are marked by thick highstand systems tracts, with or without thin lowstand deposits preserved as shell-gravel lags or thin, lensoid, sand bodies. On the eastern, sediment-starved cratonic platform, the typical expression of second- and third-order sequences is again an asymmetrical cyclothem with little or no transgressive systems tract preserved other than transgressive lags of fine siliciclastic debris, shell and bone fragments and phosphate pebbles. Here, maximum flooding surfaces are characterised by condensed beds containing shell and bone fragments within clay-shale and carbonate facies, as well as firm grounds with benthic colonisation surfaces. Highstand systems tracts dominate regressive phases, and are commonly composed of gradually upward-coarsening shales, silty shales, fine siltstones, and sandstones (Kauffman, 1991).

Within the seaway (as mentioned previously), the maximum water depth varied from potentially as much as 600 metres to 100 to 300 metres or less (Asquith, 1970; Kauffman, 1969, 1977; Weimer, 1983). From Albian to Maastrichtian time, five transgressive-regressive depositional cycles with durations between 5 to 10 m.y. have long been recognised: Kiowa-Skull Creek, Greenhorn, Niobrara, Clagget and Bearpaw (Cross, 1986). The Mesaverde Formation was deposited during the Niobrara, Clagget and Bearpaw cycles (Cross, 1986). The Niobrara cycle spans the time span from the Turonian to Early Campanian, a period of more than 9 m.y. The Claggett cycle spans the Middle Campanian, a period of about 5 m.y., with intensive volcanic activity occurring during the initiation of this cycle. The Bearpaw cycle marks the end of marine sedimentation in the Cretaceous Western Interior Basin and has a duration of 9 m.y. (Kauffman, 1969).

In contrast, Cant and Stockmal (1989) correlated the generation of six successive sequences (each unconformity-bounded and dominated by an eastward-thinning, coarse-grained, clastic-wedge with terminal non-marine deposits) to the emplacement and cratonward displacement, of six discrete allochthonous terranes. The accreted and deplaced terranes are assumed to have created, directly and indirectly, the tectonic loads that induced lithospheric flexure and, thus, the temporal correlation of the accretionary event and the clastic-wedge sequences are considered to imply mechanical linkage. However, eustatic fluctuations in sea level operating on finer time scales than the tectonic loading episodes are believed to have controlled the internal stratigraphy and sedimentology of clastic-wedge associations and the generation of thinner, higher frequency sequences (Vail et al., 1977; Haq et

al., 1987). Krystinik and Blakeney (1995) integrated biostratigraphic and lithostratigraphic data to create a chronostratigraphic framework for the Campanian and lower Maastrichtian of the Western Interior Seaway and recognised that some of the obtained profiles do not compare favourably with the eustatic curves of Vail et al. (1977) and Haq et al. (1987). They showed that, although seven third-order relative sea-level falls and subsequent rises occurred during the Campanian to early Maastrichtian, little evidence of a uniform predictable response can be see in the sedimentary record of the Western Interior Seaway due to local tectonic activity typical of tectonically active basins. Thus, they infer that tectonic activity rather than solely eustasy during this time played a major role in creating the complex interfingering relationships and stratal architecture.

I-3.2. TECTONICS

Late Mesozoic and Early Cenozoic deformation in the Rocky Mountains region traditionally has been categorised as two temporally distinct compressional events termed the Sevier and Laramide orogenies, although the temporal change from Sevier to Laramide deformational style is not coeval throughout the Western Interior Seaway (Armstrong and Oriel, 1965; Oriel and Armstrong, 1966). The former is characterised by thin-skinned thrust and folds of decollement style which usually did not involve basement whereas the latter is marked by basement block faulting (Cross, 1986). Deformation along the Sevier foreland fold-and-thrust belt was confined to strata of the westward thickening Precambrian, Paleozoic and Mesozoic sedimentary prism. Laramide structures are characterised by basement-cored uplifts and asymmetric anticlines typically bounded by high-angle reverse and

thrust faults. Such basement-involved deformation was confined to the southern and central Rocky Mountains of New Mexico, Colorado, Wyoming and southern Montana (Armstrong, 1984). In this sector, deformation along the Sevier fold-and-thrust belt ceased shortly before initiation of Laramide basement-involved deformation. This style of deformation was latitudinally restricted to the central and southern Rocky Mountains and was contemporaneous with thin-skinned deformation to the north and south. Thus, although the terms Laramide and Sevier are traditionally used as temporal distinctions of deformational events throughout the Rocky Mountains, their temporal distinctiveness is equivocal and such usage should not be implied.

During the Sevier orogeny, thrusting occurred from the latest Jurassic to the Early Eocene and the ages of thrust faults decreases to the east and are mostly foreland propagating structures (Armstrong and Oriel, 1965; Oriel and Amstromg, 1966; DeCelles et al., 1995). Subsidence of sedimentary basins within the Western Interior Seaway was mainly an isostatic adjustment to tectonic loading in the fold-and-thrust belt and sedimentary loading in the basin thereby resulting in spatial and temporal variations of the wavelength of the flexural subsidence between basins (Fleming and Jordan, 1989; Jordan, 1981; Pang, 1994). In Wyoming, the flexural subsidence pattern near the thrust front is different to that in adjacent Montana and Utah. Here, the wavelength is longer, as much as 400 km and extends as far east as the Laramie and Powder River Basins. Therefore, Wyoming is marked by a broad and deep foreland basin that experienced significant thrust loading and deflection of the lithosphere. During the Niobrara cycle, subsidence accelerated rapidly in

Wyoming, in contrast to Utah, but by the beginning of the Campanian, subsidence slowed everywhere (Pang, 1994). The aforementioned spatial and temporal variations imply that gross crustal shortening over a 16 m.y. interval was centered in the Idaho-Wyoming salient rather than being evenly distributed along the Sevier Belt and that the Western Interior foreland basement was most likely segmented into the Wyoming, Montana and Utah blocks (Lawton et al., 1994).

In the foreland basin, the basin axis progressed eastward during the times of motion on the Paris, Meade and early Absaroka thrusts marked by widespread unconformities and major regressive-transgressive cycles. Jordan (1981) indicated that the outer bulge or "forebulge" was located at the Moxa arch, as suggested by Elliot (1977), and sloped gently (less than 1.5 degrees) eastward. For Jordan (1981), lithospheric loading by thrusting and subsequent redistribution of the load by sedimentation was the primary cause of the subsidence of the seaway flanking the Idaho-Wyoming thrust belt. She considered sea-level change as merely modifing an existing downwarp.

DeCelles (1995) showed that during Coniacian through Palaeocene time, thrusting followed an overall eastward progression but was interrupted by local out-of-sequence and hinterland-verging events. Several episodes of synchronous displacement on two or more thrusts can be demonstrated and shortening appears to have occurred in three main episodes: the first (89-84 m.y.) involved 33 km of shortening; the second (84-62 m.y., with a break between 75-69 m.y.) involved 30 km of shortening, mainly along the Absaroka thrust and development of an additional 6 km of structural relief in the culmination; the third (56-50 m.y.) was on

the Hogsback thrust and involved 21 km of horizontal shortening and produced no significant increase in structural relief in the culmination.

Cross (1986) summarises the Sevier orogeny as formed during a period of normal subduction (from before 92 to about 80 m.y.) and that thin-skinned, decollement style deformation occurred opposite to the convergent margin. Coeval subsidence of the foreland basin was confined to a relatively narrow zone to the east of the Sevier belt. Along the axis of the foreland basin, subsidence began as early as 115 m.y. with a major episode of rapid subsidence initiated by about 90 m.y. From about 80 to 67 m.y., rapid subsidence occurred over a broad region centered about Colorado and Wyoming. This episode of subsidence is attributed to sub-lithospheric loading and cooling induced by the shallowing of the dip of the subducting oceanic plate (Jordan, 1981). Another effect of low-angle subduction was the transfer of deformation from the Sevier belt (termination about 75 m.y.) to the eastern and northern margins of the Colorado Plateau, coincident with the position of greatest contrast in mechanical properties of the lithosphere. This initiated Laramide-style basement-cored uplifts at about 69 m.y.

The pattern of volcanism also displays spatial and temporal variability and explains the differences in mechanical properties of the lithosphere. During 60-45 m.y., the northern limit of magmatism is clearly defined by centres of volcanism and plutonism in southern Idaho and south-western Montana. Between 80 to 45 m.y. there was igneous activity in southern Arizona and south-western New Mexico (Armstrong, 1984). The region in between SW Wyoming and Utah is known as the magmatic gap and is considered a consequence of low-angle subduction (Armstrong,

1984). Magmatism was renewed in the southern Rocky Mountains in Colorado and New Mexico, during 45 to 35 m.y. and expanded rapidly between 35 to 25 m.y. as a consequence of steepening of the previously shallow subduction zone (Armstrong, 1984).

Armstrong (1984) noticed these coincident events and succinctly related them to the cessation of Sevier-style deformation in Utah and Wyoming, the initiation of Laramide-style deformation in the central and southern Rocky Mountains and the history of igneous activity in the western United States. He attributed the abrupt change from thin-skinned to basement-involved deformation and the attendant eastward displacement of deformation to a ductile contrast within the continental lithosphere. Sevier-style deformation was coeval and latitudinally conterminous with Andean-type volcanism and plutonism. The response to these compressive stresses was predominantly ductile shortening within the crust heated by magmatism, and detachment and internal imbrication of the overlying westward thickening sedimentary prism. Cessation of igneous activity in the Sierra Nevadan arc and formation of the magmatic gap at 80 m.y. caused this back-arc region to dissipate. Consequently, the lithosphere in the vicinity of the magmatic gap (located between SW Wyoming and Utah), cooled, thickened and became resistant to deformation as a consequence of its increasing strength. By contrast, the lithosphere to the north and south of the magmatic gap, opposite the volcano-plutonic arcs, remained hot and more ductile, thereby producing thin-skinned deformation. This model does not explain the eastward displacement of deformation, or the curvature and specific loci of Laramide structures that are orientated approximately north-

south and coincident with the eastern margin of the Colorado Plateau. As Laramide structures are traced into the central Rocky Mountains, structural trends rotate anticlockwise first to the NW-SE and then to east-west. To explain this, Gries (1983) suggested a relative motion between the Colorado Plateau microplate and the continental interior which produced a east-west relative motion during Late Cretaceous through early Palaeocene time and a north-south relative motion during the late Palaeocene through late Eocene time.

In Wyoming, the age of initial loading inferred from geohistory analysis is 114-107 m.y. (Jordan, 1981). Ages of deformation obtained from most well-documented structures indicate that thrusting ceased by 57 m.y. (Armstrong, 1984). Laramide uplifts consist of broad asymmetrical anticlines in which the over-steepened limb is faulted. The north-west Wind River Mountains (Figure I-2) are the largest Laramide uplift in Wyoming with a length of 220 km (137 miles) and a width of 70 km (44 miles). This style of Laramide deformation dominated by basement-cored, fault-bounded uplifts continued during the Early Eocene. Molzer et al. (1995) pointed out that there are east-west basement cored arches in central Wyoming that are oblique to the average northwesterly trend of foreland faults and folds and one of those, the Owl Creek arch (Figure I-1) forms the northern boundary of the Wind River basin. This arch connects the Bighorn and Casper arches to the east with the Wind River and Beartooth arches to the west. In the Owl Creek Mountains there are a series of faults that indicate sinistral oblique-slip in the east-west-trending, high-angle northern Owl Creek fault zone. Blackstone (1990) explains the Owl Creek Mountains as developing over an east-west-striking, north-dipping oblique ramp that

underwent south-west-directed oblique thrusting and attained its structural elevation by southwest tectonic transport on a series of northerly-dipping thrust faults.

In summary, the Sevier foreland fold-and-thrust belt occurred as an Andean-type volcano-plutonic arc in lithosphere rendered ductile by high heat flow in the arc and back-arc region. The Laramide orogeny occurred within a region devoid of magmatism and above an inferred shallowly-inclined, subducted oceanic plate. Therefore, the change from one type of deformation to another was not synchronous through the Rocky Mountain region. This, together with the differences in behaviour of the lithosphere, explain the resultant changes in timing and sedimentary patterns found in similar rocks located in different basins through the Rocky Mountain area.

I-3.3. WATERMASS DYNAMICS

The Mesaverde Formation forms a clastic wedge that prograded with several pulses into the Interior Seaway. Therefore, the watermass dynamics play a key role in the development of the marine-influenced deposits that correspond to this formation.

Even given the tectonic factors, it is generally accepted that recurrent, eustatically influenced flooding of the Western Interior Seaway by both northern cool-temperate and southern warm-temperate to subtropical water-masses created dynamic oceanographic changes in the basin (Arthur et al., 1997) and these have influenced shallow-marine facies distribution. Chemical composition, current-circulation patterns, temperature gradients, and water depth commonly changed and the stratification of the water column was disrupted by mixing and overturn. The north-south elongation of the basin and its seaway restricted oceanic circulation and

the effects of the inferred catchment area in the orogenic highlands of the Cordillera provided an intricate linkage between regional climate, water-column structure, sediment supply and the chemistry of middle and bottom waters in the seaway (Kauffman et al., 1991). Slingerland et al. (1996) proposed a mechanism to explain the Cenomanian to early Turonian patterns of lithofacies, marine faunas, organic carbon enrichment, isotopes and trace elements in the Western Interior seaway by modelling the linkages between fresh water-masses entering from the eastern and western margins of the seaway that mixed with the Tethyan and Boreal waters under a Cretaceous mean annual wind field and meridional temperature gradient. The net result was a strongly accentuated counterclockwise circulation in the seaway.

When eustatic fluctuations are superimposed in these factors, they produce long-term intervals of organic-carbon accumulation on the sea floor due to varying anoxic to dysoxic conditions. For example, Kauffman (1984) inferred episodic oxygen reduction and anoxia in bottom to mid-column water-masses of the basin (as shown by the discontinuous intervals of organic-carbon enrichments that comprise major source rocks). These are associated with transgressive, peak flooding, and earliest highstand systems tracts of the Middle and Late Cretaceous cyclothems. Broad areas of density stratification, diminished downward mixing of oxygenated surface waters, reduced benthic oxygenation, and organic-carbon accumulation in the Western Interior Seaway are proposed to have occurred as follows (Kauffman, 1984): during initial sea-level rise (represented by early transgressive systems tracts), salinity stratification was enhanced by internal fresh-water runoff coupled with very low levels of circulation during the Albian. During mid to late sea-level

rise (represented by late transgressive systems tracts) and early sea-level fall (highstand systems tracts), warm marginal Tethyan water-masses overstepped the southern topographic barrier to the seaway and became thermally stratified above denser, cooler, northern Boreal water-masses occupying the basin. This diminished downward mixing of oxygen-rich surface waters. During that time and around peak sea-level rise, major northward incursions of an expanded oxygen-minimum zone from the proto-Gulf of Mexico and Caribbean basins may have broadly flooded the lower water column of the seaway with an oxygen-depleted water-mass, which then became stratified in the deeper portions of the basin below normal saline surface waters from the south, or cooler, slightly brackish water-masses from the north. Also, widespread organic-rich deposits in the Western Interior Seaway may also have been formed by various upwelling phenomena. Upwelling brings large quantities of nutrients to the surface, enhancing productivity and organic carbon production (Parrish et al., 1984).

Several lines of evidence, therefore, suggest that broad-scale oxygen depletion leading to organic-carbon accumulation within the Cretaceous Western Interior Basin reflect long-term density-stratification events and episodic upwelling and downwelling phenomena. Mid-water oxygen minima zones developed in adjacent oceanic basins, especially the proto-gulf of Mexico and Caribbean basin, became enhanced during eustatic rise and global warming (Parrish et al., 1984), and may have spilled frequently into the epicontinental seaway as dysoxic or anoxic bottom water or mid-water masses during and near eustatic highstand influencing shallow and deep marine facies architecture and stacking patterns.

I-3.4. CLIMATE

Glancy et al. (1993) believe that the short-term climatic changes in the basin area could have developed in response to two mechanisms: (1) a latitudinal differences in Cretaceous landmass distribution; (2) Milankovitch-scale changes in insolation, even in the absence of permanent polar ice and extensive glaciation.

Palynology studies have established the terrestrial biostratigraphy as well as delineating climatic zones based on the flora. Upchurch and Wolfe (1993) described the Cretaceous palaeofloras as being dominated by ferns and gymnosperms. North of palaeolatitude 50-55^0 N, deciduous plants, including gingkophytes with well-developed dormancy mechanisms, dominated. South of this palaeolatitude, predominantly evergreen conifers, cycadophytes, and tree ferns were major components. After a transition period marked by the diversification of angiosperms there was an ecological displacement of more primitive conifer, fern, cycadophyte and ginkgophyte floras. Cenomanian through Maastrichtian (Upchurch and Wolfe, 1993) terrestrial floras of North America were dominated by different communities of angiosperms from pole to equator. Low-latitudinal temperature gradients are indicated by these Western Interior floral and, also, reptilian distribution patterns and suggest that there was little or no freezing south of 55^0 N. Based on floral assemblages Early Cretaceous climates were generally moist, but they became gradually drier from the Cenomanian to Maastrichtian (time of Mesaverde deposition). An abrupt increase in rainfall occurred at the time of the Cretaceous-Tertiary transition and may have been, in part, responsible for a major plant extinction at the end of the Cretaceous. Figure I-4 shows representative floral fossils

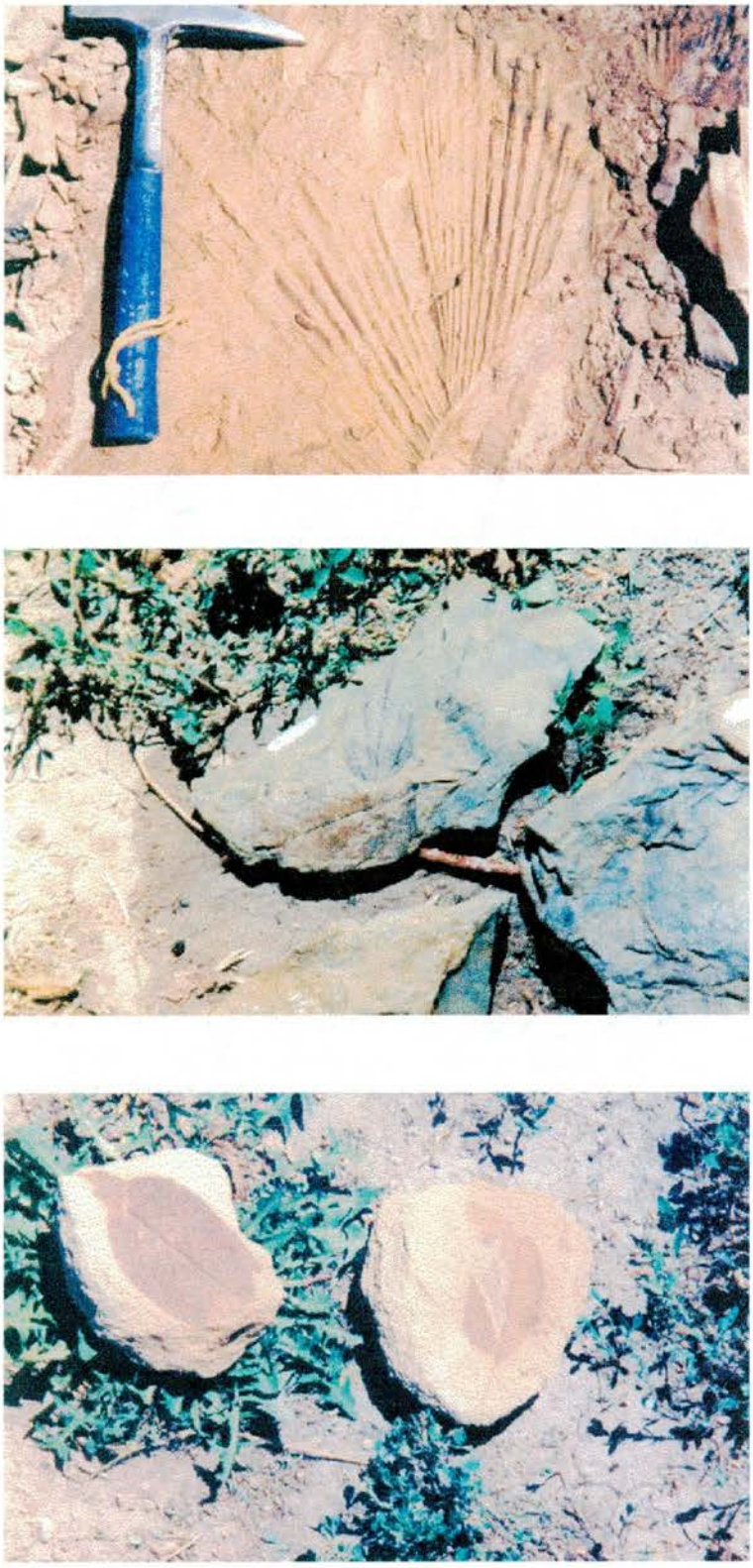

Figure I-4: Photographs of plants found in the Middle Member of the Mesaverde Formation in the Wind River Basin.

found in the Mesaverde Formation. Although these have not been identified to generic and species level, they are leaves typical of those described by Upchurch and Wolfe (1993).

I-4. BACKGROUND AND PREVIOUS STUDIES OF THE MESAVERDE FORMATION IN THE WIND RIVER BASIN

The Wind River Basin has been exploited for commercial quantities of oil and gas for over 100 years with most of the production in the Wind River Basin focused on structural or combined structural-stratigraphic traps (Keefer and Rich, 1957). In addition to being a potential oil and gas reservoir, the Mesaverde Formation contains economically important coal deposits, especially in its lower units (Berryhill et al., 1950; Thompson and White, 1952). In 1993, a preliminary geologic characterisation of Upper Cretaceous and Lower Tertiary low-permeability gas bearing rocks in the Wind River Basin designated the Mesaverde Formation as a tight sandstone and it contains mainly gas-prone type III organic matter with a thermal maturity level of Rm 0.73 percent (Johnson, 1993).

The Mesaverde Formation was first defined by W.H. Holmes (1877) from exposures in Montezuma County in southwestern Colorado, although the Mesaverde in the Wind River Basin differs considerably from its type locality. Detailed studies of the stratigraphy and structural evolution of the Wind River Basin have been publisher by Yenne and Pipiringos (1954), Keefer and Troyer (1956-1964), Barwin (1959), Weimer (1960), Merewether and Cobban (1970) and Johnson and Rice (1993). The nomenclature of the Mesaverde Formation in the Wind River Basin presents a problem because of complex intertonguing of marine, transitional and

nonmarine deposits (see Figure I-2 for a summary). Tables of applicable stratigraphic nomenclature were presented by Hills (1956), Gower (1978) and Love et al. (1987).

In addition, detailed maps of the area have been published by Tourtelot and Thompson (1948), Masursky (1952), Troyer and Keefer (1955), Murphy et al. (1954), Keefer and Troyer (1964), McGrevy et al. (1969), Keefer (1970), Maughn (1972) and Love and Christiansen (1985).

In 1986, the Geological Survey of Wyoming, US Department of the Interior, and the Bureau of Land Management (BLM), entered into Cooperative Agreement N^0 Wy-910-CA7-C1. This agreement established that geologic information collected with public funds or in response to a Federal mandate may be released to the public through the Geological Survey of Wyoming.

Previous workers (Keefer and Troyer, 1964; Keefer and Johnson, 1993) have defined the Mesaverde Formation as composed of 3 separate members; basal, middle and Teapot. The unconformity at the base of the Teapot Member was described by Gill and Cobban (1966) and Reynolds (1966). Although some sedimentary logging has been completed on the Reservation, no sequence stratigraphic framework has been suggested for the rocks in this area.

I-5. BIOSTRATIGRAPHY OF THE MESAVERDE FORMATION

For the Cretaceous Western Interior Seaway, ammonite zonations are well established (Kauffman, 1977). In addition to ammonites which are restricted to the geographic centre of the seaway, inoceramids, dinoflagellates and foraminifers are also useful in supplementing the biostratigraphic record. Marine biostratigraphy can

resolve 200 k.y.-500 k.y. cycles from ammonites and dinoflagellates thereby dividing the Late Cretaceous into six intervals of time. For the Campanian stage, three different intervals are subdivided and the Mesaverde Formation in the Wind River Basin (Cobban, 1984; Robinson Roberts et al., 1995) includes rocks from the Campanian I and Campanian II: Campanian I extends from the zone of *Scaphites leei III* through *Baculites asperiformis* (83.5-79 m.y.) and the Campanian II spans the ammonite zones *Baculites sp* to *B. cuneastus* (79-72 m.y.). The remainder of the Campanian includes one ammonite zone which continues into the Maastrichtian (72-65.5 m.y.) and is defined at the base by the ammonite zone *B. reesidei* and at the top by the last appearance of the dinosaur *Triceratops* (Robison Roberts et al., 1995).

Chapter II

METHODOLOGY

The study undertaken is based primarily on the outcrop analysis of exposures of the Mesaverde Formation in the Wind River Basin, Wyoming. The Mesaverde Formation crops out in a series of folds oriented N30W and the outcrop quality is superb. The reservoir characterisation is based on detailed measurement of sections and lateral tracing of beds over several kilometres and is supplemented by thin section analysis, isopach distributions and wireline-log analysis from subsurface units within the basin.

II-1. FIELD-WORK

The first part of the research involved recognising and defining the different parts of the Mesaverde Formation in outcrop and the definition of the contacts separating it from the formations above and below.

- ***Measurement of sections:*** The measurement of sections was accomplished with a Jacob Staff which is ruled in a decimetre scale. The topographic maps used were from the U.S.G.S. from Denver, prepared by Intrasearch, as well as the geologic map of Wyoming (Love, J.D. and Christiansen, A.C., 1985). The location of the sections to measure was chosen by starting with the most lateral limits of the outcrop-belt and completing additional sections in the areas in between in order to identify both vertical and lateral changes between different areas. The measurements of the sections were made in centimetre-scale detail and included information on grainsize, composition, sedimentary structures (scale and type within the different facies),

palaeocurrent data, vertical and lateral relationships between the different facies units, organic matter content and fossil evidence. Sampling was made by collecting representative rock samples of the different facies both laterally and vertically. Once the description of facies was accomplished, detailed analysis of contacts and lateral facies changes was made by walking out the length of the exposure. Contacts, as well as observations of the geometry and stacking pattern of the different units were also recorded. For example, the Basal Member was traced throughout almost the entire exposure in the Maverick Springs area (50 km) (Figure II-1). The next stage involved section logging along the eastern exposures of the Mesaverde in the basin. The resulting field database permitted defining changes in facies character basin-wide and the development of the depositional framework.

II-2 WIRELINE-LOG ANALYSIS

Because facies changes occur between the different exposures across the outcrop belts, correlations between them are not straightforward. Use of intervening subsurface data is therefore necessary in order to analyse the areas between outcrops. With the purpose of establishing the wireline-log characterisation of the Mesaverde Formation at the different localities several studies were made:

- Analysis of cores at the USGS core facility in Denver, with the resultant comparison of the core with the closest outcrop section
- Comparison of the core with its correspondent wireline-log from the USGS (Denver).

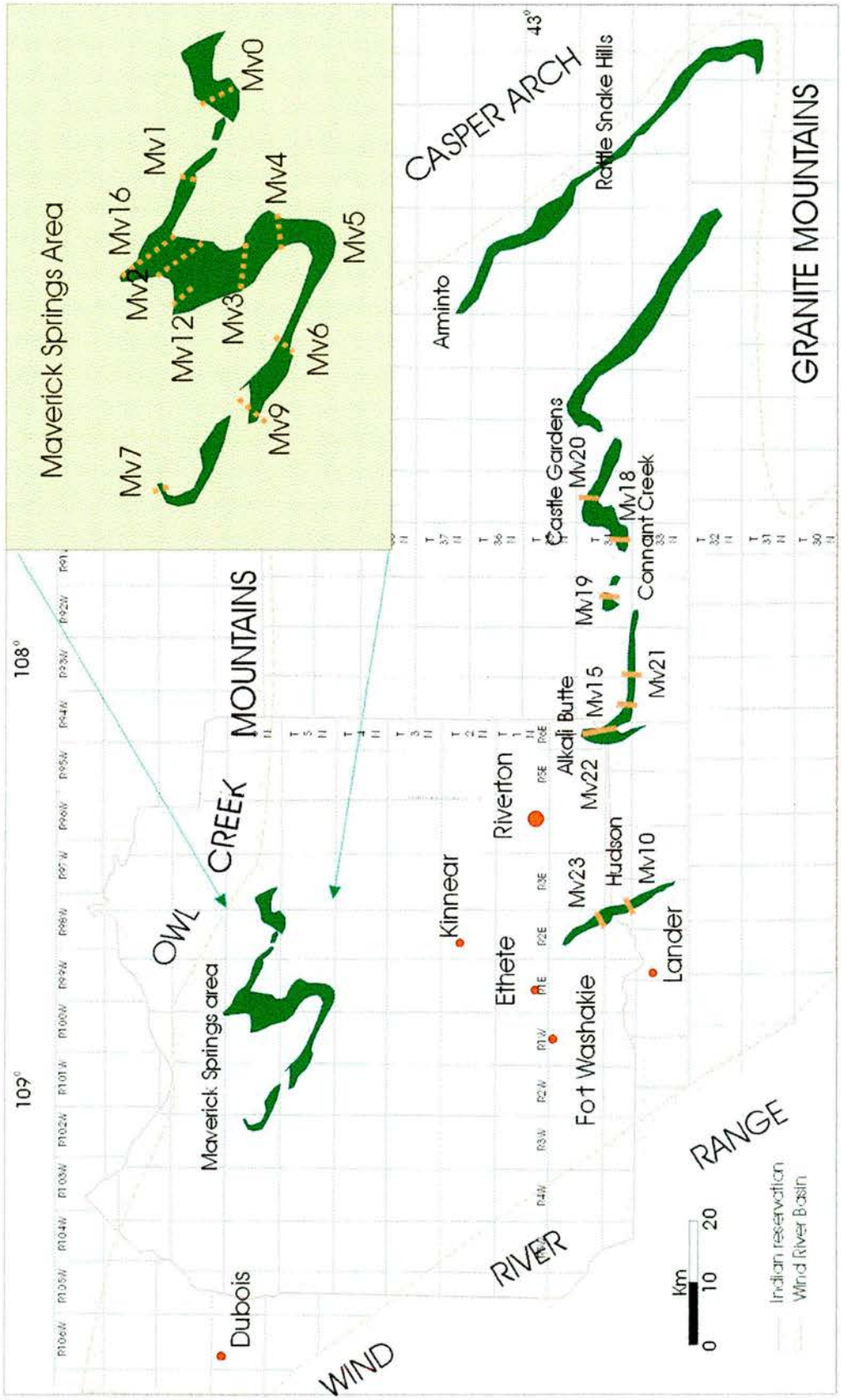

Figure II-1: Location of the Mesaverde outcrop in the Wind River Basin and position of the measured sections.

- Use of a gamma-ray scintilometer on the core (reading spacing of 0.5 metre) and comparison of the gamma-ray log obtained with the well wireline-log.
- Hand-held gamma-ray logs were also measured on particular outcrop sections (3 metres spacings) in order to create a comparison with the wireline-logs from the subsurface.

II- 3. LABORATORY WORK

In order to characterise the different facies present in the Mesaverde Formation, the samples obtained in the field work where studied using the following techniques.

- ***Thin-section analysis:*** Thin-section analysis was performed on samples representing sandstones and siltstones. The samples were treated with methyl-blue in order to measure and discriminate the porosity content. Observations about the minerals, rock fragments, porosity, cement, matrix, as well as relationships between the different components, were made in order to establish the diagenetic history of the samples. The microscope used was a James Swift Polarising Microscope Model MP3502B (BL) (Dual purpose-combined incident/transmitted light). Point counting of 100 points on each slide allows the percentages of different mineral species to be quantified for each of the samples. The point counting analysis was accomplished using a James Swift automatic point-counting model "F" and it was made taking into account the main mineral components as well as rock fragments, cement, matrix, porosity

and a category of "other" including heavy minerals or rock fragments not common in the samples. The results of the point-counting were statistically treated, looking for possible trends in the mineral content for the different samples. The statistical analysis was performed using the statistical software "Minitab"10.

- ***XRD/XRF analysis:*** These two techniques were used to obtain the geochemistry of the shales, as well as the chemical composition of representative sandstones and siltstones. The XRF analysis was done using a Philips PW 1450/20 Automatic Sequential Spectrometer with a RH X-ray tube for primary excitation. Calibration is done by reference to a monitor (H12) supplied by K. Norrish, and using 25 international rock standards. For consistency, all calculations are performed by an on-line computer. XRD is a technique used mainly for the analysis of fine-grained material which are difficult to study in thin-section analysis. The crystallinity of minerals results in each having a unique X-ray diffraction pattern. When a sample is bombarded with high energy X-rays, particular wavelengths and intensities are emitted by the sample dependent on the elements present. Measurement of the intensity of the characteristic radiation for a particular element gives a value reflecting its concentration in the sample. The sample is analysed and a graph is obtained with the diffractometre traces of the different minerals present in the sample; the x-axis represents the 2θ angle characteristic of each mineral and the y-axis represents the intensity of the diffracted peak

above background. The XRD analysis is performed with the Philips PW 1050 Difractometer/Hiltonbrooks DG2. The X-ray tube contains Cu or Co and the analyses are made with the interpretation software Siemens diffrac-AT version 3.2. This technique is ideal for the determination of major and minor elements, such as Si, Al, Mg, Ca, Fe, K, Na, Ti, S and P.

- ***Palynology:*** Palynological samples of coals and organic-rich shales representative of the different stratigraphic positions and localities of the outcrop were taken in order to obtain biostratigraphic control and possible correlation lines throughout the basin. Analyses are currently being conducted under the supervision of Professor David Batten at the University of Aberystwyth and are not included in this dissertation, but will be presented in future publications.

Chapter III

FACIES AND THIN-SECTION ANALYSES

III-1. INTRODUCTION

The area of study covers the Mesaverde outcrop throughout the Wind River Basin (Figure III-1). In this area, the Campanian Mesaverde Formation includes all rocks between the top of the underlying Cody Formation and the base of the Lewis, Lance, Meeteetse and Fort Union Formations (Keefer and Van Lieu, 1966). The lower contact of the Mesaverde Formation is placed at the base of the massive, generally littoral deposits (see below). The underlying Cody Formation is composed of shelf and lower and middle shoreface deposits. The top of the Mesaverde contact is well recognised where the Teapot Member is present and is placed at the top of the last white sandstone bed in the Teapot Member. In areas where the Teapot is not present, the top of the Mesaverde Formation is chosen at the marine flooding surface of the Lewis Shale or the Lance Formation. At some localities, like Hudson (Figure III-1), the top is truncated by the angular unconformity at the base of the Fort Union Formation (Figure III-2).

In the northwestern part of the basin (Figure III-1), the outcrop displays a vertical change from marine to non-marine continental deposits, whereas in the southern and southeastern parts of the basin, the Mesaverde Formation reflects repeated episodes of marine and marine-influenced deposition.

III-2. FACIES ANALYSIS

In order to establish the depositional framework of the Mesaverde Formation, the first goal of the research (see Chapter I) is to provide the stratigraphic and sedimentological analysis of the exposed rocks throughout the

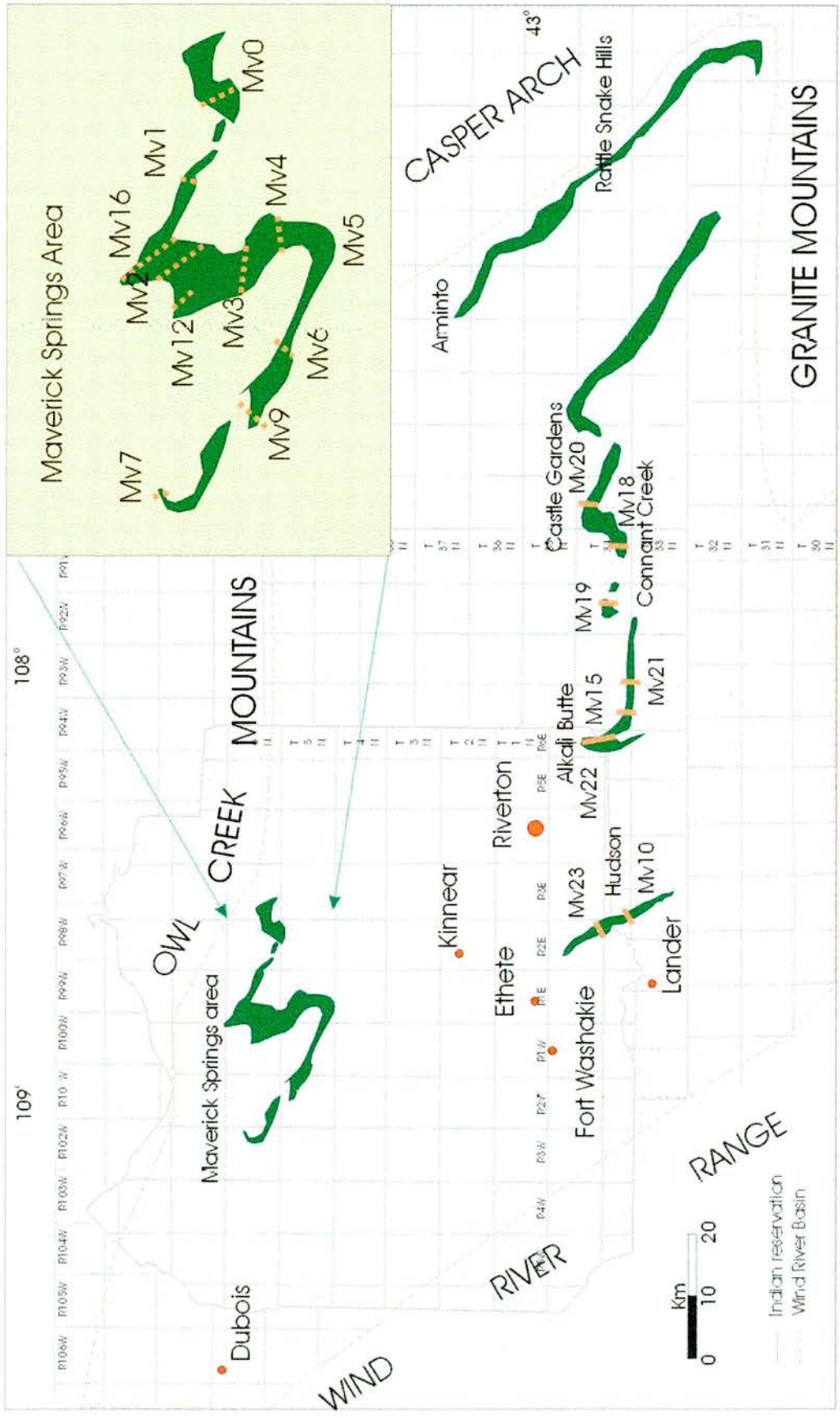

Figure III-1 Location of the Mesaverde Formation in the Wind river Basin. Location of measured sections.

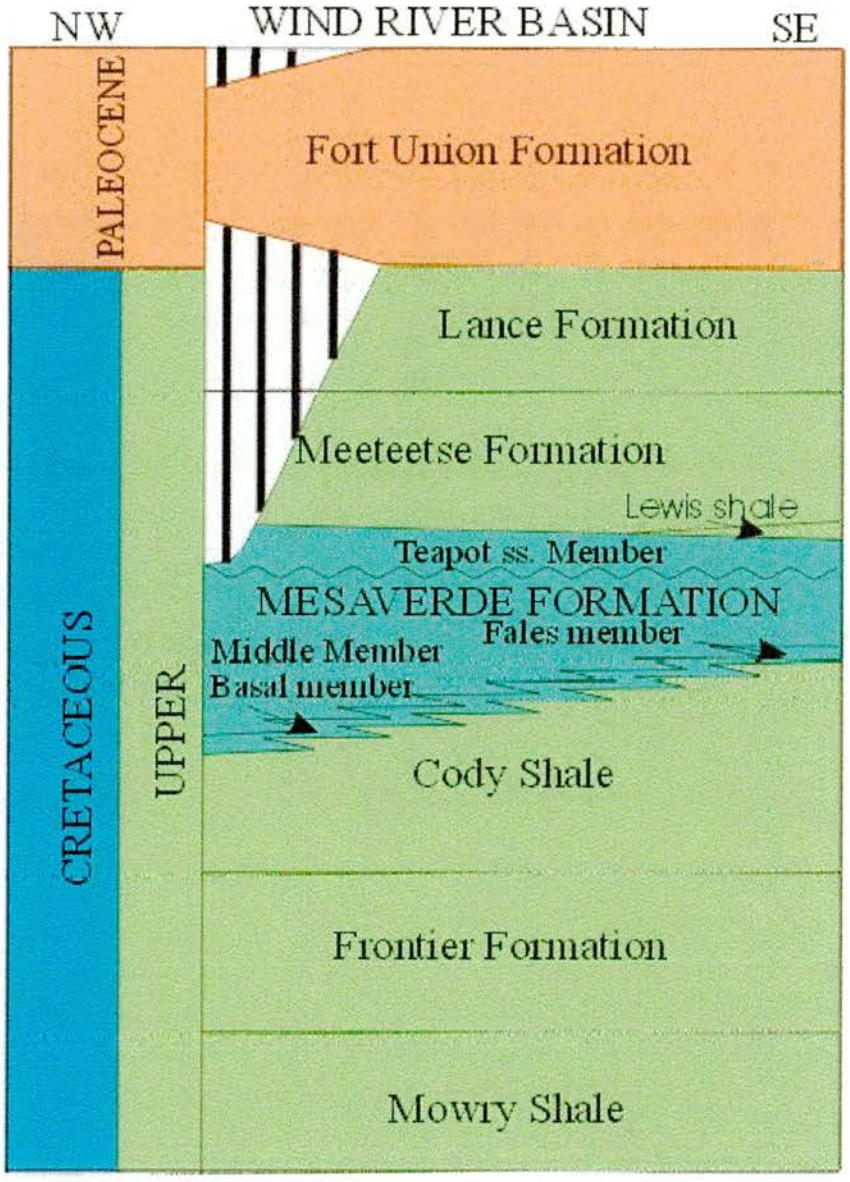

Figure III-2: Stratigraphy of the Upper Cretaceous in the Wind River Basin

Wind River Basin. The facies synthesis and the interpretations of depositional environments provide the foundation on which stratigraphic architectural interpretations and conclusions are based. Distinguishing sedimentologic and stratigraphic characteristics of each sedimentary facies and facies association, as well as the contacts separating them, are described and interpreted below. Facies associations 1, 2, and 3 correspond to the upper part of the Cody Formation, but their study is necessary to develop a context for the basin-wide depositional framework of the Mesaverde Formation.

Facies association 1: mudstones with hummocky cross-stratified sandstones

Description

This facies association consists mainly of grey mudstone intervals ranging in thickness from metres to tens of metres. Locally interbedded with these mudstones are very fine-grained tan to reddish sandstones which, together with the mudstones, form coarsening-and-thickening upward cycles typically 30 to 50 metres in thickness (Figure III-3A). The sandstones bodies are 10 to 20 centimetres thick and display variable lateral continuity from only two metres in some cases, up to several hundreds of metres in others. These sandstone beds display sharp bases, with wavy, parallel and low-angle planar-lamination, centimetre-thick climbing ripples and in some cases hummocky cross-stratification. Trace fossils such as *Ophiomorpha nodosa* (Seilacher, 1967; Mieras et al., 1993; Pemberton et al., 1992) as well as some shell fragments, are present, but in general these are not abundant. Towards the top of the sequence, cycles coarsen and thicken upward and the uppermost sandstones typically exhibit current, symmetrical and combined-flow ripples (Table III-1: Fa 1).

Interpretation

The sandstone bodies represent episodic storm deposits under oscillatory-dominated combined flows as reflected in the hummocky cross-stratification and the wavy, low-angle cross-lamination and climbing ripples (Swift et al., 1987). The mudstones reflect quieter environmental conditions deposited below storm wave base and reflect pelagic deposition between storms. Cycles of more abundant mudstones reflect less impact of storm events. Sharp contacts between sandstones and mudstones represent abrupt deepening across flooding surfaces (Van Wagoner et al., 1990).

Facies association 2: amalgamated sandstone bodies

Description

This facies is composed of very fine-grained sandstone bodies, with a combined thickness of a few metres to tens of metres that are laterally continuous for up to hundreds of metres (Figure III-3C). The main sedimentary structures in these sandstone bodies are cross-cutting sets of gently dipping concave-up laminae (0.5 metres thick and 2-3 metres width) which gradually flatten upwards. Flat lamination and structureless beds are also present. Lenticular beds up to 1 to 2 metres thick occur locally at the base of the sequence between the sandstone bodies. These beds have undulating upper and lower surfaces, contain internal convolute bedding and decimetre-scale intraclasts of sandstone eroded from underlying layers (some of the clasts show hummocky cross-stratification). Some of the amalgamated sandstone bed bases are erosional and, in some locations, are concave in shape. Vertical and lateral amalgamation of beds is common, with individual beds difficult to trace and distinguish. In places, the sandstone tops can display thin (less than 1 centimetre thick) layers of mudstone (mud drapes), shell fragments (*Inoceramus*), and even thin beds of well-cemented red sandstone that appear to pinch-and-swell. Following these layers down

depositional dip (towards the south-east) over many 10's to several 100's of metres, it is observed that the thickness of the sandstone bodies decreases and undergo a facies change into thin sandstone beds of facies association 1 with hummocky cross-stratification. These latter beds are typically more laterally continuous for hundreds of metres. In the south-eastern parts of the basin (Figure III-1, Alkali Butte and Castle Gardens sections), the tops of some of these beds contain a lag of pebbles, pelecypods, shells, shark teeth and vertebrate bone fragments. Towards the top of the sequences, oscillatory and climbing ripples appear to be more abundant. Trace fossils, such as *Ophiomorpha nodosa* (Seilacher, 1967; Mieras et al., 1993; Frey and Pemberton, 1992) appear rarely. At some localities, facies association 2 is not present. (Table III-1: Fa 2).

Interpretation

The sedimentary structures and rarity of fossil content infer high energy conditions with the substrate under continuous agitation. These characteristics are typical of middle and upper shoreface environments. The sandstones with concave-up laminae sets are interpreted as swaley cross-stratification. The convolute, lenticular beds with large intraclasts are interpreted as slump deposits of the underlying storm deposits of facies association 1. The downdip "splitting" of the sandstone bodies is interpreted as a normal lateral facies change from shoreface to inner shelf settings. Therefore, the tops of the beds from facies association 1 can be correlated with the tops of thin layers of mudstone with shell fragments represent flooding surfaces (Van Wagoner et al., 1990). Similarly, the tops of the laterally traceable sandstone beds in distal parts of the basin which are commonly marked by a lag of pebbles, shark teeth, shell fragments, pelecypods and vertebrate bone fragments are interpreted as regional transgressive surfaces (Van Wagoner et al,, 1990). Soft-sediment deformation, massive beds and the

scarcity of wave-formed features suggest rapid rates of sediment accumulation, possibly in a delta front region of a river-dominated delta (Coleman and Gagliano, 1965; Coleman and Prior, 1982). Dewatering and loading features result from sediment instabilities and density contrasts between rapidly deposited clay, silt, and sand.

Facies association 3: massive sandstone bodies, with erosive bases and basal lags

Description

This facies association appears only in certain localities (Figure III-1: Mv2, Mv5 and Mv1). It is composed of erosive-based sandstone bodies up to 25 metres in thickness and 100 to 200 metres in width, that change upwards into laminated, bioturbated shale intervals. These fine-to medium-grained sandstone bodies cap shoreface deposits and commonly, but locally cut down through their entire thickness (Figure III-3B). The bases of the sandstone bodies have rip-up clasts and, in places, *Teredolites* burrows, as well as *Ophiomorpha nodosa* traces on the bed tops (Seilacher, 1967; Mieras et al., 1993; Frey and Pemberton, 1992). Locally, bidirectional palaeocurrent indicators can be observed, but they are rare. At some localities, the sandstone bodies contain reactivation surfaces, with trough cross-bedding (palaeocurrents ~110^0 and 310^0) (See section III-3 for discussion of palaeocurrents) and appear multistory in character forming sandstone packages up to 15 metres thick.

Interpretation:

The multistorey channelised character, with erosive bases and lags and the locally bidirectional indicators, imply tidally influenced fluvial deposits that scour into underlying shoreface deposits. The high amount of bioturbation in

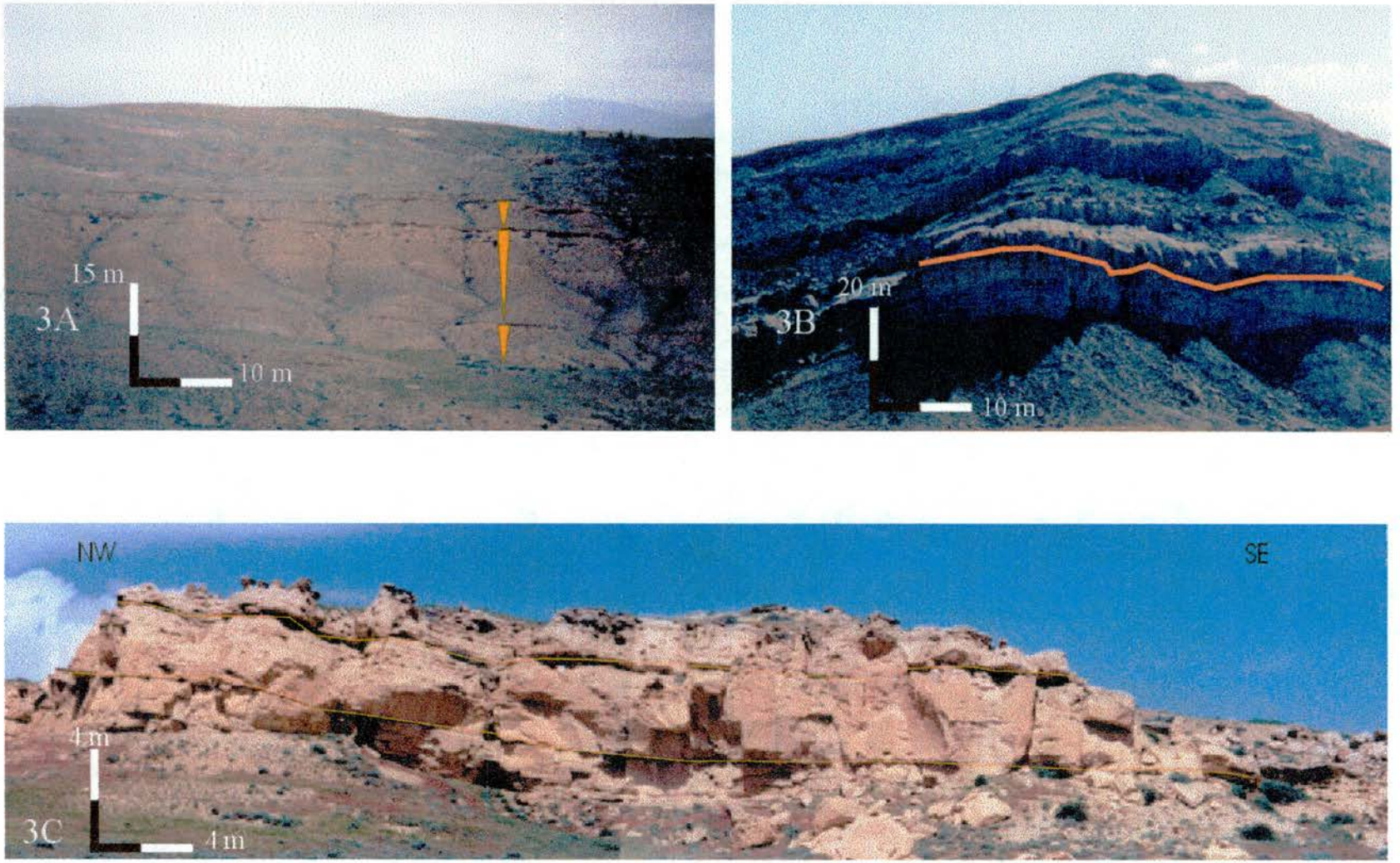

Figure III-3: A) General view of the coarsening and thickening-upwards cycles of the Cody Formation (section Mv9). B) Erosive based sandstone bodies at top of the Cody Formation cutting-down into the shoreface deposits below (section Mv2). C) Shoreface clinoform of the Cody Formation at Alkali Butte section. See Figure III-1 for locations.

both sandstones and shales, together with the bidirectional palaeoflow indicators may reflect an estuarine environment (Table III-1: Fa 3).

Facies association 4: amalgamated sandstone bodies with bidirectional flow indicators capped with organic-rich beds

Description

This facies consists of several amalgamated, medium grain-size sandstone bodies that range in thickness from 3 to 5 metres which are white in colour and typically cap facies association 2 (Figure III-4A). Along the outcrop, they exhibit trough cross-lamination (10-30 centimetres thick cosets) (Figure III-4B), herringbone cross-lamination (20 to 30 centimetres thick) and flat lamination (Figure III-4C) and commonly contain vertical trace fossils and shell fragments. Locally, they grade laterally into carbonaceous shales and coal beds. To the south at Hudson (Figure III-1), tabular-bedded sandstones with high-angle cross-stratification (up to 50 centimetres thick and approximately 2 metres width) occur at the top of the white sandstones. These sandstones appear as bodies up to 20 metres thick and 300 metres in width and reflect vertical changes in palaeocurrent direction (south-east to north-west) that show landward-dipping laminae capped by steeply dipping foresets of cross-bedded units up to 1 metre thick and inclined landward at high angles) (For palaeocurrent discussion see section III-3). Truncation surfaces and wave ripples are common. In south-eastern parts of the basin, this facies association appears repeated several times (Figure III-4D). The contact between this facies association and facies association 2 and 3 appears transitional, although in more distal sections like Mv10 and Mv15 (Hudson and Alkali Butte; Figure III-1), the contact is very sharp and erosive. The tops of these sandstone bodies are capped by a coal bed or

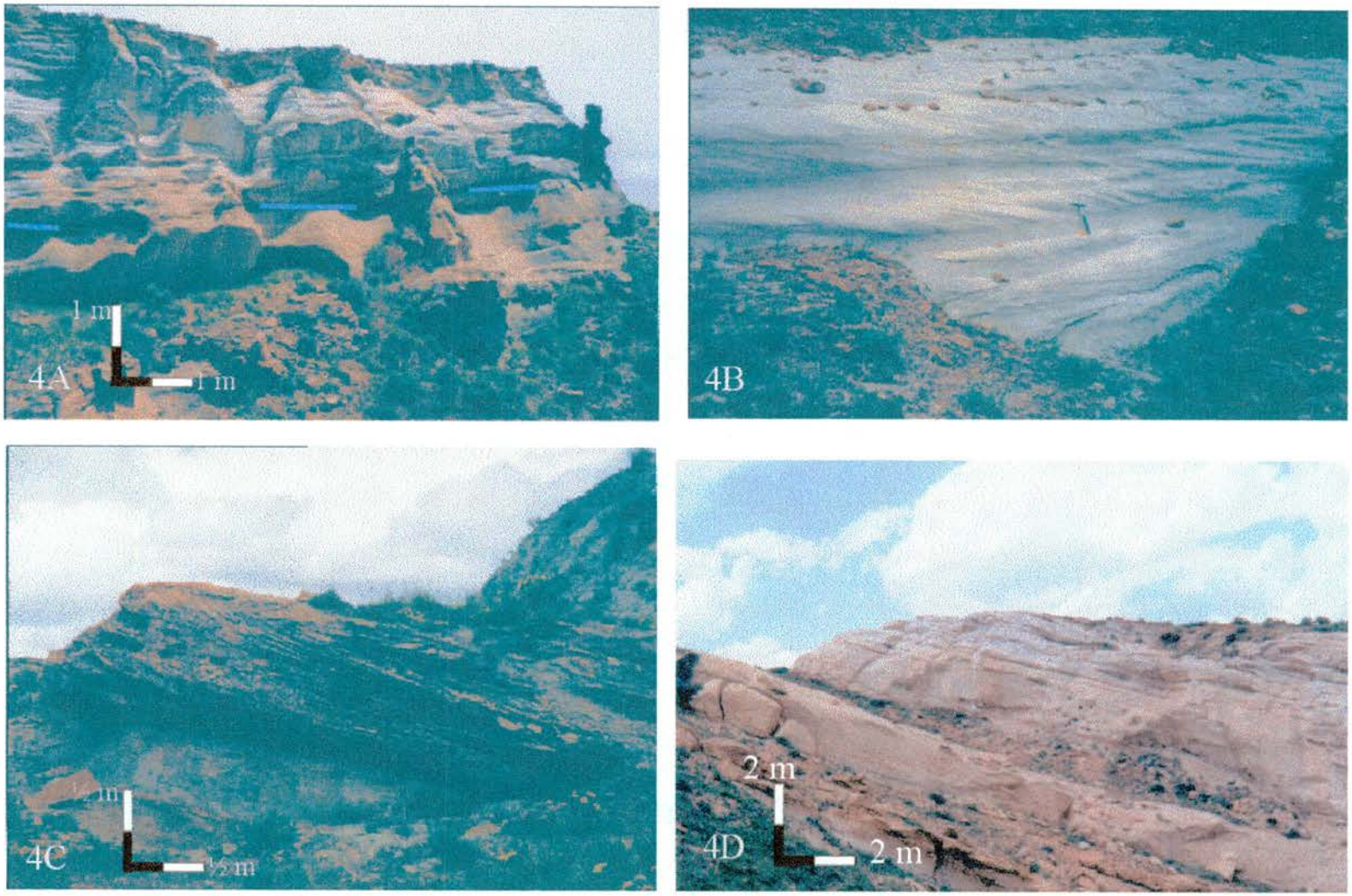

Figure III-4: A) Contact between the Cody Formation (below) and the Mesaverde Formation (Hudson section Mv 10). B) Planar cross-bedding of the Basal Member of the Mesaverde Formation at top of the foreshore deposits at Hudson. C) Trough cross-bedding at top of the foreshore deposits of the Basal Member (Hudson section). D) Amalgamated shoreface deposits of the Mesaverde Formation in the section of Alkali Butte. (See Figure III-1 for location of sections).

organic-rich shale with plant and wood fragments, except at section Mv16 (north of Muddy Creek; Figure III-1), where the organic layer is eroded by a channelised sandstone of the Middle Member of the Mesaverde Formation (Table III-1: Fa 4).

Interpretation

These sandstone bodies represent foreshore and wave-influenced shoreface settings (Plint and Walker, 1987) that are vertically capped by, or laterally grade into, lagoonal or distal coastal plain (carbonaceous shales and coal beds) deposits. The low trace faunal diversity implies that this setting may have been stressful for organisms (Frey and Pemberton, 1992).

Facies association 5: interbedded mudstones, siltstones and sandstones with coals

Description

This facies association consists of shales, coals, siltstones and sandstone bodies that form fining-upward cycles typically 25 to 35 metres in thickness. The sandstone bodies are cross-stratified (cosets are 10's of centimetres thick, and 1 to 2 metres in width), fine-grained, erosively based and can be either sheet-like or lenticular in geometry depending on the orientation of the outcrop with respect to depositional strike. They also show lateral accretion surfaces. Locally, the base of these sandstones contains a lag of silty pebbles eroded from deposits immediately below. In some localities (Mv9; Figure III-1), the base of the sandstone bodies contain *Teredolites* burrows (Figure III-5A). The sandstones appear either as single-storey bodies up to 4-5 metres thick or multistored up to 15-20 metres thick. Their lateral extent varies between ~50 to ~400 metres. Tidal bundles and mud drapes become more common in sandstone bodies in sections towards the southeast. Palaeocurrent indicators show dominant flows of 140^0.

Thin, 1 metre thick (or less) sandstone bodies with symmetrical and asymmetrical ripples appear related to the lenticular-shaped deposits. Laterally, or at the top of both types of sandstone bodies, carbonaceous shales and ~1 metre thick coals interbedded with thin siltstone beds form the bulk of the depositional cycles. The shales are carbonaceous-rich and locally change into coal beds. The coal beds are laterally continuous for 10's of metres, but scouring of channelised sandstones makes them difficult to trace laterally for long distances. The siltstone beds are lenticular, have lateral extents of a few metres and thicknesses of less than 1 metre. They have some relict stratification, with plant leaves and roots on tops, and in some cases contain nodules. These cycles average approximately 30 metres in thickness, with sandstone/shale ratios between 1 and 1.8. The sequence generally coarsens upward (Table III-1: Fa 5).

Interpretation

These sandstone bodies are interpreted as distributary systems with limited tidal influence (Figure III-5B), encased in floodplain mudstones and siltstones. They occur both as bodies that represent relatively complete cycles of distributary channel deposition, accretion and abandonment, whereas thicker, multistored occurrences represent stacked distributary channel deposits. The shales, siltstones and coals appear laterally to the channelised complexes and represent interdistributary swamps, vegetated islands, and marshes. The siltstone beds represent small ponds formed laterally to the distributary channels during times of low deposition of clastic material. If the time of low deposition was long enough, the ponds became vegetated and pedogenic activity started, generating weakly developed palaeosols (probably entisols or inceptisols) (Aslan and Austin, 1998; Bown and Kraus, 1981, 1987). The palaeosol development was enhanced in the floodplains that were stable due to a balance between

sedimentation and erosion (McCarthy et al. 1997). The thin sandstone beds with symmetrical and asymmetrical ripples suggest break out of the main distributary onto a floodplain, forming crevasse complexes, which show some wave and tidal influence as well as high abundance of climbing ripples. Altogether, this facies association represents a distal delta-plain environment with some wave and limited tidal influence.

Facies association 6: sandstones with combined flow ripples

Description

This facies association is formed by sandstone units which generally exhibit an upward increase in grain-size from fine to medium and contain low-angle parallel laminations. Carbonaceous debris drapes accentuate the laminae and bedding. Biogenic structures are sparse to absent. Sandstones range in thickness from 5 to 13 metres and extend laterally for up to 100 metres. They have scoured bases and are typically lenticular in shape. Symmetric and combined-flow ripple laminations (10-30 centimetres thick) are present at some localities. A thicker sequence of this facies association appears towards the east of Maverick Springs (Sheep Creek Road section, MV0; Figure III-1) (Table III-1: Fa 6)

Interpretation

This facies association is interpreted as broad channelised deposits in a distal deltaic setting. The predominance of flat-laminated sandstones and organic laminae suggests suspension fallout during sediment deposition. Scouring, in association with the predominantly unidirectional palaeocurrents, suggests erosion by traction currents emanating within fluvial dominated distributary channels (see section III-3 for palaeocurrent analysis). Localised low-angle

stratification and symmetrical and combined-flow ripple lamination suggest intermittent wave and possibly storm influence (Walker, 1992).

Facies association 7: mudstones, siltstones and sandstones beds with lateral accretion surfaces

Description

This facies association is composed of mudstones, interbedded with siltstones and sandstone beds. The sandstone beds are laterally continuous for ~100 metres with thicknesses between 5 and 15 metres (Figure III-5C). Trough cross-bedding (sets are approximately 40 centimetres in thickness and 1 metre in width), erosive bases and basal lags of plant material are common. Palaeocurrents show a wide range of flow directions between 290^0 and 160^0 (See section III-3 for palaeocurrents discussion). Lateral-accretion surfaces migrating orthogonally to the main palaeoflow directions are also common. Laterally and vertically adjacent to the main sandstone bodies are up to 1 metre thick sandstones that are continuous for many tens of metres and display sharp bases and tops. These sandstone beds contain abundant climbing ripples. Although individual beds fine upwards, they commonly stack together to define an overall coarsening upward trend. In general, they contain small-scale trough cross-bedding (Table III-1: Fa 7). Siltstone beds traceable for tens of metres appear laterally adjacent to the main sandstone bodies. They have sparse root traces and traces of what could have been some stratification. Carbonaceous shales form a high proportion of the cycles.

Interpretation

This facies association is interpreted as single and/or multistorey deposits of a fluvial system with meandering trunk channels (the thicker cross-bedded sandstones) and contain lateral accretion surfaces with associated crevasse splay

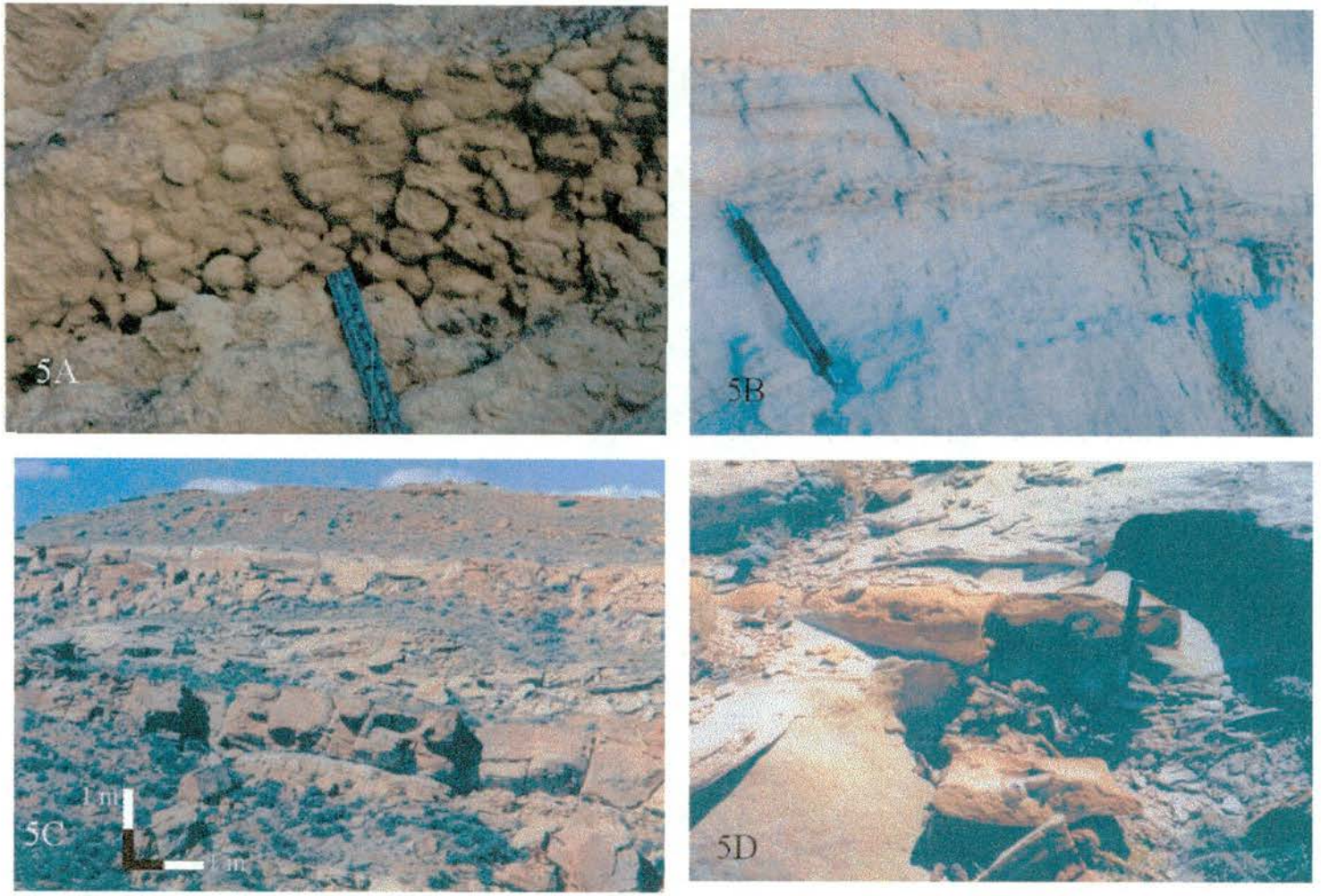

Figure III-5: A) Teredolites burrows at the base of a channelised body in the lower part of the Middle Member (Maverick Springs area). B) Tidal bundles in a channelised deposit of the lower submember of the Mesaverde Formation in Maverick Springs area. C) General view of the Middle Member of the Mesaverde Formation in Maverick Springs area displaying lateral accretion surfaces encased in a broad but lenticular sandstone.. D) Tree trunk in the upper Middle Member in Maverick Springs area. See Figure III-1 for locations.

complexes (thinner, tabular sandstones). Palaeosols (Krauss, 1987; Brown et al., 1988) and fine-grained deposits formed laterally to channelised areas.

Facies association 8: coal, mudstones and ribbon shaped sandstones

Description

Like facies associations 5 and 7, this facies association consists of sandstones, shales, abundant coal beds and siltstones. However, sandstone bodies have "ribbon-like" geometries and the content of plant material is generally higher than in previous facies with tree trunks (Figure III-5D) as large as 1 meter in length at the base of the sandstones. Thin sandstones (less than 1 metre thick), which contain climbing ripples (Figure III-6A) and display sharp bases and tops and in some places a high concentration of plant leaf fossils and root traces (Figure III-6B), occur laterally to the "ribbon like" sandstone bodies. They show a decreasing trend in thickness and grain-size away from the thicker sandstone bodies. Carbonaceous shales and siltstones are more abundant and siltstone beds are laterally continuous for tens of metres and are heavily rooted at the top (Figure III-6A). Several sandstone bodies with "ribbon-like" geometries appear at the same stratigraphic position, and appear separated by the fine-grained material or the thin sandstones with climbing ripples. Palaeocurrents show mean directions of about 150^0 (Figure III-6) (See section III-3 for discussion of palaeocurrents) (Table III-1: Fa 8).

Interpretation

This facies association represents an anastomosed distributary system flowing through a broad floodplain. The thin "ribbon-like" (Figure III-6C) sandstones are the distributaries encased in floodplain fines and soils. The anastomosing character is interpreted based in the appearance of several channelised deposits at the same stratigraphic position, the appearance of

crevasse splay complexes and vegetated islands between them and the high content of organic material. The carbonaceous shales reflect the abundance of available vegetable matter, conditions of low sediment accumulation and burial under reducing conditions. The carbonaceous shales, sandstones and siltstones were deposited on floodplains and within marginal swamps and lakes during times of flood. Some of the siltstones represent poorly developed palaeosols similar to facies association 5 (Krauss, 1987; Brown et al., 1988). The "ribbon-like" geometry of sandstone beds, absence of marine fauna, abundant carbonaceous material, leaves and finely disseminated particles of coal indicate dominant continental conditions with no marine influence.

Facies association 9: amalgamated sandstone bodies with scarce mudstones, siltstones and coals

Description

This facies association is only observed in the Teapot Sandstone Member, which is composed of three separate units arranged vertically (Figure III-6D). Facies association 9-A corresponds to the lower and top sub-units of the Teapot Member, and Facies association 9-B corresponds to the middle sub-unit.

A) The lower and upper sub-units are formed by lenticular-shaped medium-to coarse-grained sandstone bodies. These beds amalgamate to form sandstone packets between 5 and 10 metres thick. The individual lenticular-shaped sandstones are usually 4 to 6 metres wide and 0.5 to 1 metre thick. They are filled by sets of trough cross-stratification, with palaeocurrent mean directions of 170^0 dominating the lower submember and a wider range of between 30^0 and 160^0 for the top submember (See section III-3 for discussion of palaeocurrents). The sandstones contain decimetre-scale planar cross-

Figure III-6: A) Climbing ripples from a crevasse-splay complex in Maverick Springs area. B) Palaeosol deposit from the upper part of the Middle Member in Maverick Springs area. C) Ribbon-like channelised deposit from the upper part of the Middle Member in Maverick Springs area. D) General view of the Teapot Member in sheep Creek Road (section Mv0). See Figure III-1 for locations.

stratification and lateral migration surfaces are also present in 1 metre thick bed-forms but are not abundant. The lenticular sandstones amalgamate laterally and vertically, forming a package up to 25 metres thick and continuous for hundreds of metres. Minor amounts of siltstone and shale are present, appearing as stringers isolated between the sandstones. The succession fines-upwards.

B) The middle sub-unit contains much more siltstone and shale. It is composed of medium-grained sandstone bodies that display trough and planar cross-bedding (up to 1 metre in thickness) and scoured basal surfaces. Lateral accretion surfaces are present with palaeoflow means of 40^0 and 180^0. The palaeocurrent directions of the main sandstone bodies are 150^0 and 50^0 (See section III-3 for discussion of palaeocurrents). The sandstone bodies are continuous for up to 100 to 160 metres, but eventually grade laterally into shales, siltstones and coal stringers.

Interpretation

The Teapot Member of the Mesaverde Formation can be interpreted as a fluvial system. It consists of three distinct units with different combinations and scales of stacking pattern. In general, the grain size in each unit decreases upwards. The basal and top units (facies association 9A) represent sandy braided systems with channels and bars; floodplain deposits are not abundant. Facies association 9B represents a broad channelised system containing lateral accretion surfaces orthogonal to the main palaeoflow orientation. The latter sandstone bodies have low lateral extent and are associated with abundant shale and sandstone. This facies association is interpreted as a meandering fluvial system with point bar deposits within an extensive floodplain (Table III-Fa 9A and 9B).

Facies association	Lithology	Texture Sorting	Physical structure	Biogenic structure	Depositional environment	Section (metres)
FA 1	Grey mudstone, very-fine grained reddish sandstone.	Claystone to very fine grained.	Wavy, parallel and low angle-planar-lamination, climbing ripples, hummocky cross-stratification. Sharp bases. Sole marks at bases. Coarsening-upward sequences.	Trace fossils: *"Ophiomorpha nodosa"*.	Shelf-lower shoreface environments.	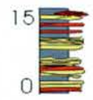
FA 2	Sandstone. minor mudstone.	Very-fine grained; claystone.	Swaley cross-stratification; flat lamination. Internal convolution and decimetre-scale intraclasts. Undulating upper and lower surface. Centimetre thick layers of mudstone. Well-cemented sandstones with hummocky cross-stratification. Pebble lags. At top oscillatory and climbing ripples. Fluid-escape features.	Trace fossil *"Ophiomorpha nodosa"*. *"Inoceramus"* shell fragments. Sharks teeth. Vertebrate bone fragments.	Middle shoreface deposits. Delta-front, prodelta environments. Slump deposits.	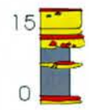
FA 3	Sandstone, minor mudstone drapes along reactivations surfaces.	Claystone to very-fine sandstone.	Multistorey to single storey channelised deposits. Massive, but some bidirectional palaeocurrent indicators. Pebble lags and slump deposits.	Trace fossil *"Ophiomorpha nodosa"* at top, and at base *"Teredolites.*	Tidally influenced fluvial channels (estuarine)	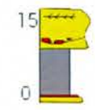
FA 4	Sandstone, coal, carbonaceous mudstones.	Very fine grained. Claystone.	Trough cross-lamination; herringbone cross-lamination and high-angle flat lamination dipping landward. Turncation surfaces. Wave ripples.	Wood fragments. Vertical trace fossils. Shell fragments. Macerated organic debris.	Upper shoreface; beach and backshore environments.	
FA 5	Mudstones, coals, siltstones and sandstones.	Fine grained; claystone.	Lateral-accretion surfaces; basal lag of silty pebbles. Symmetrical and asymetrical ripples. Tidal bundles. Carbonaceous mudstones interbedded with siltstones. Sandstone/shale ratios: 1-1.8.	Root traces. Plant leaves. Macerated organic debris. Trace fossil *"Teredolites"*.	Delta plain (distal) environment with distributaries, swamps and marshes. Wave and tidal influence (distal distributary).	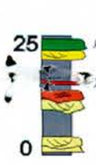
FA 6	Sandstones.	Fine- to medium fine grained.	Coarsening-upward sequences. Massive to low-angle parallel laminated. Scoured bases and lenticular in shape. Symmetrical and combined-flow ripple lamination.	Rare burrows. Carbonaceous debris abundant.	Distributary mouth bar.	
FA 7	Mudstones, siltstones and sandstones.	Claystone to fine-grained.	Trough cross-bedding; scoured bases; lateral-accretion surfaces. Sandstone bodies with sharp bases and tops. Current ripples. Coarsening-upward cycles on m. to 10's of m scales. Carbonaceous mudstones interbedded with thin laminated siltstones.Sandstone/shale ratios: 1-1.3	Plant remains. Plant leaves.	Meandering trunk channel; Crevasse complexes; Soils and floodplain deposits.	
FA 8	Mudstone, coals, siltstone and sandstone bodies.	Very fine to fine-grained sandstones.	Ribbon-like sandstone geometries; well-cemented sandstones with climbing ripples, flat tops and bases. Carbonaceous mudstones abundant. Sandstone/shale ratios: 0.5-0.7	Wood fragments. Carbonaceous debris. Root traces. Tree trunks.	Anastomosed fluvial system and floodplain deposits.	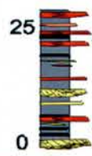
FA 9	Sandstones, with sparse mudstones and coal layers.	Fine to coarse grained; pebbles at some localities.	Fining-upward trends. 3 distinct units: A) Amalgamated, trough cross-bedded sandstone. B) Trough and planar cross-bedded sandstone with large-scale lateral accretion surfaces. C) Amalgamated trough cross-bedded sandstone with variable palaeocurrents.	Root traces. Logs. Wood fragments. Plant remains. Tree trunks.	A) Sandy braided system. B) Meandering fluvial system. C) Braided fluvial system, with higher degree of sinuosity.	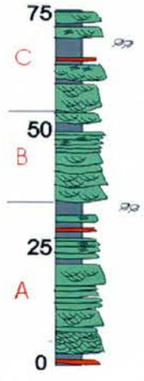

Table III-1: Summary of facies associations for the Mesaverde Formation.

III-3. PALAEOCURRENTS

Palaeocurrents have been measured based on trough cross-bedding, planar cross-bedding, current ripples, wave ripples and flutes. The main palaeocurrent indicator measured in the channelised and shoreface deposits is trough-cross bedding and the rosettes for these deposits are predominantly based on this sedimentary structure. Observations of bidirectional palaeocurrents were made, but due to the smaller number of one of the directions, the rosette plots do not show the two trends clearly in some cases. However, palaeocurrent values and type of sedimentary structure with stratigraphic position are listed in Appendix 2.

In this section, palaeocurrent trends are explained for each of the facies associations previously cited. In chapter IV the palaeocurrent trends of the facies in the different locations refer back to this section.

III-3.1 CODY FORMATION

The main palaeocurrent indicator found in the Cody Formation is trough cross-bedding from facies association 3, with bidirectional trends between ~110^0 and ~320^0 (Figure III-7A) in the Maverick Springs area. In the area of Alkali Butte (Figure III-1), a small number of palaeocurrents have been measured in sedimentary structures from facies associations which are interpreted as shelf to lower and middle shoreface deposits. The palaeocurrent indicators, which are trough cross-bedding and herringbone cross-stratification, display an along shore (south to north) and oblique offshore (~120^0) transport direction (Figure III-7B). Therefore, the Cody Formation deposits from the two different areas appear to represent different palaeocurrent trends, which can be interpreted as the predominance of shelf versus deltaic-tidal processes operating in the two areas.

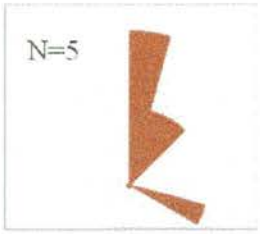

B) Palaeocurrents from trough cross-bedding in facies association 2 (middle and lower shoreface deposits).

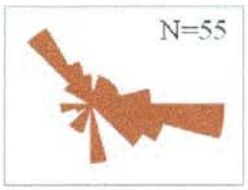

A) Palaeocurrents from trough cross-bedding in facies association 3 (channelised deposits with bidirectional indicators).

Figure III-7: A) Palaeocurrents from the upper part of the Cody Formation in Maverick Springs area; B) Palaeocurrents from the top sandstones of the Cody Formation in Alkali Butte area. See Figure III-1 for locations.

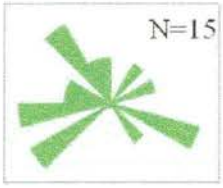

C) Palaeocurrents from trough cross-bedding from facies association 4 in Castle Gardens area (upper shoreface deposits).

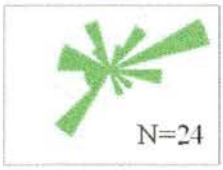

B) Palaeocurrents from trough cross-bedding from facies association 4 in the area of Alkali Butte (upper shoreface deposits).

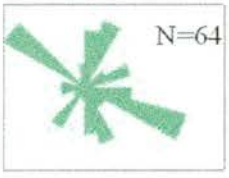

A) Palaeocurrents from trough cross-bedding from facies association 4 in Maverick Springs area (upper shoreface deposits).

Figure III-8: A) Palaeocurrents obtained for the Basal Member in Maverick Springs area; B) Palaeocurrents for the first sandstone representing the Mesaverde rocks in Alkali Butte area; C) Palaeocurrents for the first sandstone representing the Mesaverde Formation in Castle Gardens area. See Figure III-1 for locations.

Alternatively, the palaeocurrents could represent different paleoshorelines if the Cody-Mesaverde contact is becoming younger towards the center of the basin.

III-3.2 MESAVERDE FORMATION

The Basal Member of the Mesaverde Formation (facies association 4) has mainly trough, herringbone and planar cross-stratification. It has been said previously that the base of the Mesaverde is placed where the first marine-influenced to littoral deposit appears. This deposit is represented as facies association 4 in all localities, although changes in thickness and palaeocurrents trends are observed. In the area of Maverick Springs (Figure III-1), the dominant trends are 115^0 and 280^0 (Figure III-8A), measured from trough and herringbone cross-bedding indicators. Therefore, the shoreline can be interpreted as having been orientated approximately northeast to southwest. In the area of Alkali Butte and Castle Gardens the bidirectional nature of the palaeocurrents is also fairly well distinguished (Figure III-8B). The palaeocurrents for the latter locality reflect a wider range of directions, but the dominant directions are ~135^0, 210^0, 260^0 and 372^0 in the area of Castle Gardens (Figure III-8C), and ~40^0 to 205^0 in the area of Alkali Butte (Figure III-8B). The change in palaeocurrent directions from Maverick Springs eastwards could be interpreted as reflecting changes in the direction of the palaeoshoreline, although the wide range of directions and weaker but present tidal indicators, imply a tidally influenced setting.

The palaeocurrents obtained from the Middle Member are mainly from trough cross-bedding observed in channelised deposits (Figure III-9), although some climbing and current ripples were also measured. Climbing ripples from the crevasse complexes (see Appendix 2) show palaeocurrent indicators slightly oblique (~130^0) to the channelised deposits at the same stratigraphic level. Mainly, the three submembers of the Middle Member show a general

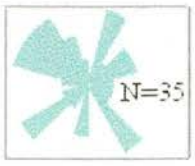

D) Palaeocurrents from trough cross-bedding of channelised deposits of facies association 7 in Alkali Butte area

C) Palaeocurrents from trough cross-bedding of channelised deposits of facies association 7 in Maverick Springs area

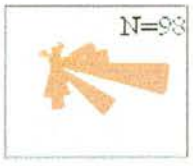

B) Palaeocurrents from trough cross-bedding of channelised deposits of facies association 5 in Maverick Springs area

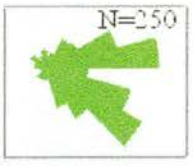

A) Palaeocurrents from trough cross-bedding of channelised deposits of facies association 8 in Maverick Springs area

Figure III-9: A) Palaeocurrents from channelised deposits from the third submember of the Middle Member in Maverick Springs area; B) Palaeocurrents from channelised deposits from the first submember of the Middle Member in Maverick Springs area; C) Palaeocurrents from channelised deposits from the second submember of the Middle Member in Maverick Springs area; D) Palaeocurrents from channelised deposits in Alkali Butte area. See Figure III-1 for locations.

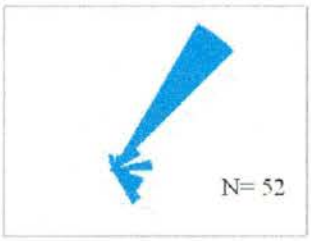

C) Palaeocurrents from trough cross-bedding of channelised deposits of facies association 7 in Maverick Springs area

B) Palaeocurrents from trough cross-bedding of channelised deposits of facies association 5 in Maverick Springs area

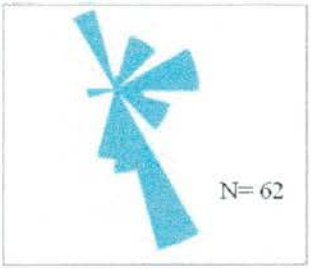

A) Palaeocurrents fromtrough cross-bedding in channelised sandstone bodies from the lower subunit of the Teapot Member.

Figure III-10: Palaeocurrents from the Teapot Member in Maverick Springs area.

southeastern trend, although the first (Figure III-9A) and second (Figure III-9B) submembers at Maverick Springs display wider ranges of directions (~170^0 to 60^0) than the third one (Figure III-9C) which shows a much more dominant trend towards 150^0. The bidirectional indicators of the middle submember are present but not abundant (see Appendix 2). However, the channelised deposits present in the Alkali Butte area present a much more clear bidirectional trend of ~150^0 and 340^0 (Figure III-9D) and illustrate the influence of tidal processes in this location.

The Teapot Member, characterised by facies association 9A and B, is composed of a braided fluvial system at its base and top, with palaeocurrent indicators formed mainly by trough cross-bedding (Figure III-10A and 10C) (~170^0 for the lower submember and ~30^0 to 160^0 for the top submember), and a meandering fluvial system with trough cross-bedding indicators of ~50^0 to 130^0 (Figure III-10B) and lateral accretion surfaces migrating orthogonal to those previous directions. The rotation of palaeocurrent trends is displayed well in Figures III-9 and III-10 and illustrates the change from southeasterly directed transport for the Middle Member to northeast transport by the top of the Teapot Member.

III-3.3 SUMMARY OF PALAEOCURRENTS ANALYSIS

- The Cody Formation represented in the northern and southeastern areas represents different environments with changes in palaeocurrent direction: in the northern area the shoreface and channelised deposits have a general trend of 110^0 and 320^0, whereas in the southern areas, the shoreface deposits contain palaeocurrents with an along shore trend (north to south), and an oblique offshore transport direction of 120^0.
- The base of the Mesaverde Formation (placed at the base of the first littoral-marine-influenced deposit) show changes in the direction of the shorelines,

changing from a northeast to southwest orientated one in Maverick Springs area to a more northwest to southeast orientation in Alkali Butte area; a northwest to southeast orientation is observed at Castle Gardens (See Figure III-1 for locations). The wide range of directions imply wave as well as tidal influence in the deposits.

- The palaeocurrent trends of the channelised deposits of the Middle Member in Maverick Springs area show a general southeastern trend with wider range of palaeocurrent directions for the first and second submember, as well as bidirectional indicators for the latter.
- The channelised deposits at Alkali Butte reflect a strong bidirectional pattern, which implies a strong tidal influence for these deposits.
- The palaeocurrents from the Teapot Member reflect a change from the southeastern trend of the Middle Member to a more eastern (and northeastern) transport direction of the Teapot systems. This implies a change of source area possibly related to tectonic events. Reiners et al. (1999) infer an age for the uplift of the Wind River Range (Figure III-1) of ~75 ± 5.3 m.y. based in apatite (U/Th)/He thermochronometry; this date does not correspond to previous studies that date placing the uplift of the Wind River Range as a Tertiary event. This ~75 m.y. age would correspond to the late Campanian (Figure III-2) and approximately with the generation of the unconformity below the Teapot Member. Thus the change of transport directions can be explained by uplift of the Wind River Range in the west of the basin and tilting of the basin towards the east.

III-4 THIN-SECTION ANALYSIS

Thin sections of 126 samples collected from the measured sections and representing the different facies and their inferred palaeoenvironments in the

Mesaverde Formation have been analysed (see Chapter II for description of methodology). The samples vary primarily in the relative abundance of quartz, feldspar, and rock fragments (Table III-2). Carbonate cement is locally abundant. The principal minerals found are quartz (in most of the samples it forms more than 40% and up to 90%), feldspar (trace amounts to a maximum of 6% based on the occurrence of plagioclase and microcline), micas appear in percentages between 0% to 7% (depending on the facies present biotite, muscovite, chlorite, or both biotite and chlorite together), rock fragments (clasts of clay, carbonate, schist, phyllite, and chert can be as much as 24% of the total components) and heavy minerals (appear in some samples in significant amounts of up to 2%). The sandstones range from quartz-arenites to litharenites, subarkoses and subgraywackes. The size, shape, sorting and roundness of the quartz grains vary widely.

Distinction between samples (and therefore facies) can be made based on proportions and presence/absence of matrix, cement and porosity, as well as the framework grains. Matrix appears in percentages between 0% and 30%, with a mean of 22%. It occurs mainly as pseudomatrix (matrix formed after the deposition of the clasts) with kaolinite and illite as the main clay minerals. In some samples, the clay occurs with organic matter and both reduce porosity. In other samples, the matrix is micritic and is locally dissolved thereby generating secondary porosity. Samples representing palaeosols and ponds have percentages of micrite up to 80%. Authigenic glauconite is characteristic of some samples in percentages no higher than 4% and fills voids, thus acting as "matrix". The cement mean is 6% and occurs in four forms: carbonate cements which have Mg-rich calcite and dolomite, iron cement (with a mean of 4%, but in Fe-stones can be as high as 62%) that locally replaces the carbonate cement and some minor

SECTION	SAMPLE	HEIGHT	FACIES	Q	FELD	MICA	S.R.F.	M.R.F.	MATRIX	CEMENT	POROSITY	FE (+)	OM	GLAUCONITE
Mv0	2	2	crevasse	6	0	2	5	0	80	0	3	4	0	0
Mv0	3	18	ch1submember	32	0	3	7	9	25	0	21	2	1	0
Mv0	21	452	ch3submember	28	2	1	4	4	24	13	24	0	0	0
Mv0	3-1 2	392	crevasse	39	2	0	8	0	16	15	9	9	2	0
Mv1	9	20	crevasse	30	0	0	0	0	5	28	20	17	0	0
Mv1	11	90	ch1submember	50	3	1	3	6	23	0	10	0	3	1
Mv1	13	130	crevasse	25	0	2	4	0	0	62	7	0	0	0
Mv1	14	265	crevasse	38	1	1	7	2	22	0	5	21	2	1
Mv1	20	415	ch2submember	55	1	3	10	12	12	3	2	2	0	0
Mv1	21	415	siltstone	10	0	0	3	0	44	0	2	41	0	0
Mv1	22	458	ch3submember	67	1	0	0	10	12	0	7	3	0	0
Mv1	22	455	w Maveric	45	0	0	0	5	31	0	17	1	1	0
Mv1	23	475	sitstone	57	1	0	1	2	12	0	18	4	5	0
Mv1	24	480	tp1	52	0	0	1	2	20	0	21	0	4	0
Mv1	26	480	tp1fr	51	3	0	5	4	18	0	17	0	1	1
Mv2	1	280	w Maverick	54	4	1	0	6	24	0	6	1	3	1
Mv2	4	300	sitstone	36	0	4	5	0	30	6	16	3	0	0
Mv2	6	400	w Maverick	58	0	2	0	5	13	0	11	8	3	0
Mv2	8	435	ch 3 submember	42	2	3	0	7	12	30	0	1	3	0
Mv2	9	445	siltstone	4	0	0	0	0	73	0	6	17	0	0
Mv2	10	460	ch 3 submember	41	4	1	15	5	15	0	16	1	2	0
Mv2	12	515	1tp	28	2	5	0	3	0	0	0	62	0	0
Mv2	13	-30	red-cody	38	0	1	4	0	18	28	11	0	0	0
Mv2	14	-20	y-cody	31	1	4	10	0	25	16	7	2	2	2
Mv2	16	-5	y-cody	34	1	0	1	1	20	23	19	0	0	1
Mv2	17	1	basal	42	3	3	4	5	32	0	9	0	2	0
Mv2	18	5	crevasse	37	2	5	0	6	40	0	4	5	1	0
Mv2	20	20	ch1submember	38	2	0	15	4	6	15	18	2	0	0
Mv2	22	75	ch1submember	43	1	4	3	4	15	23	7	0	0	0
Mv2	23	90	crevasse	43	0	2	6	0	14	0	21	14	0	0
Mv2	25	100	crevasse	61	2	1	8	3	5	17	3	0	0	0

Table III-2

Mv2	26	400	ch2submember	47	2	0	5	5	17	4	15	4	0	1
Mv2	28	220	w Maverick	57	0	1	0	5	19	0	17	1	0	0
Mv2	29	520	1tp	48	3	1	0	1	32	5	8	2	0	0
Mv2	30	520	1tp	53	1	0	2	11	16	1	14	2	0	0
Mv2	31	538	tp2fr	46	1	0	0	4	25	0	22	2	0	0
Mv2	33	538	tp2fr	43	0	2	0	0	29	0	21	2	1	2
Mv2	35	550	2tp	63	3	0	0	8	11	10	4	1	0	0
MV2	S-99	220	w Maverick	39	3	7	3	3	23	0	19	0	1	2
MV3	11	427	crevasse	48	2	5	0	4	33	0	5	0	2	1
Mv5	4	306	crevasse	47	0	0	7	0	25	10	11	0	0	0
Mv5	6	316	ch2submember	50	1	0	9	9	9	10	9	3	0	0
Mv5	10	446	ch3submember	49	0	1	12	4	12	10	7	5	0	0
Mv5	12	536	tp1	51	1	0	4	3	23	0	16	1	1	0
Mv5	17	586	3tp	65	3	1	3	3	8	0	17	0	0	0
Mv5	19	601	3tp	58	2	0	3	0	12	0	20	5	0	0
Mv5	22	6	basal	36	2	2	2	5	4	16	33	0	0	0
Mv5	23	2	basal	40	1	0	0	2	21	0	31	0	5	0
Mv5	27	18	basal	59	1	0	0	7	14	0	19	0	0	0
Mv5	28	36	crevasse	37	5	0	15	7	0	17	12	7	0	0
Mv5	29	42	ch1submember	34	3	1	10	0	19	11	14	4	2	2
Mv5	31	161	ch1submember	41	6	0	3	2	23	14	8	2	1	0
Mv5	32	161	ch 1 submember	67	2	0	1	6	13	1	10	0	0	0
Mv6	6	2	cody	20	0	0	11	0	27	5	37	0	0	0
Mv6	8	22	crevasse	31	1	2	20	4	6	14	20	2	0	0
Mv6	9	12	basal	40	0	8	0	8	22	0	14	2	2	4
Mv6	13	27	crevasse	0	0	0	0	0	100	0	0	0	0	0
Mv6	14	77	ch1submember	41	1	9	0	6	30	0	12	0	1	0
Mv6	17	117	ch2submember	38	4	4	4	3	4	34	7	0	1	1
Mv6	19	497	tp2	45	2	0	0	9	20	0	24	0	0	0
Mv6	20	470	1tp	45	2	4	0	3	29	0	17	0	0	0
Mv6	21	452	1tp	52	4	0	0	7	31	0	5	1	0	0
Mv6	22	377	ch3submember	37	2	1	4	2	31	17	6	0	0	0
Mv6	23	352	crevasse	43	3	0	4	5	1	33	10	1	0	0

Table III-2

Mv6	24	352	ch2submember	42	1	1	14	3	7	18	11	3	0	0
Mv6	25	202	crevasse	52	0	0	9	6	10	10	12	1	0	0
Mv6	26	207	siltstone	8	0	0	0	0	66	0	26	0	0	0
Mv6	27	112	ch2submember	47	0	1	4	5	29	11	3	0	0	0
Mv6	34	15	crevasse	33	0	2	8	3	25	21	4	0	1	3
Mv6	14'	7	ch 1 submember	51	0	3	7	2	23	14	0	0	0	0
Mv6	31	60	crevasse	56	2	0	0	0	31	8	3	0	0	0
Mv7	2	35	ch1submember	19	0	2	2	1	30	0	8	38	0	0
Mv7	3	5	cody	31	1	4	3	1	22	21	16	1	0	0
Mv7	6	10	ch distal	13	0	0	0	0	68	0	13	6	0	0
Mv9	2	0	cody	32	0	1	6	0	21	22	17	1	0	0
Mv9	3	2	base	45	1	0	2	3	24	0	25	0	0	0
Mv9	4	2	base	49	1	0	7	2	21	0	19	0	0	1
Mv9	5	12	ch1submember	39	1	0	7	0	26	12	14	1	0	0
Mv10	1	61	2 shoreface	39	5	2	0	2	21	0	29	1	0	1
Mv10	2	66	2 shoreface	31	3	4	0	6	27	0	28	1	0	0
Mv10	3	81	2 shoreface	32	1	1	3	5	35	0	18	3	2	0
Mv10	8	-14	cody	39	0	0	4	0	29	6	20	1	0	1
Mv10	11	21	base	50	0	1	1	1	26	0	19	0	2	0
Mv10	18	31	distalch	14	0	0	0	0	76	0	0	10	0	0
Mv17	1	1	basal	52	1	0	1	6	17	0	20	1	1	1
Mv17	3	25	2 shoreface	31	0	2	1	5	40	0	15	1	2	3
MV17	4	40	2 shoreface	42	2	2	3	1	29	0	19	0	2	0
Mv17	7	120	ch diistal	48	0	3	0	0	34	0	6	9	0	0
Mv17	8	150	ch distal	30	2	0	5	0	32	0	21	0	6	4
Mv17	9	208	crevasse/flood	43	0	1	15	0	26	0	5	0	8	2
Mv17	10	216	crev/flood	37	3	2	1	1	12	27	15	0	2	0
Mv17	12	326	ch distal	42	1	0	0	4	22	0	26	2	2	1
Mv18	3	23	RE MV?	55	0	1	0	2	10	0	32	0	0	0
Mv18	6	40	shoreface	54	0	1	0	0	9	0	18	14	4	0
Mv19	1	38	shoreface	46	0	0	1	3	29	0	19	0	0	2
Mv20	1	5	redtopflood	40	1	2	1	1	27	0	25	0	1	2
Mv20	5	117	crevasse	48	0	1	7	1	16	10	10	0	4	3

Table III-2

Mv20	7	145	ch distal	42	0	1	9	4	20	0	20	0	1	3
Mv20	10	170	ch distal	39	0	2	1	0	26	0	26	2	0	4
Mv20	9	165	siltstone	41	0	0	3	2	4	0	12	38	0	0
Mv22	2	6	basal	51	2	0	0	2	17	0	28	0	0	0
Mv22	2	25	ch distal	39	1	0	11	4	0	0	20	15	10	0
Mv26	1	5	cody	31	2	1	8	0	34	6	16	0	0	3
Mv26	2	13	ch distal	20	0	0	2	0	61	0	3	9	5	0
Mv26	5	126	1 tp	49	0	4	1	4	36	0	5	0	1	0
Mv26	6	130	2 tp	50	0	0	3	5	19	0	21	0	2	0

Table III-2: Point counting results from the thin section analysis

percentages (less than 1%) of syntaxial quartz cement. In some samples, the iron cement was precipitated prior to the formation of matrix. These observations correspond to those made by Shapurji (1978) and Pryor (1961) on Mesaverde rocks in Wyoming.

Porosity is mainly secondary and is both intergranular (by dissolution of the matrix) and, in some cases, intragranular (formed by dissolution of clay and carbonate clasts). There are samples where the porosity is intercrystalline, as a result of dissolution of the cement. Fracture porosity occurs in 5 samples. Primary porosity has been destroyed by cementation or by precipitation of matrix. The porosity ranges between a mean of 14% and a maximum of 28% of the total components of the samples (some samples present porosity contents up to 36% but this is due to problems during the thin-section preparation).

III-4.1. QUALITATIVE ANALYSIS

A qualitative classification of the samples into different categories was constructed. The criteria used to separate the samples was based on the presence or absence of the main components. Primarily, it was based on the presence of matrix and/or cement (Table III-3 and III-4) and then on:

1. presence or absence of carbonate clasts;
2. presence or absence of chert clasts;
3. presence or absence of glauconite;
4. very low content of clasts and abundant matrix;

Based on these criteria, some generalisations can be made about the samples representing different palaeoenvironments. The main characterisations obtained are:

- The samples representing sandstones from the Cody Formation have the same composition: they have carbonate cement in percentages ranging

SECTION	SAMPLE	HEIGHT	FACIES	Q	FELD	MICA	S.R.F	M.R.F.	MATRIX	CEMENT	POROSITY	FE (+)	OM	GLAUCONITE
	CEMENT	NO MATRIX	S.R.F.	M.R.F.	NO GLAUCONITE									
Mv5	28	36	crevasse	37	5	0	15	7	0	17	12	7	0	0
Mv1	13	130	crevasse	25	0	2	4	0	0	62	7	0	0	0
	CEMENT	**MATRIX**	**NO S.R.F.**	**NO M.R.F.**		**NO GLAUCONITE**								
Mv1	9	20	crevasse	30	0	0	0	0	5	28	20	17	0	0
Mv6	31	60	crevasse	56	2	0	0	0	31	8	3	0	0	0
	CEMENT	**MATRIX**	**NO S.R.F.**	**M.R.F.**	**NO GLAUCONITE**									
Mv2	29	520	1tp	48	3	1	0	1	32	5	8	2	0	0
Mv2	35	550	2tp	63	3	0	0	8	11	10	4	1	0	0
Mv2	8	435	ch 3 submember	42	2	3	0	7	12	30	0	1	3	0
	CEMENT	**MATRIX**	**S.R.F.**	**NO M.R.F.**		**NO GLAUCONITE**								
Mv9	5	12	ch1submember	39	1	0	7	0	26	12	14	1	0	0
Mv2	13	-30	cody	38	0	1	4	0	18	28	11	0	0	0
Mv9	2	0	cody	32	0	1	6	0	21	22	17	1	0	0
Mv6	6	2	cody	20	0	0	11	0	27	5	37	0	0	0
Mv5	4	306	crevasse	47	0	0	7	0	25	10	11	0	0	0
Mv0	3-1 2	392	crevasse	39	2	0	8	0	16	15	9	9	2	0
Mv2	4	300	sitstone	36	0	4	5	0	30	6	16	3	0	0
	CEMENT	**MATRIX**	**S.R.F.**	**NO M.R.F.**		**GLAUCONITE**								
Mv5	29	42	ch1submember	34	3	1	10	0	19	11	14	4	2	2
Mv10	8	-14	cody	39	0	0	4	0	29	6	20	1	0	1
Mv2	14	-20	cody	31	1	4	10	0	25	16	7	2	2	2
Mv26	1	5	cody	31	2	1	8	0	34	6	16	0	0	3
	CEMENT	**MATRIX**	**S.R.F.**	**M.R.F.**	**NO GLAUCONITE**									
Mv2	30	520	1tp	53	1	0	2	11	16	1	14	2	0	0
Mv5	22	6	basal	36	2	2	2	5	4	16	33	0	0	0
Mv5	32	161	ch1submember	67	2	0	1	6	13	1	10	0	0	0
Mv5	31	161	ch1submember	41	6	0	3	2	23	14	8	2	1	0
Mv6	14'	7	ch1submember	51	0	3	7	2	23	14	0	0	0	0
Mv2	22	75	ch1submember	43	1	4	3	4	15	23	7	0	0	0
Mv2	20	20	ch1submember	38	2	0	15	4	6	15	18	2	0	0
Mv5	6	316	ch2submember	50	1	0	9	9	9	10	9	3	0	0
Mv6	22	377	ch3submember	37	2	1	4	2	31	17	6	0	0	0

Table III-3

Mv6	24	352	ch3submember	42	1	1	14	3	7	18	11	3	0	0
Mv0	21	452	ch3submember	28	2	1	4	4	24	13	24	0	0	0
Mv5	10	446	ch3submember	49	0	1	12	4	12	10	7	5	0	0
Mv6	27	112	ch3submember	47	0	1	4	5	29	11	3	0	0	0
Mv1	20	415	ch3submember	55	1	3	10	12	12	3	2	2	0	0
Mv7	3	5	cody	31	1	4	3	1	22	21	16	1	0	0
Mv17	10	216	crev/flood	37	3	2	1	1	12	27	15	0	2	0
Mv2	25	100	crevasse	61	2	1	8	3	5	17	3	0	0	0
Mv6	8	22	crevasse	31	1	2	20	4	6	14	20	2	0	0
Mv6	23	352	crevasse	43	3	0	4	5	1	33	10	1	0	0
Mv6	25	202	crevasse	52	0	0	9	6	10	10	12	1	0	0
	CEMENT	**MATRIX**	**S.R.F.**	**M.R.F.**	**GLAUCONITE**									
Mv6	17	117	ch2submember	38	4	4	4	3	4	34	7	0	1	1
Mv2	26	400	ch2submember	47	2	0	5	5	17	4	15	4	0	1
Mv20	5	117	crevasse	48	0	1	7	1	16	10	10	0	4	3
Mv6	34	15	crevasse	33	0	2	8	3	25	21	4	0	1	3
Mv2	16	-5	y-cody	34	1	0	1	1	20	23	19	0	0	1

Table III-3: Samples with carbonate cement as a component

SECTION	SAMPLE	HEIGHT	FACIES	Q	FELD	MICA	S.R.F	M.R.F.	MATRIX	CEMENT	POROSITY	FE (+)	OM	GLAUCONITE
	MATRIX	**NO S.R.F.**	**NO M.R.F.**	**NO GLAUCONITE**										
Mv17	7	120	ch distal	48	0	3	0	0	34	0	6	9	0	0
Mv7	6	10	ch distal	13	0	0	0	0	68	0	13	6	0	0
Mv10	18	31	ch distal	14	0	0	0	0	76	0	0	10	0	0
Mv6	13	27	crevasse	0	0	0	0	0	100	0	0	0	0	0
Mv18	6	40	shoreface	54	0	1	0	0	9	0	18	14	4	0
Mv2	9	445	siltstone	4	0	0	0	0	73	0	6	17	0	0
Mv6	26	207	siltstone	8	0	0	0	0	66	0	26	0	0	0
	MATRIX	**NO S.R.F.**	**NO M.R.F.**	**GLAUCONITE**										
Mv2	33	538	2 tp fr	43	0	2	0	0	29	0	21	2	1	2
	MATRIX	**NO S.R.F.**	**M.R.F.**	**NO GLAUCONITE**										
Mv2	12	515	1tp	28	2	5	0	3	0	0	0	62	0	0
Mv6	20	470	1tp	45	2	4	0	3	29	0	17	0	0	0
Mv6	21	452	1tp	52	4	0	0	7	31	0	5	1	0	0
Mv6	19	497	2 tp	45	2	0	0	9	20	0	24	0	0	0
Mv2	31	538	2 tp	46	1	0	0	4	25	0	22	2	0	0
Mv5	23	2	basal	40	1	0	0	2	21	0	31	0	5	0
Mv22	2	6	basal	51	2	0	0	2	17	0	28	0	0	0
Mv5	27	18	basal	59	1	0	0	7	14	0	19	0	0	0
Mv6	14	77	ch1submember	41	1	9	0	6	30	0	12	0	1	0
Mv1	22	458	ch3submember	67	1	0	0	10	12	0	7	3	0	0
Mv2	18	5	crevasse	37	2	5	0	6	40	0	4	5	1	0
Mv18	3	23	RE MV?	55	0	1	0	2	10	0	32	0	0	0
Mv10	2	66	shoreface 2	31	3	4	0	6	27	0	28	1	0	0
Mv1	22	455	w Maveric	45	0	0	0	5	31	0	17	1	1	0
Mv2	6	400	w Maverick	58	0	2	0	5	13	0	11	8	3	0
Mv2	28	220	w Maverick	57	0	1	0	5	19	0	17	1	0	0
	MATRIX	**NO S.R.F.**	**M.R.F.**	**GLAUCONITE**										
Mv6	9	12	basal	40	0	8	0	8	22	0	14	2	2	4
Mv17	12	326	ch distal	42	1	0	0	4	22	0	26	2	2	1
MV3	11	427	crevasse	48	2	5	0	4	33	0	5	0	2	1

Table III-4

Mv10	1	61	shoreface 2	39	5	2	0	2	21	0	29	1	0	1
Mv2	1	280	w Maverick	54	4	1	0	6	24	0	6	1	3	1
	MATRIX	**S.R.F.**	**NO M.R.F.**	**NO GLAUCONITE**										
Mv5	19	601	3tp	58	2	0	3	0	12	0	20	5	0	0
Mv26	2	13	ch distal	20	0	0	2	0	61	0	3	9	5	0
Mv0	2	2	crevasse	6	0	2	5	0	80	0	3	4	0	0
Mv2	23	90	crevasse	43	0	2	6	0	14	0	21	14	0	0
Mv1	21	415	siltstone	10	0	0	3	0	44	0	2	41	0	0
	MATRIX	**S.R.F.**	**NO M.R.F.**	**GLAUCONITE**										
Mv17	9	208	crevasse/flood	43	0	1	15	0	26	0	5	0	8	2
Mv20	10	170	ch distal	39	0	2	1	0	26	0	26	2	0	4
Mv17	8	150	ch distal	30	2	0	5	0	32	0	21	0	6	4
	MATRIX	**S.R.F.**	**M.R.F.**	**NO GLAUCONITE**										
Mv22	2	25	ch distal	39	1	0	11	4	0	0	20	15	10	0
Mv1	24	480	1 tp	52	0	0	1	2	20	0	21	0	4	0
Mv5	12	536	1 tp	51	1	0	4	3	23	0	16	1	1	0
Mv26	5	126	1 tp	49	0	4	1	4	36	0	5	0	1	0
Mv26	6	130	2 tp	50	0	0	3	5	19	0	21	0	2	0
Mv5	17	586	3tp	65	3	1	3	3	8	0	17	0	0	0
Mv2	17	1	basal	42	3	3	4	5	32	0	9	0	2	0
Mv10	11	21	base	50	0	1	1	1	26	0	19	0	2	0
Mv9	3	2	base	45	1	0	2	3	24	0	25	0	0	0
Mv2	10	460	ch 3 submember	41	4	1	15	5	15	0	16	1	2	0
Mv7	2	35	ch1submember	19	0	2	2	1	30	0	8	38	0	0
Mv0	3	18	ch1submember	32	0	3	7	9	25	0	21	2	1	0
MV17	4	40	shoreface 2	42	2	2	3	1	29	0	19	0	2	0
Mv10	3	81	shoreface 2	32	1	1	3	5	35	0	18	3	2	0
Mv20	9	165	siltstone	41	0	0	3	2	4	0	12	38	0	0
Mv1	23	475	sitstone	57	1	0	1	2	12	0	18	4	5	0
	MATRIX	**S.R.F.**	**M.R.F.**	**GLAUCONITE**										
Mv1	26	480	1 tp fr	51	3	0	5	4	18	0	17	0	1	1
Mv17	1	1	basal	52	1	0	1	6	17	0	20	1	1	1
Mv9	4	2	base	49	1	0	7	2	21	0	19	0	0	1

TableIII-4

Mv20	7	145	ch distal	42	0	1	9	4	20	0	20	0	1	3
Mv1	11	90	ch1submember	50	3	1	3	6	23	0	10	0	3	1
Mv1	14	265	crevasse	38	1	1	7	2	22	0	5	21	2	1
Mv20	1	5	redtopflood	40	1	2	1	1	27	0	25	0	1	2
Mv19	1	38	shoreface	46	0	0	1	3	29	0	19	0	0	2
Mv17	3	25	shoreface 2	31	0	2	1	5	40	0	15	1	2	3
MV2	S-99	220	w Maverick	39	3	7	3	3	23	0	19	0	1	2

Table III-4: Point counting results. Samples having carbonate cement and matrix as components

from 5 to 28%; matrix content is always higher than 10% with a maximum value of 34%; they contain 1-11% of sedimentary rock fragments (note that no metamorphic or igneous rock fragments were observed); all the samples have glauconite, although the content is very low (between 1-3%); porosity ranges from 7-28% with the mean around 15%. None of the samples have organic matter and iron cement is absent or in very low proportions.

- Samples with both carbonate cement and matrix represent either samples from the Cody Formation or channelised and/or crevasse splay deposits from the Middle Member of the Mesaverde Formation.
- There is a correspondence between the presence/absence of sedimentary or metamorphic/igneous rock fragments in channelised deposits and crevasse deposits of the Mesaverde Formation relative to stratigraphic height. The content of both types of rock fragments decrease upwards.
- The samples representing marine-influenced environments, distal channels and shorefaces in the south and southeastern parts of the basin (these units were defined as the Unnamed Middle Member by Barwin, 1961), as well as the base of the Mesaverde Formation, very rarely (two samples) have carbonate cement. They also have variable amounts of sedimentary and metamorphic/igneous rock fragments.
- Samples representing distributary channelised deposits in the south and southeastern areas do not contain metamorphic or chert fragments.
- The samples representing mouth bar deposits of the Middle Member do not have carbonate cement. They can contain glauconite.

- Samples representing siltstones from floodplain deposits in the Middle Member do not have carbonate cement or glauconite.
- Generally, the samples from the Teapot Member do not have carbonate cement (three exceptions) or glauconite (two exceptions).

Plotting the results of the point counting analysis into ternary diagrams (Figure III-11) shows that, although samples representing similar environments appear grouped for some areas, no clear distinction is made between environments of deposition. Thus, apart from the aforementioned generalisations, various facies can not be readily discriminated using ternary diagrams which implies the rocks have shared similar provenance histories.

III-4.2. STATISTICAL ANALYSIS

Statistical analysis of the point counting results was conducted in order to quantitatively and objectively determine (a) the petrographic characterisation of the different facies and (b) changes related to stratigraphic position in the sections. This resulted in separating the samples based on composition. The analysis was made using the software package MINITAB 10. A data matrix was constructed of *n* samples by *m* variables and the analysis attempts to resolve if the *n* samples are related to the *m* variables (Walden and Smith, 1995). To examine many variables simultaneously, multivariate methods are necessary and the method chosen is Factor analysis. This method attempts to reduce the dimensionality of the problem by looking for the underlying trends within the data (for example, establishing if several variables are highly correlated). Therefore, factor analysis tends to discern simplifying relationships, although interpretations can only be made based on knowledge of the geological system (Swan et al., 1995). The principle of this method is that the total variation in the dataset can be represented by a small number of geological "factors", each

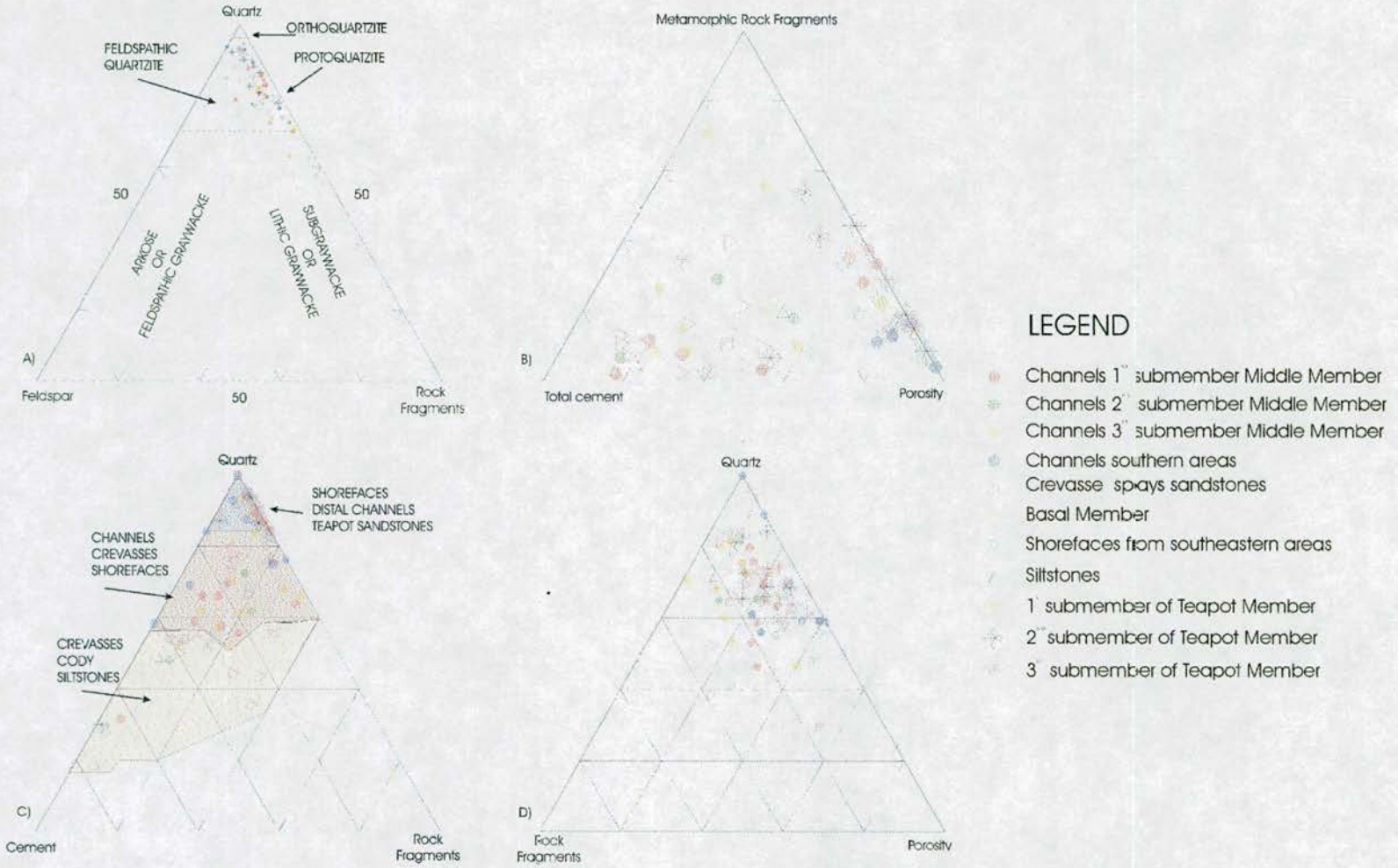

Figure III-11: Ternary diagrams of the point counting results: A) Quartz, feldspar, rock fragments; B) Metamorphic rock fragments, total cement and porosity; C) Quartz, cement and rock fragments; D) Quatz, rock fragments and porosity. See Figure III-1 for locations.

manifested in a degree of correlation in the data scatter. Therefore, factors are chosen so as to maximise the correlation between the original variables and then transforming the original variables into a smaller number of mutually uncorrelated underlying factors (Walden and Smith, 1995). The number of factors chosen for this study has been 2. More factors could be chosen, but enough discrimination are obtained with two.

Each of the factors occupies a set of mutually orthogonal axes in a multidimensional factor space. There are also "factor loadings" for each of the original variables on each of the new factors. The size of each of these factor loadings is related to the amount of variance of each variable represented by each individual factor. Variables that plot in close proximity are generally highly correlated (Walden and Smith, 1995).

The original data requires a transformation because numerical values based on observations of different variables range widely from variable to variable. In this case, quartz is the main component in most samples thereby generating a difference between the scale of the variables used in the study. The values are transformed so that the quartz content does not have an undue weighting influence with respect to the other components of the samples. After this transformation, no clear separations were found between samples. The next transformation made for this study was to divide the values of each variable by the highest value observed for that variable. Therefore, the different variables have been normalised. Following transformation, meaningful similarity coefficients between samples can be calculated.

Figure III-12 shows (A) the loading of the components for all the samples and (B) the result of the factor analysis. Factor 1, in this case, is formed by the direct correlation of quartz, feldspar, metamorphic and sedimentary rock

fragments. More weakly correlated with these variables are the content of carbonate cement and the amount of porosity. Characterising this factor is the negative loading generated by the content of matrix, and then the weakly correlated content of glauconite, organic matter, mica and iron cement. Factor two is characterised by the positive loadings of porosity, organic matter and glauconite, with weak correlation to matrix and quartz and the negative loadings of both types of cement, with weaker correlation to the content of rock fragments, feldspar and mica. Figure III-12-B illustrates that three separations are obtained with some samples located away from the general clustering trends. These are:

(1) the marine-influenced deposits (basal member of the Mesaverde Formation, mouth bars of the Middle Member, shoreface deposits of the south and southeastern parts of the basin) appear grouped with values of Factor 1 ranging from –1 to 1 and values of Factor 2 ranging between 0 and 2 and the correlation is generally positive;

(2) the Cody Formation sandstones appear clearly separated from the marine-influenced sandstones of the Mesaverde Formation, showing values of Factor 1 between –1 and 0, and Factor 2 between –1 and 1. Again, the correlation is positive. These characteristics imply that the separation between marine-influenced sandstones of the Mesaverde Formation and the marine sandstones of the Cody Formation are due to the comparative low values of Factor 1 and Factor 2. That is explained by the cement content in the Cody samples, the complete lack of cement in the samples representing Mesaverde marine-influenced sandstones, as well as the low content of rock fragments

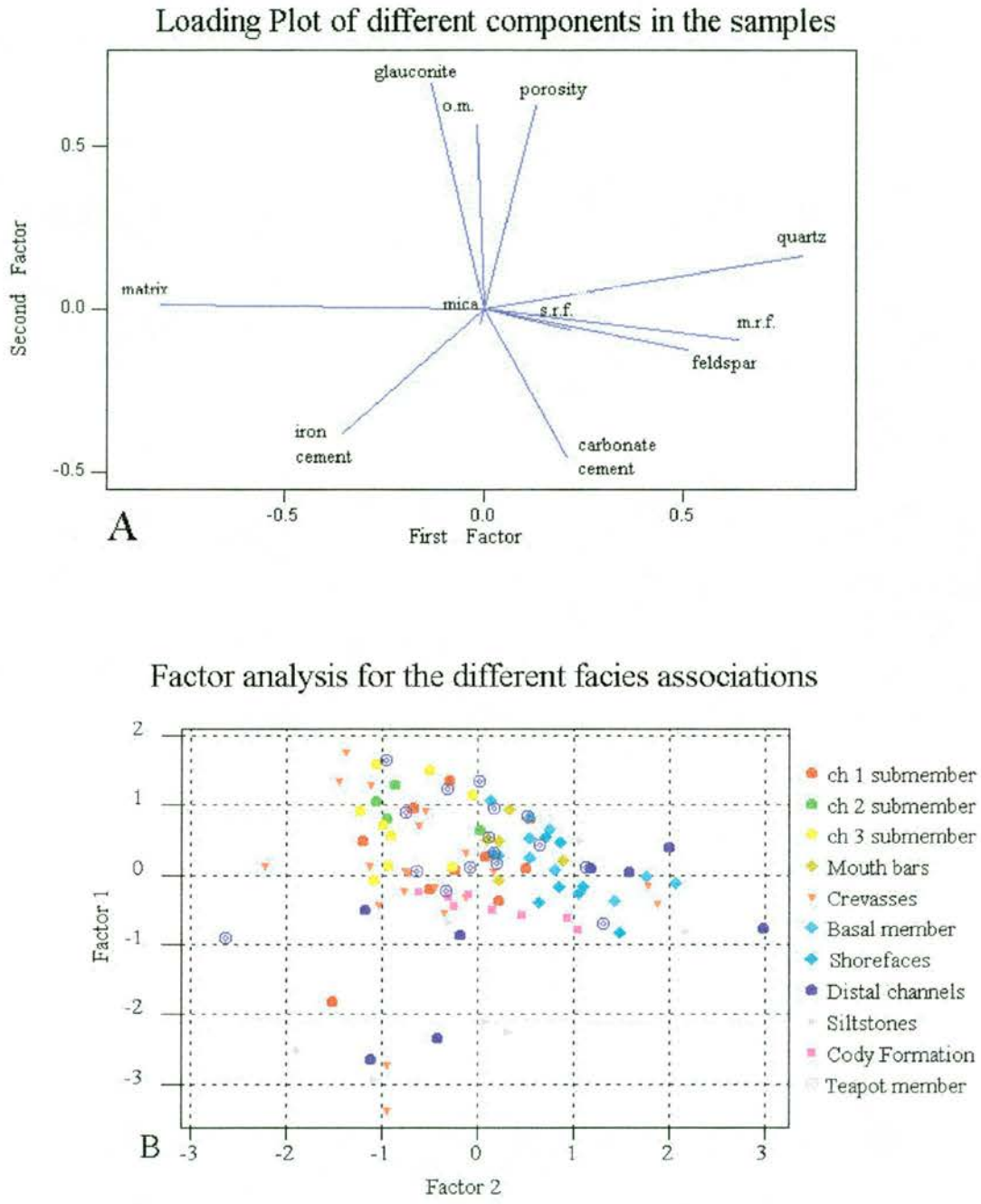

Figure III-12: A) Factor loadings for the variables taken into account in the statistical analysis of all the samples (s.r.f.: sedimentary rock fragments; m.r.f.: metamorphic rock fragments; o.m.: organic matter); B) Results of the factor analysis (ch: channelised deposits). Legend for figures III-12, 13 and 14: Ch 1 submember: channelised deposits of the first submember of the Middle member; Ch 2 submember: channelised deposits of the second submember of the Middle Member; Ch 3 submember: channelised deposits of the third submember of the Middle Member; Distal channels: Channelised deposits from the Middle Member in the southeastern parts of the basin. Cody Formation: sandstones from the upper part of the Cody Formation. Teapot Member: sandstones from the Teapot Member

for the Cody Formation samples relative to their higher proportion in the Mesaverde Samples;

(3) the other clustering of the samples is formed by channelised deposits which have positive values of Factor 1 (0 and 2) and negative values of Factor 2 (around –1), reflecting mainly the content and amount of matrix present in the sample and lack of carbonate cement. The main difference between the channelised deposits of the Mesaverde Formation and the Cody sandstones is the content of iron cement, being higher for the channelised deposits.

By separating the main facies into individual factor analyses, these conclusions can be furthered tested and several observations and interpretations are made. The factor analysis for the channelised deposits (Figure III-13) shows that channels from distal parts of the basin can be separated from the rest based on their lack of quartz, feldspar, carbonate cement and rock fragments, although both Factors have a broad dispersal pattern. Looking at the composition of the samples, it is observed that another difference between the distal channels and the rest of the channelised deposits is the higher content of organic matter in the former. The rest of the channelised deposits appear grouped in areas with positive Factors 1 and 2.

Plotting the marine-influenced deposits (Figure III-14) shows a clear distinction between the Cody and Mesaverde sandstones due to differences in cement and rock fragments content. The difference in rock fragment content increases in the Mesaverde Formation and suggests that the Cody and Mesaverde Formations may have different provenances.

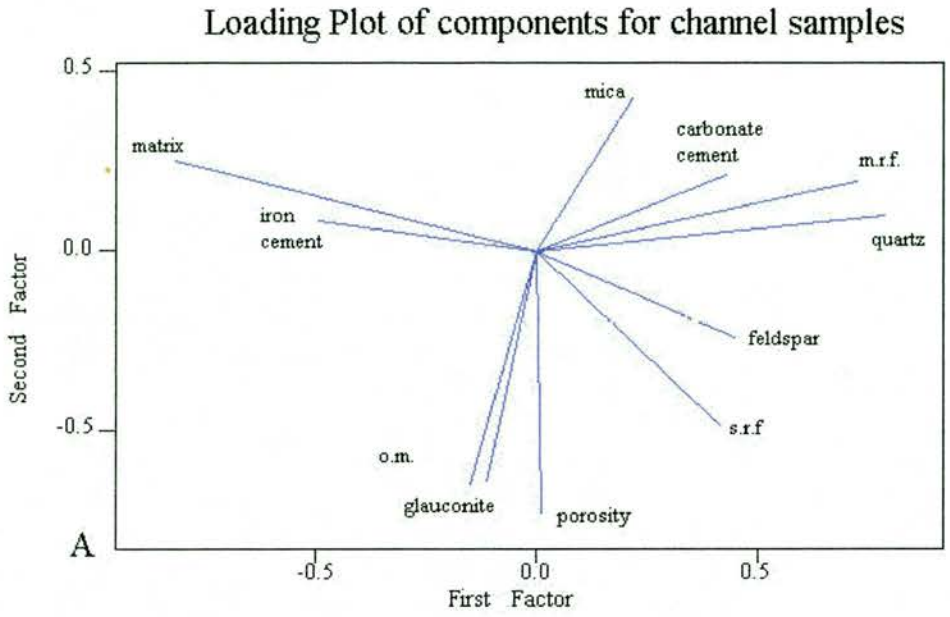

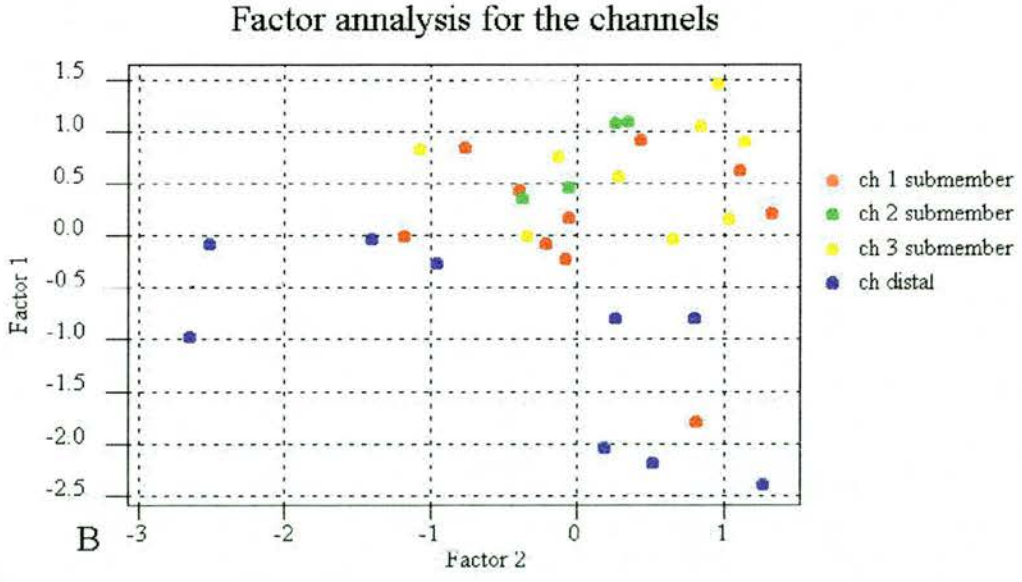

Figure III-13: A) Factor loadings for the samples representing channelised deposits (s.r.f.: sedimentary rock fragments; m.r.f.: metamorphic rock fragments; o.m.: organic matter); B) Results of the factor analysis (ch: channelised deposits from the Middle Member in Maverick Springs area). See Figure III-1 for location.

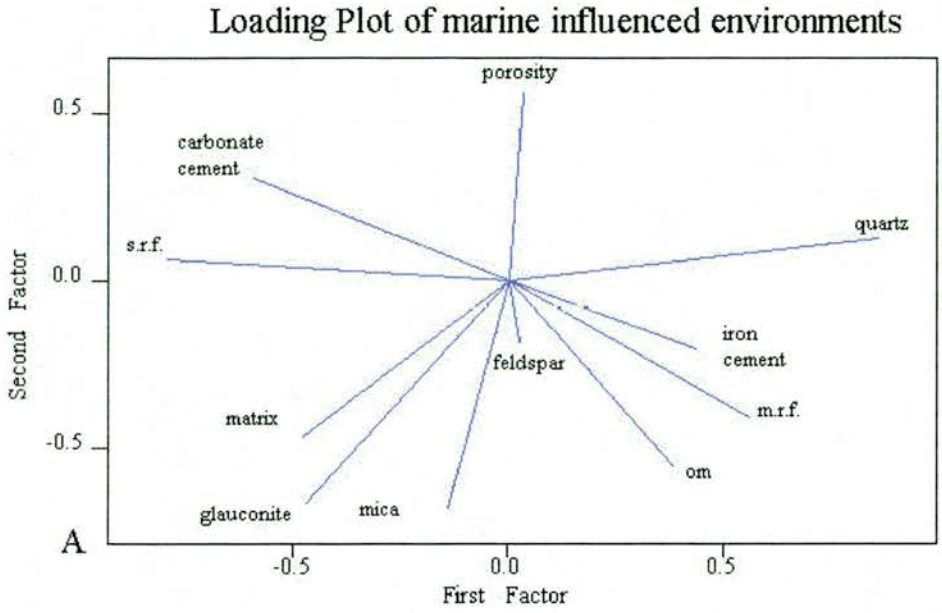

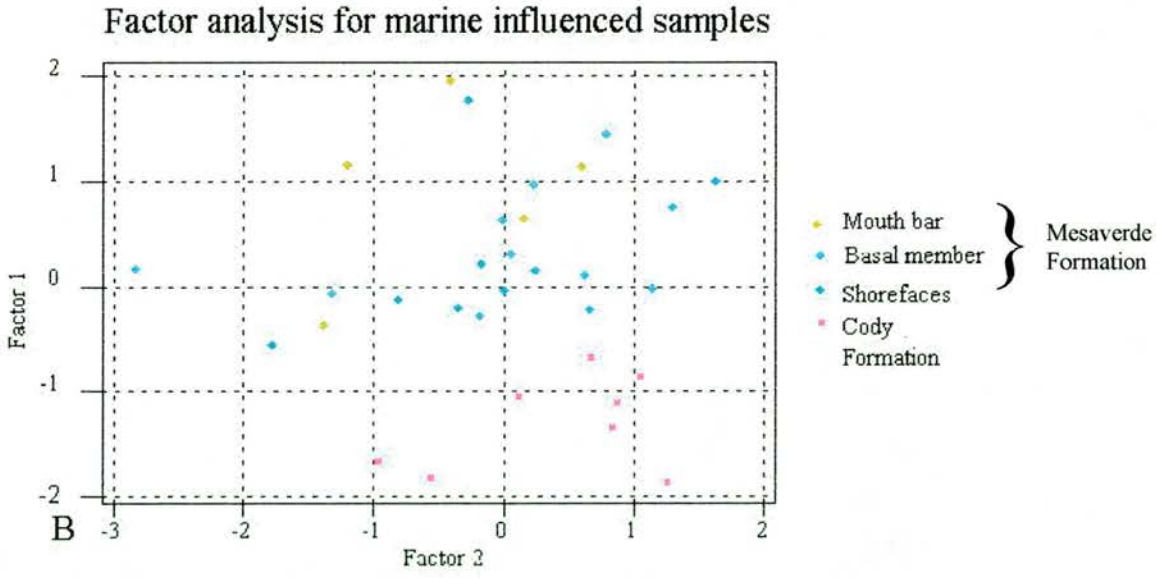

Figure III-14: A) Factor loadings for the samples representing marine environments (s.r.f.: sedimentary rock fragments; m.r.f.: metamorphic rock fragments; o.m.: organic matter); B) Results of the factor analysis.

III-4.3. XRF/XRD ANALYSIS.

The thin-section analysis presented some complications. Some of the mineral species were not easy to discriminate and supportive evidence was required for the composition of matrix and cement. Two techniques (XRD and XRF analysis) are useful for determining the composition of carbonate cement, the discrimination between cement and clays like illite, or the composition of the iron cement. It also produces quantitative results that were compared to the ones obtained by the thin section analysis.

X-Ray Diffraction (XRD) is a technique used mainly for the analysis of fine-grained material, which is difficult to study in thin-section analysis. First of all, the sample is reduced in grain size to a mean particle diameter of 5-10μm. Quartering is then done to obtain a representative sample. The sample is then taken, analysed and a graph is obtained with the diffractometer traces of the different minerals present in the sample. The graph of Figure III-15 shows two axes: the x-axis represents the 2θ angle characteristic of each mineral, and the y-axis represents the intensity of the diffracted peak above background. Because all minerals are crystalline, they posses a unique X-ray diffraction pattern. Quantitative analysis can be done by XRD because the intensity of the diffraction pattern of a mineral in a mixture is proportional to its concentration, so it is possible to make estimations of the relative proportions of the mineral in a sample by measuring their relative peak heights or areas. With this, XRD provides the most efficient method for the determination of clay minerals in sedimentary rocks.

Twelve representative samples of the Mesaverde Formation were chosen for XRD analysis in order to characterise them geochemically. These were picked because they are representative samples from different stratigraphic

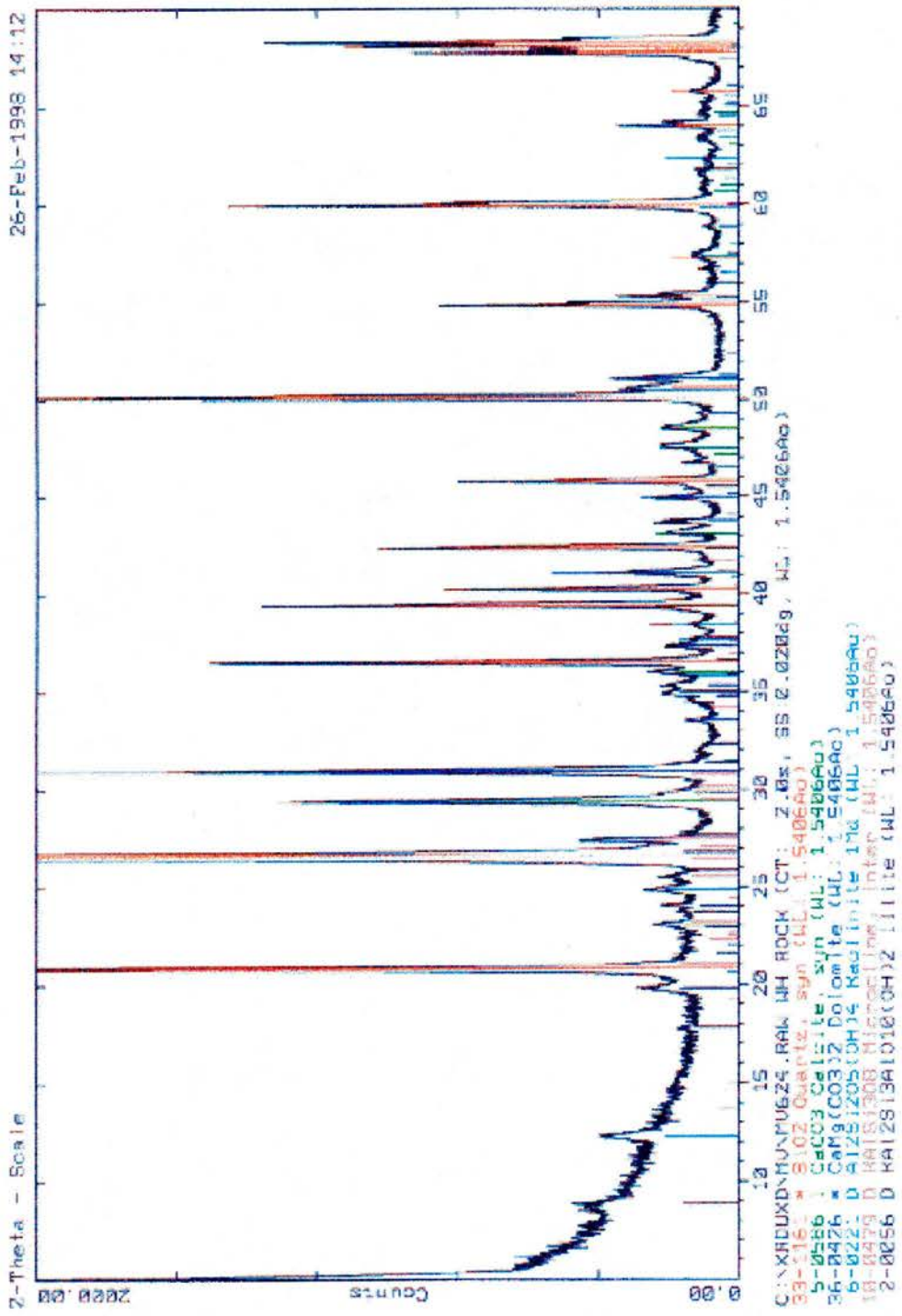

Figure III-15: XRD analysis performed in sample Mv6 24 channelised sandstone deposit from the Middle member in Maverick Springs area). See Figure III-1 for location.

positions and geographic localities of the Mesaverde Formation. They were also samples that presented problems in the identification of the mineral species. The results (Table III-5) show that the main component of all the samples is quartz and that separation of samples can be based on the presence or absence of carbonate clasts or calcite/dolomite cement. The appearance of microcline as the dominant feldspar present, as well as the appearance of illite and kaolinite as clay minerals correspond to the results obtained from the thin-section analysis. Samples were studied because Mv2-29 and Mv2-30 are from the same sandstone from the Teapot Member, except that Mv2-30 is from a highly fractured locality. As can be seen in Table III-5, no significant differences were found although the percentages of cement, illite and kaolinite are lower for the fractured sandstones.

SAMPLE	QUARTZ	CALCITE	DOLOMITE	KAOLINITE	ILLITE	MICROCLINE	PYRITE	GOETHITE	JAROSITE	HEMATITE
MV1 20	75	2	5	5	4	8	1			
MV1 23	87			3	3	3			2	2
MV2 29	86			6	5	3				
MV2 30	91			3	2	4				
MV2 9	17	57	13	4	4	2	1			2
MV5 12	88	1		5	3	3				
MV5 22	77	7	3	6	4	3				
MV5 27	89			5	3	3				
MV5 32	84			8	4	4				
MV6 13	20	51	7	3	4	3		12		
MV6 23	53	28	8	4	3	4				
MV6 24	71	6	11	5	2	5				

Table III-5: Results of the XRD analysis for samples of the Mesaverde Formation. Results are given in weight percentages.

Samples Mv1-20, Mv2-9 and Mv6-13 represent siltstone deposits characterised as ponds and poorly developed palaeosols. The latter two samples have the least amount of quartz than the samples representing other environments and they have the highest amount of carbonate, which is present in the micritic matrix. Sample Mv5-22 is a sample from the Cody Formation and Mv5-27 and Mv5-32 are samples from the basal and mouth-bar deposits of the Mesaverde Formation. The results correspond to those obtained from the thin-section

analysis, highlighting the carbonate content of the Cody Formation and the lack of carbonate content in the two marine-influenced deposits (see section III-4.1. in this chapter). Samples Mv6-23 and Mv6-24 represent a crevasse and a channelised sandstones, respectively, and contain lower amounts of quartz and are grouped in the thin-section analysis as having carbonate cement present. Note the considerably higher calcite content in the crevasse samples.

X-Ray Fluorescence analysis (XRF) is a technique used in hard-rock petrology, but it is also used for the whole-rock analysis of mudrocks. The principle behind this technique is that when a sample is bombarded with high energy X-rays, particular wavelengths and intensities are given off the sample dependent on the elements present. Measurement of the intensity of the characteristic radiation for a particular element gives a value reflecting its concentration in the sample. This technique is ideal for the determination of major and minor elements, such as Si, Al, Mg, Ca, Fe, K, Na, Ti, S and P.

SAMPLE	SiO_2	TiO_2	Al_2O_3	Fe_2O_3	MnO	MgO	CaO	Na_2O	K_2O	P_2O_5	PLoos	Total
MV3	81.86	0.49	8.99	1.03	0	0.64	0.47	0.42	2.17	0.05	3.60	99.72
MV5 20	65.66	0.75	18.86	1.10	0.01	0.44	0.41	0.41	0.80	0.06	10.70	99.36
MV014	48.25	0.34	6.79	7.36	0.21	3.64	13.23	0.39	1.46	0.18	18.00	99.85
MV39	56.29	0.49	11.39	3.15	0.04	4.50	6.39	0.65	2.65	0.24	13.90	99.69
MV3 12	80.32	0.52	9.84	1.06	0.01	0.51	0.42	0.45	1.93	0.04	4.30	99.40
MV28	80.74	0.48	9.05	1.61	0.02	0.74	0.15	0.50	1.72	0.06	4.10	99.17
MV55	72.45	.053	12.99	2.15	0.01	1.15	0.45	0.52	2.45	0.05	7.00	99.75
MV1 61	63.56	.058	15.19	2.82	0.02	2.06	1.76	0.56	2.98	0.11	10.10	99.74
MV29	19.19	0.19	3.96	3.88	0.65	3.45	35.19	0.20	1.06	0.28	32.7.	100.7
MV09	62.74	0.61	22.32	0.59	0.01	0.33	0.72	0.71	1.27	0.06	10.10	99.46

Table III-6: Results of the XRF analysis of some samples of the Mesaverde Formation. Results in weight percentages.

III-4.5. PROVENANCE OF THE MESAVERDE SEDIMENTS

The composition of the Mesaverde sediments indicates that sedimentary terranes supplied most of the material. Chert is present in almost all samples which implies that limestones or other chert-bearing rocks were also supplying sediments throughout Mesaverde time. Quartz was derived from source areas

containing both igneous and metamorphic rocks and these latter two increased in proportion from Cody to Mesaverde time. The contrast in size and roundness of the quartz grains indicates mixing of material by addition of "new" quartz to a recycled suite. This supports the inference that, in part, Mesaverde sandstones represent reworking of older sandstones (Eardley, 1951; Pryor, 1961). No traces of volcanic-derived clasts were observed in the Mesaverde rocks of the study area. This implies that no volcanic terranes contributed to sediment infilling in the Wind River Basin during Mesaverde time. This is intriguing because the equivalent strata in the Bighorn and Powder River Basins have abundant volcanic detritus, most notably, the Ardmore bentonite (Roberts and Kirschbaum, 1995).

III-4.6. DIAGENETIC HISTORY

Studying the packing of grains, contacts between clasts, cements, matrix and porosities, a diagenetic sequence of events for each of the samples has been established. It is observed that different samples can be grouped depending on the order of these events. Based on this, the samples are grouped into three main categories of diagenetic "histories":

(A) Diagenetic history 1: The samples that correspond to this history are representative of the Cody Formation and crevasse splay deposits from the Middle Member of the Mesaverde Formation. These samples are characterised by the presence of carbonate cement surrounding grains of quartz, rock fragments and micas. Some of the grains and portions of cement are dissolved and replaced by kaolinitic matrix, that is itself dissolved later. Some of the samples, especially the Cody samples, have iron cement coating grains. Not all the samples retain evidence for every step of this diagenetic history, but in general, it can be described as follows:

1. Deposition
2. Precipitation of carbonate cement
3. Compaction
4. Dissolution of grains and cement
5. Formation of matrix
6. Dissolution of matrix and generation of secondary porosity
7. Filling of porosity by some organic matter
8. Precipitation of iron cement

(B) Diagenetic history 2: This diagenetic history is recorded in samples representing channelised deposits from the lower submember of the Middle Member of the Mesaverde Formation. The main characteristic they show is the appearance of iron coating around grains and the precipitation of clay matrix around this cement.

1. Deposition
2. Precipitation of iron coating on some grains
3. Formation of clay matrix
4. Dissolution of matrix and generation
5. Filling of porosity by organic matter (in some samples)

C) Diagenetic history 3: The samples recording this diagenetic history are those from the Basal Member (including upper shoreface deposits and shoreface deposits from the southern and southeastern parts of the basin), as well as sandstones from the lower submember of the Middle Member representing distal channelised deposits and Teapot Member samples. All these samples represent rocks which are white in colour, do not have carbonate cement and display very low content of clay matrix.

1. Deposition

2. Precipitation of micrite
3. Dissolution of micrite forming primary porosity
4. Formation of kaolinite occluding some of the secondary porosity
5. Precipitation of iron cement

III-4.7. CONCLUSIONS OBTAINED FROM THE THIN SECTION AND XRD/XRF ANALYSES

The analysis of thin sections, XRD and XRF has lead to the determination of the main composition of sandstones and shales. The statistical analysis leads to the discrimination of several characteristic relationships based on the correlations between the components of the individual samples. The main conclusions are:

1. Sandstones are quartz-arenites, litharenites and subarkoses. A few subgreywackes are also present.
2. The main components of the sandstones are quartz, micas, rock fragments, matrix, cement and porosity, and those components were obtained in both the thin section analysis as well as in the XRD/XRF analyses.
3. The main clay minerals present are kaolinite and illite, both acting as pseudomatrix filling porosity.
4. The cement present in most of the samples is calcite, but samples representing the Cody Formation, ponds from swamp areas of the floodplain of the first submember of the Middle Member, as well as crevasse and channelised deposits of the same submember present dolomite cement.
5. The porosity of most of the samples is secondary and can be either intra- or inter-crystalline.

6. The basal marine-influenced sandstones of the Mesaverde Formation can be separated from the sandstones of the Cody Formation based on the absence of carbonate cement and presence of rock fragments in the former.
7. There is no clear distinction between the sandstones of the Middle Member and the sandstones of the Teapot Member except that the latter samples display higher black chert rock fragments and lower amounts of cement.
8. Based on the absence of cement and the higher percentage of organic matter, the channelised deposits representing distal distributaries in the south and southeastern parts of the basin can be separated from the distributaries in the northern parts of the basin, which represent more proximal parts of the system and have carbonate cement and lower amounts of organic matter percentages.
9. The source areas for the Mesaverde Formation were to the north-west of Wyoming. The variety of sedimentary, igneous and metamorphic rock fragments and predominance of quartz grains infer a mixed lithology provenance. This is readily attributed to the older sedimentary and crystalline formations throughout that part of the Rocky Mountain region.

Chapter IV

DEPOSITIONAL FRAMEWORK OF THE OUTCROP BELT

IV-1. MAVERICK SPRINGS AREA

Description

Through township and ranges T6N R3W to T6N R3E (inside the Wind River Indian Reservation), the Mesaverde Formation crops out in a series of folds oriented N30W (Figure IV-1). These represent the most northwestern exposures of the formation in the Wind River Basin. The Mesaverde Formation in this area is composed mainly of three distinct members, the Basal, Middle and Teapot (Keefer and Troyer, 1964; Keefer, 1972) (See appendix 2 for measured sections). Below the Mesaverde Formation is the Cody Formation which is characterised by coarsening-upward cycles of facies association 1 followed by lower and middle shoreface deposits of facies association 2 (See Chapter III). By laterally tracing these units, it can be seen that individual shoreface deposits change to lower shoreface or shelf deposits towards the south-east over many hundreds of metres. In the Muddy Creek and Five Mile Creek sections (Figure IV-1: Mv2 and Mv5), the top of the Cody Formation consists of sandstone packages up to 15 metres thick and several hundreds of metres in width. The bases of these packages display scouring and commonly contain lags of rip-up clasts. Many of the packages define channelised deposits that erode the top part of the underlying shoreface deposits (Figure IV-2, 3 and 4). Capping these upper Cody units is the Basal Member of the Mesaverde Formation. It is composed principally of facies association 4 and contains sandstones that are ~5 to ~25 metres in thickness and are amalgamated vertically. Individual sandstones are white-to-grey in colour, locally appear massive but generally exhibit herringbone

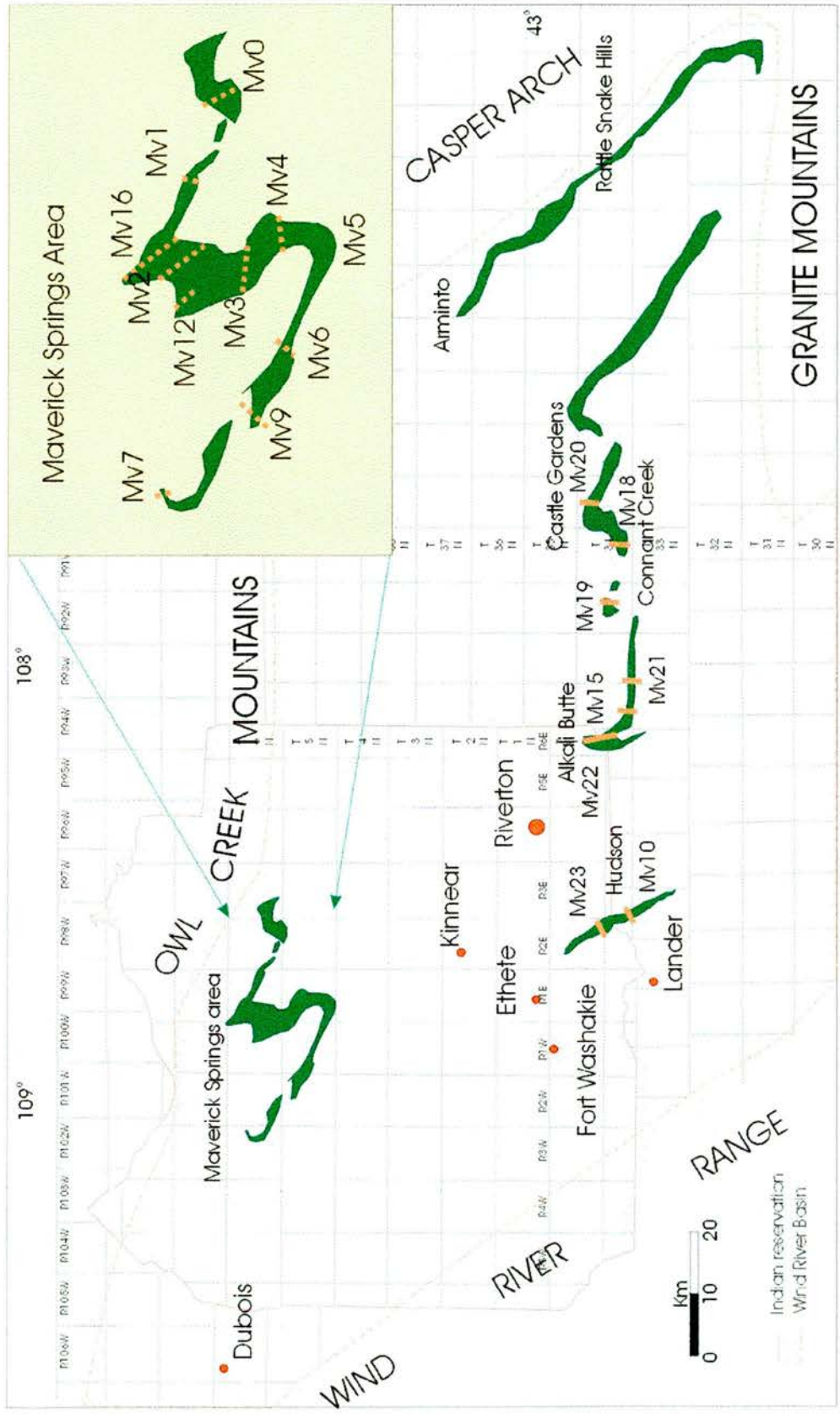

Figure IV-1: Location of the Mesaverde outcrop in the Wind River Basin and position of the measured sections.

cross-stratification, trough cross-bedding and, in places, are heavily burrowed. Although in many places the contact with the underlying Cody Formation appears transitional, careful facies analysis and lateral tracing of contacts reveals that the upper shoreface deposits of the Basal Member of the Mesaverde Formation define a laterally continuous shallow-marine sandstone body that everywhere rests erosionally upon and sharply truncates the underlying middle and lower shoreface deposits of the Cody Formation. Thus, the Basal Member is genetically unrelated to the Cody Formation and is interpreted as a regional sequence boundary (Figure IV-2 and 3). The Basal Member is typically between 5 and 25 metres thick in the Maverick Springs area and everywhere displays a sharp upper contact with overlying coals and/or carbonaceous shales.

The contact between the coals and carbonaceous shales (which overlie the Basal Member) and the rest of the Middle Member of the Mesaverde Formation appears transitional, although in some places distributary channel sandstones erode into the coal-carbonaceous shale and onto the white sandstones of the Basal Member. The Middle Member ranges in thickness from 442 metres in the west to 520 metres in the northeast. It is composed of decametre-scale cycles ranging from 26 to 66 metres in thickness (Figure IV-4). These cycles begin with sandstones that are between 1 to 20 metres thick and internally consist of thick tabular and trough (cut-and-fill) cross-stratified cosets and several decimetres in thickness. The sandstones have erosional bases that cut into underlying finer-grained beds and locally contain lags of mudstone rip-ups and plant material. Soft-sediment deformation structures are common in the lower part of the sandstone bodies and sandstone tops commonly display rooting. Above the sandstones are siltstone-shale intervals that grade upward into organic-rich

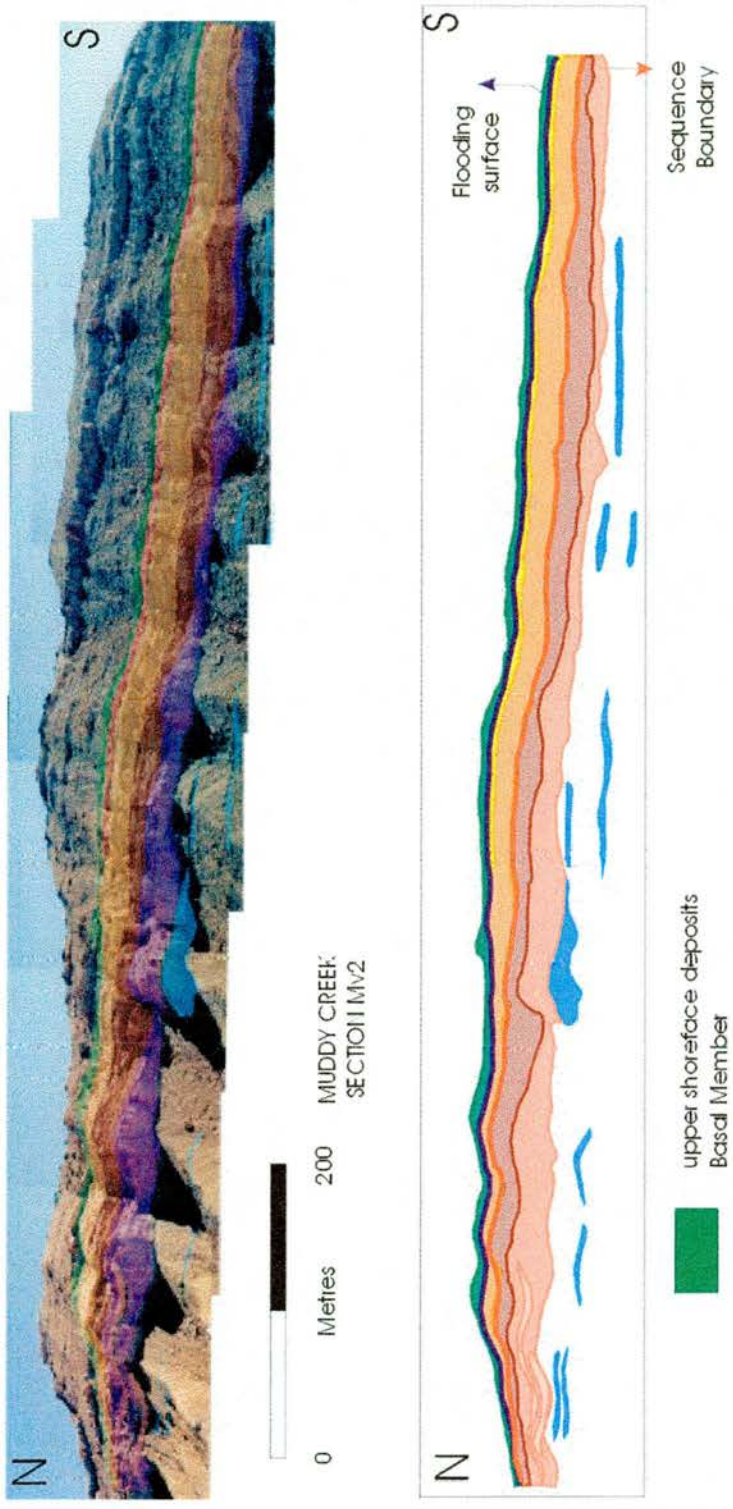

Figure IV-2: Contact between the Cody and mesaverde Formations, Muddy Creek section (Mv2)

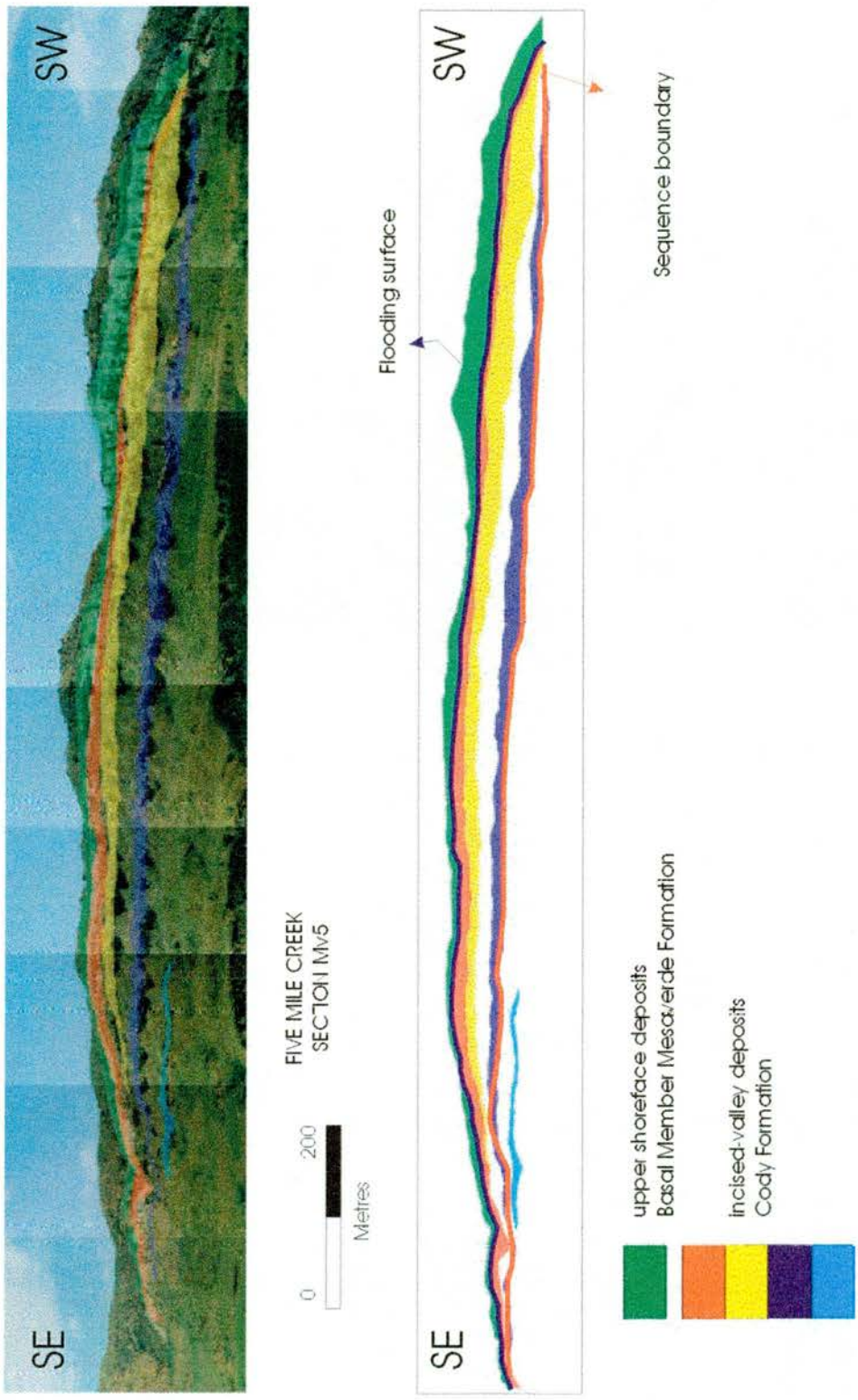

Figure IV-3: Contact between the Cody and Mesaverde Formations in Five Mile Creek section (Mv5)

mudstones and/or coal. Isolated within these shales and siltstones are thinner sandstone bodies which are lenticular in shape. They range from 4 to 60 metres in width and no more than 5 metres in thickness. Palaeocurrent data averages 130^0 (N=25) and is slightly oblique to that obtained from the thicker sandstone bodies, which average 160^0 (N=40). Siltstones typically form lenticular lenses, are orange in colour and usually are no more than 1 metre thick. In some places they contain plant material. Shales are mostly covered, although below large channel complexes, better exposed outcrops display an alternation of brown and black shales. The black interval shows higher content of organic matter. Coals are common at the top of these shale intervals, but vary considerably between areas. In the more southerly "distal" parts of the Maverick Springs area, such as Mv5 (Five Mile Creek section; see Figure VI-1) coals are more abundant but thinner relative to more northerly "proximal" sections, such as Mv2 (Muddy Creek section; see Figure VI-1), where the coals are less abundant but up to 1 metre thick. Commonly interbedded within these finer-grained intervals are thinner sandstones, less than 1 metre thick, that are very well cemented with internal climbing ripples, characterised by flat tops and bases. The tops of those sandstones can locally be highly rooted.

In general, the Middle Member is organised into three units (Figure IV-4A) and these can be correlated between all the sections (see measured sections in appendix 2 and 3). The lower unit is characterised by thinner (<30 metres) cycles that have greater sandstone/shale ratios, typically 1 to 1.8. Coal beds are common and can be up to 1 metre in thickness. The unit overall coarsens upward (facies association 5). The middle unit (Figure IV-4B) thins from 126 metres in the northeast to 50 metres in the west. It differs from the underlying unit by

having sandstone/shale ratios of 1 to 1.3 and contains fewer and thinner coals. It denotes the start of another coarsening upward cycle. The upper unit (Figure IV-4C) differs markedly to the other two. It ranges between 78 to 170 metres in thickness and is characterised by successions (typically less than 60 metres in thickness) which show a general fining upwards tendency. The sandstone/shale ratio is much lower, ranging from 0.5 to 0.7. Shales and coals are more abundant towards the south-west (Section Mv5). The regional correlation of the three submembers of the Middle Member and the change in shale content leads to the interpretation of a potential flooding surface between the middle and upper units.

Analysis of channel geometry dimensions also produces a tripartite sub-division of the Middle Member. In submember 1, channelised sandstones are more abundant. They display lateral continuity over distances of hundreds of metres, have high width/thickness relationships and are internally amalgamated. In submember 2, width/thickness relationships decrease, channel sanstones are less abundant and the shale proportion is higher. The upper unit, submember 3, is characterised by amalgamated channel sandstone bodies with the lowest width/thickness relationships (Figure IV-4).

The top member of the Mesaverde Formation in this area is correlative to the Teapot Member recognised in southeastern parts of the basin. The Teapot Member appears to unconformably overlie the Middle Member of the Mesaverde Formation. This inference is supported by: (1) systematic decrease in thickness of the Middle Member towards the northwest; (2) an angular discordance between Teapot and sub-Teapot strata in some localities (e.g.: Arapahoe Ranch Road, Mv1; see Figure IV-1); and 3) decimetre to metre-scale erosional scouring

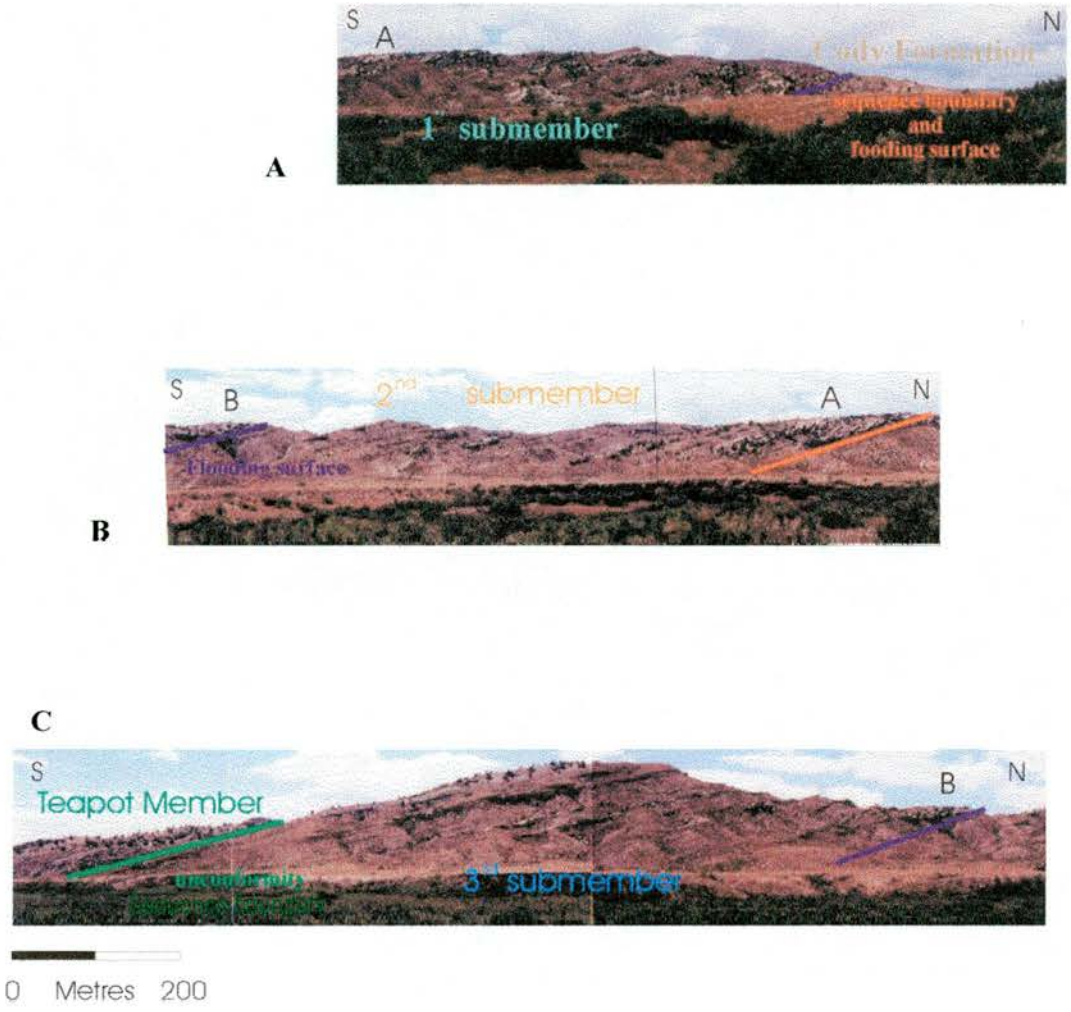

Figure IV-4: Panel with a general view of the Mesaverde Formation in the Maverick Springs area. Notice the differences in the stacking pattern of the channelised deposits, as well as the differences in the amount of sand between the three submembers of the Middle Member.

of the base of the Teapot into the underlying strata of the Middle Member. This surface is therefore interpreted as a regional sequence boundary with regional angular discordance. Everywhere in the Maverick Springs area, the Teapot is composed of three units. The basal unit ranges in thickness from 25 to 30 metres. It consists of fine-to-medium, locally coarse-grained sandstone units of 10 to 20 metre thicknesses with scoured bases. Trough cross-bedding is common and cosets can be up to 8 metres in width and 30 centimetres in thickness. Current and climbing ripples and a characteristic "salt-and-pepper" texture (due to quartz, black chert and dark heavy mineral content) are common. In many places, dark minerals are aligned along bedding surfaces and foresets of cross-bedded units. The trough cross-bedded cosets are amalgamated and palaeocurrent data show very little dispersal with indicators towards the southeast (see Chapter III.3). Basal rip-ups, iron concretions, bioturbation, rooting, and plant material, such as tree trunks in channel bases, are common. Grain size decreases upwards in many of the sandstone bodies, but overall trends in grain size are not well defined. Depending on locality, the sandstones can contain interbedded carbonaceous siltstones, shales, and locally, thin lenticular coal seams. Where present, the siltstone-shale beds range in thickness from 0.5 metre to 1 metre and the contact with the overlying sandstones is commonly erosional. Sandstone/shale ratios range between 3 to 3.5. This unit and overlying units of the Teapot are very friable with low cementation, abundant fracturing and good porosity (15-20 %).

The second unit of the Teapot Member ranges in thickness from 15 to 25 metres. It is marked by a decrease in the sand/shale ratio to between 1.6 to 2.6. Within this unit, sandstone beds are similar to those described previously but are usually 2-3 metres thick and the shale intervals are 0.5 to 1 metre thick. Coals

occur locally, but generally are less than 1m thick. Wedge-shaped units of lateral accretion bedding were observed.

The upper unit displays an increase in shale content and in some places sandstones contain wave ripples. Sandstone/shale ratios vary between 1 and 1.5. In some localities, the Teapot units have a distinctive red-yellow color but no clear differentiation could be seen in thin-section analysis other than a slight increase in the percentage of hematite. Palaeocurrent directions (see chapter III section 3; Figure III-9) show a gradual change of transport direction from the Middle Member to the top of the Teapot (from a southeastern to a northeastern direction).

IV-2. HUDSON AREA

Two sections have been measured in this area (See appendix 2B for measured sections). The sections are only 75 to 90 metres thick due to erosional removal beneath the basal unconformity of the Fort Union Formation. The Cody Formation in the southwestern part of the basin is similar to the Cody Formation in Maverick Springs and Alkali Butte areas with coarsening-upward cycles of vertically and laterally amalgamated sandstone bodies. These bodies are up to 25 metres thick and contain hummocky and swaley cross-stratification with locally distributed vertical burrows and scattered rip-up clasts. These facies are typical of facies association 2.

The lowermost Mesaverde Formation strata (Figure IV-5) can be assigned to facies association 4, i.e, white fine-to-medium sandstone bodies between 3 to 8 metres thick that amalgamate to form a unit as much as 25 metres in thickness. They display decimetre scale trough cross-stratification with palaeocurrent mean directions between 230^0 and 140^0 (Appendix 2) and vertical

burrows are locally common at the tops of beds. Some of the sandstone bodies contain interbedded lenses of organic-rich and carbonaceous shales. Where these occur, root traces can be commonly observed to penetrate downward into the underlying white sandstone. Above the white sandstone unit, interbedded brown shale, siltstones and thin sandstone beds (1 to 3 metres thick) display climbing ripples, trough cross-stratification, soft-sediment deformation, wave ripples (crest orientation is north-south approximately), vertical burrows, shell fragments and scattered rip-up clasts; these strata are part of facies association 5.

This facies succession of thick, white sandstone units of facies association 4 overlain by organic-rich shales and thin sandstones of facies association 5 is stratigraphically repeated over the remaining 25 metres of the section up to the basal unconformity of the Fort Union Formation. Palaeocurrents trends in the upper white sandstones display means between 100^0 and 340^0 (Appendix 2B). Overall the white sandstones thin towards the south and in the northern part of the Hudson outcrop they are absent. At that locality, a 10 metre thick interval of carbonaceous shales interbedded with coal bearing strata and organic-rich siltstone lenses occurs beneath the Fort Union unconformity. As in Maverick Springs area, the contact between the Cody and Mesaverde Formations is interpreted as a flooding surface.

IV-3. ALKALI BUTTE AND CONANT CREEK ANTICLINES

In this area (Figure IV-1) (See appendix 2B for measured sections), the Mesaverde Formation sharply overlies the sandy upper part of the Cody Formation, which is very sand-rich in this area. It displays the characteristics of facies associations 1 and 2. An unnamed marine tongue of Cody (facies association 1) was interpreted to overlie the Mesaverde Formation in Alkali

Butte anticline (Keefer and Rich, 1957; Barwin, 1961). This unnamed unit consists of facies association 1 and is unconformably overlain by beds that are believed to be equivalent to the Lance Formation. The presence of this unit can be attributed to the intertonguing between the "Cody like" and "Mesaverde" lithologies and the extent of erosion at the base of the Lance Formation (Keefer and Rich, 1957; Barwin, 1961). From subsurface data (presented in next chapter), the unnamed Cody tongue pinches out westward several kilometres from Alkali Butte. To the east, it intertongues with the underlying Mesaverde Formation and merges with the sandy member of the Cody Shale in the south central part of the basin.

The Mesaverde Formation in this area (between the Cody Shale and unnamed unit) ranges in thickness from 200 to 300 metres. It consists of a cyclic repetition of basal white to grey, massive to cross-bedded sandstones, typically several metres in thickness (facies association 4), that grade upward into interbedded tan sandstones, siltstones, carbonaceous shales and coal beds (facies association 5) (Figure IV-6). East of Alkali Butte, this part of the Mesaverde Formation thins abruptly to less than 30 metres and intertongues with the Cody Formation. (Figure V-7). This is followed by a succession that ranges from 5 to several tens of metres in thickness that is composed of a number of erosionally based sandstones, with decimetre-scale low-angle trough and planar cross-bedding that commonly display burrows and bi-directional palaeocurrents of ~45^0 and 200^0 (see chapter III, section 3; Figure III-8B). This succession decreases in thickness towards the east where it is replaced by facies association 2, marked by convolute beds (1-2 metres in thickness) and tan-coloured

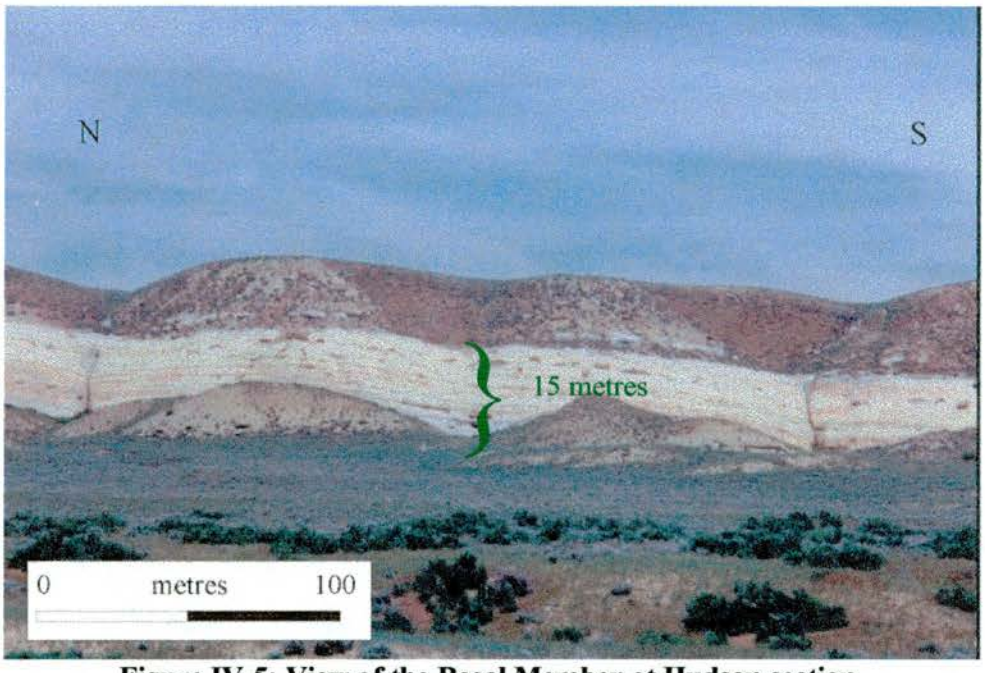

Figure IV-5: View of the Basal Member at Hudson section.

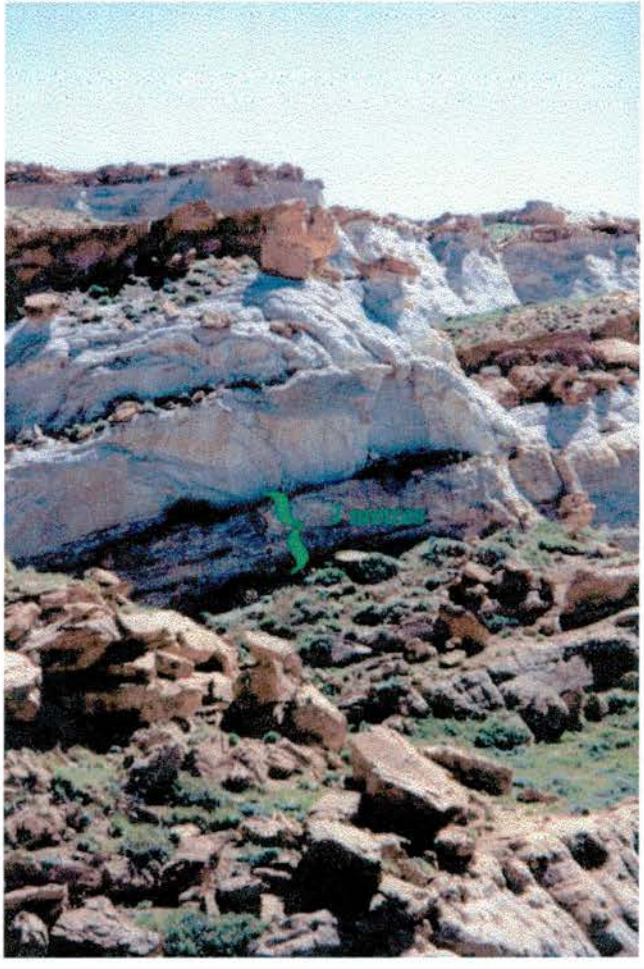

Figure IV-6: View of amalgamated upper shoreface deposits of the Mesaverde Formation at Alkali Butte section.

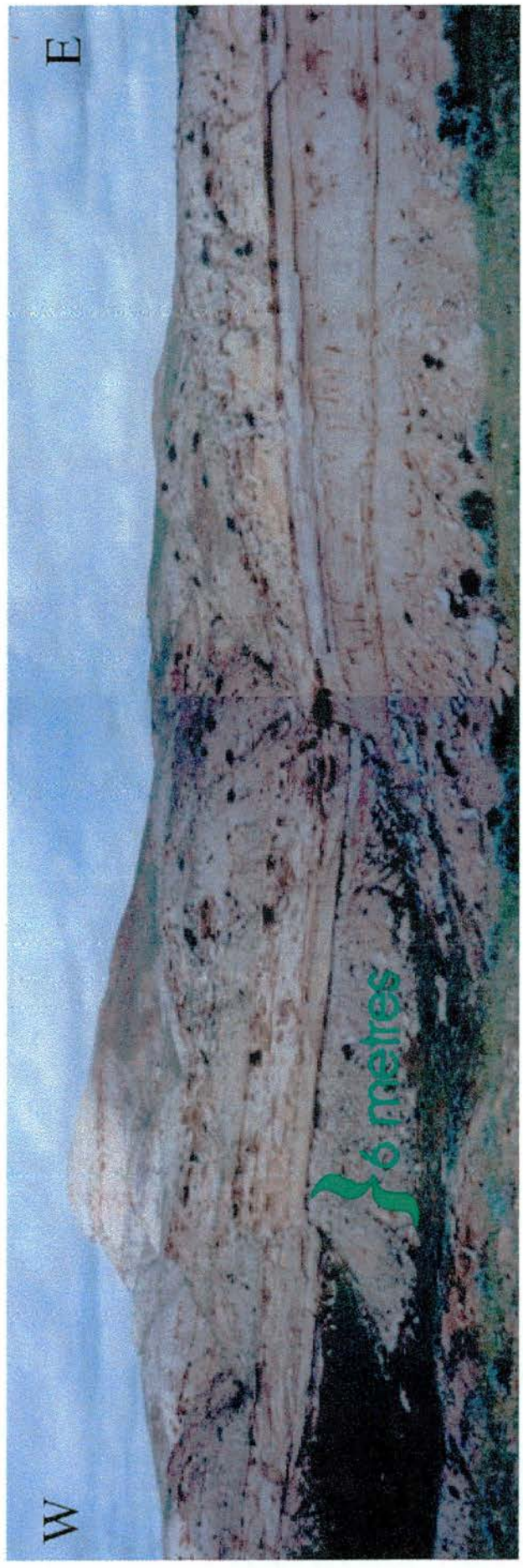

Figure IV-7: General view of the measured section at Alkali Butte. Channelised sandstone from the second submember of the Middle Member at the base, interbedded with carbonaceous shales and coals.

sandstones with swaley and hummocky cross-stratification. Above this, the next cycle begins with another white, massive sandstone body (up to 10 metres in thickness in the southern part of the outcrop belt) overlain by carbonaceous shales, grey sandy shales, coals (some as thick as 2 metres) and thinner sandstone bodies between 2 and 6 metres in thickness. The sandstones amalgamate vertically in some places. Towards the south, these sandstones contain multidirectional palaeocurrents with a western trend (approximately 340^0, 200^0 and 280^0 (N=8); Appendix 2B). The tops of many of these beds are marked by oscillatory wave ripples (6 centimetres height and 10 centimetres wavelength) and vertebrate fragments which occur as thin lags in ripple troughs. Towards the northwest, the cross-bedded sandstones contain abundant plant debris and have erosive bases with rip-up clasts. At Alkali Butte, overlying coals are up to 4 metres thick. These cycles are repeated up to 6 times depending on the locality. Although any facies may be omitted or repeated more regularly, the tan and white sandstones are most frequently repeated in the south-eastern part of the basin, whereas the coal and grey shale interbedded with tan sandstone bodies are less well represented in the northwest. These cyclical facies grade abruptly eastward (towards the east of the Alkali Butte outcrop belt (Figure IV-7) into the offshore marine deposits that are included in the Cody Formation by previous authors, but they are interpreted to represent normal lateral changes to deeper marine conditions in a basinward direction. Chronologically, they are Mesaverde rocks. The contact between the sandy part of the Cody and the Mesaverde Formation appears to be represented at the top of a basinward shift of facies and a flooding surface at the top.

IV-4. CASTLE GARDENS AND DUTTON ANTICLINES

These sections represent the south-eastern part of the Wind River Basin (Figure IV-1) (See appendix 2B for measured sections). From a basinal perspective, these locations are the most "distal" Mesaverde units. Here, the succession consists of the Cody Formation, the Fales Member of the Mesaverde Formation (Keefer and Rich, 1957), the marine Wallace Creek Tongue of the Cody Formation, the middle unnamed member of the Mesaverde Formation, the Teapot Member and the marine Lewis Shale (Chapter III; Figure III-2).

The Cody Formation (facies association 1) in this area is characterised by dark grey, clay-rich shale interbedded with layers less than 1 metre thick of calcareous siltstone, platey sandstones and thin sandstone beds (no thicker than 2 metres) that become more abundant upward. Above this lies the Fales Member of the Mesaverde Formation (Keefer and Rich, 1957). It is composed of three distinct sub-units that show an upward progradational trend (facies association 4). A basal 15 to 25 metre thick unit consists of light grey, fine to medium-grained sandstones that grade laterally into carbonaceous shales and coal beds of up to 1.5 metres thickness (Figure IV-8). Locally, the sandstone is massive but in most places decimetre-scale trough-cross bedding is present and yields palaeocurrent means of 72^0 (N=5), and/or bidirectional indicators of 290^0 and 108^0(N=10) (Appendix 2B). Locally, the tops of beds display reddish staining, pelecypods and vertical burrowing. The degree of amalgamation of the sandstone bodies appear to increase towards the southeast, whereas shales interbedded with coals increase towards the northwest. Above the basal unit is a carbonaceous shale up to 10 metres thick and composed of dark-brown to purplish-black mudstone, lignitic in part, with very fine- to fine-grained carbonaceous

Figure IV-8: General view of the Castle Gardens measured section. Shoreface deposits define the base of the succession (white sandstone bodies) and are overlain by coastal swamp deposits (interbedded coals, shales and sandstones on top of the white sandstones).

sandstones with rooted tops. The third and uppermost unit of interbedded sandstones (up to 1 metre thick), siltstones (typically less than 1 metre thick) and shales and coals (up to 2 metres thick) averages 30 metres in thickness. The contact of the Fales Member with the underlying Cody Formation represents a basinward shift in facies and lends support to the interpretation of a regional sequence boundary between the "Cody-like" lithology (Basal Member and lower submember of the Middle Member in maverick Springs area) and the Mesaverde Formation in this area (correlative to the middle submember of the Middle Member in Maverick Springs area). The contact with the overlying marine Wallace Creek represents a flooding surface. Laterally, towards the northwest, the Fales Member becomes thinner. Thus, the Fales Member of the Mesaverde Formation represents a lowstand wedge bounded by a sequence boundary below and by a fooding surface above. The Wallace Creek Tongue of the Cody Formation (Barwin, 1959, 1961) is composed of 45 metres of grey shale (at Castle Gardens section; see figure IV-1) that becomes dark-grey clay shale towards the east. Locally, this unit can be more arenaceous or silty and becomes interbedded with tan, poorly consolidated sandstone. The thickness of this marine tongue increases towards the southeast where it is considered to completely interfinger with the "Cody-like" deposits. It is considered to represent the base of the Mesaverde Formation in this southeastern part of the basin. Clearly, in a temporal framework, the Wallace Creek Tongue is deposited during Mesaverde time, being Cody Formation in lithological appearance only.

The Middle Member of the Mesaverde Formation (the "unnamed" Middle Member) is represented by interbedded sandstones, shales, siltstones and carbonaceous shales (facies association 5). It sharply overlies the Wallace Creek

Tongue in both the Castle Gardens and Dutton anticline areas (Keefer and Rich, 1957; Barwin, 1961). The thickness of the Middle Member is approximately 75 metres. The basal 5-10 metres contains light grey to buff, very fine- to medium-grained sandstones that gradually thin to the west and become thicker to the south-east. The sandstone typically forms 1 metre thick bodies which display clay rip-ups, vertical burrows and plant remains. Some *Teredolites* burrows appear at the base, as well as oscillatory wave ripples with palaeocurrents of about 344^0 - 164^0 (N≈4), and crest directions of 262^0 and 33^0 (Chapter III, section 3, Figure III-8B)). Higher in the succession, interbedded sandstones, shales and carbonaceous shales occur. The sandstone beds are normally buff to yellowish tan, as much as 5 metres thick, fine- to medium-grained and extremely lenticular. Decimetre-scale trough cross bedding is common and yields palaeocurrent mean directions of 56^0 (N=20), Appendix 2B). Locally well-cemented sandstone beds up to 1 metre in thickness form resistant lenses that are 4 to 30 metres in width and contain trough cross-bedding which displays palaeocurrent means of 33^0 (N=15) (Appendix 2B). Vertebrate bone fragments are common in these sandstones. Siltstone lenses are locally abundant, up to as much as 20 metres in width and no more than 1 metre in thickness, and contain high proportions of plant remains and even wood fragments (facies association 5). The Mesaverde Formation is unconformably overlain by the Lewis Shale. The Teapot Member is reported to be absent in this area (Keefer and Rich, 1957).

IV.5 FLUVIAL STYLE IN THE MESAVERDE FORMATION

In fluvial systems, past studies have mainly focused on the channelised deposits (width/thickness ratios, sedimentary structures, shape, etc.) but fine-grained material, if present, gives information about the behaviour of the

channels and an indication of the evolution of the floodplain and the controls upon its character. Studies from modern rivers demonstrate the importance of fine-grained overbank material in understanding the evolution of the system (Smith et al., 1986).

The Mesaverde outcrop in the Wind River Basin contains a high amount of fine floodplain material. To understand the origin, evolution and depositional framework of the Mesaverde Formation, it is necessary to establish the architectural arrangements between both channelised and fine-grained deposits. In general, the fluvial part of the Mesaverde Formation contains 40-60% lenticular sandstone units, but, at any given locality, the sandstone is not evenly distributed in the stratigraphic section. In some intervals, stacking of the channels produces highly sandy sections several metres thick, whereas in other intervals, few channels exist. The stacked channel intervals are not persistent and grade laterally into less sandy intervals.

IV-5.1 River belt.

The lower and upper submembers of the Middle Member of the Mesaverde Formation appear to have channelised deposits at the same stratigraphic position in different parts of the outcrop belt which are separated by vegetated areas and crevasse splay complexes; the latter contain smaller-scale channelised deposits. These two submembers are interpreted to have an anastomosing pattern. The middle submember displays unique channelised deposits with some degree of sinuosity and lateral accretion surfaces (inferred by the palaeocurrents) surrounded by floodplain fine-grained deposits and is interpreted as a meandering system.

The channels found in the Mesaverde Formation have either sheet-like or

ribbon-like geometries. The former appear in amalgamated bodies up to 50 metres thick, with individual bodies being 5 to 9 metres in thickness. Generally, sheet-like bodies are associated with lateral accretion surfaces. The sandstone bodies that show ribbon-like geometries can have various width/thickness ratios at the same stratigraphic level and can be either amalgamated or isolated

IV-5.2. Floodplain deposits

Generally, floodplain deposits are shales, siltstones, fine-grained sandstones and coals. Coal thicknesses range from less than 1 metre in "distal" parts to 1 metre in more "proximal" parts. The siliciclastic facies define metre-scale coarsening upward cycles. These cycles are interpreted as "crevasse splay complexes" which are generated during times of overbank flooding. The coarsening-upward trend reflects aggradation of the floodplain during an ongoing avulsion event. Smith et al. (1986) have established a sequence of depositional events that reflect the development of a new trunk channel pathway. After the avulsion a new channel is complete and the abandonment of the area takes place, the zone becomes sediment starved, and floodplain soils (and subsequently coals) start to develop. Thus, the floodplain contains variable thicknesses of sandstone which grade laterally into fine-grained material. The sandstones are encase in fines and may be "connected" to the trunk channel sandstones. The lower submember of the Middle Member contains the most abundant and connected sandstone architecture.

IV-5.5. Stacking patterns

The stacking pattern of the channelised deposits and also their inteconnectedness has been considered to be an indicator of changes in sedimentation rate (a proxy for subsidence rate) (Leeder, Allen and Bridge,

1972). Other models (Heller and Paola, 1996) consider that the main factor that controls the stacking pattern together with the changes in sedimentation rates is the dependence of avulsion frequency on local sedimentation rate within the active channel belt. Therefore, the stratigraphic arrangement, stacking density and interconnectedness of preserved amalgamated channel sand bodies and floodplain material may record relative changes in local subsidence rates. If average avulsion frequency is constant, periods of increased subsidence/sedimentation rate should result in more frequent superposition of channel belts on one another. This increase in stacking density leads to greater vertical connectivity of sand bodies and higher sandstone/shale ratios in the alluvial succession and is associated with the ribbon-like sandstones in the lower and upper submembers. With avulsion frequency constant, the average density and interconnectedness of sandy amalgamated channel-belt deposits is proportional to sedimentation rate (the higher the sedimentation rate, the thicker the sediment deposited in the channel belt and adjacent floodplain between each avulsion event). Conversely, with lower sedimentation rates, sediment deposition is thinner and more widespread producing sheet-like sand bodies similar in geometry to the middle submember of the Middle Member.

IV-6. SHOREFACE DEPOSITIONAL STYLE

Many Upper Cretaceous shoreline sandstones units of the Rocky Mountain region (Campbell, 1971; Howard, 1972; Ryer, 1977; Walker , 1991; Plint, 1991) are progradational shoreface and beach sequences, evidently deposited on coasts with moderate to high wave energy. They have the typical coarsening–upward sequence discussed previously and in chapter III.

The shoreface deposits near the landward margin, where the shoreline sandstone lies with disconformable contact on older non-marine or lagoonal deposits, consists of cross-stratified upper shoreface deposits overlain by beach deposits. Farther seaward, lower shoreface deposits were laid down before upper shoreface and beach deposits, and the complete sequence is present. Because a prograding beach-to-offshore sequence is an offlap sequence, time lines slope seaward in the direction of progradation, through successively lower facies and into marine shales. In some cases this is recorded by seaward-sloping surfaces marked by erosion, heavy-mineral placers, glauconite or clay-rich partings.

Intertonguing marine and marine-influenced rocks include coastal-marine sandstones interpreted as complete to incomplete progradational sequences separated by transgressive erosional surfaces. The erosional surfaces have low relief but are commonly overlain by thin conglomerates with shell fragments. These surfaces may record shoreface erosion during transgressive episodes, but the amount of erosion is unknown. Some progradational sequences may be incomplete at the top because of their location on the shelf, rather than because of substantial shoreface erosion.

As is typical of nearshore-marine to coastal-plain deposits formed on the western margin of the Late Cretaceous Interior Seaway, the Mesaverde succession consists of three distinct depositional systems. The lower one is interpreted as lower-middle shoreface environments formed during a period of high sediment influx relative to subsidence or sea-level change. The second system consists of a progradation of upper beach and shoreface environments alternating with episodes of deltaic progradation. The upper shoreface units thin to the west against deltaic sandstone deposits, with very thin contemporaneous

lagoonal sediments. The relatively rapid progradation of the delta plain could have resulted from an abundant supply of sand from rivers or distributaries. The thickest succession of shoreface-beach sandstones is located in the Hudson and alkali Butte areas (Riverton Dome) (Figure IV-1) and they are encapsulated in siltstones and shales.

IV-7. STRATIGRAPHIC INTERPRETATION OF OUTCROP LOCALITIES

As discussed below, the Mesaverde Formation is a net southeast-directed progradational succession across the Wind River Basin in Wyoming. In the Maverick Springs area (northernmost exposures; Figure IV-3), the Cody Formation at the base of the Mesaverde Formation displays, based on the relationships of facies associations 1 and 2, a series of depositional packages that comprise progradational, coarsening-upwards set (10's of metres thick) of parasequences of shallow marine (delta front) deposits. Facies association 1 represents a storm-dominated shelf (lower delta front) and appears widespread throughout the basin. Facies association 2, higher up in the vertical sequence at any one section, represents shallower, more landward storm-generated deposits. The lateral correlation over tens of kilometres of the tops of facies association 2 (middle shoreface sandstones) with the tops of the laterally continuous thin sandstones with hummocky cross-stratification (lower shoreface), is based on lateral tracing of these surfaces and a characteristic concentration of *Inoceramus* shells, nodular bedding appearance and mm-scale interbeds of mudstone. These features appears genetically related, are developed coincident with a flooding surface and reflect increases of relative sea-level (Van Wagoner, 1990). The prograding delta front environment, represented by the repeated coarsening-

upward cycles of facies association 1 and 2 and the lateral transition of facies association 2 to facies association 1 in a progradational direction, is typical of shallow marine clinoforms in the Cretaceous Wester Interior (e.g. Swift et al, 1987; Walker et al, 1991; Plint, 1991). This progradational sequence is capped by a major erosion surface of regional extent, which in turn is capped by three laterally discontinuous packages of fluvial /estuarine channelised deposits (Facies association 3; see chapter III).This basinward shift of facies is interpreted as an incised valley, formed as a result of a rapid fall in relative sea level above a sequence boundary with the erosion of the upper shoreface deposits of the Cody clinoforms and bypass of sediment towards more distal areas. It is predicted that a lowstand shoreline should be found in the south or southeastern parts of the basin and that the deposition within the valleys is a response to a relative rise in sea level during a transgression period. In places, the sequence boundary and flooding surface are coincident. On top of this succession appear upper shoreface deposits of the Basal Member of the Mesaverde Formation forming an aggradational and progradational set. The flooding surface at the base of this Member is therefore also responsible for the new incursion of marine influenced deposits in the section, separating the Cody and Mesaverde Formation, and the deposits above the sequence boundary therefore represent a transgressive to highstand system tract (Vail et al., 1977). Due to the autocyclic nature of deltaic systems and the possible lateral switching of deltaic lobes, the system tract interpretations do not necessarily reflect eustatic changes.

In the same area (Maverick Springs area) the Mesaverde Formation is divided into several depositional packages of 1) wave dominated upper shorefaces; 2) coastal-plain deposits with some wave influence; 3) trunk channels

with floodplain deposits; 4) distributary channels; and finally, 4) braided and meandering systems of the Teapot Member. The outcrop clearly reflects changes in facies relationships and sand body morphology and quality. The shoreface deposits are typically quite clean and uniform and laterally continuous until northwestwards, over hundreds of metres, they change into carbonaceous shales and coals. The overlying coastal plain/fluvial succession makes up the largest volumetric percentage of the Formation in this area (up to 70%) and contains less clean sandstones which are laterally discontinuous. The coastal plain deposits at the base of the sequence are wave influenced, fed by a series of distributary networks that must be in close proximity to the shoreline, interpreted to be close to the eastern part of the Maverick Springs outcrop belt from the appearance of mouth bar deposits at the top of some cycles and the previously mentioned wave influence. The overall progradational character of the formation is interpreted from the vertical succession of delta plain (lower submember of the Middle Member) to fluvial deposits (middle and upper submembers of the Middle Member), which at this locality appear to reflect a steady basinward shift of environment. The fluvial deposits are first meandering and evolve into a tributary, anastomosing channel system. Finally, the angular unconformity at the base of the Teapot Member reflects a new fall of relative sea-level (and generation of a sequence boundary) and the generation of a widespread alluvial plain.

In southern and south-eastern parts of the basin (Figure IV-1) the facies character changes drastically. In these areas (Hudson, Alkali Butte and Castle Gardens; see Figure IV-5, 6, 7 and 8), the sequences are formed by interfingering marginal marine, foreshore and lower shoreface to shelf deposits, forming cycles

which reflect the progradational-retrogradational character of the shoreline during Mesaverde time. Overall, the sequence progrades. Each regressive cycle is separated by a transgressive tongue of marine deposits (lithologically, but not temporally; see chapter VI for explanation) of the Cody Formation. In Hudson and Alkali Butte areas, the Cody Formation through proper is considerably more sandstone-rich than to the northwest and represents lower-shoreface environments (facies association 1 and 2). The tops show truncation overlain by deposits of nearshore marine, littoral and coastal swamp environments (facies association 4), grading abruptly eastward into the offshore marine deposits included in facies association 1. The surface between the Mesaverde and Cody Formations is therefore interpreted as a sequence boundary. At the top of this succession, nearshore/coastal plain sedimentation occurs (Middle Mesaverde Member), but most of the Mesaverde rocks are removed by erosion on the unconformity at the base of the Fort Union Formation. In Castle Gardens (the most south-eastern studied outcrop; Figure IV-3), the Cody Formation mainly represents an offshore inner shelf deposit. The Fales Member (Keefer, 1957) represents the base of the Mesaverde Formation and abruptly emplaces littoral, nearshore marine (forebeach deposits), brackish-water lagoonal environments and marshes over the inner shelf deposits of the Cody Formation. This surface separating the Fales Member and the Cody clearly represents a basinward shift of facies and is interpreted as a sequence boundary. The top of the succession is capped by the Wallace Creek Tongue that represents a return to deeper marine conditions, reflecting a westward readvance of the sea and therefore the surface at its base is a flooding surface. However, at each of the southeastern sections, a second regression occurs during the deposition of the fluviatile-dominated

Middle Member (or equivalent) of the Mesaverde Formation (Barwin, 1961). The nature of the regressive cycle is highly variable. Some regressive cycles consist of a single, regionally persistent, upwards-coarsening beach sandstone that is overlain by a very coaly, lower-coastal-plain or deltaic deposit. Other cycles consist of several less regionally persistent marginal-marine sandstones and much less coaly lower-coastal-plain deposits. These are overlain by fluvial sequences consisting of point-bar and overbank deposits. The lower lenticular channel sandstones in the regressive cycles are generally thinner and less laterally persistent than channel sandstones in the fluvial sequences above the regressive cycles. The juxtaposition of these fluvial successions on marginal marine and coastal plain deposits could be a steady progradation or it may represent another basinward shift in facies.

Chapter V

WIRELINE-LOG CHARACTERISATION OF THE MESAVERDE FORMATION

The wireline-log characterisation of the Mesaverde Formation incorporates four data sets: (1) 30 wireline-logs; (2) gamma-ray logs of outcrop generated with a hand-held scintilometer; (3) core analysis; and (4) the outcrop based measured sections. All the wireline-logs used for this study contain the complete Mesaverde Formation and the thicknesses vary from 650 metres to less than 100 metres. The wireline correlation is based on two surfaces; a bentonite marker bed in the Cody Formation (Steve Parks, Tom Brown Inc.) and the top of the Teapot Member. By hanging the correlations on these two surfaces, it will be demostrated below that the Basal Member sandstones of the Mesaverde Formation appear successively higher up in the wireline logs towards the southeast part of the basin. Therefore, although the base of the Mesaverde is defined as the Basal Member in the Maverick Springs area, the first appearance of similar sandstones in the wireline logs (and outcrop) in the southeastern part of the basin do not represent the base of the Mesaverde chronostratigraphically. Correlation of the logs is complicated by the fact that facies successions show abrupt changes in character and thickness and there are no easily recognisable marker beds. Consequently, the correlations are based on matching distinctive log patterns on the basis of log shapes over intervals that represent characteristic vertical facies successions and then they are compared to outcrop observations. This methodology has been termed "electrosequence analysis" by Rider (1996) and an electrosequence is defined as *"an interval defined on wireline-logs, through which there are consistent or consistently changing log responses and*

characteristics, sufficiently distinctive to separate it from other electrosequences".

V-1.1. WIRELINE-LOGS DISCUSSION

Gamma-ray log shapes generally reflect variations in clay (shale) content. The highest values represent higher shale content and vice versa. There is also a relationship between gamma-ray log and sandstone grain-size (Serra and Sulpice, 1975), with higher values interpreted as recording smaller grain size.

The sonic log measures the formations capacity to transmit sound waves whose velocity depends on lithology and rock texture, notably porosity. High velocities are typically associated with carbonate rocks, intermediate velocities with sandstones and shales, and lower velocities with shales. Note though, that the sonic log is not necessarily diagnostic of a particular lithology but can be a function of changes in texture and interstitial fluid content (Rider, 1996).

The density and neutron logs can be used to measure porosities. The density tool emits gamma radiation which is scattered back to the detector in amounts proportional to the electron density of the rock, which is usually related to the density of the solid material and the amount and density of pore fluids. These logs are good indicators of lithology and are sensitive to permeability (sand) and impermeability (shales).

V-1.2. WIRELINE LOGS CHARACTERISATION

Observations made at the outcrop have been used to define the distinguishing characteristics of the members and submembers that comprise the Mesaverde Formation in the Wind River Basin. The most typical vertical patterns seen on gamma-ray logs can be seen in Figure V-1 (after Cant, D, 1992). Interpretations based on log curve shape alone is extremely imprecise, so in this

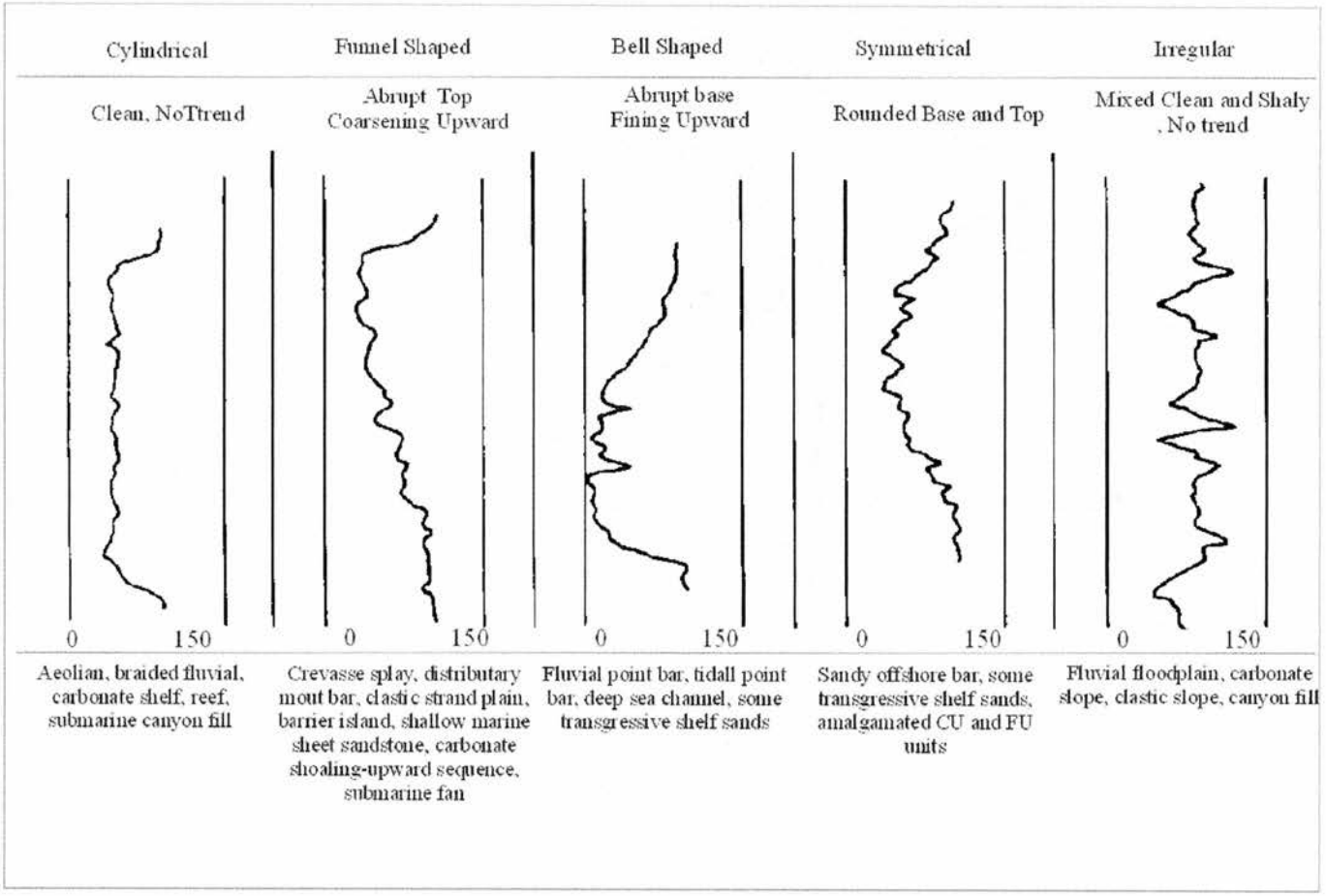

Figure V-1: The most common idealised log curve shapes seen on gamma-ray logs (From Cant, 1992)

chapter the log patterns have been calibrated to well-understood depositional facies successions in cores and in outcrops. The following characteristics are used to guide wireline log correlations:

1- The upper part of the Cody Formation is composed of shelf, lower and middle shoreface deposits represented by coarsening-upward parasequences. These will appear on the wireline logs as a succession of stacked funnel-shaped log responses (Figure V-1).

2- The Basal Member of the Mesaverde Formation is represented in outcrop by a 5 to 25 metres thick, white, upper shoreface (medium grained) deposits (Facies association 4, chapter III). This sandstone should appear as a laterally continuous cylindrical unit (Figure V-1) above the Cody coarsening-upward depositional cycles. Gamma-ray counts should decrease upwards due to the decreasing amount of clay material from the top of the Cody into the Basal Mesaverde.

3- The Middle Member of the Mesaverde Formation consists of delta plain deposits overlain by fluvial deposits. From outcrop data, the facies character changes over relatively short distances thus wireline-log response should display variable character from log to log. In general, log shapes are expected to be funnel, bell and mixed shaped (Figure V-1).

4- The sandstone/shale ratio differences of the three submembers of the Middle Member should be reflected in the wireline-logs. The lower submember is 1.3, the middle is 1.2 and the upper is 0.6 sandstone/shale ratio (Figure V-2). Sandstone/shale ratios were calculated taking into account the amount of sandstone against the amount of shales, siltstones and coal beds in separate

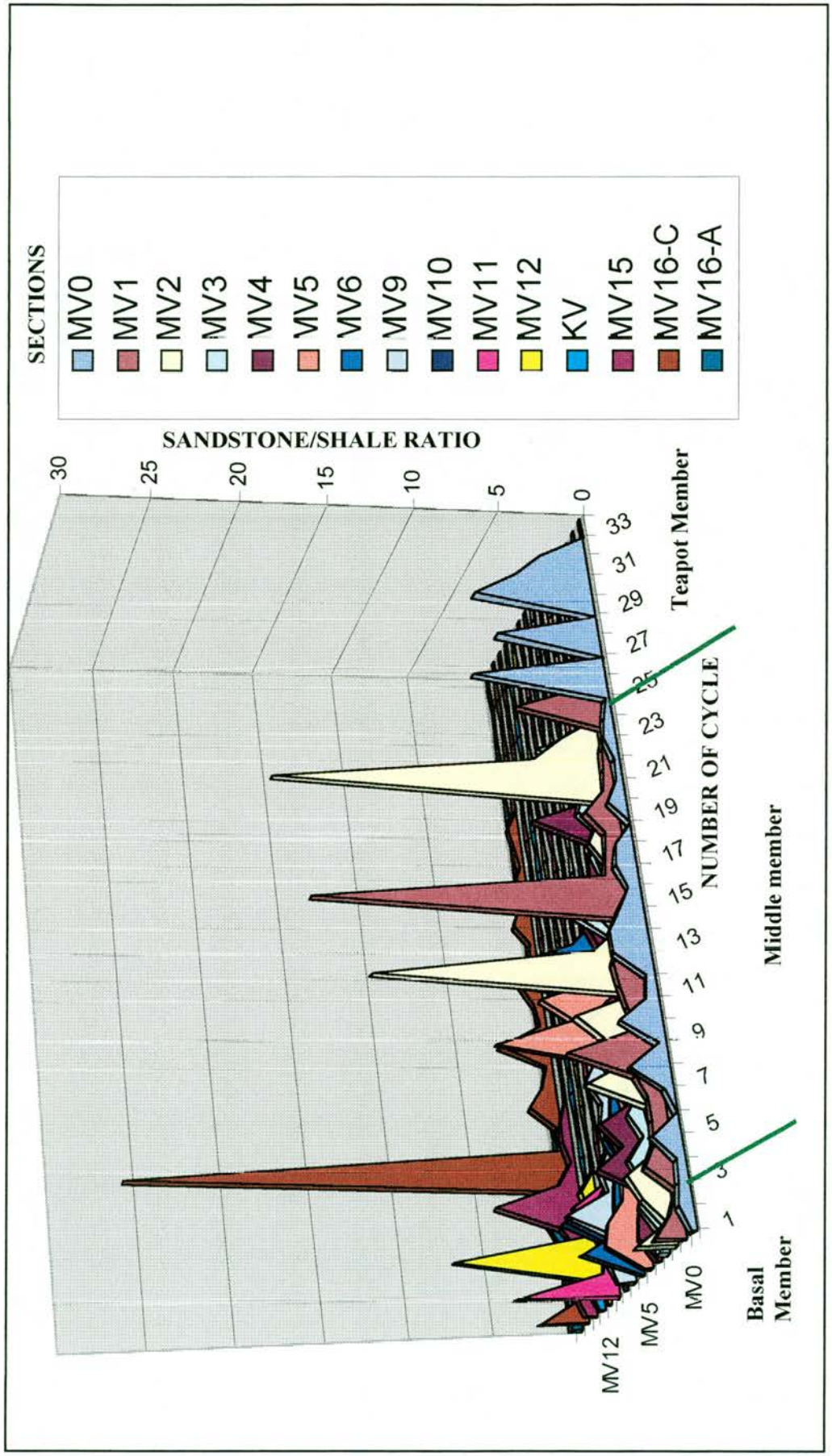

Figure V-2: Diagram showing the sandstone/shale ratios for some of the measured sections see Figure V-3 for localities).

fining or coarsening-upward cycles for each of the submembers and members.

5- The Teapot Member will reflect high sandstone/shale ratios (Figure V-2). It occurs as clean medium to coarse-grained sandstone bodies emplaced sharply on the interbedded sandstones and shales of the Middle Member of the Mesaverde. Thus, the base of the Teapot, which is an unconformity, should be a readily recognisable surface on the wireline-logs. The logs shapes are expected to be cylindrical and bell (Figure V-1).

6- The Mesaverde Formation is overlain either by the Meeteetse, Lance and Fort Union Formations which have a lower sandstone/shale ratio than the Mesaverde and this should be reflected in the log character. The base of the Fort Union Formation defines a basinwide unconformity and this should be recognisable as a downcutting surface on the logs.

In order to obtain the wireline-log characterisation of the Mesaverde Formation, log shapes are studied as overall successions rather than individual bodies (Parker, 1977). Where possible, gamma-ray, density and sonic logs were examined together and used to define characteristic intervals. Based on their position on the logs and their comparison to appropriate outcrop intervals, the variations in log shape within a given interval can be related to specific facies variations and hence palaeoenvironmental setting.

V-1.3. HAND-HELD GAMMA-RAY SCINTILOMETER

Hand-held gamma-ray logs of outcrops have been generated in order to compare/contrast the outcrop with the gamma-ray signatures and demostrate the reliability and potential pitfalls of subsurface wireline-log correlations to the facies associations. This technique is helpful in visualising the depositional

geometries and lateral facies changes of subsurface strata thereby reducing the degree of uncertainty associated with correlations (Slatt et al., 1992).

The scintilometer has the capability of measuring either total or individual radioelement concentrations (Myers and Wignall, 1987). Measurements were made at 1.5 or 3 metres intervals and the result is a gamma-ray log that is calibrated to facies interpreted from the outcrop and thus can be used to aid interpretations of nearby subsurface gamma-ray logs.

Two complete Mesaverde sections have been measured with the gamma-ray scintilometer (Mv3 and Mv0). The results show that the general patterns can be compared with wireline-logs approximately 6 km away (Figure V-3).

A USGS core was logged with the scintilometer (CBM-8 Pilot Butte) and compared to the wireline-log 4n2e2211 to test how well the scintilometer and downhole gamma-ray tool compare (Figure V-4). The comparison shows that both tools give similar results and correlations can be made at ~ 15 metre scale. The coarsening-upward trend of the BasalMember as well as the fining-upward trend of the lower submember of the Middle Mesaverde are clearly correlated.

The Mv3 section (Figure V-5) appears to have 5 units well discriminated: the Basal Member, 15 metres thick, formed by the amalgamation of two upper shoreface sequences (facies association 4); and the 3 submembers of the Middle Member and the Teapot Member. As can be seen on Figure V-4, the lower submember log responses reflect the sandier base (low gamma-ray), but sandstone becomes less important towards the top and shale intervals become thicker (up to 5 metres thick). The base of the middle submember (170 metres thick) shows the abrupt emplacement of thick sandstone bodies at the base; when correlated to an adjacent well, the basal sandstones of the middle submember

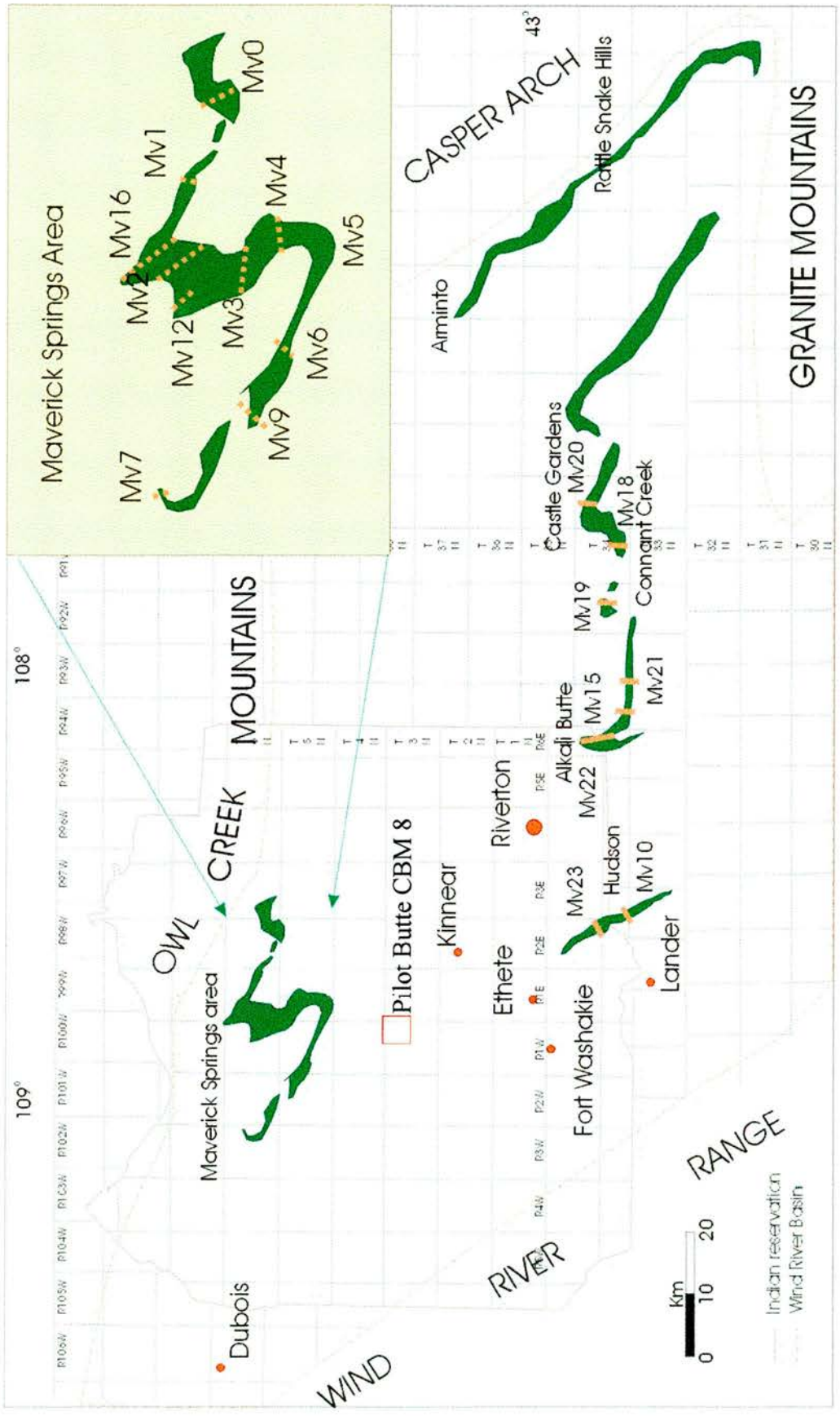

Figure V-3 Location of the Mesaverde Formation in the Wind river Basin. Location of measured sections.

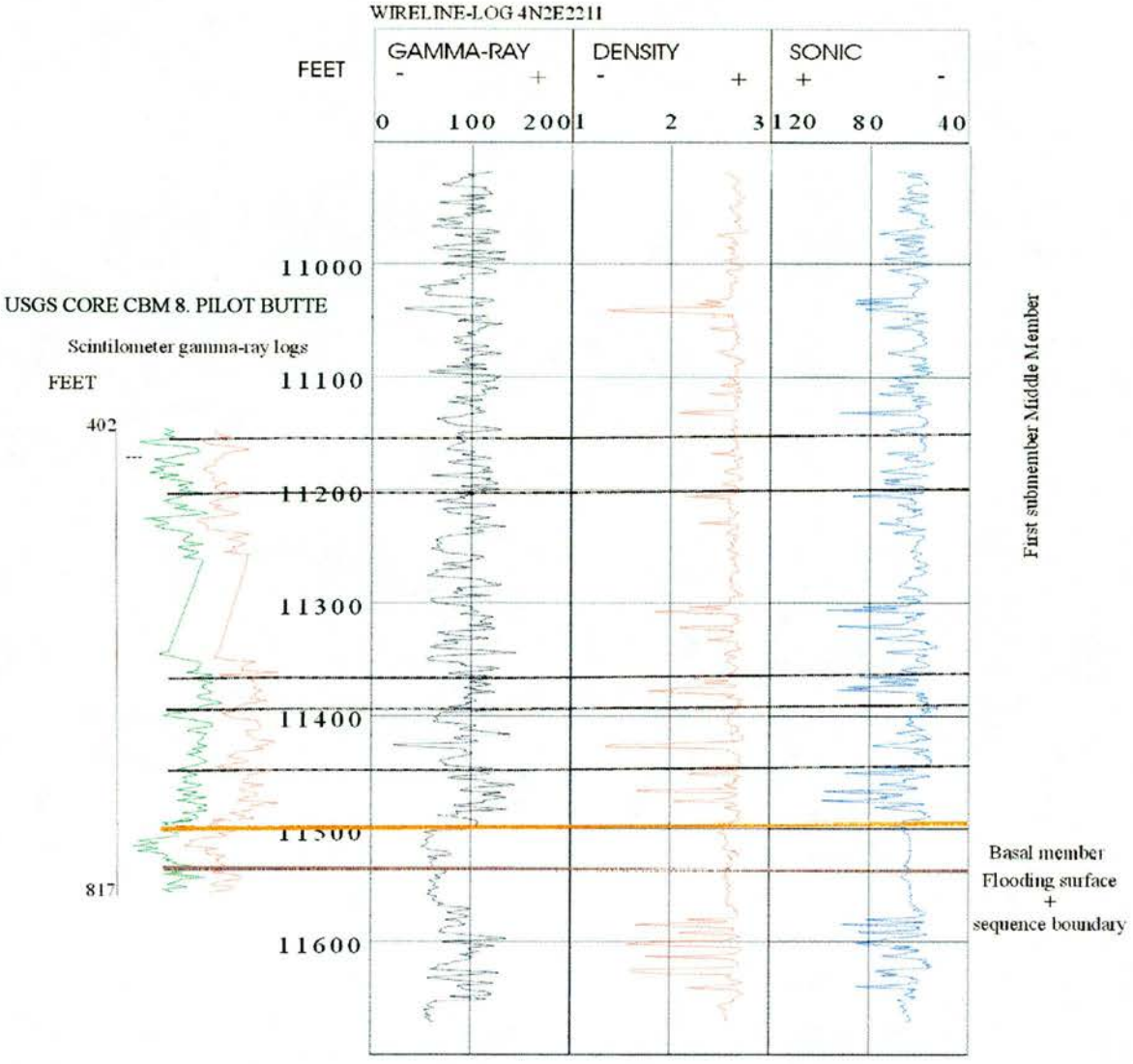

Figure V-4:Comparison of the wireline-log 4n2e2211 with the gamma-ray log from the USGS core CBM 8, Pilot Butte obtained with the scintilometer. See Figure V-3 for locations.

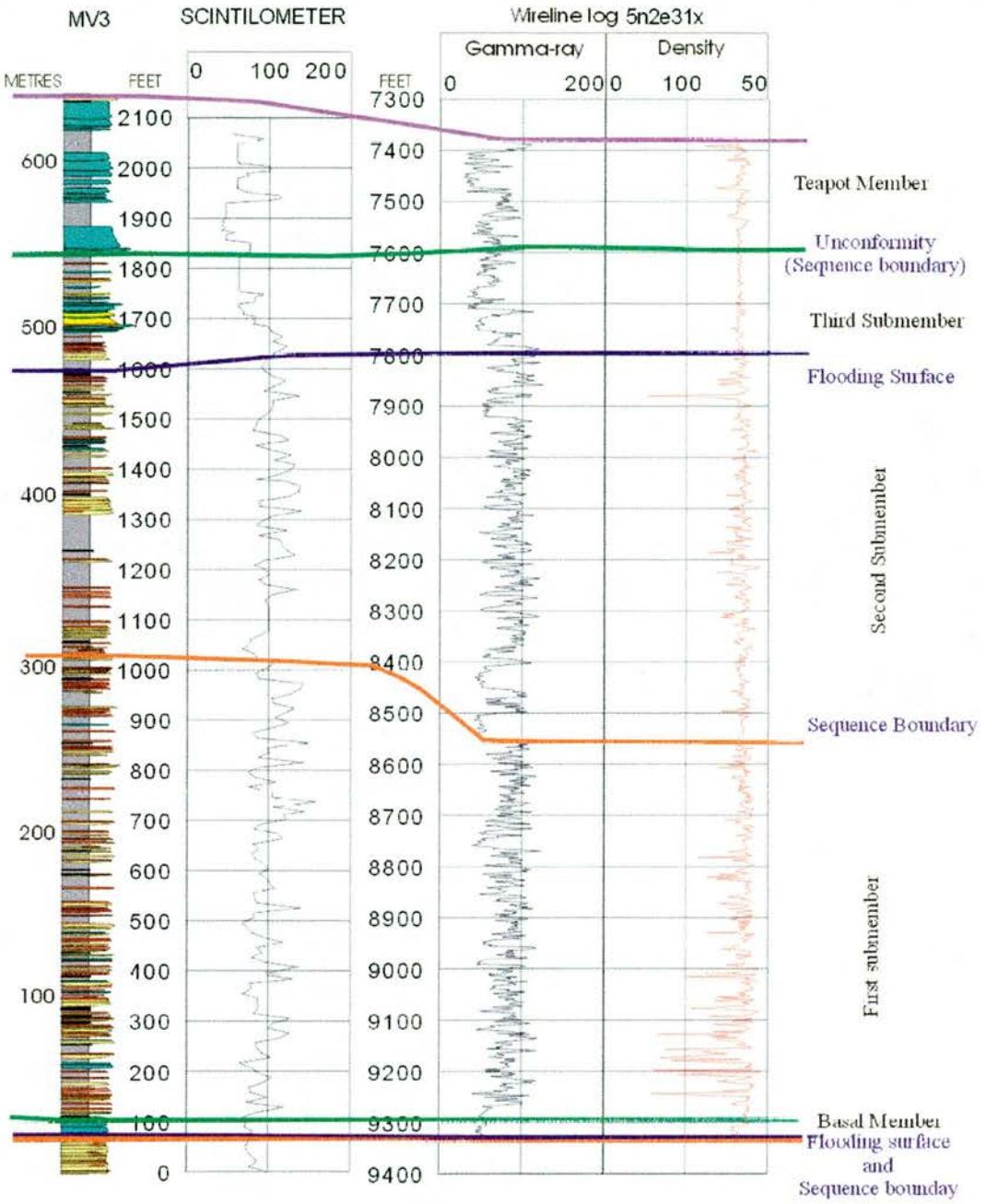

Figure V-5: Comparison of the measured section Mv3, with the gamma-ray log obtained with the scintilometer and the wireline-log 5n2e31x (closest wireline log to the outcrop area) See Figure V-3 for location of section and Figure V-10 for location of wireline log.

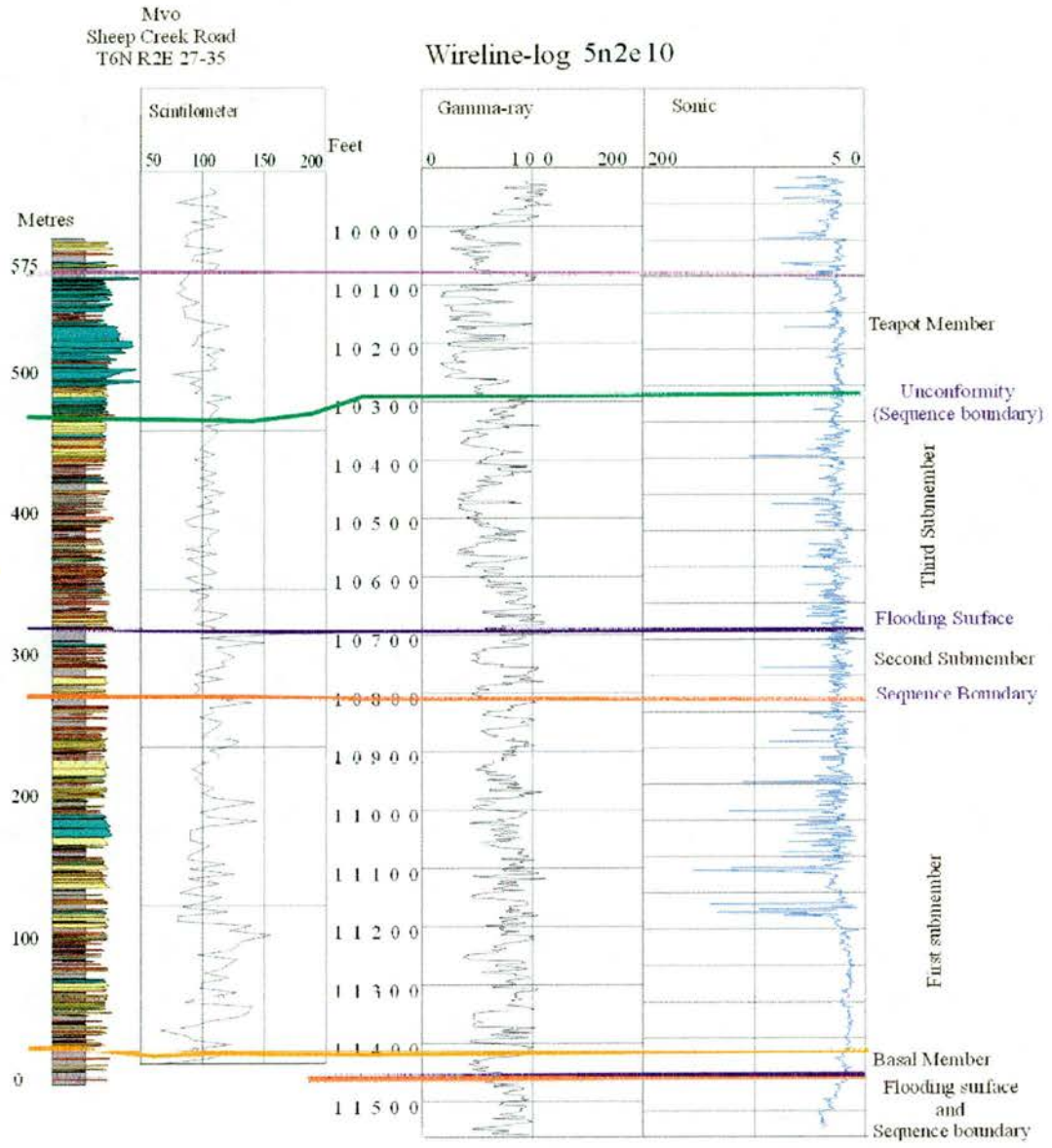

Figure V-6: Comparison of the measured section Mv0 (Sheep Creek Road), with the gamma-ray log obtained with the scintilometer and the wireline-log 5n2e10 (closest wireline log to the outcrop area). See Figure V-3 for location of section and Figure V-10 for location of wireline log.

scour into the underlying member by as much as 50 metres (Figure V-5). The upper submember is characteristic in its response and shows a coarsening-upwards followed by finning-upwards trend representing an increase in sandstone upward and the initiation of the more shaley uppermost unit which in turn is truncated by the Teapot Member (Figure V-5). The Teapot Member is characterised by the thick, cylindrical sandstone signatures. The section Mv3 can be correlated to the wireline-log 5n2e31x, which is aproximately 5 km from the measured sections. The general signatures of the subunits from the gamma-ray scintilometer can be correlated with the wireline-log although changes in thickness of the packages can be observed. The lower submember of the Middle Member is the least similar in character to the wireline-log. In section Mv0 (Figure V-5), correlation to the 3 km appart wireline-log, 5n2e10, is quite straightforward. From the sedimentary log the Basal Member in this area appears to be cut out by carbonaceous shales interbedded with sandstones and siltstones from facies association 4. The lower submember of the Middle Member appears sandier than in Mv3 and composed of 3-4 fining-upwards cycles. This character is reflected in the wireline log although the number of cycles is higher. The middle submember of the Middle Member in this case is much thinner than the previous example, with only ~30 metres of sandy shales and sandstone bodies at the base. The upper submember appears thicker, with more sandstone bodies towards the middle and top. The increase of thickness of this submember seems to be related to the appearance of this topmost sandy cycle. The Teapot Member, with the unconformity at its base truncates the member below and reflects its sandy nature in the wireline-log, the scintilometer log and the measured section.

Section Mv 15 has been compared to the wireline-log 36n94w25 (20 km away) (Figure V-7). The comparison of the measured section to the gamma-ray log reveals a unit formed by three-four fining-upward sequences composed of marine-influenced, lagoonal and finally delta plain environments. These sequences become sandier but thinner towards the top. The next sequence is characterised by a new fining-upwards trend but the sonic log reflects less carbonaceous material on top of the cycles.

Two sections have additionally been compared to wireline-logs: Alkali butte W (section Mv21) is compared with the wireline-log 1s5e13 and Alkali Butte E (section Mv23) is compared with the wireline-log 34n90w23 (see Figure V-3 for location of sections and wireline-logs). The correlation between Alkali Butte W and the wireline-log 1s5e13 (Figure V-7) shows how the sandstone bodies that appear in the wireline-log represent the basal (cylindrical-shaped) shoreface deposits of facies association 4 and change upwards into channelised (bell-shaped) sandstone bodies interbedded with carbonaceous (mixed-shapes) shales and coals of facies association 5. The Mesaverde Formation in this area is truncated by the Fort Union unconformity and, therefore, the measured section is not complete. The correlation of the section at Alkali Butte E (Mv23) (Figure V-9) and the wireline log 35n92w31 shows how the base of the formation is composed of a shoreface deposit described in chapter IV and overlain by bell-shaped channelised deposits interbedded with carbonaceous shales. This represents the unnamed middle Member (Keefer and Rich, 1957) in this area and is correlated to the middle submember of the Middle Member in the Maverick Springs area (see wireline correlations below). The sequence at the top of this submember appears as a rip-up clast lag, with pebbles and shell fragments on top

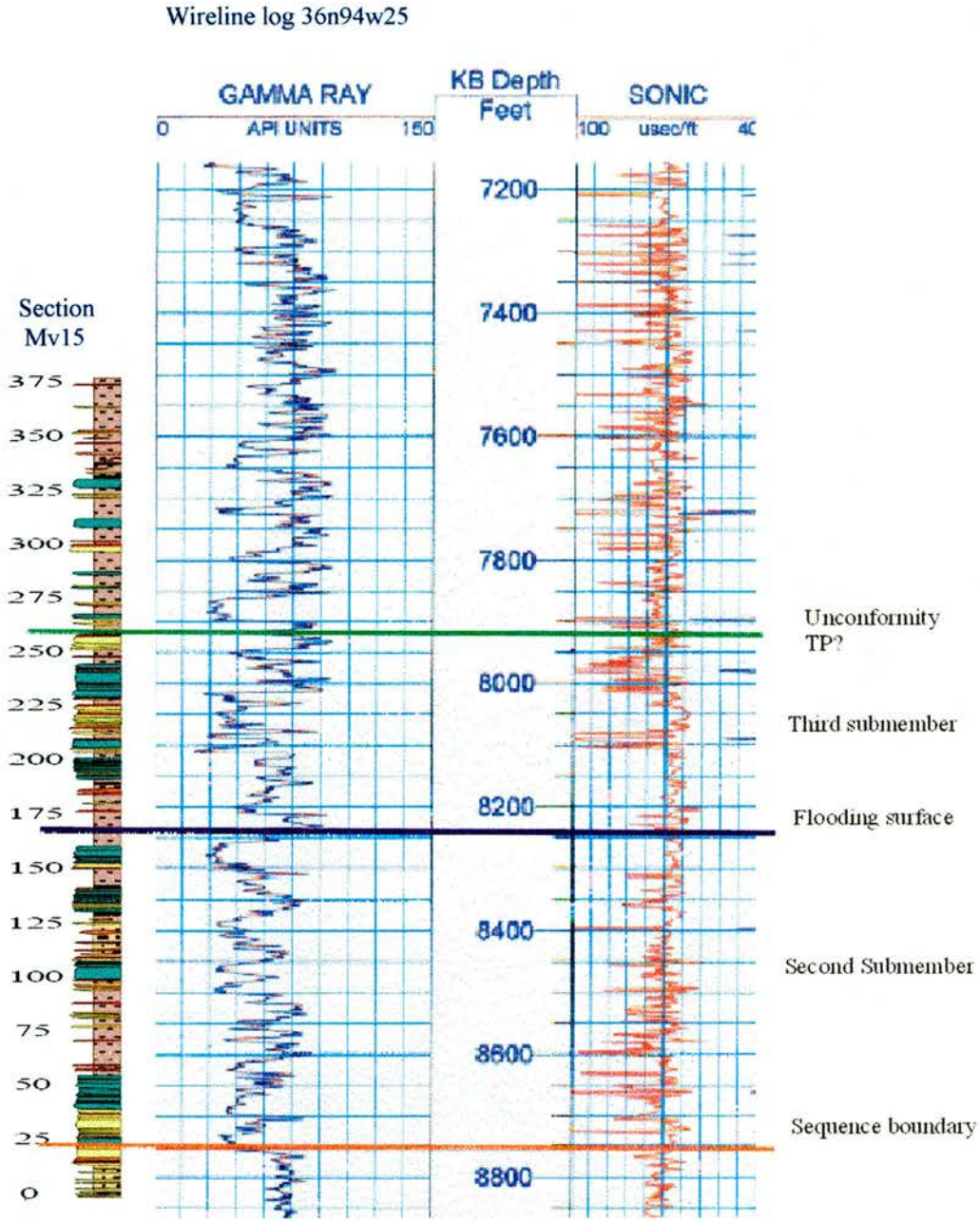

Figure V-7: Comparison of the measured section Mv15 (Alkali Butte), with the wireline log 36n94w25 closest to the outcrop area. See Figure V-3 for location of section and Figure V-9 for location of wireline log.

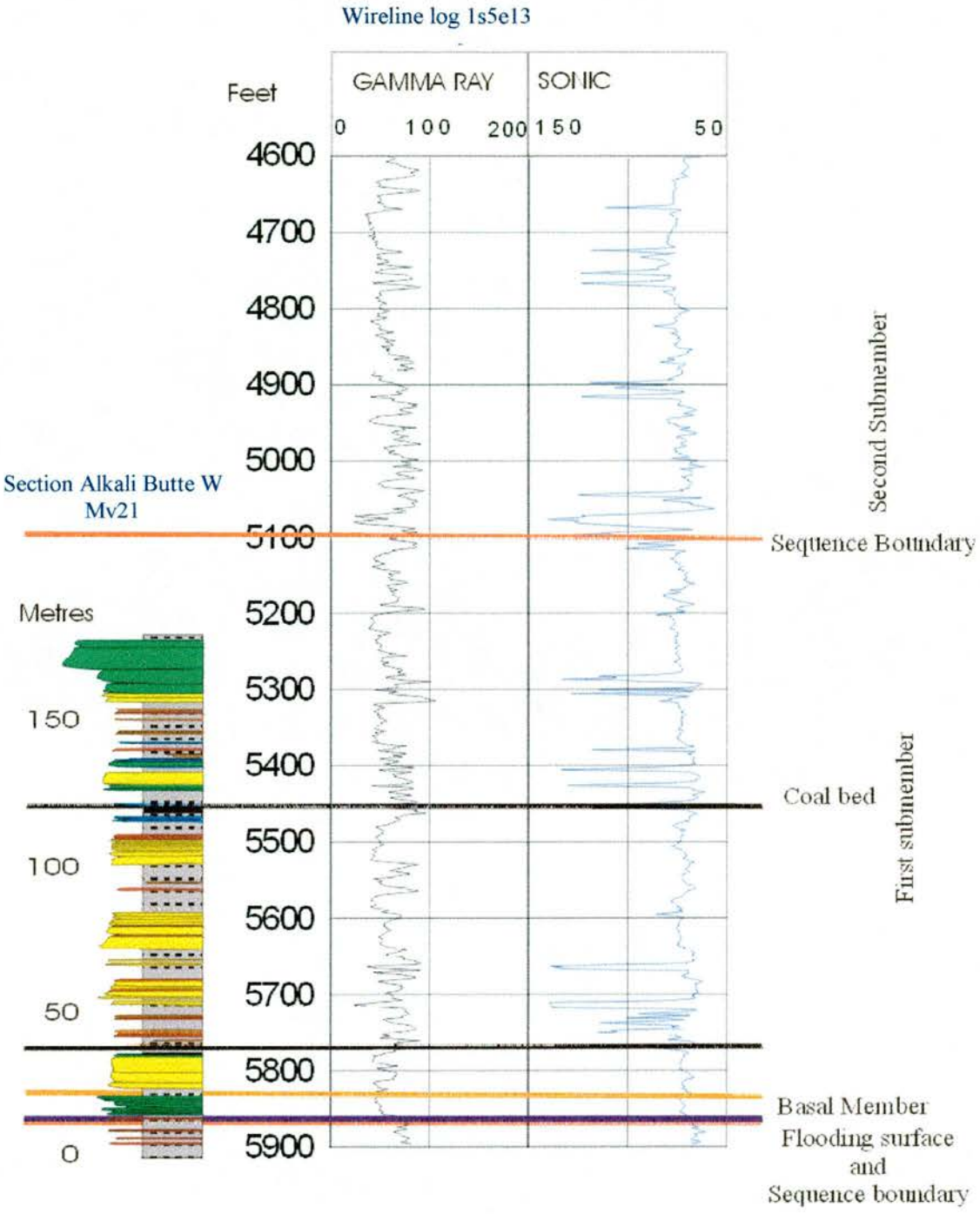

Figure V-8: Comparison of the measured section Mv21 (Alkali Butte W), with the wireline-log 1s5e13 (closest wireline log to the outcrop area). See Figure V-3 for location of section and Figure V-10 for location of wireline log.

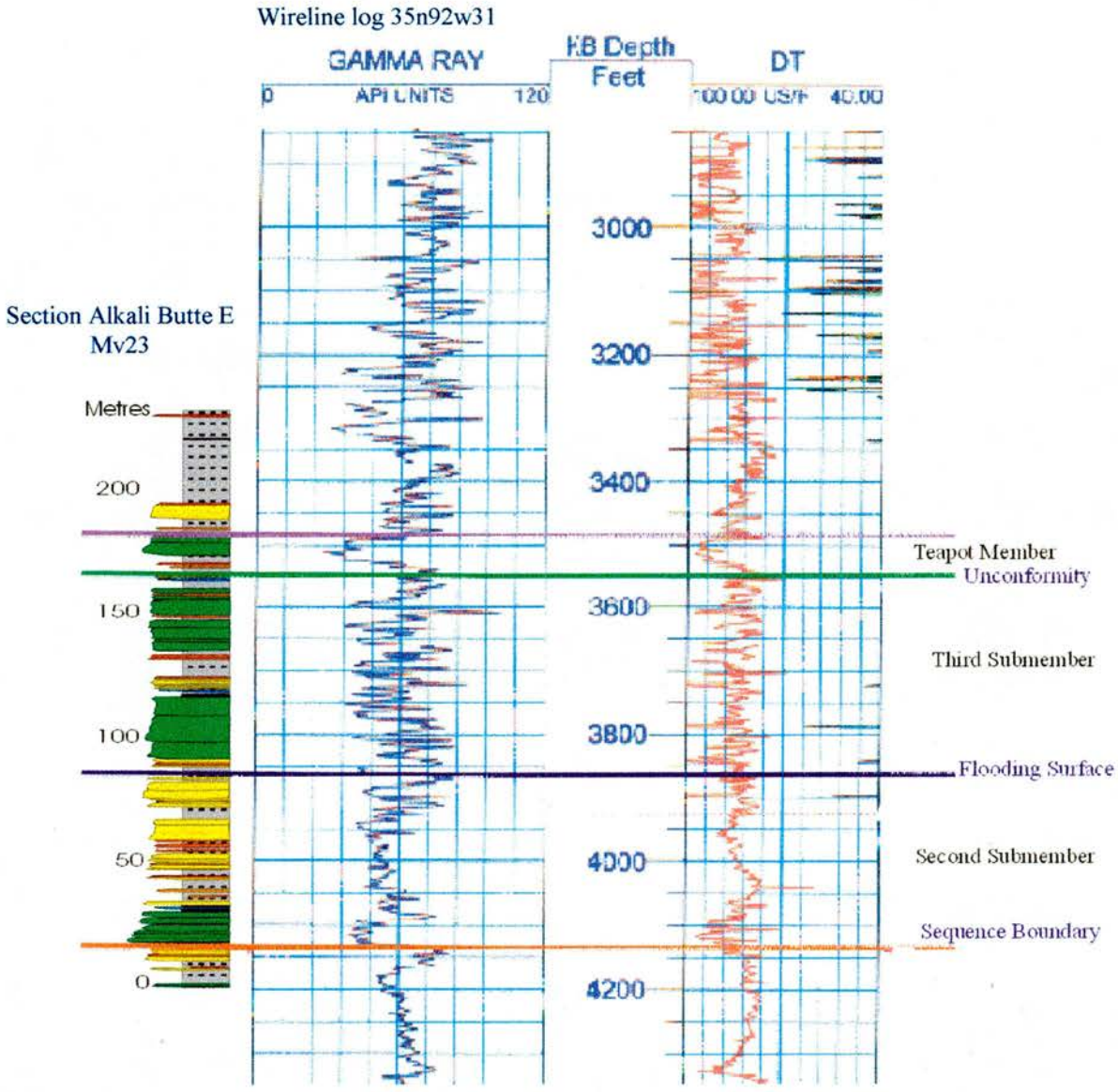

Figure V-9: Comparison of the measured section Mv23 (Alkali Butte E), with the wireline-log 35n92w31 (closest wireline log to the outcrop area). See Figure V-3 for location of section and Figure V-10 for location of wireline log.

of a sandstone body, and overlain by marine-influenced deposits; it is interpreted as a flooding surface (see Chapter III, facies association 1 and 2). The upper submember is composed of marine influenced deposits, and based on its relationship to the underlying regional flooding surface is correlative to the upper submember of the Middle Member in Maverick Springs area. The Teapot Member is less than 20 metres thick at this locality. Overall, the three units display the general signatures characteristic of the wireline-logs.

V-1.4. WIRELINE-LOGS : MESAVERDE FORMATION

The remaining 35 wireline logs for the Wind River Basin have similarly been correlated. In the northwestern part of the basin, the base of the Mesaverde Formation (Figure V-4, 5 and 6) can be distinguished by the presence of several 10's of metres thick, low gamma-ray reading (Basal Member) on top of coarsening-upward cycles that represent the Upper Cody Formation (Table V-1: EF1-2). The top of the Mesaverde Formation (Figure V-3 and 4) is distinguished by the appearance of a 30 to 70 metres thick packet of cylindrical-shaped sandstone bodies that have low gamma-ray readings and are attributable to the Teapot Member (Table V-1: EF5). Within the Middle Member, differences between the three submembers can be distinguished by comparing the gamma-ray, density and sonic logs (See Appendix 4). The lower submember is composed of sandstone packets interbedded with shales and display an irregular or bell-shaped pattern on gamma-ray, density and sonic logs. Channel sandstones, with abrupt erosional bases pass steadily upward to finer-grained deposits over 25 metres thick successions (ie. fining-upward trends into overbank shales and coals) and this yield a shoaling gamma-ray log motif (Table V-1: EF4). The shales are easily distinghished in the density log due to their low permeability.

From outcrop, these shales are known to be carbonaceous and some coal beds can be detected on the logs. The thickness of this member varies from 200 metres to 60 metres.

The middle submember is characterised by a similar facies motif to the lower submember. However, it is distinguished by the appearance of thicker and more abundant sandstones at its base. The succession defines an overall fining-upwards trend, characterised by a bell-shaped base overlain by a mixed-shaped interval which overall varies in thickness from 50 metres to more than 100 metres. When the base of this submember is correlated from log to log, it is shown to incise into the underlying submember by almost 200 metres. The significance of this incision is discussed below.

The upper submember is characterised easily in the three types of wireline-logs: the gamma-ray log shows an initial coarsening-upward followed by a fining-upward trend and appears to be sandier than the previous submembers. The density and sonic logs are more uniform, showing either no significant content of carbonaceous material throughout the submember or its permeability may be fracture-controlled. The base of this submember appears to define a relatively flat surface that can be traceable throughout the basin. In some cases this surface corresponds to a coal bed (noticeable in the density and sonic logs). This surface is interpreted as a flooding surface (see Chapter IV).

The base of the Teapot member is very sharp, normally with a high peak of the gamma-ray log (Table V-1: EF5). This surface incises up to 20 metres in some sections and is a regional unconformity recognised in outcrop. Above this surface, the Teapot Member is characterised by very low gamma-ray values and a cylindrical-shaped log motif defining 5 to 20 metres thick sandstone packages.

In some wireline-logs, the sandstones appear to contain shales. The top of the Mesaverde Formation is placed at the top of the last clean blocky (cylindrical) sandstone. Above this, are the more variable log responses of the shales and sandstones characterise the Meeteetse, Lance or Fort Union Formations. Towards the south and south east of the basin, some variations to the above sequence occur. At Hudson area, the Fort Union unconformity cuts down and removes almost half of the Mesaverde Formation and therefore, the characteristic signature of the Teapot is not present in all localities in this area. Also, the Basal Member (Figures VI-5, 6 and 7) appears much thicker formed by several successions of low gamma-ray, clean sandstones that appear amalgamated in some localities (Table V-1: EF3). The lower submember in this area appears as several cycles with clean sandstones at the base (low gamma-ray readings) followed by the carbonaceous shales, coals and channelised deposits which interfinger with shales and coals. This sequence is repeated several times, and in general, they form first fining-upward cycles followed by coarsening-upwards cycles (e.g. Figure V-8), reflecting that the sequence is more marine influenced than the north-west. At Alkali Butte, the Basal Member proper and the lower submember of the Middle Member do not appear and the middle submember (at Maverick Springs) changes laterally into marine-influenced deposits and represents the base of the Formation.

The upper submember appears towards the east of this area (Rattlesnake Hills area) where it changes again into marine influenced deposits, with coarsening-upward cycles (Figure V-3). It increases in thickness more than doubles relative to the northern areas. This is partially due to the less important

Name	"Electrofacies" association	Gamma-ray motif	Depositional environment
EF 1	Coarsening-upwards trend, 30 to 50 metres thick.	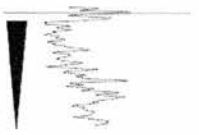	Middle and Lower shoreface deposits. Shelf deposits.
EF 2	Very low gamma-readings from packets of sandstone 30 to 60 metres thick located on top of coarsening-upward trends.		Upper shoreface deposits composed of clean sandstone bodies.
EF3	Very clean sandstone with funnel shape gamma-ray motifs. Mudstones and coals at its top or base. 5 to 10 metres thick. Appear isolated or with similar deposits amalgamating.		Mouth bar deposits, or marine-influenced parts of channelised systems.
EF4	Finning-upward cycles, 20 to 25 metres in thickness. Interbedded sandstones with mudstones, siltstones and coals.		Fluvial successions showing channelised deposits surrounded and interbedded with fine-grained material from the floodplain.
EF5	Finning-upward trends, with very low content of fines. Very low gamma-ray counts.		Fluvial deposits with low content of fine-grained material.

Table V-1: Main "electrofacies" found in the Mesaverde Formation

erosion of the Teapot unconformity in this part of the basin, but also to accommodation space increases southeastwards.

V-2. CORRELATION OF WIRELINE-LOGS

Wireline-log correlation of several lines (Appendix 4) both orthogonal, as well as parallel or sub-parallel, to depositional dip have been analysed (Figure V-10). The correlations of the wireline-logs are then compared with the gamma-ray obtained with the hand-held scintilometer and with the measured sections. The resultant correlations (Figure V-11; Appendix 4, 5 and 6) illustrate the geometries and relationships between the different members of the Mesaverde Formation and its stratigraphically adjacent formations in a basinwide context. Based on these correlations, it is observed that the Basal Member becomes thicker towards the south (around Riverton Dome; Figure V-3), with four important progradational events and the appearance of new shoreface deposits higher up in the succession (Figure V-12). The isopac map for this Member (Figure V-13) shows a northeast-soutwest depositional strike, with a depocenter located in the southwestern part of the basin. The lower submember of the Middle Member is genetically related to the Basal Member. It is formed by the delta-plain facies that correspond to the landward lateral facies change of the shoreface deposits of the Basal Member (Figure V-14). The isopach map (Figure V-15) reflects the decrease of thickness of this submember towards the southeast, and the location of the depocenter for this submember in the western part of the basin. The Basal and lower submember of the Middle Member form part of the same system, which shows an southeastern- directed progradation of the shoreline, that migrated from Hudson towards the southeastern corner of the Wind River Indian Reservation area (Alkali Butte). The thickness of this system

varies, depending on the scouring from the submember above, from 50 to 300 metres. In Alkali Butte this member is reduced to only the shoreline deposits that correspond to the upper part of the lower submember of the Middle Member in Maverick Springs. East and southeast of this area, this submember is not present. The middle submember appears scouring down up to 200 metres of the submember below it, based on correlations of the wireline-logs (Figure V-16). This submember appears locally and seem to be orientated from northwest to southeast and formed by a distributary system that represents an incised valley. The top of this sequence is placed at a coaly interval that separates it from the overlying submember and represents a flooding surface. Thicknesses of the middle submember vary depending on the amount of scouring it effects on the submember below, but the thickness also decreases towards the southeast (Castle Gardens area) and disappears in the Rattlesnakes Hills area. The isopach map (Figure V-17) shows how this submember appears only in certain parts of the basin. At the top of this interval in Maverick Springs area a coarsening-upward sequence of variable, but no more than 100 metres thickness, which changes in thickness due to the unconformity on top (Figure V-18) is interpreted as the upper submember. This submember is present all the way through the basin, even in Rattlesnakes Hills, and correlation lines indicate progradation as well as increase in thickness in a southeastern direction, from 100 metres in Maverick Springs area to almost 300 metres in the area of Hudson (Figure V-19), and the depocenter has changed from western areas for the middle submember to a more central position in the basin. The thickness variation from northwest to southeast is due to: 1) erosional thining under the Teapot unconformity which is greater to the west; and 2) accomodation space increase on the flooding surface with

increase to the southeast (Figure V-20). The Teapot Member increase in thickness towards the northwest, from less than 50 to 150 metres. The isopach map (Figure V-21) shows that the depositional centre of the Teapot is located in the northeast of the basin.

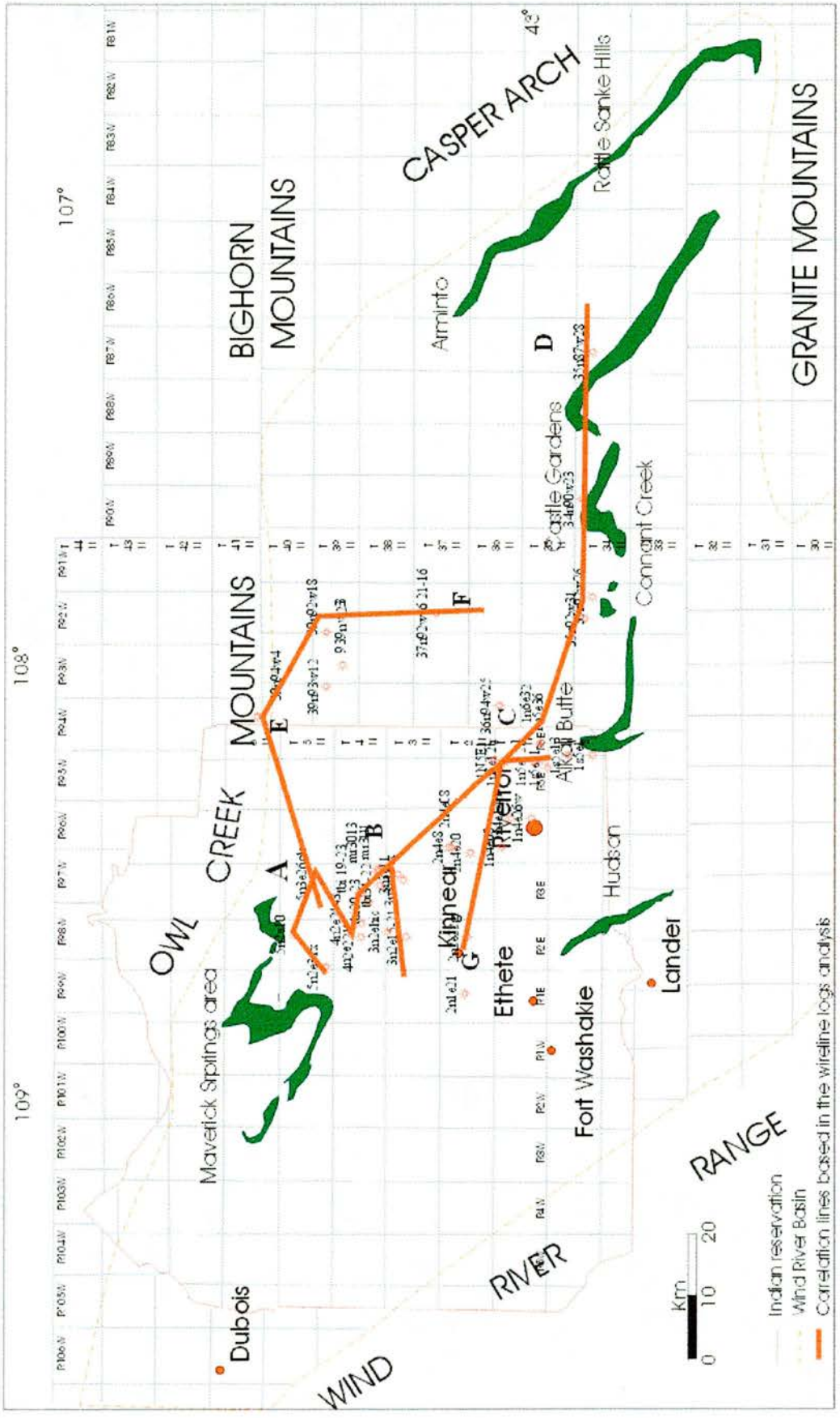

Figure V-10: Map showing location of wireline-logs, correlation lines and locations A-F of the panels.

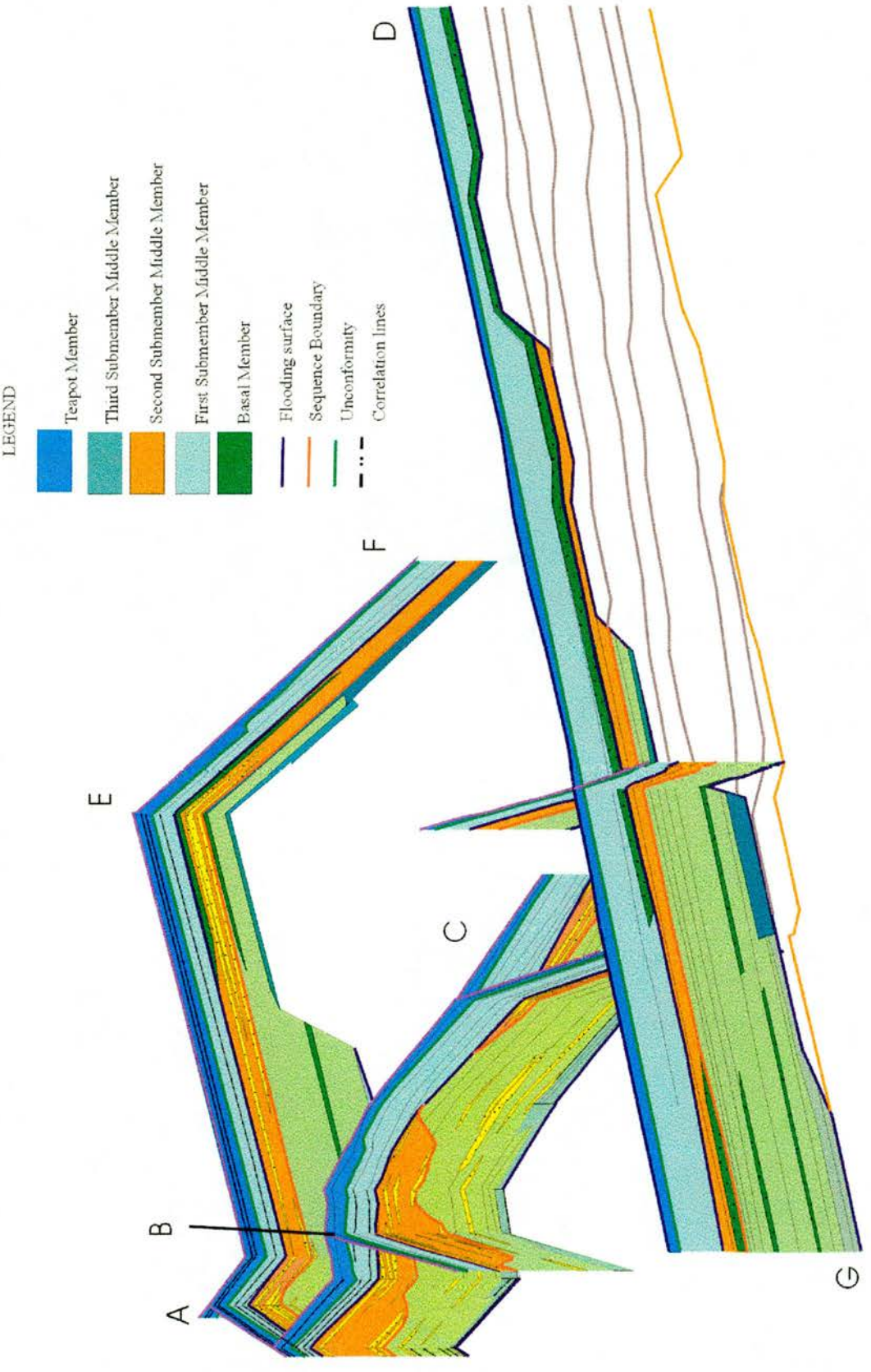

Figure V-11: Panel showing the results of the wireline-logs correlations (See Appendix 5). For locations A-F see Figure V-10.

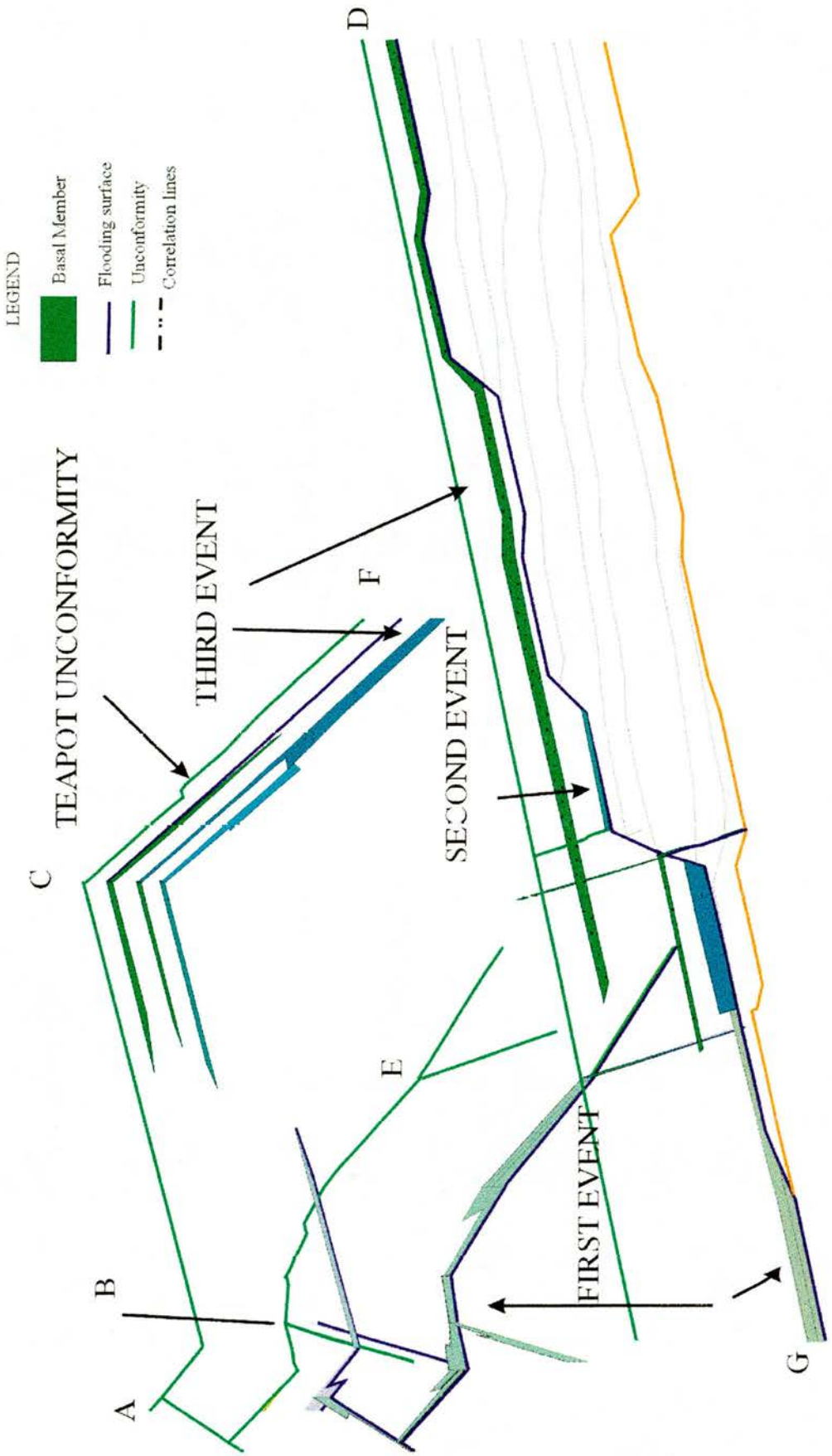

Figure V-12: Panel showing the results of the wireline-logs correlations for the Basal Member (See Appendix 5). For location of A-F see Figure V-10.

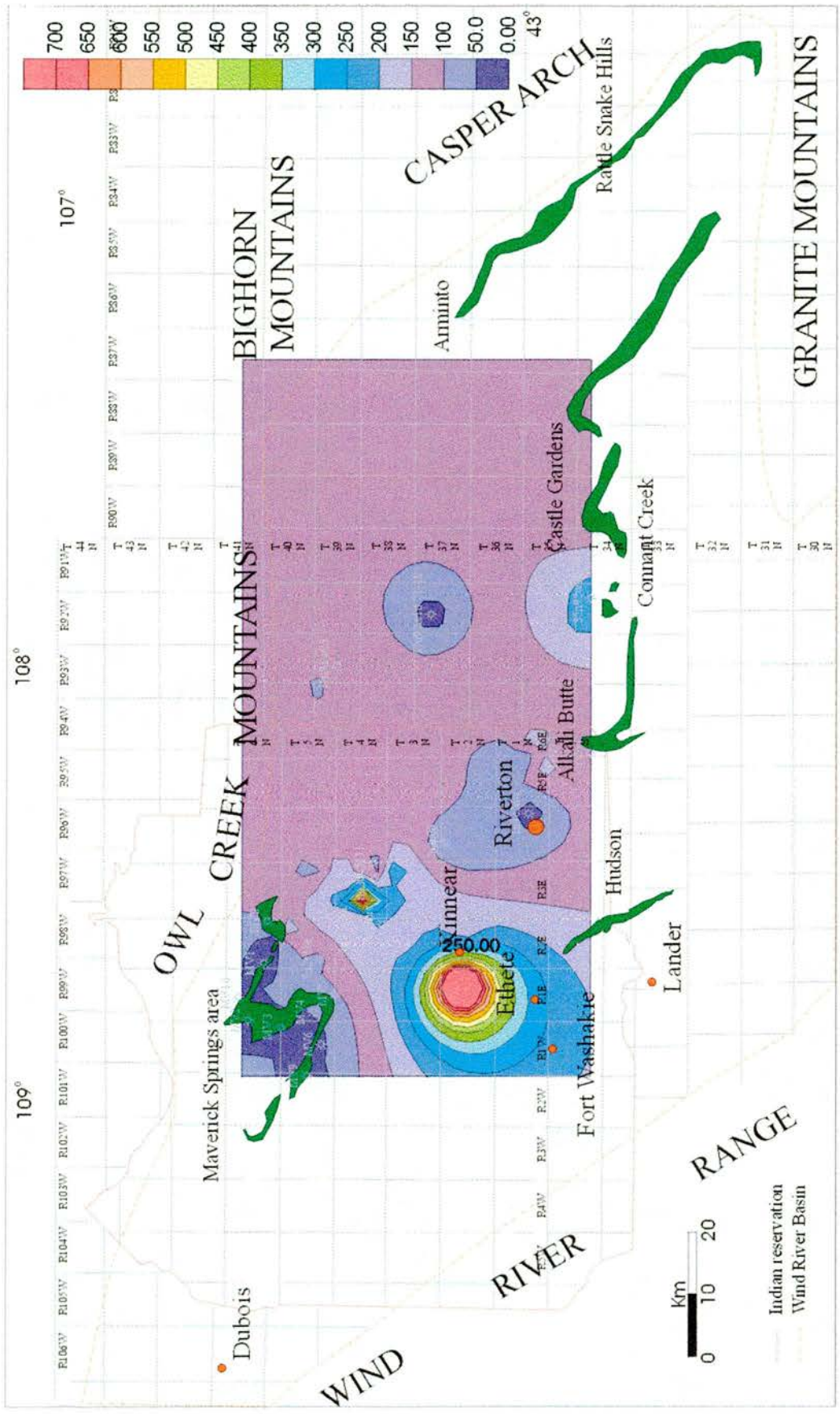

Figure V-13: Isopach map for the Basal Member of the Mesaverde Formation. Isopachs are based on both wireline-logs and outcrop measured sections.

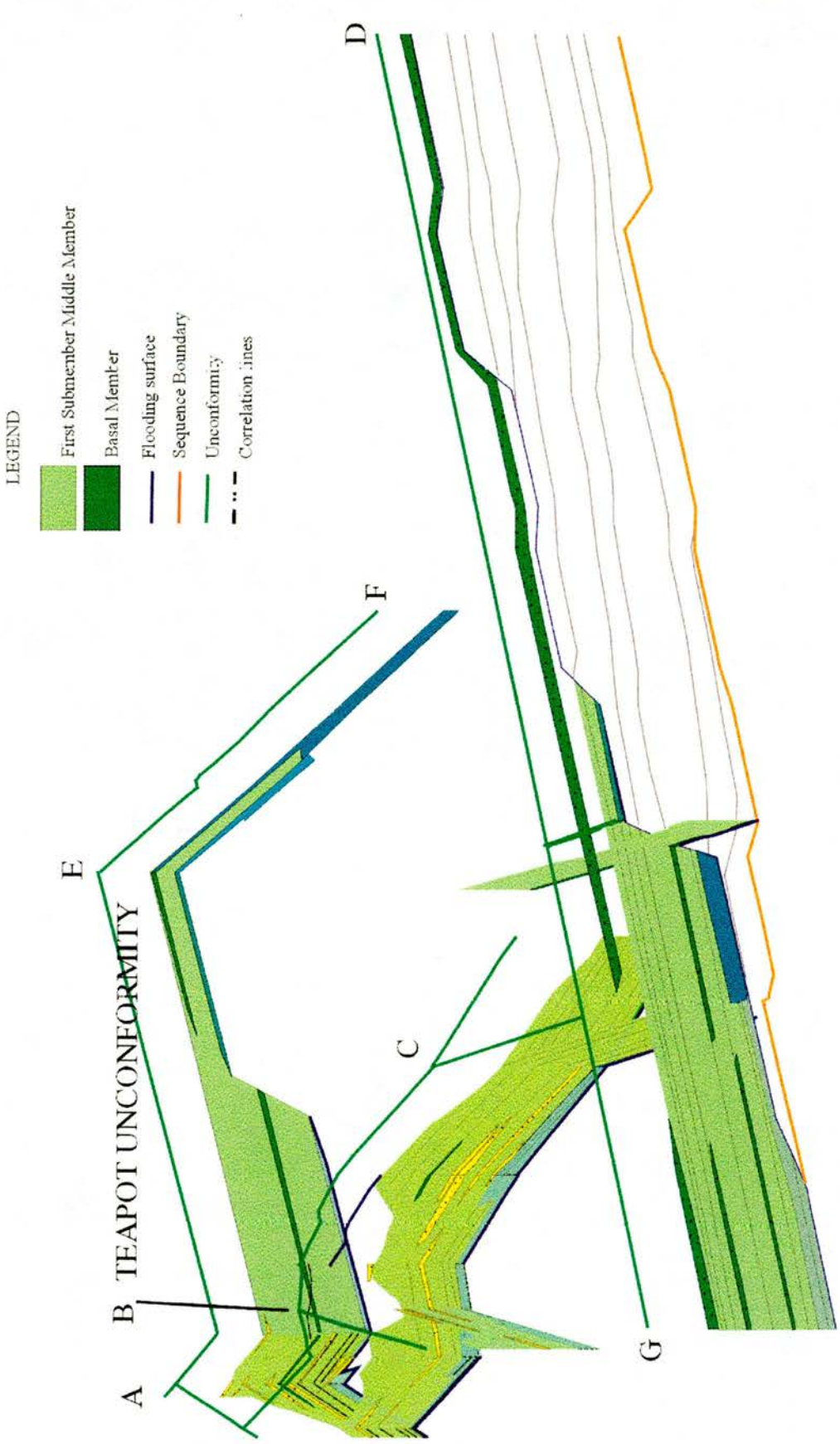

Figure V-14: Panel showing the results of the wireline-logs correlations for the first submember of the Middle Member(See Appendix 5). For locations A-F For locations A-F see Figure V-10.

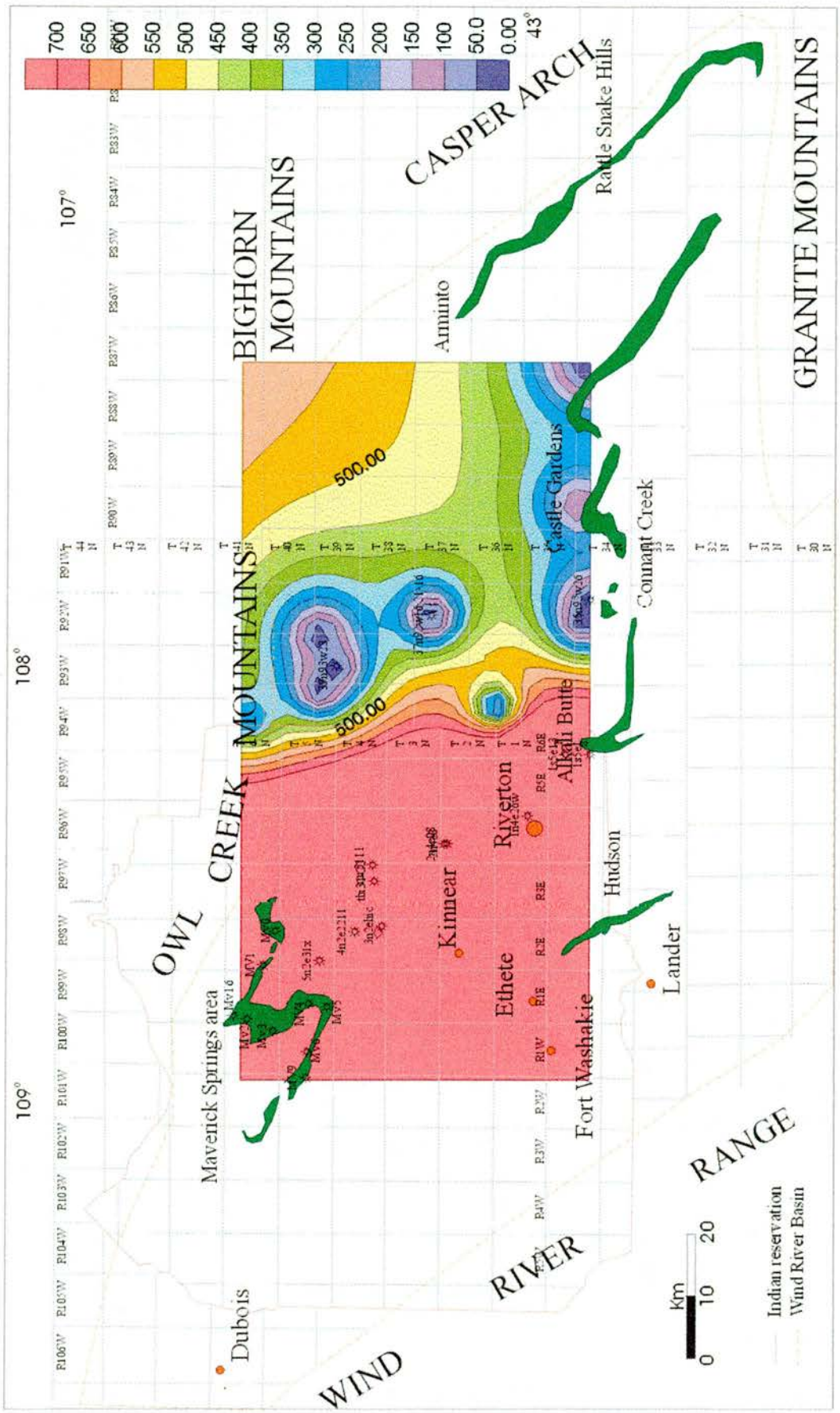

Figure V-15: Isopach map for the first submember of the Middle Member of the Mesaverde Formation. Isopachs based on both wireline-logs and outcrop measured sections.

Figure V-16: Panel showing the results of the wireline-logs correlations for the middle submember of the Middle Member (See Appendix 5). For locations of A-F see Figure V-10.

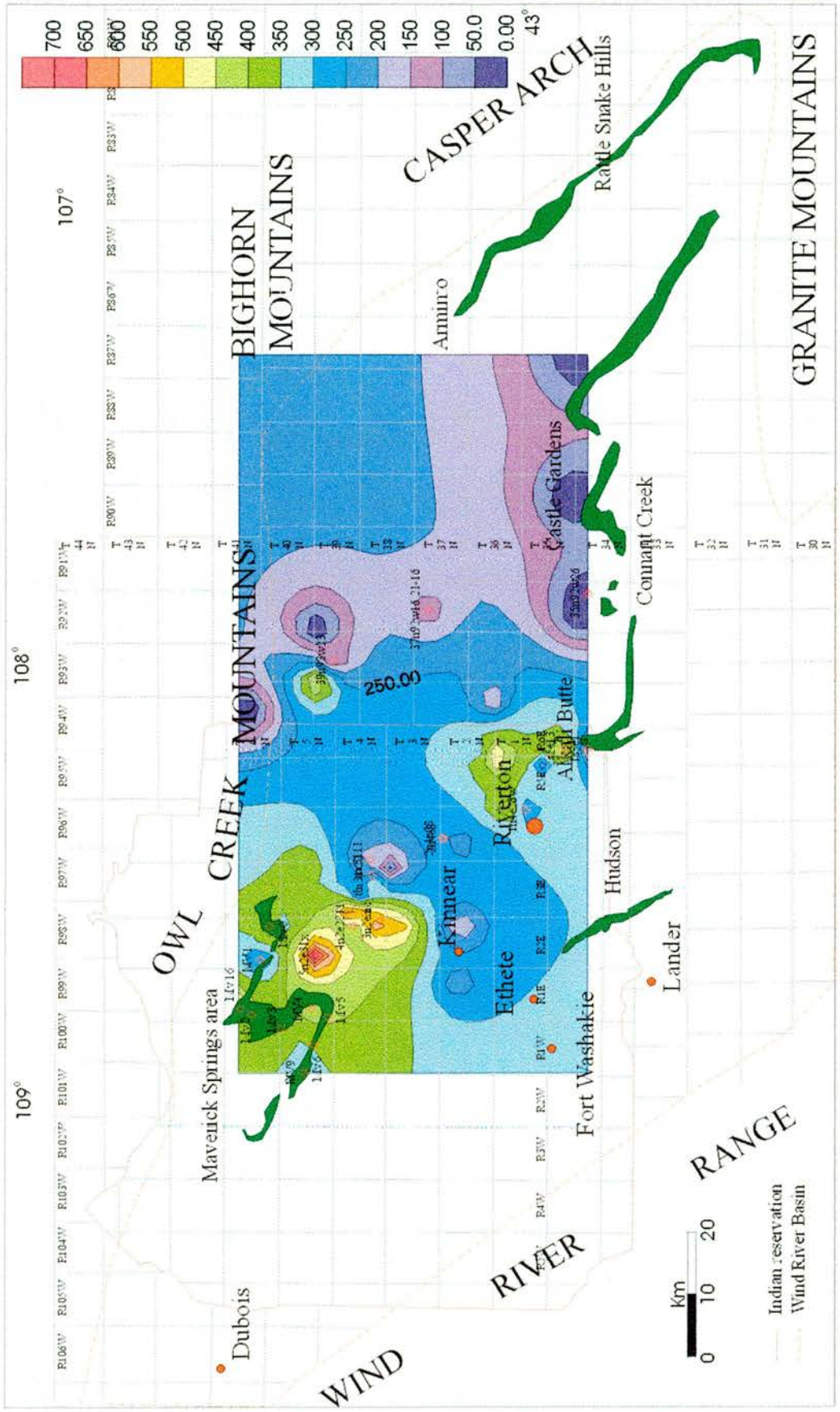

Figure V-17: Isopach map for the middle submember of the Middle Member the Mesaverde Formation. Isopachs based on both wireline-logs and outcrop measured sections.

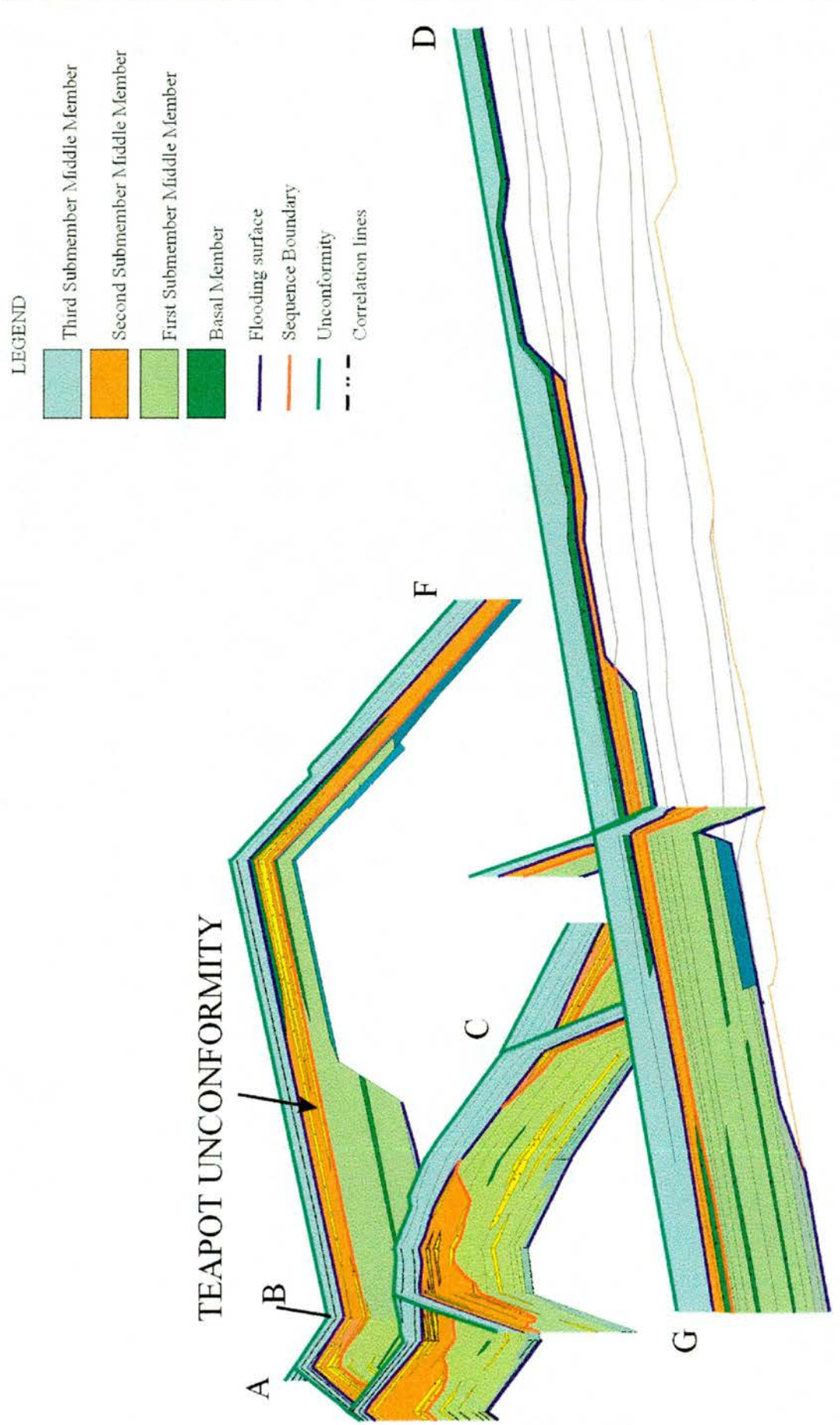

Figure V-18: Panel showing the results of the wireline-logs correlations for the upper submember of the Middle Member (See Appendix 5). For location of A-F see Figure V-10.

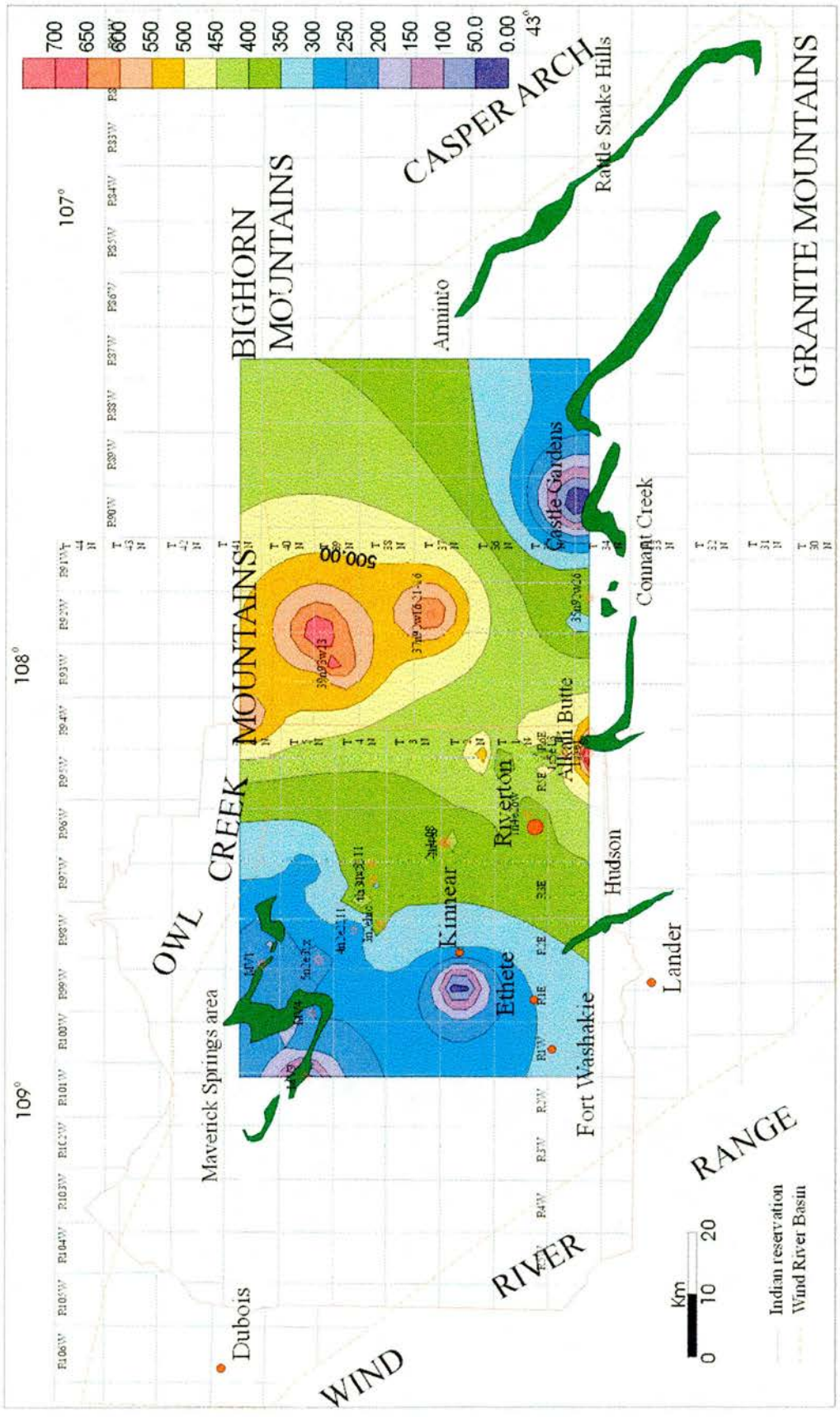

Figure V-19: Isopach map for the upper submember of the Middle Member of the Mesaverde Formation. Isopachs based on both wireline-logs and outcrop measured sections.

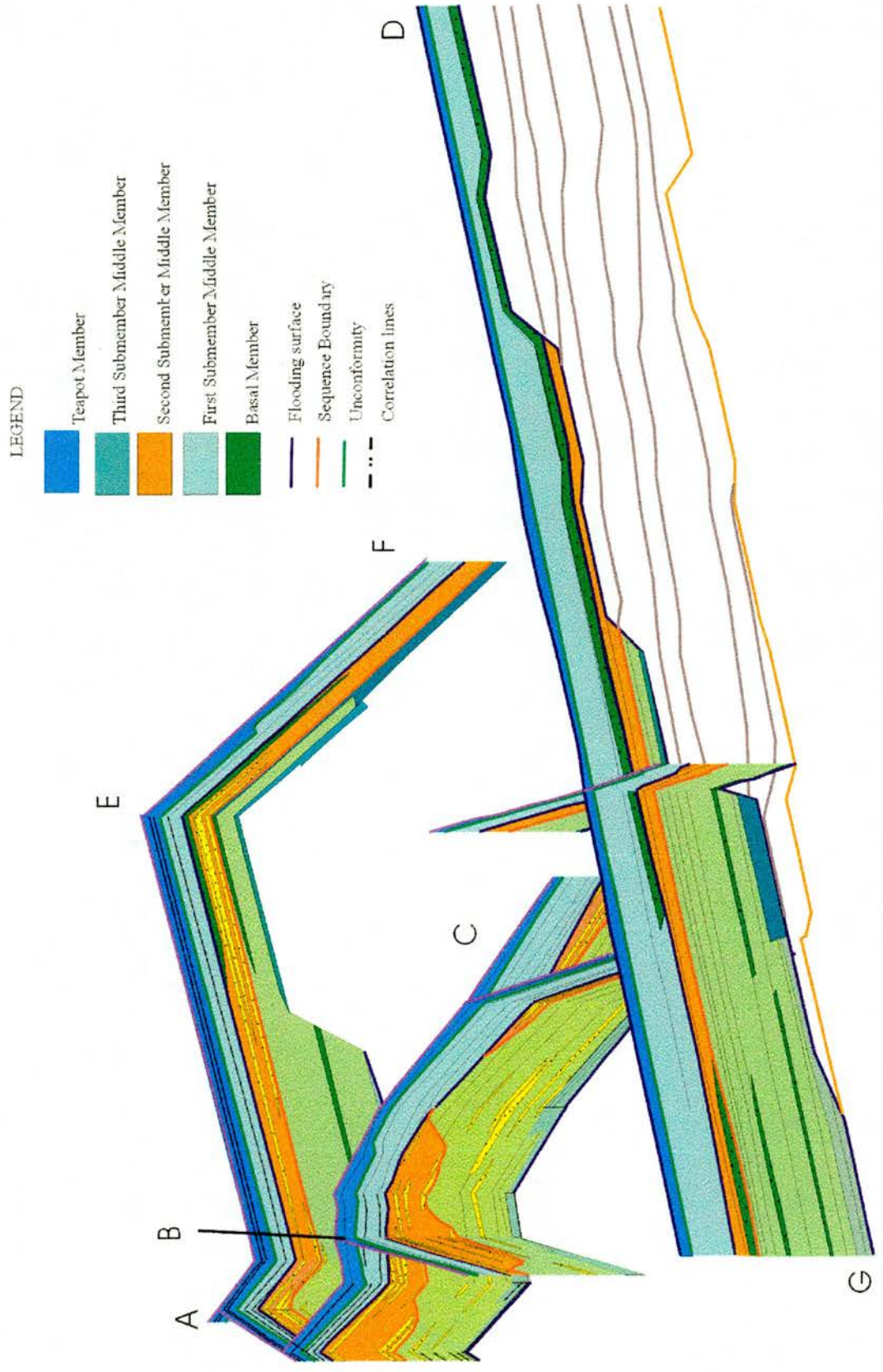

Figure V-20: Panel showing the results of the wireline-logs correlations for the Teapot Member (See Appendix 5). For location of A-F see Figure V-10.

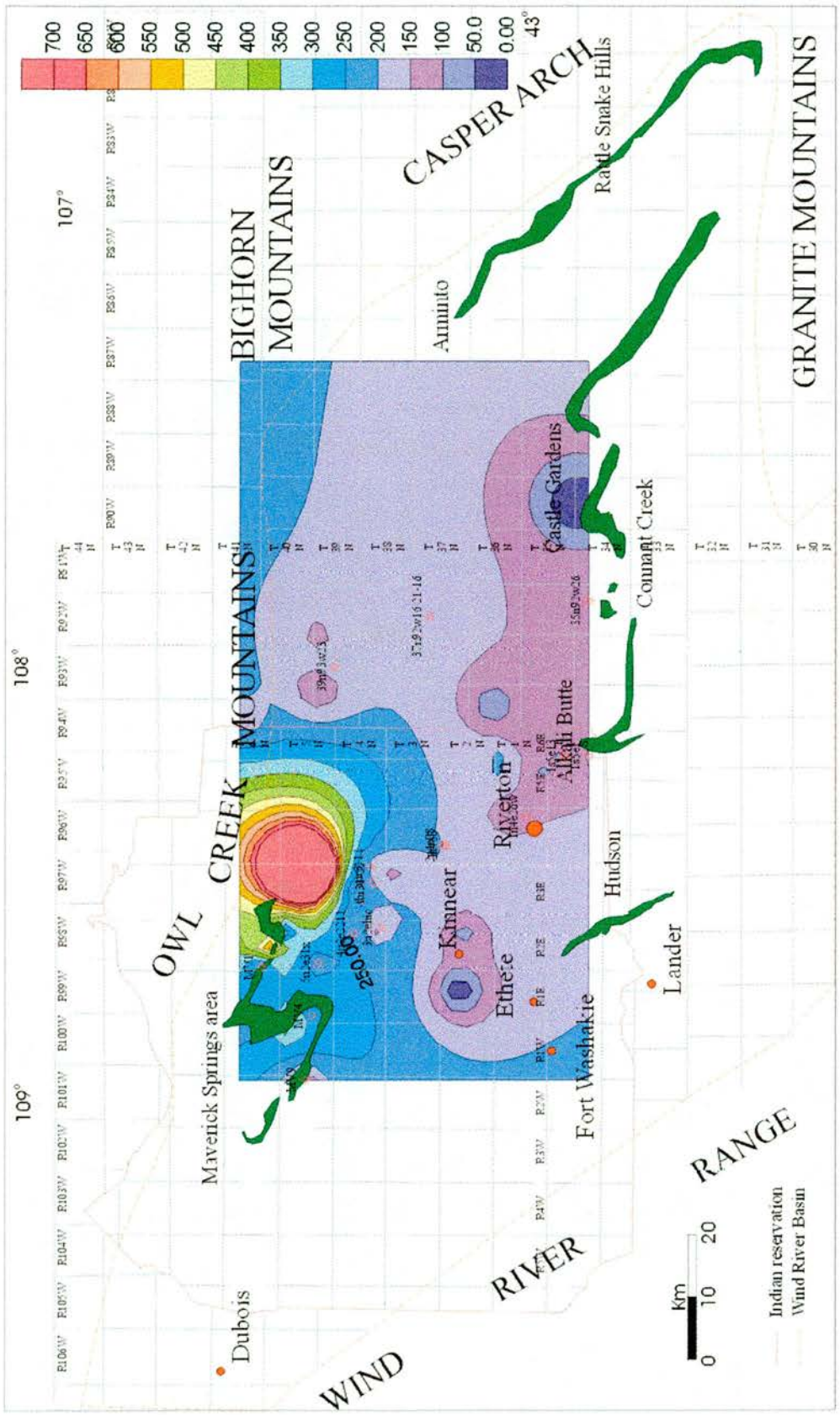

Figure V-21: Isopach map for the Teapot Member of the Mesaverde Formation. Isopachs based on both wireline-logs and outcrop measured sections.

Chapter VI

STRATIGRAPHY, DEPOSITIONAL FRAMEWORK AND RESERVOIR POTETIAL OF THE MESAVERDE FORMATION IN THE WIND RIVER BASIN

The analysis of the outcrop (see Chapter IV, Figure IV-1), the generation of outcrop analogues and the interpretation and correlation of events into the subsurface by comparing them to downhole wireline logs, leads to a new basinwide interpretation of the stratigraphy of the Mesaverde Formation in the Wind River Basin (Appendix 7-1 to 7-6).

In the northwestern exposures (Maverick Springs area), the upper Cody Formation is composed of a series of lower and middle shoreface deposits that change laterally into shelf deposits in a southern direction and represent a highstand system tract (Appendix 7-1). Although those deposits have porosities up to 20%, the high content of matrix and carbonate cement may reduce the permeability and suggests that they may have a moderate potential for being good reservoir rocks. Above these deposits, a regional erosive event took place (result of a relative rapid fall in sea level), with the generation of a sequence boundary (Appendix 7-2). This erosion generated a lowstand wedge deposit which, based in the analysis and correlation of wireline-logs, is interpreted to be a lowstand system tract, located towards the southern part of the basin (Riverton Dome). This lowstand wedge, composed of amalgamated shoreface sandstone bodies has a thickness of around 80 metres, is approximately 5-6 km wide and forms a linear belt trending northeast-southwest. This unit is very similar in geometry and architecture to other detached shoreface deposits of the Western

Interior Seaway, such as the Shannon, Sussex and Blair sandstones (Kristynik et al., 1995). Accomodation space then increased following a transgressive period, with the generation of laterally discontinuous estuarine/fluvial deposits that represent a basinward shift of facies at the top of the Cody Formation in Maverick Springs area (transgressive system tract) (Appendix 7-2). These deposits have high porosities (27%), but less carbonate cement is present (5%). The deposits are embedded in fine material and therefore represent potential good quality reservoirs in the localities of north of Riverton Dome.

Capping these deposits is a maximum flooding surface, above which occurs marine-influenced deposits in the Maverick Springs area (Appendix 7-3); these represent the upper shoreface dposits of the Basal Member. This Basal Member, linked genetically to the lower submember of the Middle Member above, appears to reflect a period of aggradation and progradation of the Mesaverde formed during a highstand system tract. I has porosities of ~29% and no carbonate cement and appears to increase in thickness towards the south of the Maverick Springs area (towards Pavillion), where it is composed of several amalgamated clean upper shoreface deposits (high potential for good reservoir quality). The delta plain deposits of the lower submember of the Middle Member are interpretd as the prograding landward equivalents to the Basal Member with an anastomosing fluvial style and high vertical interconnectivity of the sandstone bodies that are embedded in floodplain gines. These sandstones have porosities ranging between 10 and 18%, and the matrix and cement, although present, are not important constituents of the rocks, although they are not as laterally continuous as the shoreface deposits below. They represent potentially good reservoi units in the area south of Pavillion. The Basal Member and lower

submember of the Middle Member form a deltaic system that, in the area of Alkali Butte, records a facies change into correlative marine shelf deposits. These marine deposits appear to be lithologically like the lower and middle shoreface depoists of the Cody Formation, but the wireline-log and outcrop correlations lead to the interpretation of these deposits as being time equivalent to the Basal and lower submember of the Middle Member in the Maverick Springs area.

On top of this succession appears a new sequence boundary that forms the base of the middle submember of the Middle Member in the Maverick Springs area (interpretation based on wireline-log correlations), and this sequence boundary can be traced into the Ratlesnake Hills area, where it appears at the base of the Fales Member (Appendix 7-4). The middle submember (in the Maverick Springs area), composed of meandering fluvial deposits, is laterally correlative to the marine-influenced deposits represented by the Fales Member. In the Rattlesnake Hills area, the top of the Fales Member is placed at a regional flooding surface and is overlain by shelf deposits that have been called the Wallace Creek Tongue of the Cody Formation, The flooding surface at the top of the Fales Member can be correlated in the wireline-logs into the northwestern part of the basin, where it forms the base of the upper submember of the Middle Member (Appendix 7-5). Therefore, the Fales Member, with the sequence boundary at its base and capped by a flooding surface is interpreted as a lowstand deposit which was formed at the time of the generation of the sequence boundary, which also appears (albeit cryptically) at the base of the middle submember of the Middle Member in the Maverick Springs area. The Fales Member of the Mesaverde represents a very good quality reservoir unit, with

laterally continuous clean shoreface deposits with porosities up to 27% and no carbonate cement present, while the middle submember of the Mesaverde represents medium quality reservoir due to the low connectivity of the channelised deposits.

The upper submember of the Middle Member, on top of the flooding surface that can be traced into the Rattlesnake Hills area, is composed by a new anastomosing fluvial system (Appendix 7-5). This submember appears to have sandstone bodies with high connectivity, but reservoir quality may be reduced because although porosities can get up to 27%, matrix and cement are present in high amounts and this reduces the permeability. A new sequence boundary on top of this submember has been characterised in outcrop (Appendix 7-6). This sequence boundary is represented by an angular unconformity that in this study is thought to be controlled by uplift of the Wind Tiver Range around 75 m.y. (Reiners et al., 1999), with the resultant erosion of material and the generation of a broad alluvial plain, These deposits represent the Teapot Member, and contain sediment transport indicators that rotate from southeast to northeast through the member, and additionally record a decrease of incision in the same direction. The Teapot sandstones appear to be of good reservoir quality, with porosities of ~15-20%, but the density of the fractures found in some outcrops (which in the thin-section analysis appears characterised as containing no carbonate cement) could act as flow pathways for the hydrocarbons, reducing the Teapot's ability to act as a stratigraphic or structural trap (personal cmmunication; Parks, 1999).

As a result of the outcrop analysis and the wireline log correlations, it is observed that, although in outcrop in the southeastern areas the contact between the base of the Mesaverde has historically been placed at the surface between the

first marine-influenced sandstone and the "Cody like" lower and middle shoreface deposits, the lower and middle shoreface deposits are laterally equivalent to the deltaic system formed by the Basal and lower submember of the Middle Member in Maverick Springs area, Therefore, the good quality upper shoreface deposits that appear in Alkali Butte are part of this distal part of a delta system. In the Castle Gardens and Rattlesnake Hills areas, the good quality shoreface deposits are part of the Fales Member which represents the lowstand wedge equivalent to the sequence boundary at the base of the middle submember of the Middle Member in Maverick Springs area.

COMPARISON OF THE DEPOSITIONAL FRAMEWORK OF THE MESAVERDE FORMATION IN THE WIND RIVER BASIN, THE BIGHORN BASIN AND THE ROCK SPRINGS UPLIFT.

In the Bighorn Basin, northwestern Wyoming, the Mesaverde Group is comprised of two major clastic wedges (Fitzsimmons and Johnson, 2000). Here, the Mesaverde Group is classically divided into four formations, the Eagle, Claggett, Judith River and Teapot Sandstone (Mackenzie, 1975), names normally adopted in Montana. The Cody Formation in this area is composed of offshore and open shelf deposits, capped by a regional flooding surface and deltaic deposits that form the Eagle Formation that is part of the Mesaverde Group. Overlying the Eagle, is the Claggett Formation, composed of Offshore and open shelf deposits with a retrogradational stacking pattern (Fitzsimmons and Johnson, 2000). This succession is overlain by the Judith River Formation with a strongly progradational trend. Higher in the succession, the Teapot Formation is composed of estuarine deposits. Johnson et al. (1998) divided the Mesaverde strata into Basal, Middle and Teapot Members. For them, the Basal Member is

composed of shoreface deposits that have correlative delta-plain environments in a landward directions. The Middle part is also a lateral equivalent of the lower submember, and contains continental strata with channelised deposits in certain areas, whereas in other localities, the bulk of the deposit is composed of mainly fine-grained material and floodplain fines. In an easterly directions, these deposits become more marine-influenced. The contact with the overlying Teapot Member appears poorly defined, although this member appears thicker than in northern basins. Gill and Cobban (1966) believed that the base of the Teapot Sandstone Member marked a major hiatus throughout much of Wyoming as is found in the Wind River Basin.

In the Rock Springs Uplift, southwestern Wyoming, the Mesaverde Group is composed of four formations, the Blair, Rock Springs, Ericson Sandstone and Almond Formations (Martinsen et al., 1998). The Blair Formation is located on top of the Baxter Shale in sharp, sometimes erosional, contact. The deposits are laterally equivalent to the offshore deltaic environments of the lower Rock Springs Formation to the north; regional correlations record an abrupt seaward loss of coarse clastic deposition and the top records a maximum flooding surface on the top of the Blair. The Rock Springs Formation represents deltaic/shoreline deposits, overlain by coastal-plain to fluvial successions. The coastal-plain to fluvial succession is mud-dominated with discontinuous coals and single-storey, laterally accreting channelised sandstone bodies. Most of the progradational units observed in the northern part appear to intercalate and pinch-out into the Blair Shale. The Ericson Formation is composed of three members: the Trail Member (single-storey channel architecture with an unconformity at the base), the Rusty Member (delta plain facies and incised

estuarine valley-fill facies), and the Canyon Creek Member (formed by nested channels and meandering channels). The Ericson contains two unconformities; one at the base of the Trail Member and one at the base of the Canyon Creek Member (Martinsen et al., 1999). The top boundary with the underlying Almond Formation is erosional and interfingers with the Lewis Shale (Gill and Cobban, 1970). The Almond Formation is interpreted as being deposited in an inter-deltaic enbayment. It is formed by delta plain deposits that change upwards into shoreface and offshore sediments reflecting the transgressive nature of the succession (Martinsen et al., 1998).

Therefore, analysing the three basins, it seems possible that the Cody Formation in the Wind River Basin can be correlated to the Cody Formation in the Bighorn Basin and the Blair Formation in the Rock Springs Uplift; the Basal Member and lower submember of the Middle Member appear to be similar in depositional environments to the Eagle in the Bighorn Basin and the Rock Springs to the south (Rock Springs Uplift); the middle submember of the Middle Member may represent the time equivalent to the respective Clagget (in the north) and Trail and Rusty Members of the Ericson (in the south), although the Clagget may represent lowstand wedge deposits correlative to the Gales Member in the Wind River Basin. The upper submember of the Middle Member appears to be similar in nature to the Judith River to the north and the Canyon Creek Member of the Ericson Formation to the south. Finally, the Teapot appears to be represented to the north, and to correlate to the Almond Formation in the Rock Springs Uplift. Although no chronostratigraphy is presented to substantiate these potential correlations, the surface architecture and depositional trends appear similar in the three basins.

Chapter VII

CONCLUSIONS

As a result of this study, a new stratigraphic and depositional framework is constructed for the Mesaverde Formation in the Wind River Basin. The main new conclusions are summarised as follows:

- Of the three distinct members composing the succession (the Basal, Middle and Teapot Members) each of the Middle and Teapot Members are further subdivided into three submembers.

- From the outcrop analysis, 10 facies associations can be recognised and they record a wide range of environments: marine, marine-influenced, fluvial/estuarine, delta-plain, meandering, anastomosed and braided fluvial deposits.

- The continental deposits are found mainly in the northwestern part of the basin where the bulk of the sediment is composed of channelised and floodplain deposits, with the exception of the Basal Member that represents upper shoreface deposits.

- Towards the south and southeastern parts of the basin, the fluvial deposits become thinner and are more marine-influenced. Towards this area (between Hudson and Alkali Butte), a lateral facies change from fluvial deposits to their correlative marine-influenced and marine deposits occurs.

- Palaeocurrent trends indicate a general southeastern trend of transport, with a northwestern source area of material, for the Basal and Middle Members. However, palaeocurrent directions for the Basal Member vary somewhat at different localities and reflect changes in the strike of the shoreline

for these localities. The Teapot composition and palaeocurrent indicators reflect the progressive change to a western source area with a transport trend towards the east. This change of source area and transport direction could be related to the uplift of the Wind River Range, that recent studies (Reiner et al., 1999) date at ~75 m.y., and corresponds to the timing for the base of the Teapot Member approximately (Barwin, 1961; Keefer and Rich, 1957).

- Based on the thin-sections analysis, the Mesaverde sandstones are classified as quartz-arenites, litharenites and subarkoses. A few subgraywackes are present.

- The thin-section and statistical analyses of the data lead to the differentiation of the Upper Cody sandstones from the Basal Member of the Mesaverde Formation, based on the lack of rock fragments and carbonate cement in the latter. The lack of rock fragments implies differences of source of material. Differences between the percentages of metamorphic rock-fragments in the Middle Member and Teapot Member sandstones are also found and this also reflects the change of source material between these two members of the Mesaverde Formation. Changes in cement content are found between the channelised deposits of the Middle Member in northern and southeastern parts of the basin, and this is interpreted to be related to increased marine influence in the southern part of the basin.

- Correlations made between wireline-logs, measured sections and gamma-ray logs obtained with a hand-held scintilometer appear to be useful in the characterisation of "electrofacies" and the interpretation of those as the facies association explained earlier.

- With the "electrofacies" characterisation and the characterisation of the different members present in the Mesaverde Formation, correlation between wireline-logs and the outcrop permit the development of a stratigraphic framework of the Mesaverde Formation in the Wind River Basin. It can be summarised as:

1) The lower and middle shoreface deposits of the Cody Formation were subject to local transgressive events that eroded their upper shoreface deposits. A fall in relative sea level generated a regional erosive surface at the top of these deposits that was followed by a transgressive period with the generation of laterally discontinuous fluvial/estuarine deposits on top of the surface. These two surfaces are therefore interpreted as flooding surfaces coincident with sequence boundaries.

2) The regional flooding event is interpreted as representing the limit between the Cody and Mesaverde Formations in the sense of Galloway (1989).

3) In Maverick Springs area, Mesaverde deposition begins with the upper shoreface deposits of the Basal Member overlain by its landward equivalents represented by the lower submember of the Middle Member; these are interpreted as wave influenced delta-plain environments with a clear progradational trend towards the southeast. The Basal Member appears to prograde in a southeastern direction through four "jumps". Together, the succession is interpreted as a deltaic complex which is present till the area of Alkali Butte, where it grades into delta front facies (Cody-like lithologies).

4) A new regional relative fall in sea level at top of the lower submember of the Middle Member generates a sequence boundary and the concomitant regression. This appears as a basinward shift of facies (that is particularly evident in the southeast), with the formation of the following transgressive event and the generation of fluvial/estuarine deposits that form the middle submember of the Middle Member (Maverick Springs area) and these are traceable into Rattlesnake Hills area, where their lateral marine-influenced equivalent, the Fales Member, grades farther basinward into "Cody like" deposits.

5) After this, a flooding event recognised by wireline-logs into the Maverick Springs area, forms the limit between the deposits of the middle submember and the anastomosing fluvial deposits of the upper submember of the Middle Member. Therefore, the Fales Member, with the sequence boundary at its base and the flooding surface at its top, is interpreted as a lowstand wedge.

6) On top of the upper submember of the Middle Member, an erosional surface cuts down into almost two thirds of the upper submember thickness in the western part of the Maverick Springs area (section MV9). This angular unconformity is interpreted as a new sequence boundary that separated the anastomosing fluvial system of the upper submember of the Middle Member from the braided deposits that form the basal unit of the Teapot Member.

7) The generation of braided, meandering and then braided deposits of the Teapot Member form the top member of the Mesaverde Formation in this basin.

- This stratigraphic framework records 3 periods of low rates of accommodation space within an overall progradational stratigraphic arrangement.
- The "Cody-like" deposits found in southeastern areas are interpreted as being chronostratigraphically equivalent to the Basal and lower submember of the Middle Member in Maverick Springs area, and therefore, they do not represent marine Cody tongues interpreted by other authors (Keefer and Rich, 1957; Barwin, 1961; Gill and Cobban, 1966).

REFERENCES

ALLEN, J.R.L. *"Studies in fluviatile sedimentation; six cyclothems from the lower Old Red Sandstone, Anglowelsh Basin"*. SEDIMENTOLOGY, V.3. N. 3. (1964). PP. 163-198.

ARMSTRONG, F.C. *"Sevier Orogenic belt in Nevada and Utah."* NORTH AMERICAN THRUST-FAULTED TERRANES. SELECTED PAPERS FROM THE AAPG, N. 27. (1984). PP. 405-434.

ARMSTRONG, F.C. AND ORIEL, S.S. *"Tectonic development of the Idaho-Wyoming thrust belt"*. AAPG BULLETIN, V.9, N.11. (1966). PP.1847-1866.

ASLAN, A. AND AUSTIN, W.J. *"Holocene flood-plain soil formation in the southern lower Mississippi valley: implications for interpreting alluvial paleosols"*. GSA BULLETIN, V. 110. (1998). PP. 433-440.

ASQUITH, D.O. *"Depositional topography and major marine environments, Later Cretaceous, Wyoming"*. AAPG BULLETIN, V. 54. (1970). PP. 1184-1224.

BARWIN, J.R. *"Stratigraphy of the Mesaverde Formation in the southern part of the Wind River Basin, Wyoming"*. WYOMING GEOLOGICAL ASSOCIATION GUIDEBOOK. (1961). PP. 171-179.

BERRYHILL, H.L., BROWN, D.M., BROWN, A. AND TAYLOR, D.A. *"Coal resources of Wyoming"*. U.S. GEOLOGICAL SURVEY CIRCULAR 81. (1950). PP. 78.

BOWN, T.M. AND KRAUS, M.J. *"Integration of channel and floodplain suites; I. Developmental sequence and lateral relations of alluvial paleosols"*. JOURNAL OF SEDIMENTARY PETROLOGY, V. 57. (1987) PP. 587-601.

BOWN, T.M. AND KRAUS, M.J. *"Geology and paeoenvironment of the Oligocene Jebel Qatrani Formation and adjacent rocks, Fayum depression, Egypt"*. U.S. GEOLOGICAL SURVEY PROFESSIONAL PAPER 1452. (1988). PP. 64.

BRIDGE, J.S. AND LEEDER, M.R. *"A simulation model of alluvial stratigraphy"*. SEDIMENTOLOGY, V. 26. N. 5. (1979). PP. 617-644.

CAMPBELL, C.V. *"Truncated wave-ripple laminae"*. JOURNAL OF SEDIMENTARY PETROLOGY, V. 36. (1966). PP. 825-828.

CANT, D. *"Subsurface facies analysis"*. In: FACIES MODELS: RESPONSE TO SEA LEVEL CHANGE. AMERICAN ASSOCIATION OF CANADA. (1992). PP. 27-47.

CANT, D.C. AND STOCKMAL, G.S. *"The Alberta foreland basin-relationship between stratigraphy and cordilleran terrane-accretion events.* CANADIAN JOURNAL OF EARTH SCIENCE, V. 26. (1989). PP. 1964-1975.

COBBAN, W.A. AND HOOK, S.C. *"Mid-Cretaceous molluscan biostratigraphy and paleogeography of southwestern part of Western Interior, United States"*. JURASSIC-CRETACEOUS BIOCHRONOLOGY AND PALEOGEOGRAPHY OF NORTH-AMERICA. GEOLOGICAL ASSOCIATION OF CANADA SPECIAL PAPER 27. (1984). PP. 257-271.

COLEMAN, J.M. AND GAGLIANO, S.M. *"Cyclic sedimentation in the Mississippi River deltaic plain"*. TRANSATIONS GULF COAST ASSOCIATION OF GEOLOGICAL SOCIETIES, 14. (1964). PP. 67-80.

COLEMAN, J.M. AND PRIOR, D.B. *"Deltaic environments"*. SANDSTONE DEPOSITIONAL ENVIRONMENTS. MEMOIR AMERICAN ASSOCIATION OF PETROLEUM GEOLOGISTS, 31. (1982). PP. 139-178.

CROSS, T.A. *"Tectonic controls of foreland basin subsidence and Laramide style deformation, Western United States"*. SPECIAL PUBLICATION INTERNATIONAL ASSOCIATION SEDIMENTOLOGISTS, 8. (1986). PP. 15-39.

DeCELLES, P. *"Late Cretaceous-Paleocene synorogenic sedimentation and kinematic history of the Sevier thrust belt, northeast Utah and southwest Wyoming"*. GEOLOGICAL SOCIETY OF AMERICA BULLETIN, V. 106. (1994). PP. 32-56.

DeCELLES, P.G. AND GILES,K.A. *"Foreland basin systems"*. BASIN RESEARCH. BLACKWELL SCIENCE LTD. (1996). PP. 105-123.

DeCELLES, P.G., LAWTON, T.F. AND MITRA, G. *"Thrust timing, growth of structural culminations, and synorogenic sedimentation in the type Sevier orogenic belt, Western United States"*. GEOLOGY, V. 23. (1995). PP. 699-702.

DICKINSON, W.R. AND SNYDER, W.S. *"Plate tectonics of the Laramide orogeny"*. In: LARAMIDE FOLDING ASSOCIATD WITH BASEMENT BLOCK FAULTING IN THE WESTERN UNITED STATES. MEMORIA GEOLOGICAL SOCCIETY AMMERICA, 151. (1978). PP. 355-366.

EARDLEY, A.J. *"Structural geology of North America"*. HARPER AND BROTHERS, NEW YORK. (1951). PP. 624.

EICHER, D.L. *"Foraminifera from Belle Fourche Shale and equeivalents, Wyoming and Montana"*. JOURNAL OF PALEONTOLOGY, V. 41. N. 1. (1967). PP. 167-188.

FLEMING, P.B. AND JORDAN, T. *"A synthetic stratigraphic model of Foreland Basin development"* JOURNAL OF GEOPHYSICAL RESEARCH, VOL.94. N.94. (1989), PP 3851-3866.

FLEMING, P.B. AND JORDAN, T. *"Stratigraphic modeling of foreland basins: Interpreting thrust deformation and lithosphere rheology."* GEOLOGY, V.18. (1990). PP.430-434.

GILL, J.R. AND COBBAN, W.A. *"Muddy sandstone-Wind River Basin"*. WYOMING GEOLOGICAL ASSOCIATION. GEOLOGICAL SURVEY RESEARCH PROFESSIONAL PAPER 550-B. (1966). PP. B20-B27.

GLANCY, Jr T.J., ARTHUR, M.A., BARRON, E.J. AND KAUFFMAN, E.G. *"A paleoclimate model for the North American Cretaceous (Cenomanian-Turonian) epicontinental sea"*. GEOLOGICAL ASSOCIATION OF CANANDA SPECIAL PAPER 39. (1993). PP. 219-241.

GRIES, R. *"Oil and gas prospecting beneath Precambrian of foreland thrust plates in Rocky Mountains"*. AAPG BULLETIN, V. 67. N. 1. (1983). PP. 1-28.

HAQ, B.U., HARDENBOL, J. AND VAIL, P.R. *"Mesozoic and Cenozoic chronostratigraphy and cycles of sea level change"*. In: SEA LEVEL CHANGES: AN INTEGRATED APPROACH. SOCIETY OF ECONOMIC PALEONTOLOGISTS AND MINERALOGISTS, SPECIAL PUBLICATION, 42. (1988). PP. 71-108.

HELLER, P.L. AND PAOLA, C. *"Stream changes in alluvial architecture: an exploration of controls on channel-stacking patterns"*. JOURNAL OF SEDIMENTARY RESEARCH, VOL. 66. N. 2. (1996). PP. 297-306.

HOLMES, W.H. U.S. GEOLOGICAL AND GEOGRAPHICAL SURVEY TERR. (HAYDEN), 9TH ANNUAL REPORT. (1877). PP. 237-276.

HOWARD, J.D. *"Trace fossils as criteria for recognizing shorelines in stratigraphic record"*. In: RECOGNITION OF ANCIENT SEDIMENTARY ENVIRONMENTS. SEPM SPECIAL PUBLICATION, 26. (1972). PP. 215-225.

JOHNSON, R.C. AND RICE, D.D. *"Variations in composition and origins of gases from coal bed and conventional reservoirs, Wind River Basin"*. WYOMING GEOLOGICAL ASSOCIATION GUIDEBOOK. SPECIAL SYMPOSIUM. (1993). PP. 319-336.

JOHNSON, R.C.; CLARK, A.C. AND BAKER, C.E. *"Coalbed methane potential of the Upper Cretaceous Mesaverde and Meeteetse Formations, Wind River Basin, Wyoming"*. WYOMING GEOLOGICAL ASSOCIATION GUIDEBOOK. SPECIAL SYMPOSIUM (1993). PP. 215-242.

JORDAN, T.E. *"Thrust loads and foreland basin evolution, Cretaceous, Western United States"*. AAPG BULLETIN. V. 65, N. 12. (1981).

KAUFFMAN, E.G. *"A field guide to the stratigraphy, geochemestry, and depositional environments of the Kiowa-Skull Creek, Greenhorn, and Niobrara marine cycles in the Pueblo-Canon City area, Colorado"*. In: FINE GRAINED DEPOSITS AND BIOFACIES OF THE CRETACEOUS WESTERN INTERIOR SEAWAY: EVIDENCE OF CYCLIC SEDIMENTARY PROCESSES. SOCIETY OF ECONOMIC PALEONTOLOGISTS AND MINERALOGISTS SECOND ANNUAL MIDYEAR MEETING. (1985).

KAUFFMAN, E.G. *"Illustrated guide to biostratigraphically Cretaceous macrofossils, Western Interior Basin, U.S.A."*. ROCKY MOUNTAIN ASSOCIATION OF GEOLOGISTS. DENVER. (1977). PP. 225-274.

KAUFFMAN, E.G. *"Cretaceous marine cycles of the Western Interior"*. THE MOUNTAIN GEOLOGISTS, 6. N. 4. ROCKY MOUNTAIN ASSOCIATION OF GEOLOGISTS. (1969). PP. 227-245.

KAUFFMAN, E.G., ELDER, W.P. AND SAGEMAN, B.D. *"High-resolution correlation; a new tool in chronostratigraphy"*. In: CYCLES AND EVENTS IN STRATIGRAPHY. (1991). PP. 795-819.

KAUFFMAN, E.G. AND CADWELL, W.G.E. *"The Western Interior basin in space and time"*. EVOLUTION OF THE WESTERN INTERIOR BASIN. GEOLOGICAL ASSOCIATION OF CANADA SPECIAL PAPER 39. (1993). PP. 1-30.

KEEFER, R.W. *"Structural geology of the Wind River Basin, Wyoming"*. U.S. GEOLOGICAL SURVEY PROFESSIONAL PAPER 495-D. (1970). PP. 35.

KEEFER, W.R. and JOHNSON, R. *"Stratigraphy and Oil and Gas Resources in Uppermost Cretaceous and Paleocene rocks, Wind River Basin, Wyoming."* WYOMING GEOLOGICAL ASSOCIATION GUIDEBOOK. SPECIAL SYMPOSIUM. (1993). PP. 71-86.

KEEFER, W.R. AND RICH, E.I. *"Stratigraphy of the Cody shale and younguer Cretaceous and Paleocene rocks in the western and southern parts of the Wind River Basin, Wyoming"* WYOMING GEOLOGICAL ASSOCIATION GUIDEBOOK. (1957). PP. 71-78.

KEEFER, W.R. AND VAN LIEW. *Paleozoic formations in the Wind River Basin, Wyoming"*. U.S. GEOLOGICAL SURVEY PROFESSIONAL PAPER 495-B. (1966). PP. B35-49.

KEEFER. W.R. AND TROYER, M.L. *"Stratigraphy of the Upper Cretaceous and Lower Tertiary rocks of the Shotgun Butte area, Fremont County, Wyoming"*. U.S. GEOLOGICAL SURVEY OIL AND GAS INVESTIGATIONS CHART OC-56. (1956).

KEEFER. W.R. AND TROYER, M.L. *"Geology of the Shotgun Butte area, Fremont county, Wyoming"*. U.S. GEOLOGICAL SURVEY BULLETIN 1157. (1964). PP. 123.

KEFFER, W.R. *"Frontier, Cody and Mesaverde Formations in the Wind River and southern Bighorn Basins, Wyoming"*. U.S. GEOLOGICAL SURVEY PROFESSIONAL PAPER 495-E. (1972). PP. 23.

KRAUS, M.J. *"Integration of channel and floodplain suites II. Vertical relations of alluvial paleosols"*. JOURNAL OF SEDIMENTARY PETROLOGY, VOL. 57. N. 4. (1987). PP. 602-612.

KRAUS, M.J. "*Recognizing avulsion deposits in the ancient stratigraphic record"*. GSA ABSSTRACTS WITH PROGRAMS, V. 30. N.7. (1988). A-192.

KRYSTINIK, L.F. AND BLAKENEY DEJARNETT, B. *"Lateral variability of sequence stratigraphic framework in the Campanian and Lower Maastrichtian of the Western Interior Seaway"*. In: SEQUENCE STRATIGRAPHY OF FORELAND BASIN DEPOSITS. MEMOIR AAPG, N. 64. (1995). PP. 11-26.

LAWTON, T.F.; BOYER, S.E. AND SCHMITT, J.G. *"Influence of inherited traper on structural variability and conglomerate distribution, Cordilleran fold and thrust belt, Western United States"*. GEOLOGY, V. 22. (1994). PP. 339-342.

LOVE, J.D. AND CHRISTENSEN, A.C. *"Geologic map of Wyoming"*. U.S. GEOLOGICAL SURVEY, SCALE 1:500,000. (1985).

MACKENZIE, M. G."*Stratigraphy and petrology of the Mesaverde Group: southern part of the Bighorn Basin, Wyoming"*. PH.D. THESIS .TULANE UNIVERSITY, (1975). PP.166.

MCCARTHY, P.J.; MARTINI, I.P. AND LECKIE, D.A. *"Anatomy and evolution of a Lower Cretaceous alluvial plain: sedimentology and palaeosols in the Upper Blairmore Group, South-western Alberta, Canada".* SEDIMENTOLOGY, V. 44. (1997). PP. 197-220.

MCGREEVY, L.J., HODSON, W.G. AND RUCKER, IV, S.J. *"Ground-water resources of the Wind River Indian Reservation, Wyoming".* U.S. GEOLOGICAL SURVEY, WATER SUPPLY PAPER 1375, (1969). PP 205.

MEREWETHER, E.A. AND COBBAN, W.A. *"Biostratigraphic units and tectonism in the Mid-Cretaceous foreland of Wyoming, Colorado and adjoining areas."* AAPG MEMOIR 41. PALAEOTECTONICS AND SEDIMENTATION IN THE ROCKY MOUNTAIN REGION, UNITED STATES. J.A. PETERSON. (1986). PP. 443-468.

MIALL, A.D." *The architecture of fluvial-deltaic sequences in the upper Mesaverde Group (Upper Cretaceous), book Cliffs, Utah".* BRAIDED RIVERS. GEOLOGICAL SOCIETY SPECIAL PUBLICATION, N.75. (1988). PP. 305-332.

MIERAS, B.L. SAGEMAN, B.B AND KAUFFMAN, E.G. "*Trace fossil distribution patterns in Cretaceous facies of the Western Interior Basin, North America".* In: KAUFFMAN, E.G. EDS. EVOLUTION OF THE WESTERN INTERIOR BASIN: GEOLOGICAL ASSOCIATION OF CANADA, SPECIAL PAPER 39. (1993) PP. 585-620.

MOLZER, P.C. AND ERSLEV, E.A. "*Oblique convergence during Northeast-Southwest Laramide compression along the East-West Owl Creek and Casper Mountain Arches, Central Wyoming."* AAPG BULLETIN, V. 79. N.9 (1995) PP. 1337-1394.

MURPHY, J.F. AND ROBERTS, R.W. *"Geology of the Steamboat Butte-Pilot Butte area, Fremont County, Wyoming".* U.S. GEOLOGICAL SURVEY, OIL AND GAS INVESTIGATIONS MAP 0M 151. (1954).

MYERS, K.J. AND WIGNALL, P.B. *"Understanding Jurassic organic-rich mudrocks; new concepts using gamma-ray spectrometry and plaeo-ecology; examples from the Kimmeridge clay of Dorset and the Jet Rock of Yorkshire".* In: MARINE CLASTIC SEDIMENTOLOGY; CONCEPTS AND CASE STUDIES. (1987). PP. 172-189.

NADON, G.C. *"The genesis and recognition of anastomosed fluvial deposits: data from the St. Mary River Formation, southwestern Alberta, Canada".* JOURNAL OF SEDIMENTARY RESEARCH, V. B64. (1994). PP. 451-463.

ORIEL, S.S. AND ARMSTRONG, F.C. *"Tectonic development of the Idaho-Wyoming thrust belt: authors commentary".* Adapted from AAPG BULLETIN, V. 50. N.12. (1966). PP.2612-262.

ORIEL, S.S. AND ARMSTRONG, F.C. *"Times of thrusting in Idaho-Wyoming thrust belt: Reply".* Adapted from AAPG BULLETIN, V. 50. N.12. (1966). PP. 2612-262.

PANG, M. *"Tectonic subsidence of the Cretaceous Western Interior Basin, United States".* PHD THESIS, LOUISIANA STATE UNIVERSITY AND AGRICULTURAL AND MECHANICAL COLLEGE. DEPARTMENT OF GEOLOGY AND GEOPHYSICS. (1994). PP. 222.

PARKER, L.R. AND BALSLEY, J.K. *"Paleocecology of the coastal margin coal-forming swamps in the Upper Cretaceous Blackhawk Formation of central Utah".* GEOLOGICAL SOCIETY OF AMERICA. ABSTRACTS WITH PROGRAMS, 9. N. 7. (1977). PP. 1125-1126.

PARRISH, J. T., GAYNER, G.C. AND SWIFT, D.J.P. *"Circulation in the cretaceous Western Interior Seaway of Noth america: a review".* THE MESOZOIC OF MIDDLE NORTH AMERICA. MEMOIR OF THE

CANADIAN SOCIETY OF PATROLEUM GEOLOGISTS. 9. (1984). PP. 221-231.

PEMBERTON, S.G., MCEACHERN, J.A. AND FREY, R.W. *"Trace fossil facies models; environmental and allostratigraphic significance"*. In: FACIES MODELS; RESPONSE TO SEA LEVEL CHANGE. (1992). PP. 47-72.

PIZZUTO, J.E. *"Paleoflood characteristics, sediment transport, and overbank deposition during post-settelment valley alluviation along the Brandywine Creek in Pennsylvania and Delaware"*. THE GEOLOGICAL SOCIETY OF AMERICA, 98TH ANNUAL MEETING. ABSTRACTS WITH PROGRAMS. GEOLOGICAL SOCIETY OF AMERICA, 17. N. 7. (1985). PP. 690.

PLINT, A.G. AND WALKER, R.G. *"Morphology and origin of an erosion surface cut into the Bad Heart Formation during major sea-level change, Santonian of west-central Alberta, Canada"*. JOURNAL OF SEDIMENTARY PETROLOGY, 57, N. 4. PP. 639-650.

PRYOR, W.A. "*Petrography of Mesaverde Sandstones in Wyoming*" *W*YOMING GEOLOGICAL ASSOCIATION GUIDEBOOK. SIXTEENTH ANNUAL CONFERENCE. (1961). PP. 34-46.

REINERS, P.W., FARLEY, K.A., CROWLEY, P.D., BROWN, H.E., KAYE, G.D. AND REUTER, J.M. "*Apatite (U/Th)/He thermochronometry of the Wind River and Bighorn Ranges: contrating uplift and exhumation styles of Wyoming Laramide uplifts"*.AGU ABSTRACTS. T42D-11. (1999).

RIDER, M. *"The geological interpretation of well logs"*. SECOND EDITION (1996). PP. 268.

ROBINSON ROBERTS, L.N. AND KIRSCHBAUM, M.A. *"Paleogeography of the Late Cretaceous of the Western Interior of Middle North*

America: Coal distribution and sediment accumulation". U.S. GEOLOGICAL SURVEY PROFESSIONAL PAPER 1561. (1995). PP. 115.

RUST, B.R. *"Fluvial sedimentology".* MEMOIR CANADIAN SOCIETY OF PETROLEUM GEOLOGISTS, N. 5. (1978). PP. 187-198.

RYER, T.A. *"Patterns of Cretaceous shallow marine sedimentation, Coalville and Rockport areas, Utah".* GEOLOGICAL SOCIETY AMERICAN BULLETIN, V.88. (1977). PP. 177-188.

SEILACHER, A.*"Bathymetry of trace fossils".* MARINE GEOLOGY, V. 5 (1967). PP. 413-428.

SERRA, O. AND SULPICE, L. *"Sedimentological analysis of shale-sand series from well logs".* TRANSATIONS OF THE SPWLA ANNUAL LOGGING SYMPOSIUM, N. 16. (1975). PP. 23.

SHAPURJI, S.S. "*Depositional environments and correlation of the Mesaverde Formation, Wind River Basin Wyoming".* WYOMING GEOLOGICAL ASSOCIATION GUIDEBOOK. THIRTIETH ANNUAL CONFERNCE. (1978). PP. 167- 180.

SLATT, R.M., JORDAN, D.W. D'AGOSTINO, A.E. AND GILLESPIE, R.H. *"Outcrop gamma-ray logging to improve understanding of subsurface well correlations".* In: GEOLOGICAL APPLICATIONS OF WELL LOGS, VOL. II, GEOLOGICAL SOCIETY LONDON SPECIAL PUBLICATION 65. (1992). PP. 3-20.

SLINGERLAND, R., KUMP, L.R., ARTHUR, M.A., FAWCET, P.J., SAGEMAN, B.B. AND BARRON, E.J. *"Estuarine circulation in the Turonian Western Interior seaway of North America".* GSA BULLETIN, V. 108. N. 7. (1996). PP. 941-952.

SMITH, D.G. *"Anastomosed fluvial deposits: modern examples from Western Canada".* In: MODERN AND ANCIENT FLUVIAL SYSTEMS.

INTERNATIONAL ASSOCIATION OF SEDIMENTOLOGISTS, SPECIAL PUBLICATION 6. (1983). PP. 155-168.

SMITH, N.D. AND PEREZ-ARLUCEA, M. *"Fine grained splay deposition in the avulsion belt of the lower Saskatchewan River, Canada."* JOURNAL OF SEDIMENTARY RESEACH, V. B64. (1994). PP. 159-168.

SMITH, N.D.; CROSS, T.A.; DUFFICY, J.P. AND CLOUGH, S.R. *"Anatomy of an avulsion".* SEDIMENTOLOGY, V.36. (1989). PP. 1-23.

SWAN, A.K.H. AND SANDILANDS, M. *"Multivariate methods". In:* INTRODUCTION TO GEOLOGICAL DATA ANALYSIS. CHAPTER 8. (1995). PP. 328-396.

SWIFT, D.J.P., HUDELSON, P.M., BRENNER, R.L. AND THOMPSON, P. *"Shelf construction in a foreland basin: storm beds, shelf sandsbodies, and shelf-slope depositional sequences in the Upper Cretaceous Mesaverde Group, Book Cliffs, Utah".* SEDIMENTOLOGY, V.34. N. 3. (1987). PP. 423-457.

THOMPSON, R.M. AND WHITE, V.L. *"The coal deposits of the Alkali Butte, the big sand and the Beaver Creek fields, Fremont County Wyoming".* U.S. GEOLOGICAL SURVEY CIRCULAR 152. (1952). PP. 24.

TOURLETOR, H.A. AND THOMPSON, R.M. *"Geology of the Boysen area, Central Wyoming".* U.S. GEOLOGICAL SURVEY, OIL AND GAS INVESTIGATIONS MAP, OM 91. (1948).

TROYER, M.L. AND KEEFER, W.R. *"Geology of the Shotgun Butte area, Fremont County, Wyoming".* U.S GEOLOGICAL SURVEY OIL AND GAS INVESTIGATIONS MAP OM-172. (1955).

UPCHURCH, Jr. G.R. AND WOLFE, J.A. *"Cretaceous vegetation of the Western Interior and adjacent regions of North America"*. GEOLOGICAL ASSOCIATION OF CANADA. SPECIAL PAPER 39. (1993). PP. 243-281.

VAIL, P.R., TODD, R.G. AND SANGREE, J.B. *"Seismic stratigraphy and global changes of sea level, part 5: chronostratigraphic significance of seismic reflection"*. In: SEISMIC STRATIGRAPHY, APPLICATIONS TO HYDROCARBON EXPLORATION. AAPG. MEMOIR 26. (1977). PP. 99-133.

VAN WAGONER, J.C., MITCHUM, R.M., CAMPION, K.M. AND RAHMANIAN, V.D. *"Siliciclastic sequence stratigraphy in well logs, core, and outcrops"*. AMERICAN ASSOCIATION OF PETROLEUM GEOLOGISTS. METHODS IN EXPLORATION SERIES, 7. In: SILICICLASTIC SEQUENCE STRATIGRAPHY IN WELL LOGS, CORE, AND OUTCROPS. (1990). PP. 55.

WALDEN, J. AND SMITH, J.P. *" Factor analysis: a practical application"*. In: STATISTICAL MODELLING OF QUATERNARY SCIENCE DATA. QUATERNARY RESEACH ASSOCIATION. TECHNICAL GUIDE, N. 5. (1995). PP. 39-63.

WALKER, R.G. *"Facies, facies models and modern stratigraphic concepts"*. In: FACIES MODELS: RESPONSE TO SEA LEVEL CHANGE. (1992). PP. 1-14.

WALLING, D.E., WILHELM, L.F. AND BRADLEY, S.B. *"Rates and patterns of contemporary floodplain sedimentation; a case study of the River Culm, Devon, UK"*. FLOODPLAIN ENVIRONMENTS GEOJOURNAL, 19. N. 1. (1989). PP. 53-62.

WEIMER, R.J. *"Rates of deltaic sedimentation and intrabasin deformation, upper Cretaceous of Rocky Mountain Region"*. In: DELTAIC SEDIMENT MODERN AND ANCIENT. SOCIETY OF ECONOMIC PALAEONTOLOGIST AND MINERALOGISTS. SPECIAL PUBLICATION, N. 15. (1983). PP. 270-292.

WEIMER, R.J. *"Relation of unconformities, tectonics, and sea level changes, Cretaceous of the Denver Basin and adjacent areas"*. MESOZOIC PALEOGEOGRAPHY OF THE WEST-CENTRAL UNITED STATES: SOCIETY OF ECONOMIC PALEONTOLOGISTS AND MINERALOGISTS, ROCKY MOUNTAIN SECTION, ROCKY MOUNTAIN PALEOGEOGRAPHY SYMPOSIUM 2. (1983). PP. 359-376.

WILLIS, B.J. AND BEHRENSMEYER, A.K. *"Architecture of Miocene overbank deposits in northern Pakistan"*. JOURNAL OF SEDIMENTARY RESEARCH, B: STRATIGRAPHY AND GLOBAL STUDIES, N. B64. (1994).

YENNE, K.A. AND PIPIRINGOS, G.N. *"Stratigraphic sections of Cody Shale and younger Cretaceous and Plaeocene rocks in the Wind River Basin, Fremont County, Wyoming"*. U.S. SURVEY OIL AND GAS INVESTIGATIONS. CHAT OC 49.

APPENDIX 1

RESULTS OF THE XRD AND XRF ANALYSES

Difractometre traces.

SECTION	SAMPLE N^0	HEIGH	LITHOLOGY
MV 0	9		Shale
MV 0	14	450	Shale
MV 1	20	415	Siltstone
MV 1	23	475	Siltstone
MV 1	61	435	Shale
MV 2	9	445	Siltstone
MV 2	29	520	Sandstone
MV 2	30	520	Sandstone
MV 2	8	435	Shale
MV 3		10	Shale
MV 3	9	350	Shale
MV 3	12	515	Shale
MV 5	12	536	Sandstone
MV 5	32	161	Sandstone
MV 5	5	315	Shale
MV 5	20	605	Shale
MV 6	13	27	Siltstone
MV 6	24	352	Sandstone

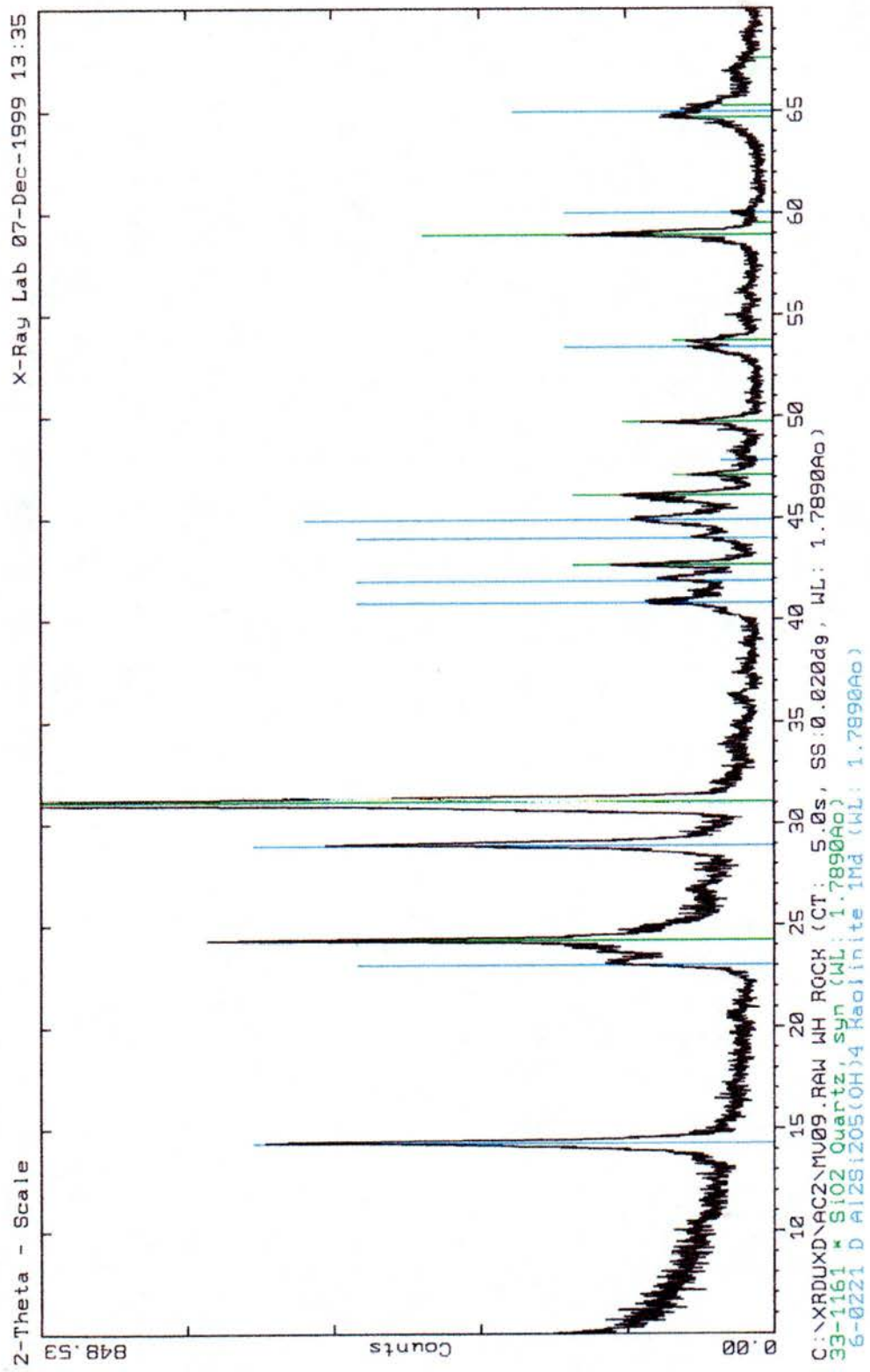
X-Ray Lab 07-Dec-1999 13:35
2-Theta - Scale
848.53
Counts
0.00
10
15
20
25
30
35
40
45
50
55
60
65
C:\XRDUXD\AC2\MV09.RAW WH ROCK (CT: 5.0s, SS:0.020dg, WL: 1.7890Ao)
33-1161 * SiO2 Quartz, syn (WL: 1.7890Ao)
6-0221 D Al2Si2O5(OH)4 Kaolinite 1Md (WL: 1.7890Ao)

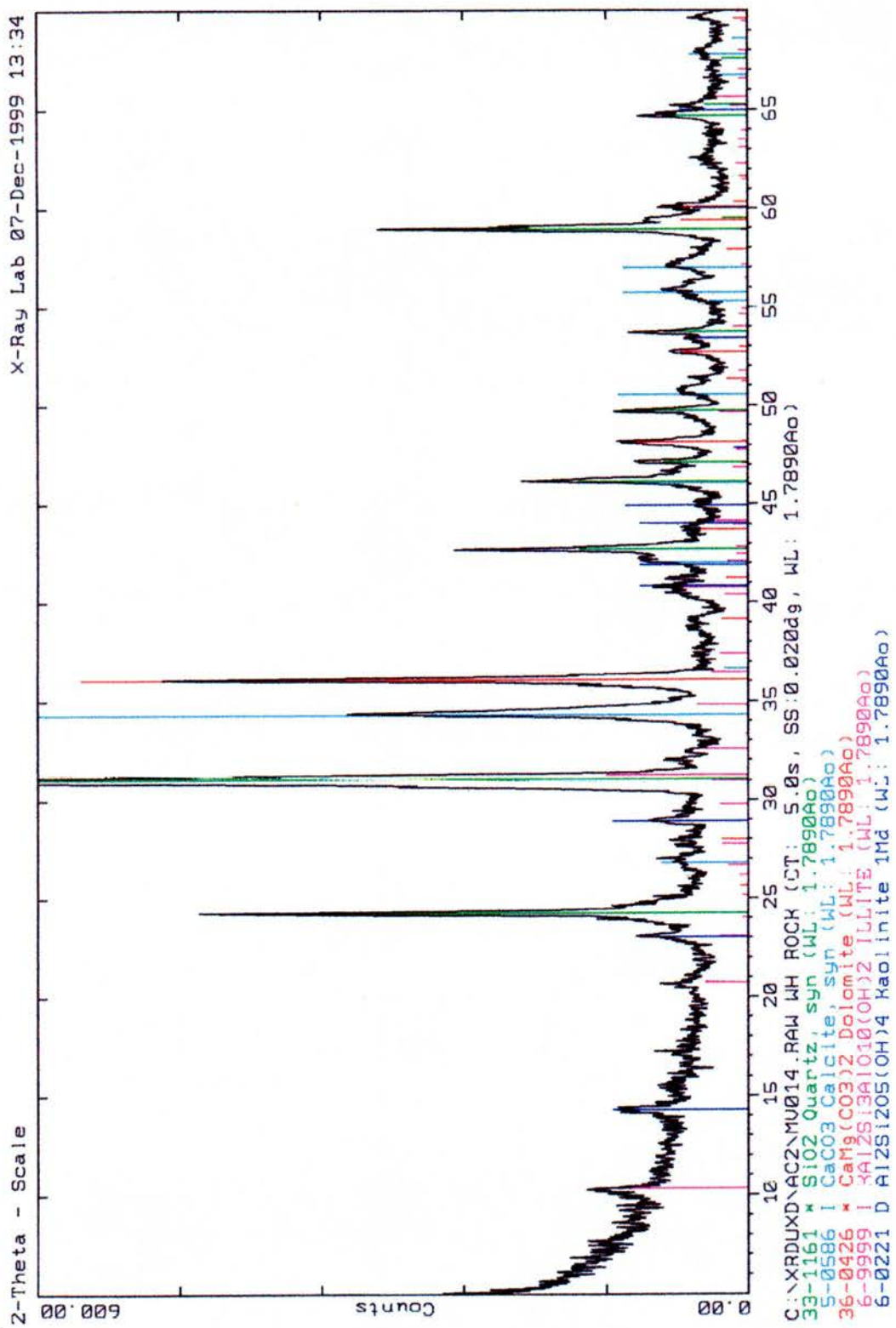
X-Ray Lab 07-Dec-1999 13:34
2-Theta - Scale
Counts
600.00
0.00
0
5
10
15
20
25
30
35
40
45
50
55
60
65
C:\XRDUXD\AC2\MV014.RAW WH ROCK (CT: 5.0s, SS:0.020dg, WL: 1.7890Ao)
33-1161 * SiO2 Quartz, syn (WL: 1.7890Ao)
5-0586 I CaCO3 Calcite, syn (WL: 1.7890Ao)
36-0426 * CaMg(CO3)2 Dolomite (WL: 1.7890Ao)
6-9999 I XAl2Si3Al010(OH)2 ILLITE (WL: 1.7890Ao)
6-0221 D Al2Si2O5(OH)4 Kaolinite 1Md (WL: 1.7890Ao)

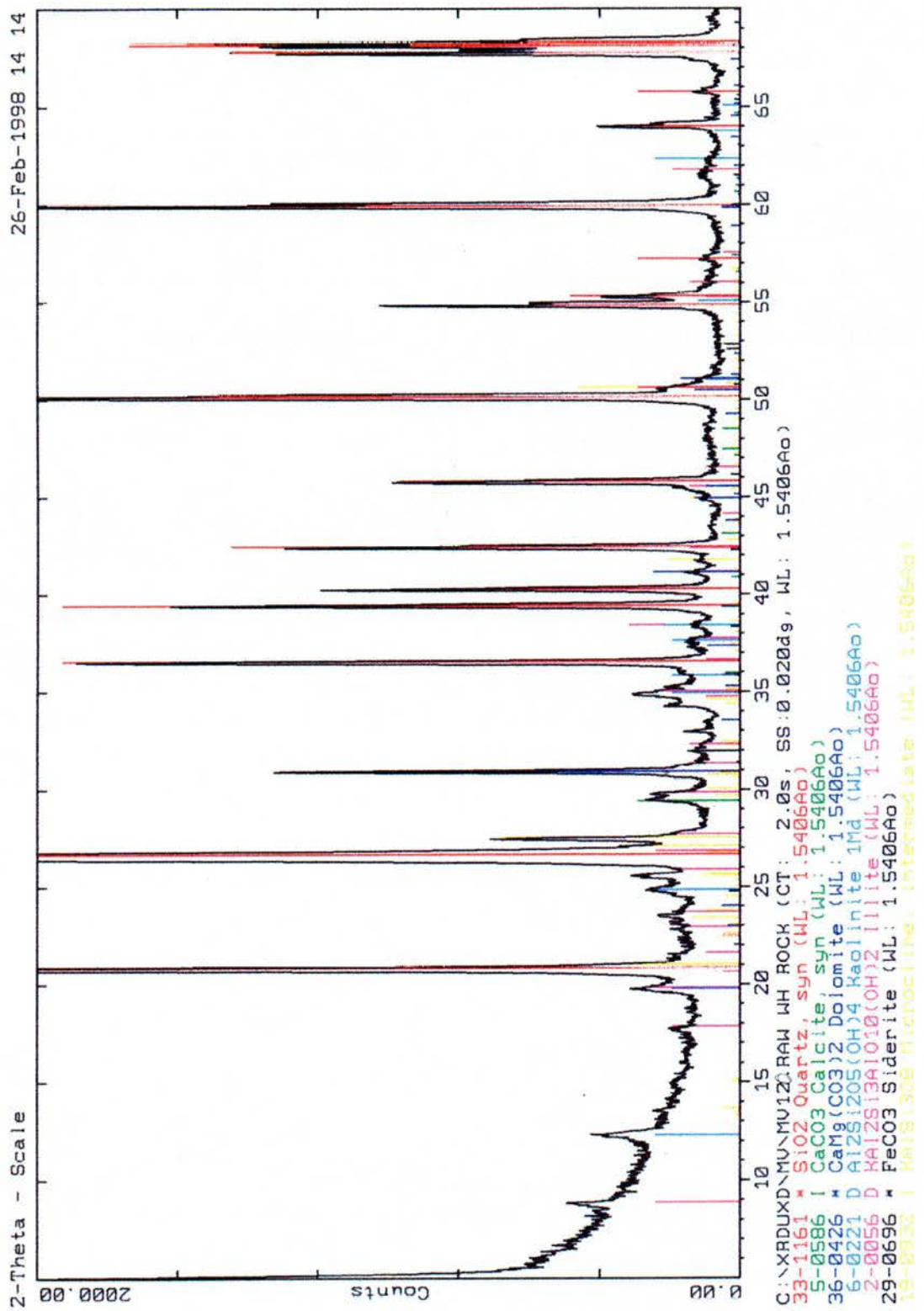
26-Feb-1998 14 14
2-Theta - Scale
Counts
2000.00
0.00
C:\XRDUXD\MV\MV12\RAW WH ROCK (CT: 2.0s, SS:0.020dg, WL: 1.5406Ao)
33-1161 * SiO2 Quartz, syn (WL: 1.5406Ao)
5-0586 I CaCO3 Calcite, syn (WL: 1.5406Ao)
36-0426 * CaMg(CO3)2 Dolomite (WL: 1.5406Ao)
6-0221 D Al2Si2O5(OH)4 Kaolinite 1Md (WL: 1.5406Ao)
2-0056 D KAl2Si3AlO10(OH)2 Illite (WL: 1.5406Ao)
29-0696 * FeCO3 Siderite (WL: 1.5406Ao)

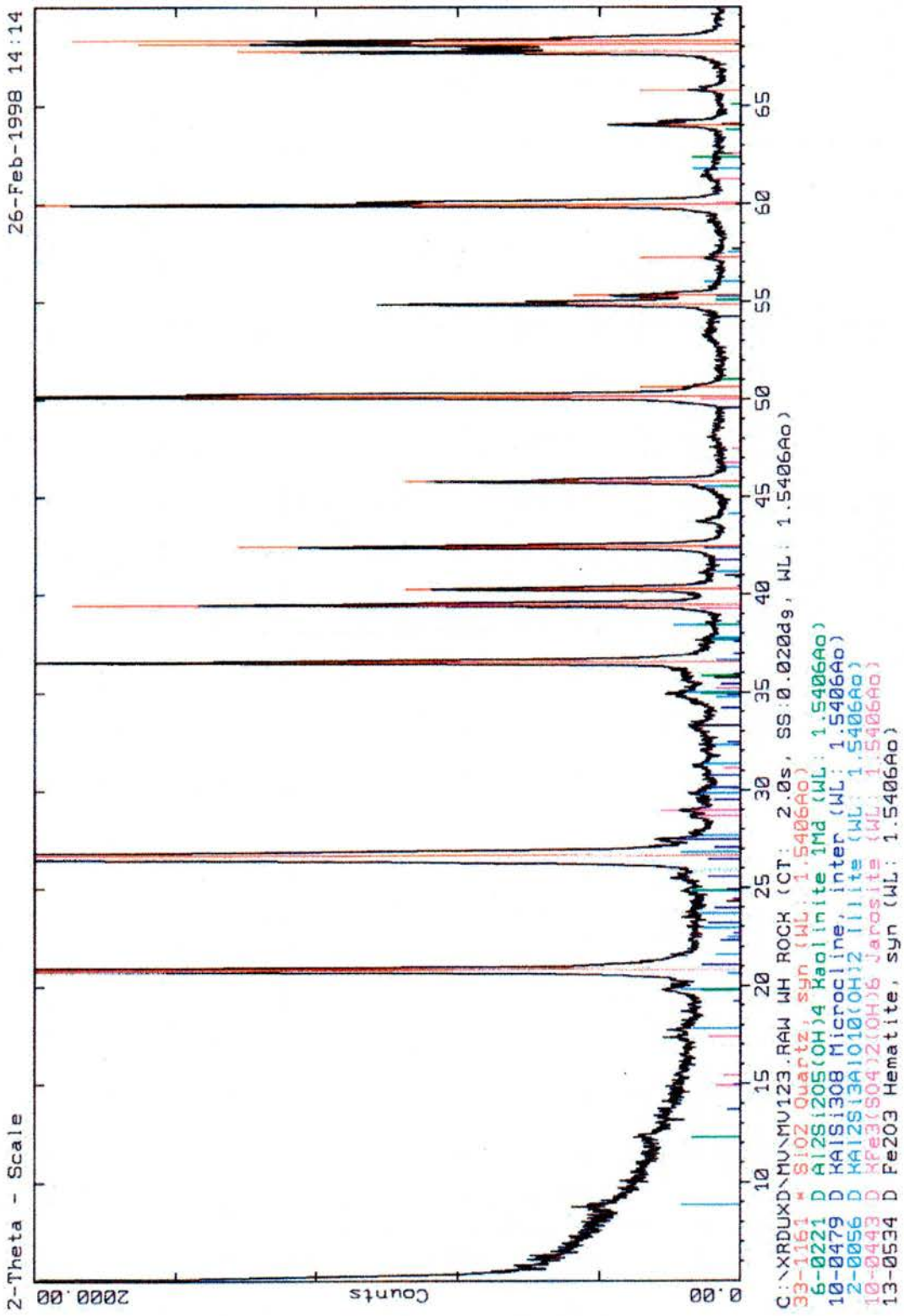
26-Feb-1998 14:14
2-Theta - Scale
Counts
2000.00
0.00
10
15
20
25
30
35
40
45
50
55
60
65
C:\XRDUXD\MV\MV123.RAW WH ROCK (CT: 2.0s, SS:0.020dg, WL: 1.5406Ao)
33-1161 * SiO2 Quartz, syn (WL: 1.5406Ao)
6-0221 D Al2Si2O5(OH)4 Kaolinite 1Md (WL: 1.5406Ao)
10-0479 D KAlSi3O8 Microcline, inter (WL: 1.5406Ao)
2-0056 D KAl2Si3AlO10(OH)2 Illite (WL: 1.5406Ao)
10-0443 D KFe3(SO4)2(OH)6 Jarosite (WL: 1.5406Ao)
13-0534 D Fe2O3 Hematite, syn (WL: 1.5406Ao)

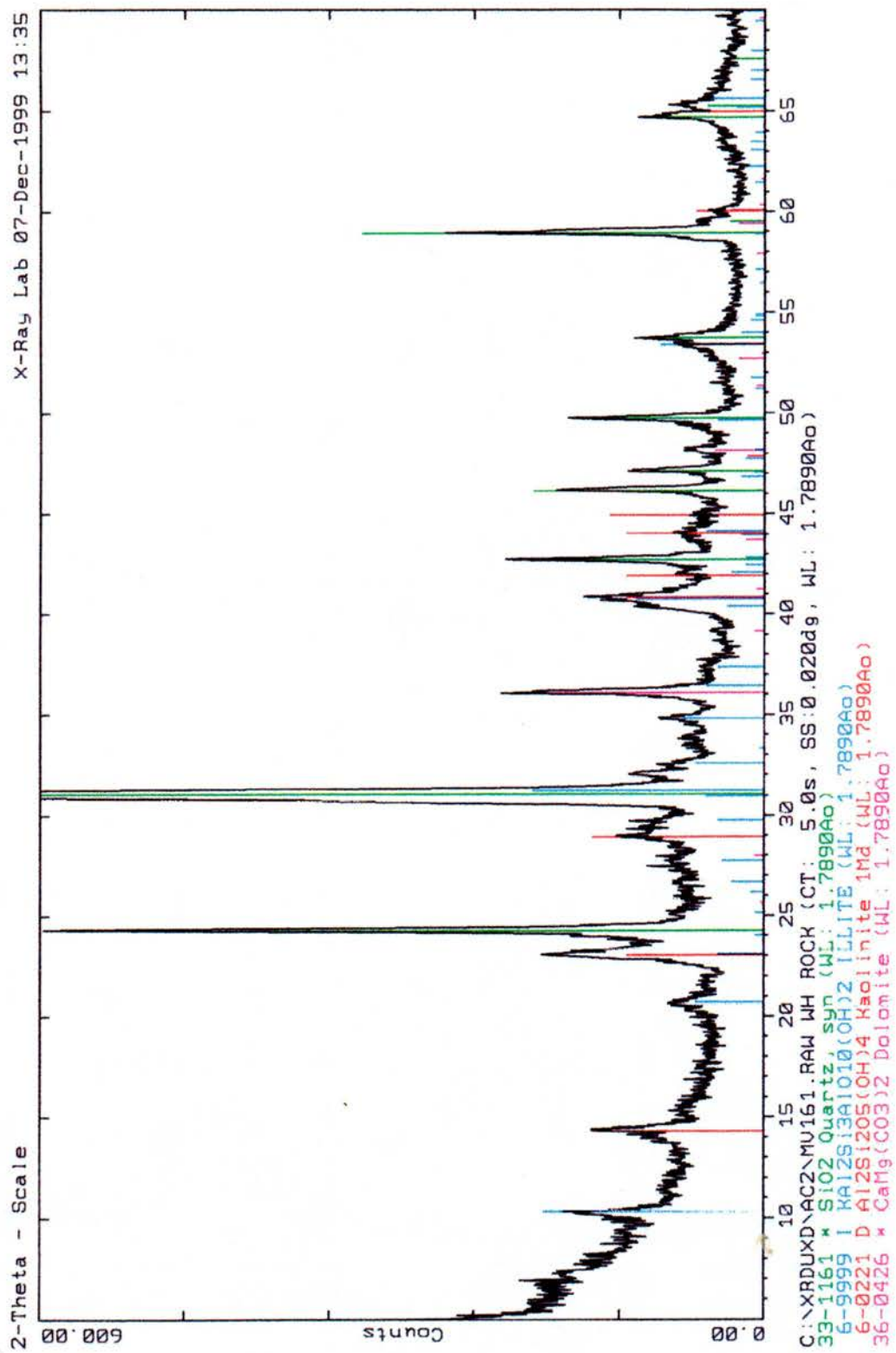
X-Ray Lab 07-Dec-1999 13:35
2-Theta - Scale
Counts
600.00
0.00
10
15
20
25
30
35
40
45
50
55
60
65
C:\XRDUXD\AC2\MU161.RAW WH ROCK (CT: 5.0s, SS:0.020dg, WL: 1.7890Ao)
33-1161 * SiO2 Quartz, syn (WL: 1.7890Ao)
6-9999 I KAl2Si3Al10(OH)2 ILLITE (WL: 1.7890Ao)
6-0221 D Al2Si2O5(OH)4 Kaolinite 1Md (WL: 1.7890Ao)
36-0426 * CaMg(CO3)2 Dolomite (WL: 1.7890Ao)

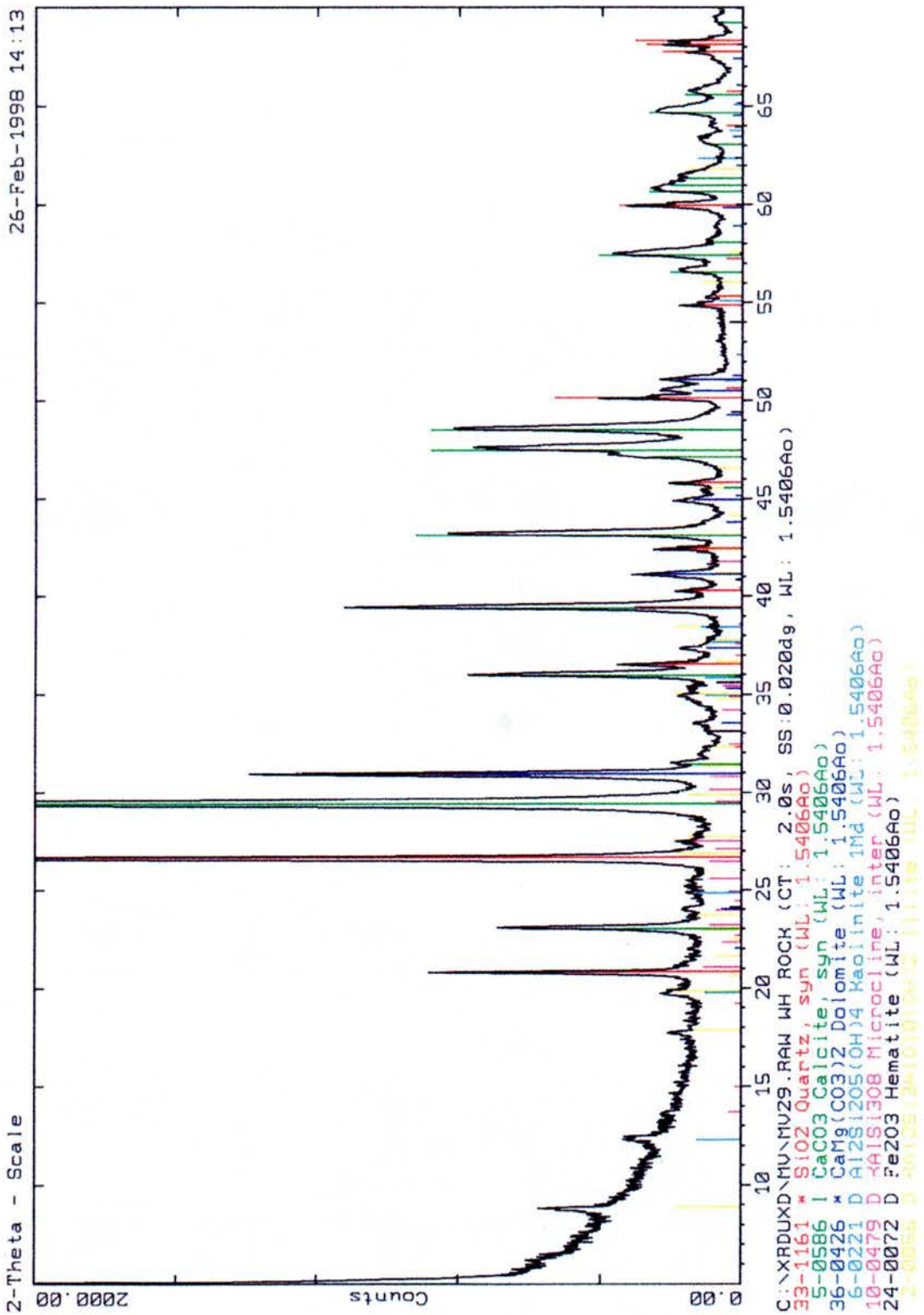
26-Feb-1998 14:13
2-Theta - Scale
Counts
2000.00
0.00
10
15
20
25
30
35
40
45
50
55
60
65
C:\XRDUXD\MV\MV29.RAW WH ROCK (CT: 2.0s, SS:0.020dg, WL: 1.5406Ao)
33-1161 * SiO2 Quartz, syn (WL: 1.5406Ao)
5-0586 I CaCO3 Calcite, syn (WL: 1.5406Ao)
36-0426 * CaMg(CO3)2 Dolomite (WL: 1.5406Ao)
6-0221 D Al2Si2O5(OH)4 Kaolinite 1Md (WL: 1.5406Ao)
10-0479 D KAlSi3O8 Microcline, inter (WL: 1.5406Ao)
24-0072 D Fe2O3 Hematite (WL: 1.5406Ao)

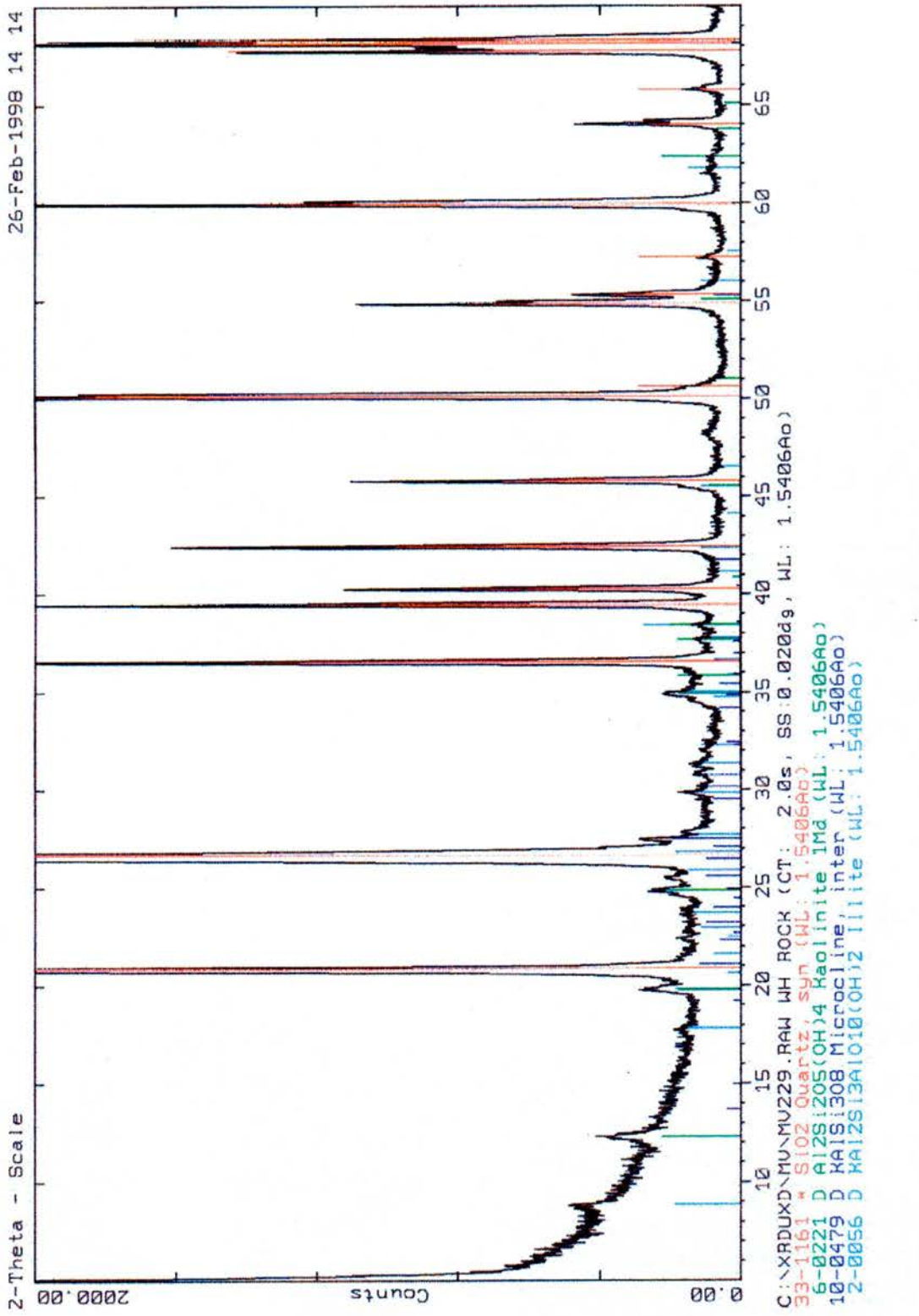
26-Feb-1998 14 14
2-Theta - Scale
Counts
2000.00
0.00
10
15
20
25
30
35
40
45
50
55
60
65
C:\XRDUXD\MU\MU229.RAW WH ROCK (CT: 2.0s, SS:0.020dg, WL: 1.5406Ao)
33-1161 * SiO2 Quartz, syn (WL: 1.5406Ao)
6-0221 D Al2Si2O5(OH)4 Kaolinite 1Md (WL: 1.5406Ao)
10-0479 D KAlSi3O8 Microcline, inter (WL: 1.5406Ao)
2-0056 D KAl2Si3AlO10(OH)2 Illite (WL: 1.5406Ao)

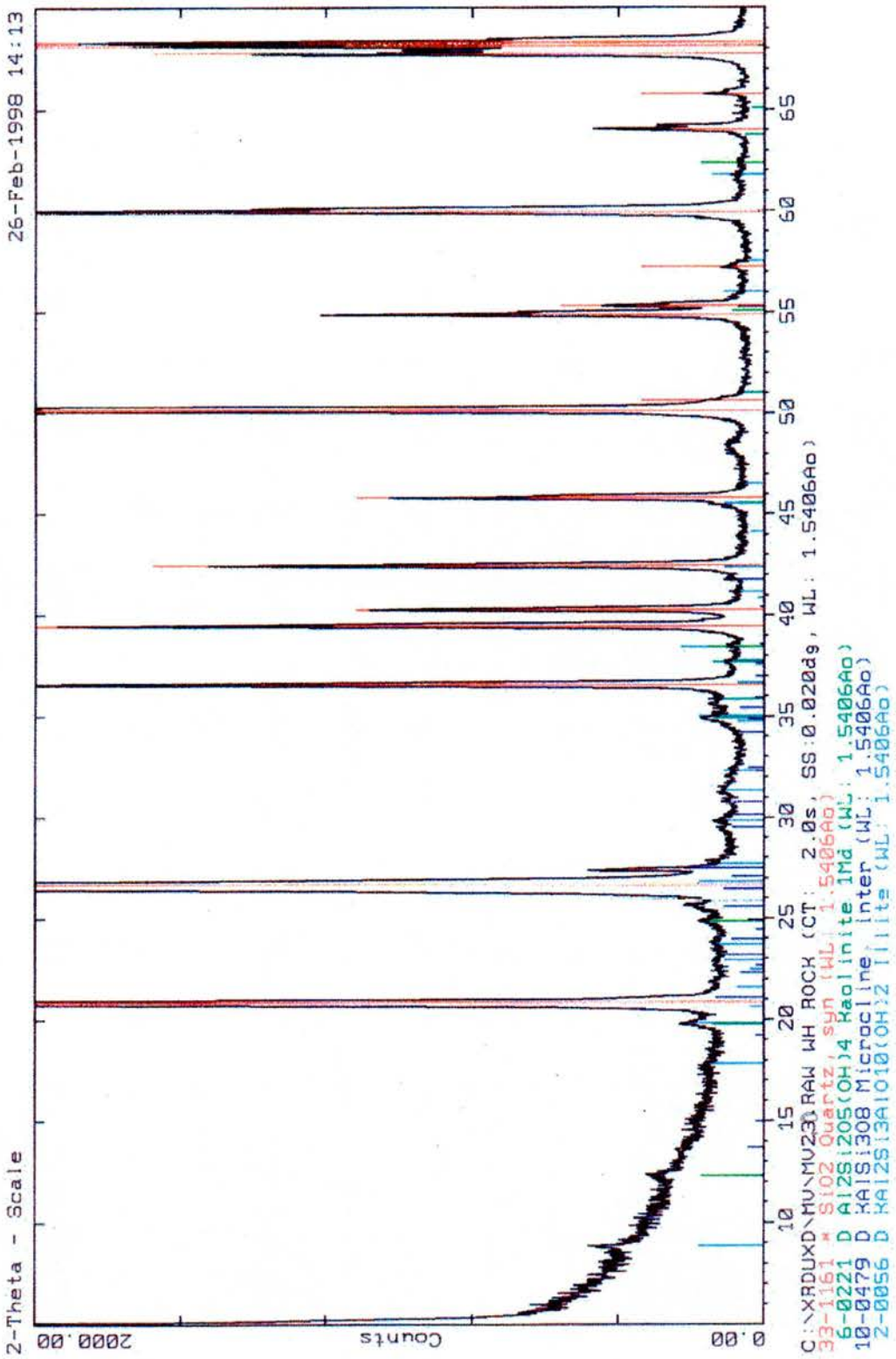
26-Feb-1998 14:13
2-Theta - Scale
Counts
2000.00
0.00
C:\XRDUXD\MV\MV23\RAW WH ROCK (CT: 2.0s, SS:0.020dg, WL: 1.5406Ao)
33-1161 * SiO2 Quartz, syn (WL: 1.5406Ao)
6-0221 D Al2Si2O5(OH)4 Kaolinite 1Md (WL: 1.5406Ao)
10-0479 D KAlSi3O8 Microcline, inter (WL: 1.5406Ao)
2-0056 D KAl2(Si3Al)O10(OH)2 Illite (WL: 1.5406Ao)

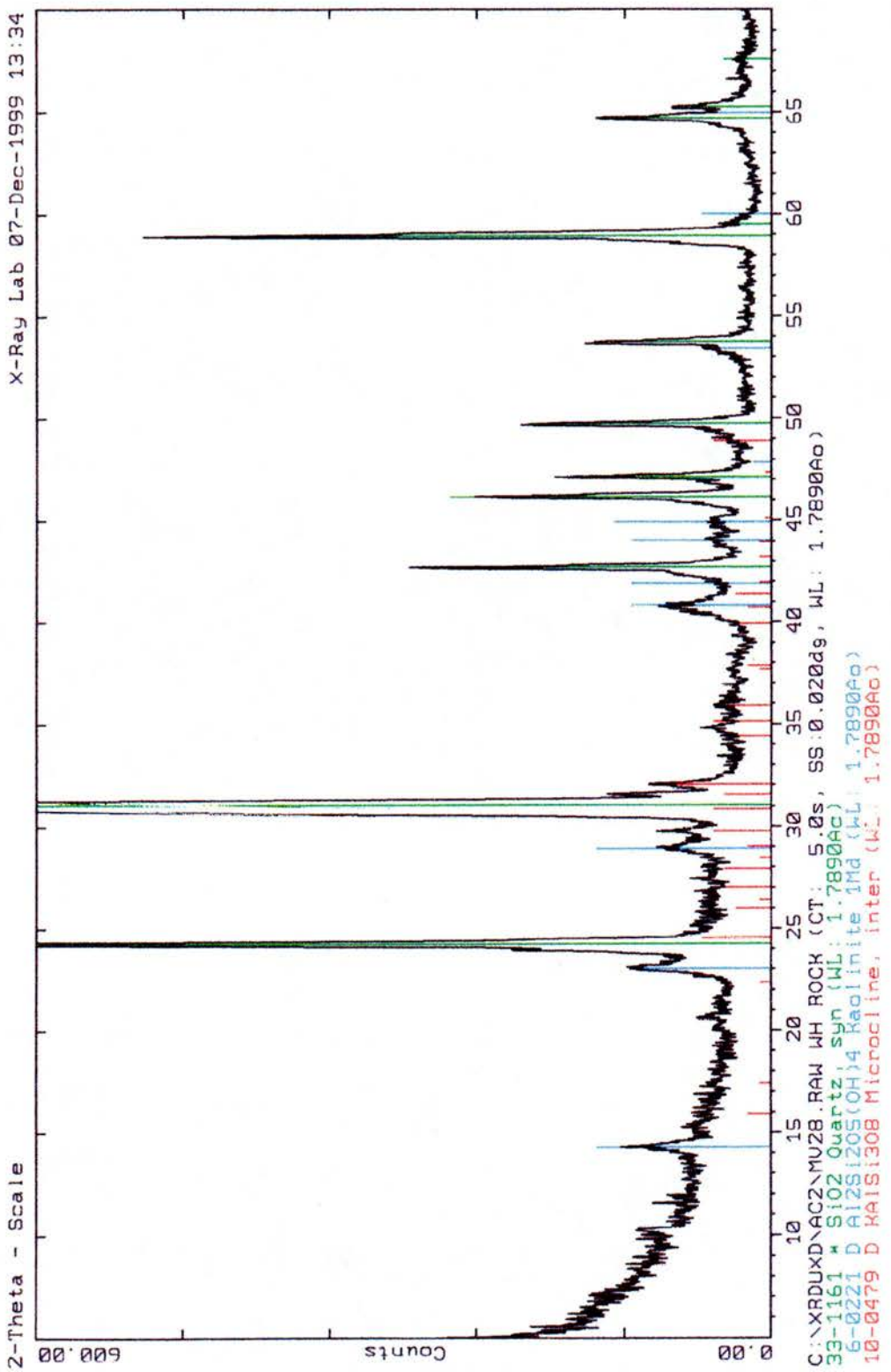
X-Ray Lab 07-Dec-1999 13:34
2-Theta - Scale
Counts
600.00
0.00
10
15
20
25
30
35
40
45
50
55
60
65
C:\XRDUXD\AC2\MU28.RAW WH ROCK (CT: 5.0s, SS:0.020dg, WL: 1.7890Ao)
33-1161 * SiO2 Quartz, syn (WL: 1.7890Ac)
6-0221 D Al2Si2O5(OH)4 Kaolinite 1Md (WL: 1.7890Ao)
10-0479 D KAlSi3O8 Microcline, inter (WL: 1.7890Ao)

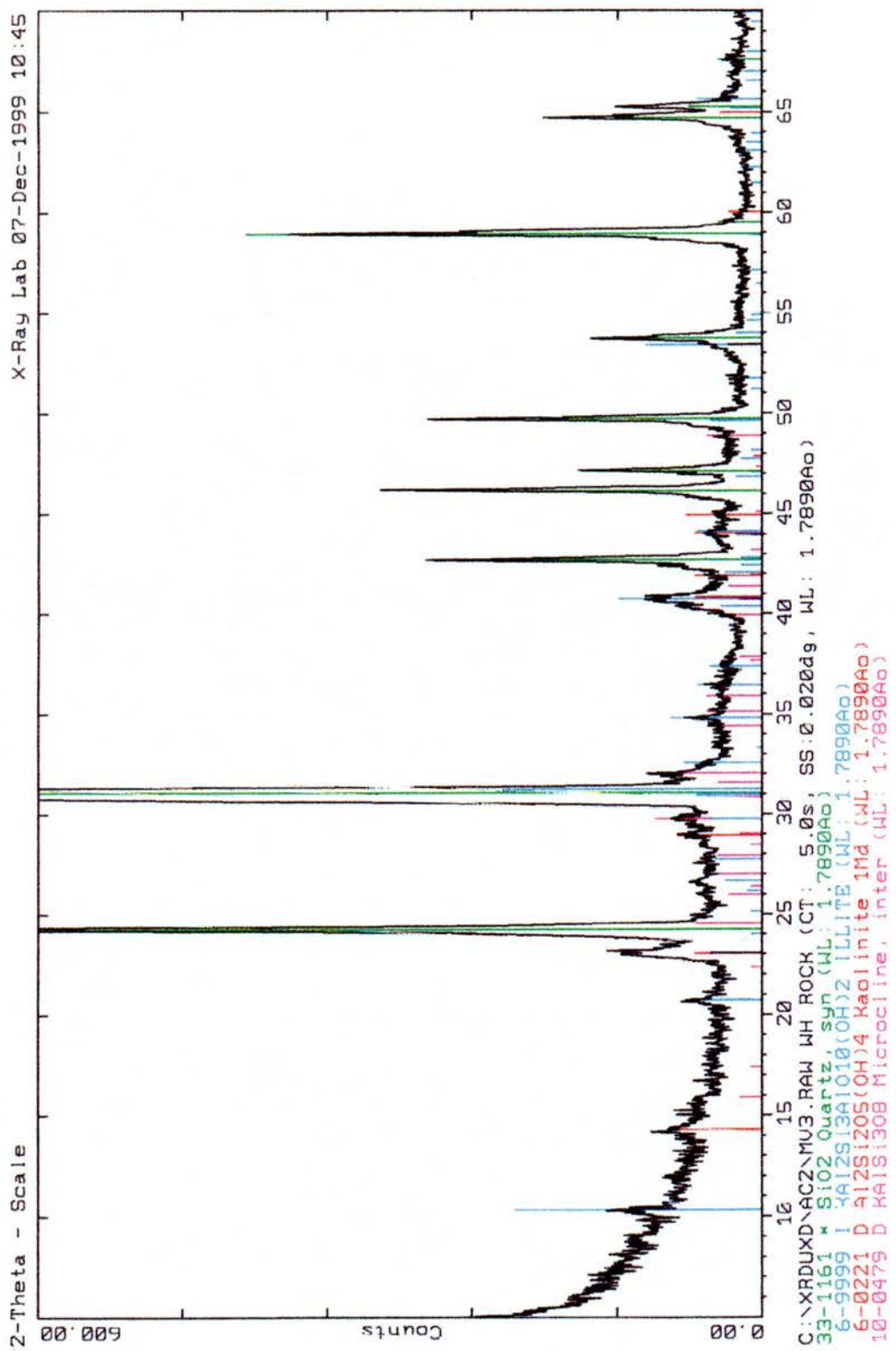
X-Ray Lab 07-Dec-1999 10:45
2-Theta - Scale
Counts
600.00
0.00
C:\XRDUXD\AC2\MU3.RAW WH ROCK (CT: 5.0s, SS:0.020dg, WL: 1.7890Ao)
33-1161 * SiO2 Quartz, syn (WL: 1.7890Ao)
6-9999 I KAl2Si3Al010(OH)2 ILLITE (WL: 1.7890Ao)
6-0221 D Al2Si205(OH)4 Kaolinite 1Md (WL: 1.7890Ao)
10-0479 D KAlSi308 Microcline, inter (WL: 1.7890Ao)

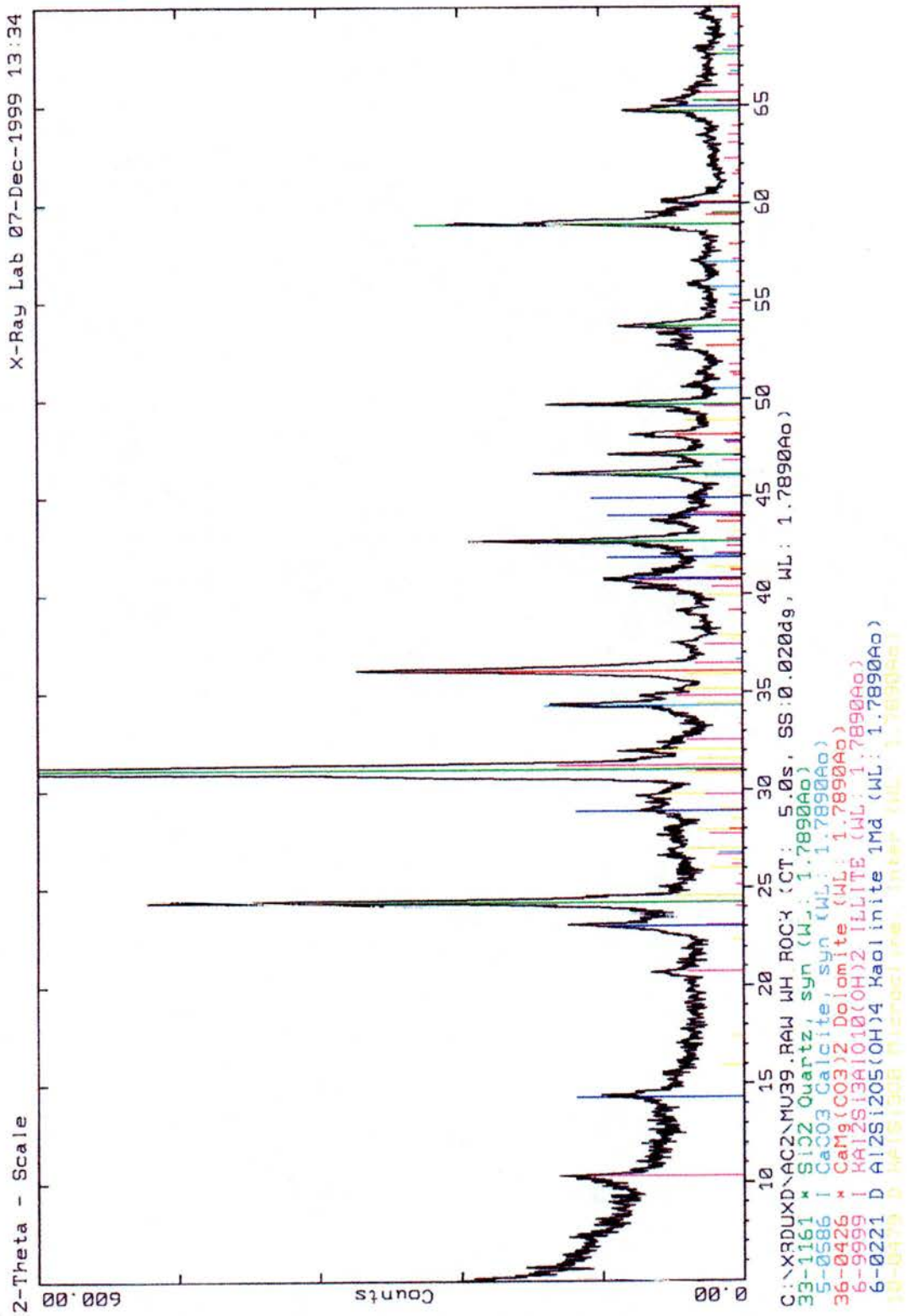
X-Ray Lab 07-Dec-1999 13:34
2-Theta - Scale
Counts
600.00
0.00
C:\XRDUXD\AC2\MU39.RAW WH ROCK (CT: 5.0s, SS:0.020deg, WL: 1.7890Ao)
33-1161 * SiO2 Quartz, syn (WL: 1.7890Ao)
5-0586 I CaCO3 Calcite, syn (WL: 1.7890Ao)
36-0426 * CaMg(CO3)2 Dolomite (WL: 1.7890Ao)
6-9999 I KAl2Si3Al010(OH)2 ILLITE (WL: 1.7890Ao)
6-0221 D Al2Si2O5(OH)4 Kaolinite 1Md (WL: 1.7890Ao)

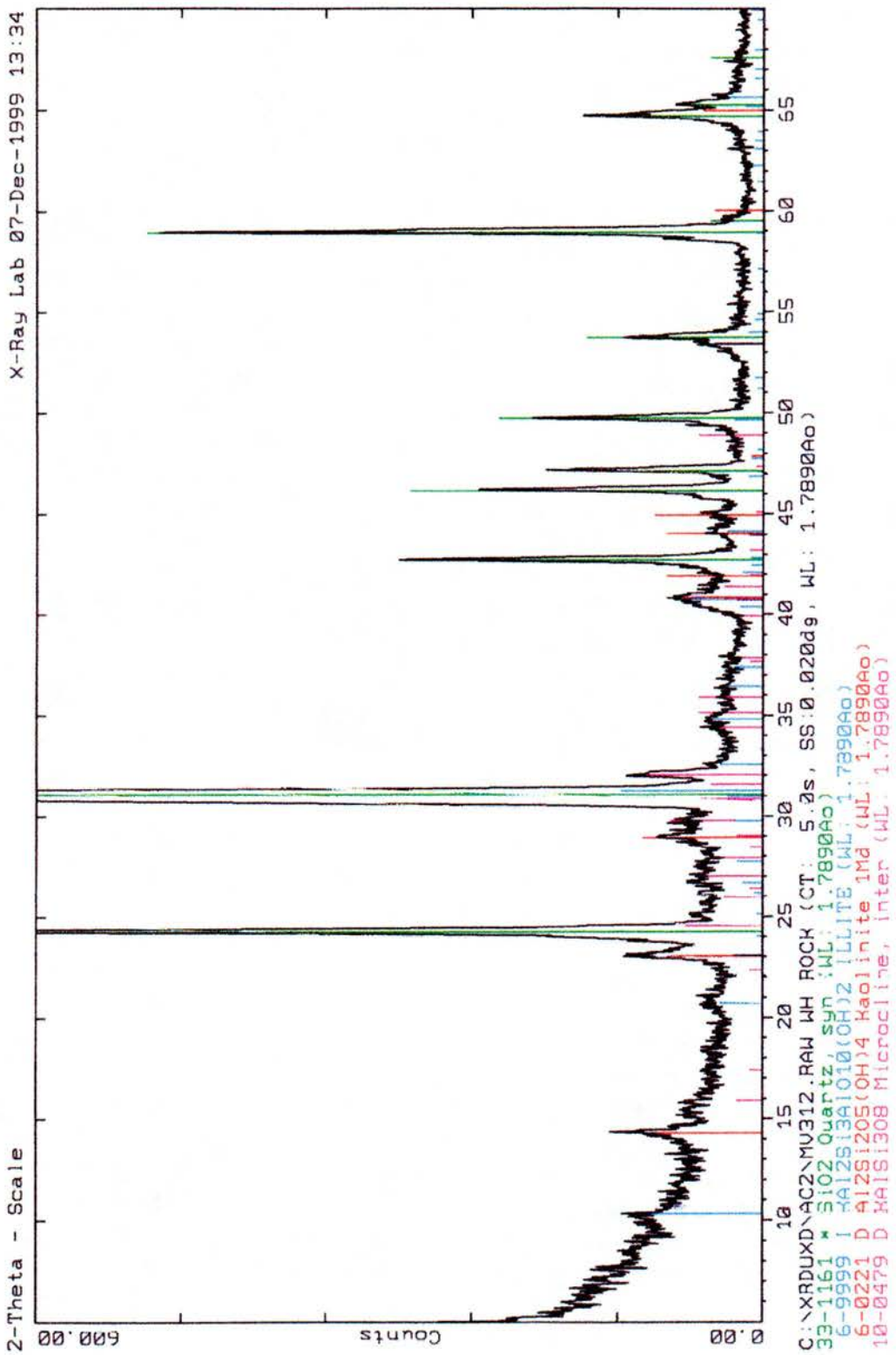
X-Ray Lab 07-Dec-1999 13:34
2-Theta - Scale
Counts
600.00
0.00
5
10
15
20
25
30
35
40
45
50
55
60
65
C:\XRDUXD\AC2\MV312.RAW WH ROCK (CT: 5.0s, SS:0.020dg, WL: 1.7890Ao)
33-1161 * SiO2 Quartz, syn (WL: 1.7890Ao)
6-9999 I KAl2Si3Al010(OH)2 ILLITE (WL: 1.7890Ao)
6-0221 D Al2Si205(OH)4 Kaolinite 1Md (WL: 1.7890Ao)
10-0479 D KAlSi308 Microcline, inter (WL: 1.7890Ao)

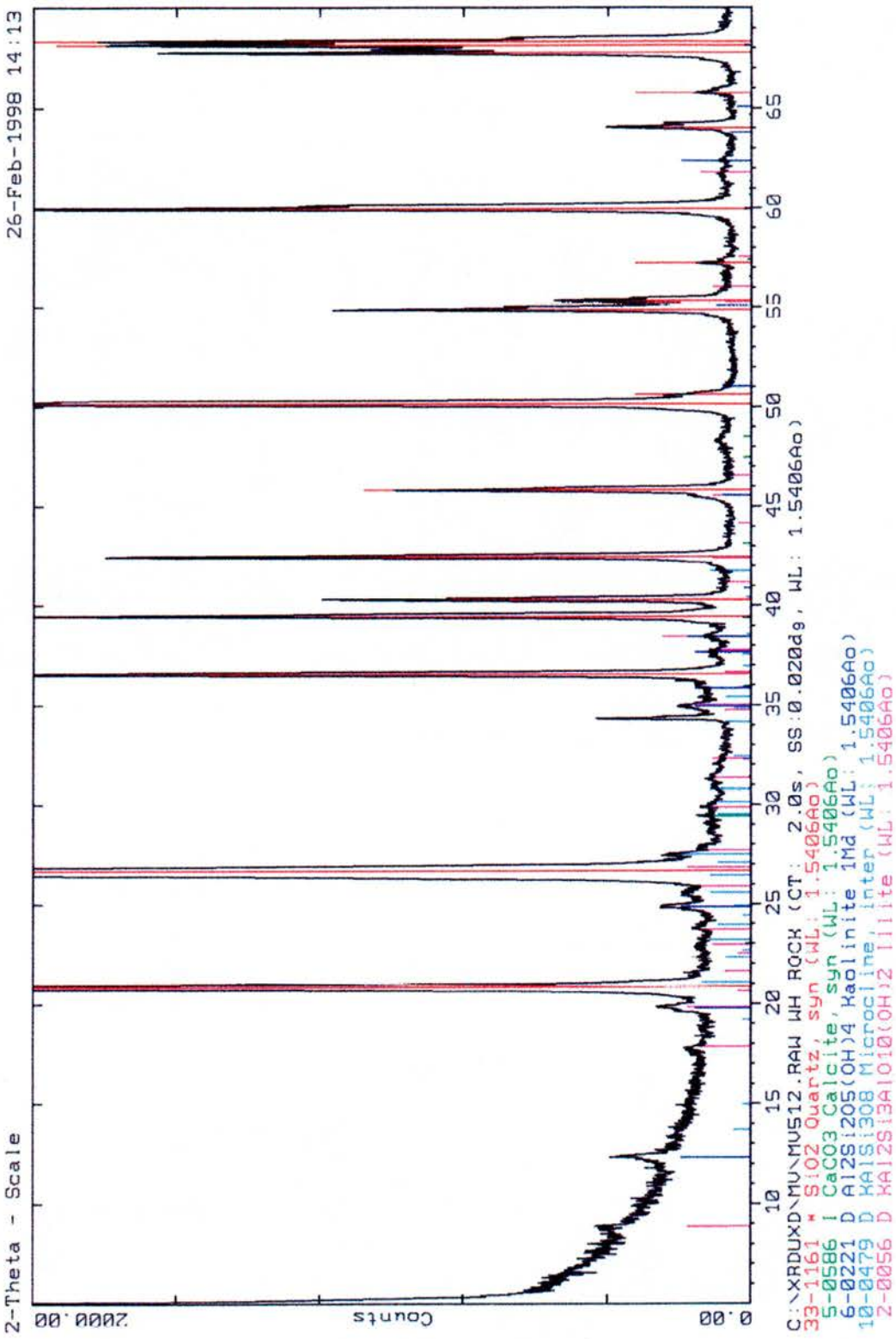
26-Feb-1998 14:13
2-Theta - Scale
Counts
2000.00
0.00
10
15
20
25
30
35
40
45
50
55
60
65
C:\XRDUXD\MV\MV512.RAW WH ROCK (CT: 2.0s, SS:0.020dg, WL: 1.5406Ao)
33-1161 * SiO2 Quartz, syn (WL: 1.5406Ao)
5-0586 I CaCO3 Calcite, syn (WL: 1.5406Ao)
6-0221 D Al2Si2O5(OH)4 Kaolinite 1Md (WL: 1.5406Ao)
10-0479 D KAlSi3O8 Microcline, inter (WL: 1.5406Ao)
2-0056 D KAl2Si3AlO10(OH)2 Illite (WL: 1.5406Ao)

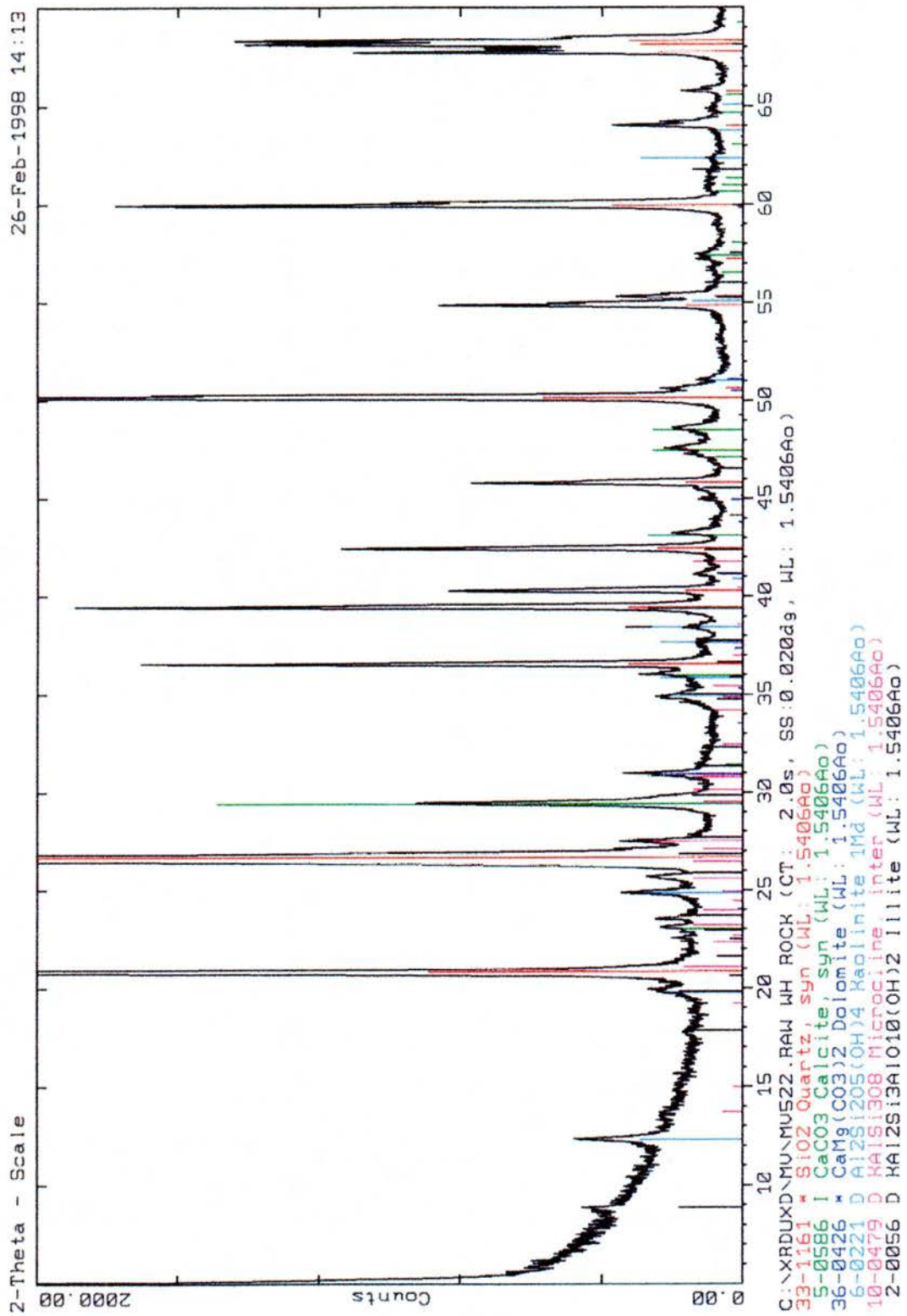
26-Feb-1998 14:13
2-Theta - Scale
Counts
2000.00
0.00
10
15
20
25
30
35
40
45
50
55
60
65
C:\XRDUXD\MU\MU522.RAW WH ROCK (CT: 2.0s, SS:0.020dg, WL: 1.54056Ao)
33-1161 * SiO2 Quartz, syn (WL: 1.5406Ao)
5-0586 I CaCO3 Calcite, syn (WL: 1.5406Ao)
36-0426 * CaMg(CO3)2 Dolomite (WL: 1.5406Ao)
6-0221 D Al2Si2O5(OH)4 Kaolinite 1Md (WL: 1.5406Ao)
10-0479 D KAlSi3O8 Microcline, inter (WL: 1.5406Ao)
2-0056 D KAl2Si3AlO10(OH)2 Illite (WL: 1.5406Ao)

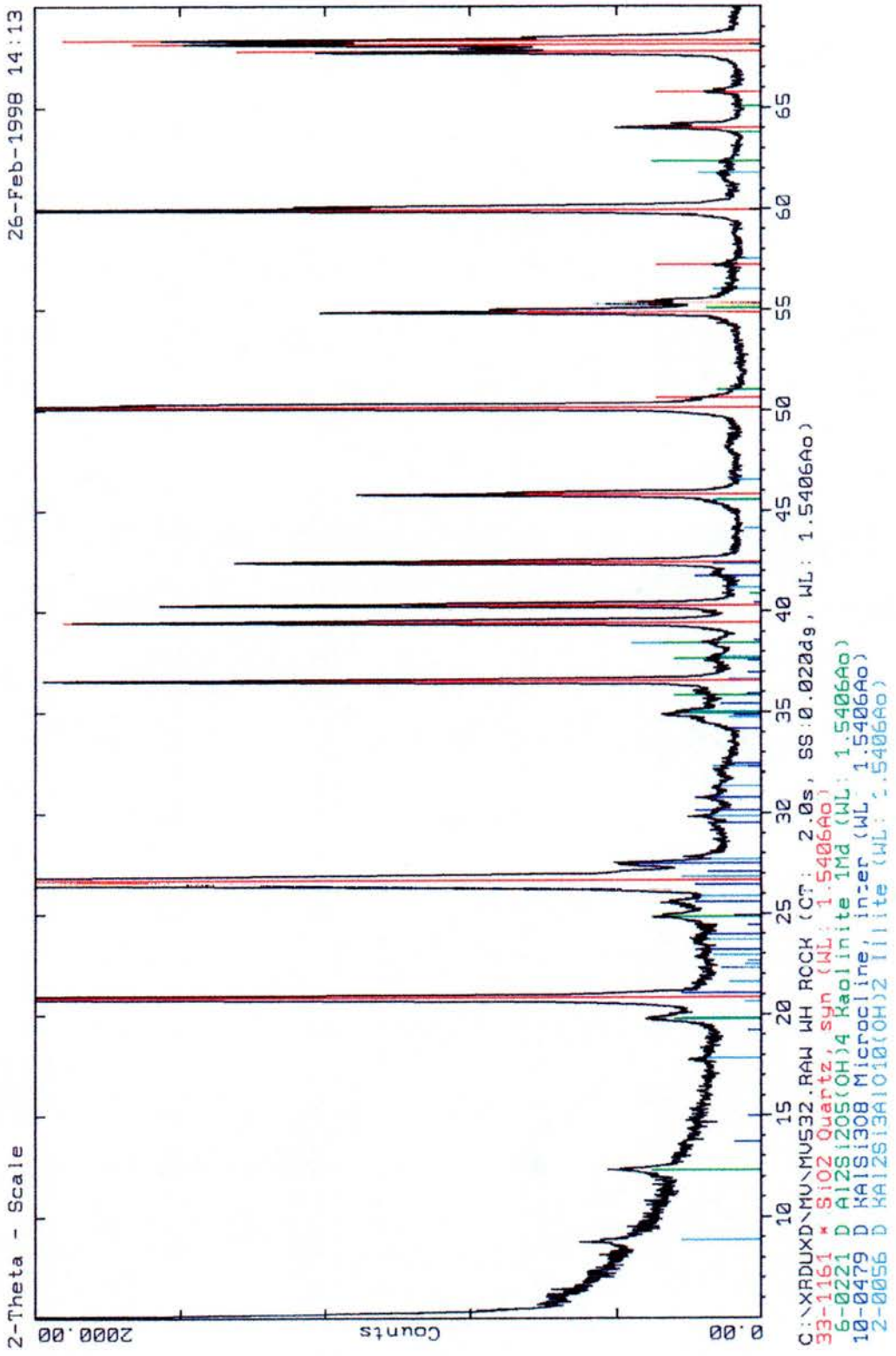
26-Feb-1998 14:13
2-Theta - Scale
Counts
2000.00
0.00
10
15
20
25
30
35
40
45
50
55
60
65
C:\XRDUXD\MV\MV532.RAW WH ROCK (CT: 2.0s, SS:0.020dg, WL: 1.5406Ao)
33-1161 * SiO2 Quartz, syn (WL: 1.5406Ao)
6-0221 D Al2Si2O5(OH)4 Kaolinite 1Md (WL: 1.5406Ao)
10-0479 D KAlSi3O8 Microcline, inter (WL: 1.5406Ao)
2-0056 D KAl2Si3AlO10(OH)2 Illite (WL: 1.5406Ao)

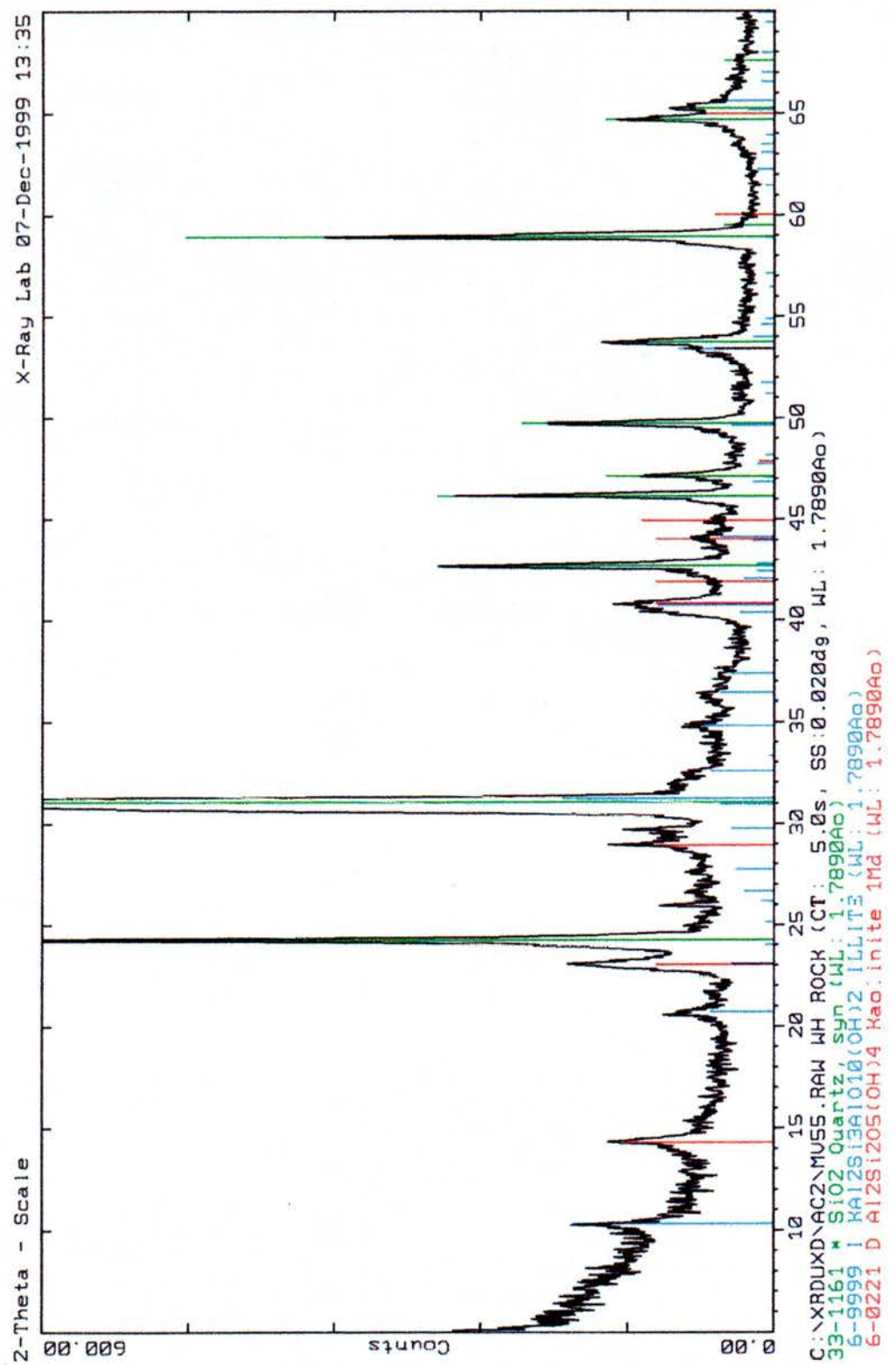
X-Ray Lab 07-Dec-1999 13:35
2-Theta - Scale
Counts
600.00
0.00
10
15
20
25
30
35
40
45
50
55
60
65
C:\XRDUXD\AC2\MU55.RAW WH ROCK (CT: 5.0s, SS:0.020dg, WL: 1.7890Ao)
33-1161 * SiO2 Quartz, syn (WL: 1.7890Ao)
6-9999 I KAl2Si3Al010(OH)2 ILLITE (WL: 1.7890Ao)
6-0221 D Al2Si205(OH)4 Kao:inite 1Md (WL: 1.7890Ao)

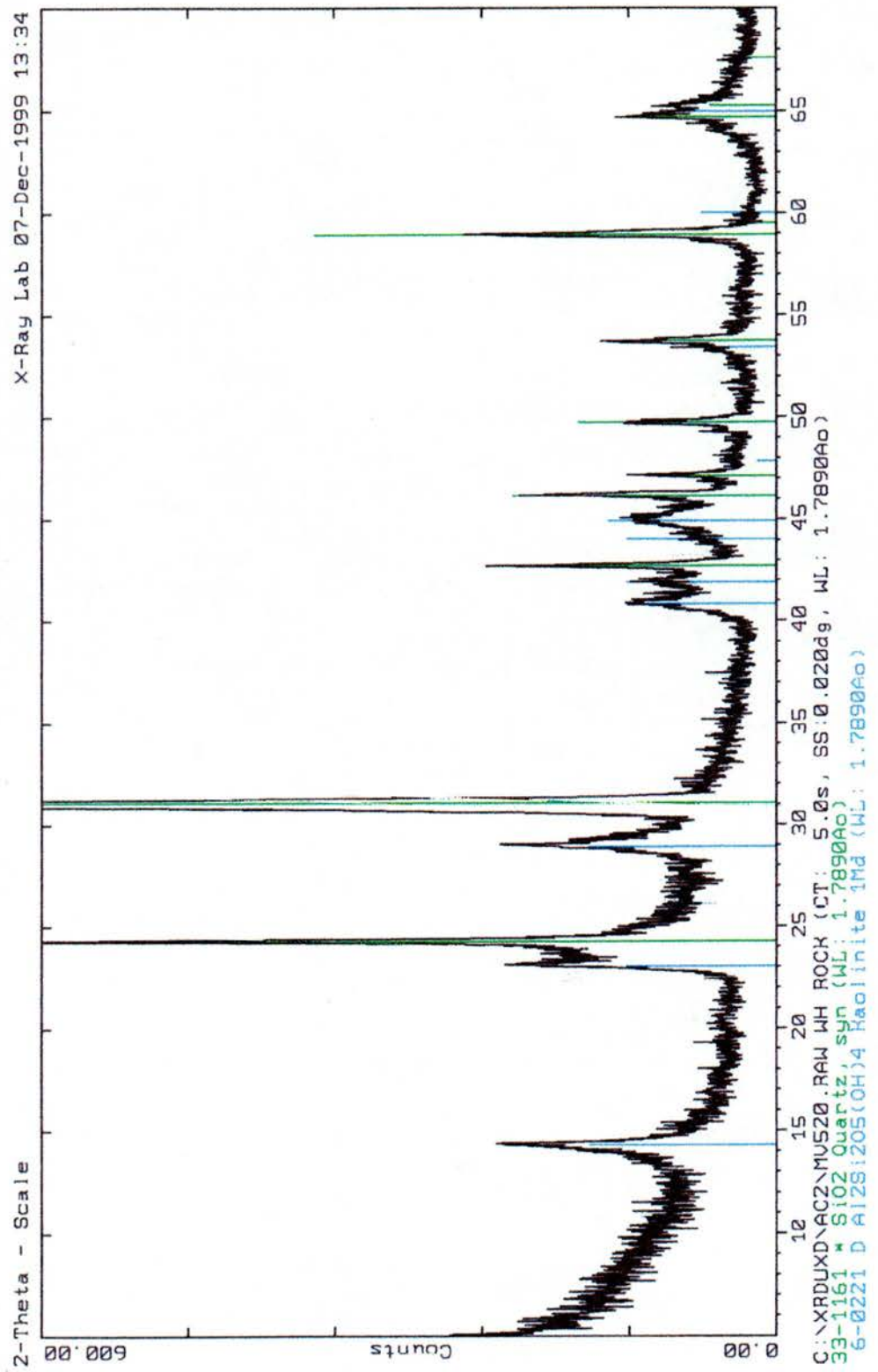
X-Ray Lab 07-Dec-1999 13:34
2-Theta - Scale
Counts
600.00
0.00
10
15
20
25
30
35
40
45
50
55
60
65
C:\XRDUXD\AC2\MV520.RAW WH ROCK (CT: 5.0s, SS:0.020dg, WL: 1.7890Ao)
33-1161 * SiO2 Quartz, syn (WL: 1.7890Ao)
6-0221 D Al2Si2O5(OH)4 Kaolinite 1Md (WL: 1.7890Ao)

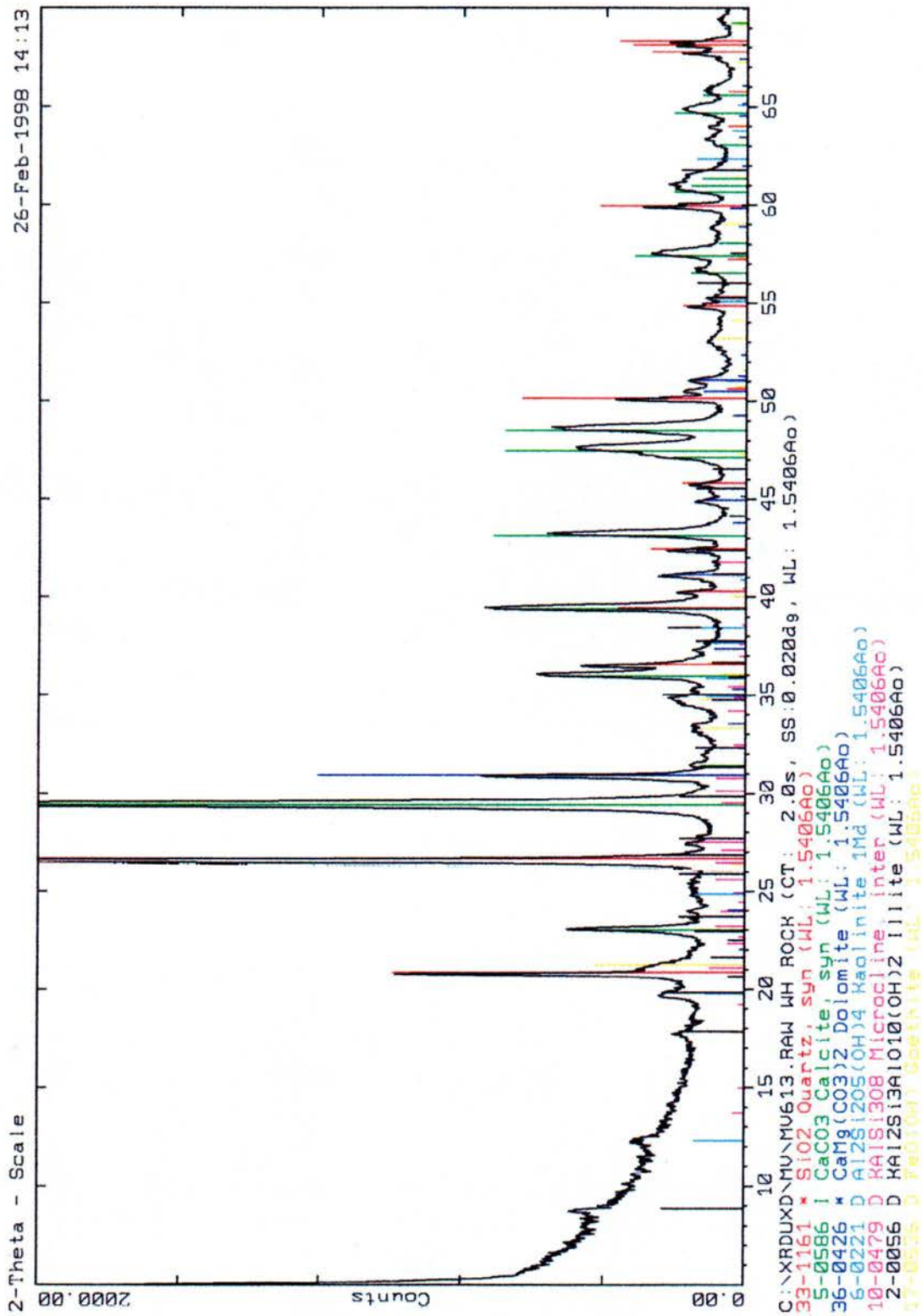
26-Feb-1998 14:13
2-Theta - Scale
Counts
2000.00
0.00
10
15
20
25
30
35
40
45
50
55
60
65
C:\XRDUXD\MV\MV613.RAW WH ROCK (CT: 2.0s, SS:0.020dg, WL: 1.5406Ao)
33-1161 * SiO2 Quartz, syn (WL: 1.5406Ao)
5-0586 I CaCO3 Calcite, syn (WL: 1.5406Ao)
36-0426 * CaMg(CO3)2 Dolomite (WL: 1.5406Ao)
6-0221 D Al2Si2O5(OH)4 Kaolinite 1Md (WL: 1.5406Ao)
10-0479 D KAlSi3O8 Microcline, inter (WL: 1.5406Ao)
2-0056 D KAl2Si3AlO10(OH)2 Illite (WL: 1.5406Ao)

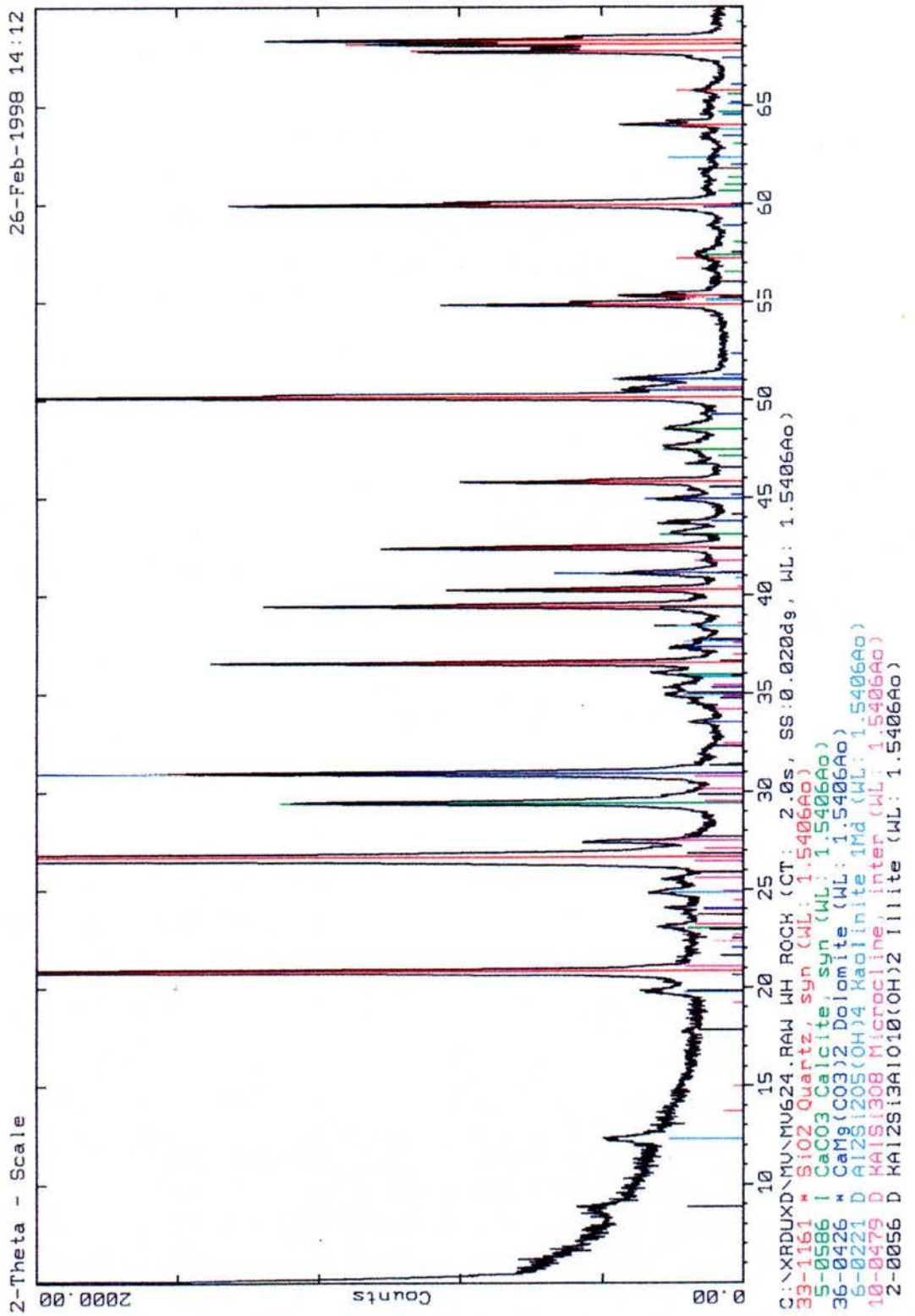
26-Feb-1998 14:12
2-Theta - Scale
Counts
2000.00
0.00
10
15
20
25
30
35
40
45
50
55
60
65
C:\XRDUXD\MV\MV624.RAW WH ROCK (CT: 2.0s, SS:0.020dg, WL: 1.5406Ao)
33-1161 * SiO2 Quartz, syn (WL: 1.5406Ao)
5-0586 l CaCO3 Calcite, syn (WL: 1.5406Ao)
36-0426 * CaMg(CO3)2 Dolomite (WL: 1.5406Ao)
6-0221 D Al2Si2O5(OH)4 Kaolinite 1Md (WL: 1.5406Ao)
10-0479 D KAlSi3O8 Microcline, inter (WL: 1.5406Ao)
2-0056 D KAl2Si3AlO10(OH)2 Illite (WL: 1.5406Ao)

APPENDIX 2

MEASURED SECTIONS

Appendix 2A: Measured sections in Maverick Springs area

SECTION	NAME	LOCATION
MV0	Sheep Creek Rd	6N2E 34-36
MV1	Arapahoe Ranch Rd	6N1E 14-23
MV2	Muddy Creek	6N1W 12; 6N1E 18
MV3	Eagle Point S	5N1W 2-1
MV4	Snakeke n1	5N1E 20-21
MV5	Five Mile Creek	5N1E 30-31
MV6	Maverick Springs Rd	5N1W 12
MV9	Oil Field large	6N2W 32-28
MV11	Oild filed short	6N2W33
MV12	Short Eagle Point	6N1W 14-23

Appendix 2B: Measured sections in south and southeastern areas

SECTION	NAME	LOCATION
MV10	Hudson S	33N98W
MV15	Alkali Butte	34N94W
MV16	North Muddy Creek	7N1W 36; 6N1E 6
MV17	Castle Gardens	43N90W
MV18	Conant Creek S	34N91W
MV19	Conant Creek N	34N92W
MV20	Alkali Butte E	34N94W
MV21	Alkali Butte W	1S6E
MV22	Hudson N	1S2E

SYMBOLS LEGEND

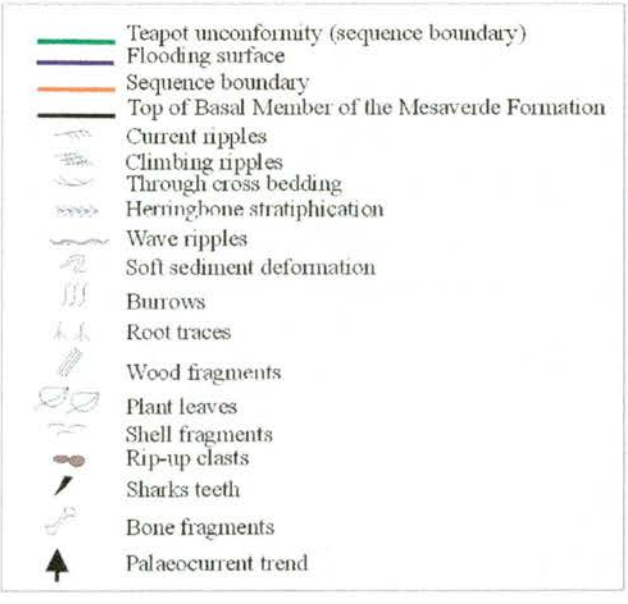

APPENDIX 3
WIRLINE-LOGS 1:

Studied wireline-logs comparing the gamma-ray, density and sonic logs.

Wireline-logs	northern	eastern	section	Top of Mv (m)	Base Mv (m)	Top of Mv (feet)	Base Mv (feet)
1n4e08	T1N	R4E	8	3185	0	10450	
1n4e14u	T1N	R4E	14	2559	3126	8395	10255
1n4e26w	T1N	R4E	26	2237	0	7340	
1n5e12tr	T1N	R5E	12	2149	2722	7050	8930
1n5e36	T1N	R5E	36	1234	1844	4050	6050
1n6e04	T1N	R6E	4	1341	1948	4400	6390
2n2e22gr	T2N	R2E	22	2274	2890	7460	9480
2n4e08	T2N	R4E	8	3630	4246	11910	13930
2n4e20	T2N	R4E	20	3467	4049	11375	13285
3n2e15-21	T3N	R2E	15	2707	3338	8880	10950
3n2ehic	T3N	R2E	3	2807	3383	9210	11100
3n3e11	T3N	R3E	11	3901	4526	12800	14850
3n3e15ex	T3N	R3E	15	3621	4237	11880	13900
4n2e2211	T4N	R2E	22	2961	3560	9715	11680
4n2e2443	T4N	R2E	24	3353	3920	11000	12860
5n2e10	T5N	R2E	10	3075	3664	10090	12020
5n2e31x	T5N	R2E	31	2256	2848	7400	9345
5n3e26ok	T5N	R3E	26	4103	5630	13460	18470
mr3013	T4N	R3E	30	3327	3901	10915	12800
mr3111	T4N	R3E	31	3319	3889	10890	12760
tbi 19-23	T4N	R3E	19	3299	3871	10825	12700
tbi20-23	T4N	R3E	20	3511	4395	11520	14420
tbi31-22	T4N	R3E	31	3261	3847	10700	12620

LEGEND

Teapot unconformity (sequence boundary)

Flooding surface

Sequence boundary

Top of Basal Member

Coincident flooding surface and sequence boundary

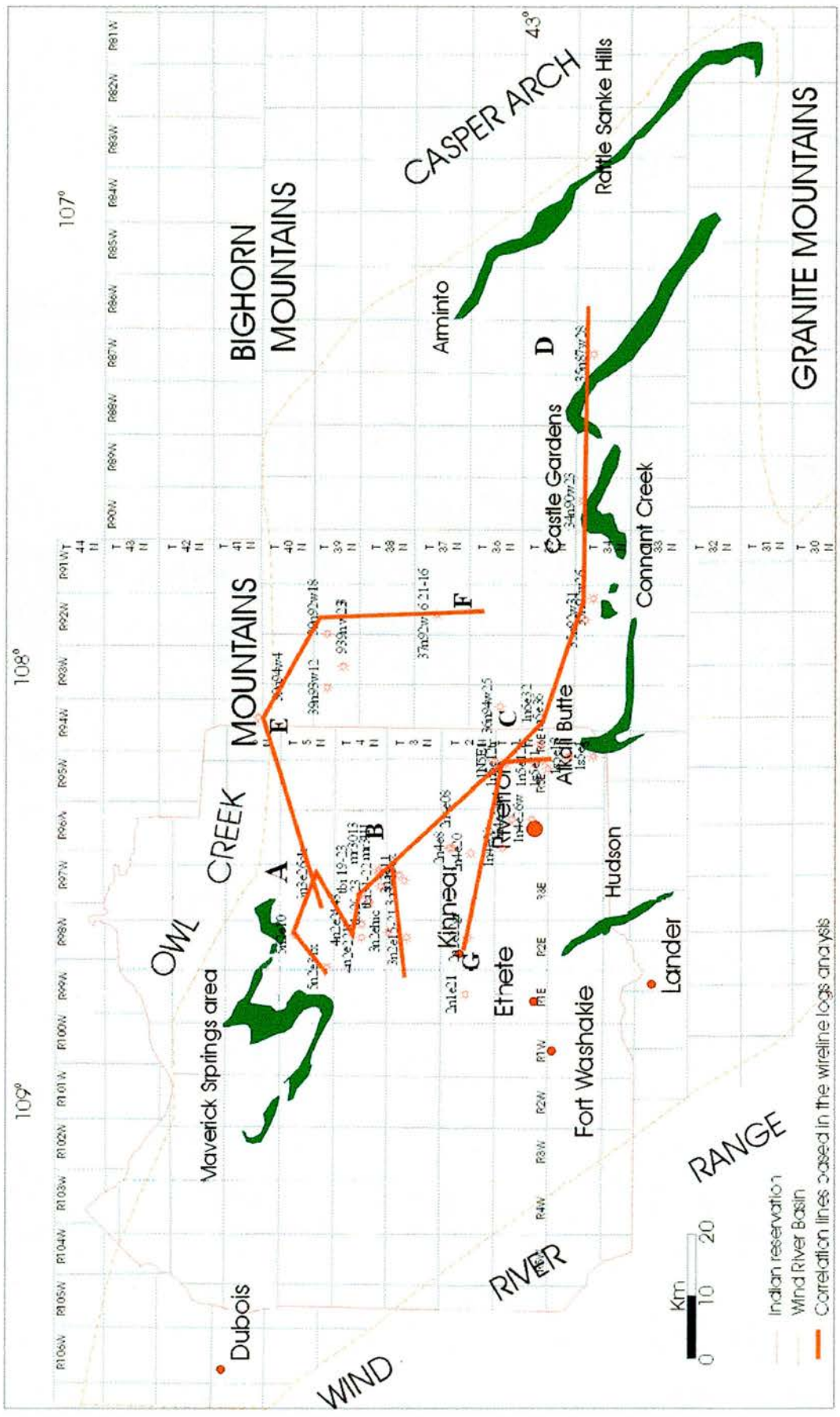

Location of wireline-logs

APPENDIX 3 WIRELINE LOGS

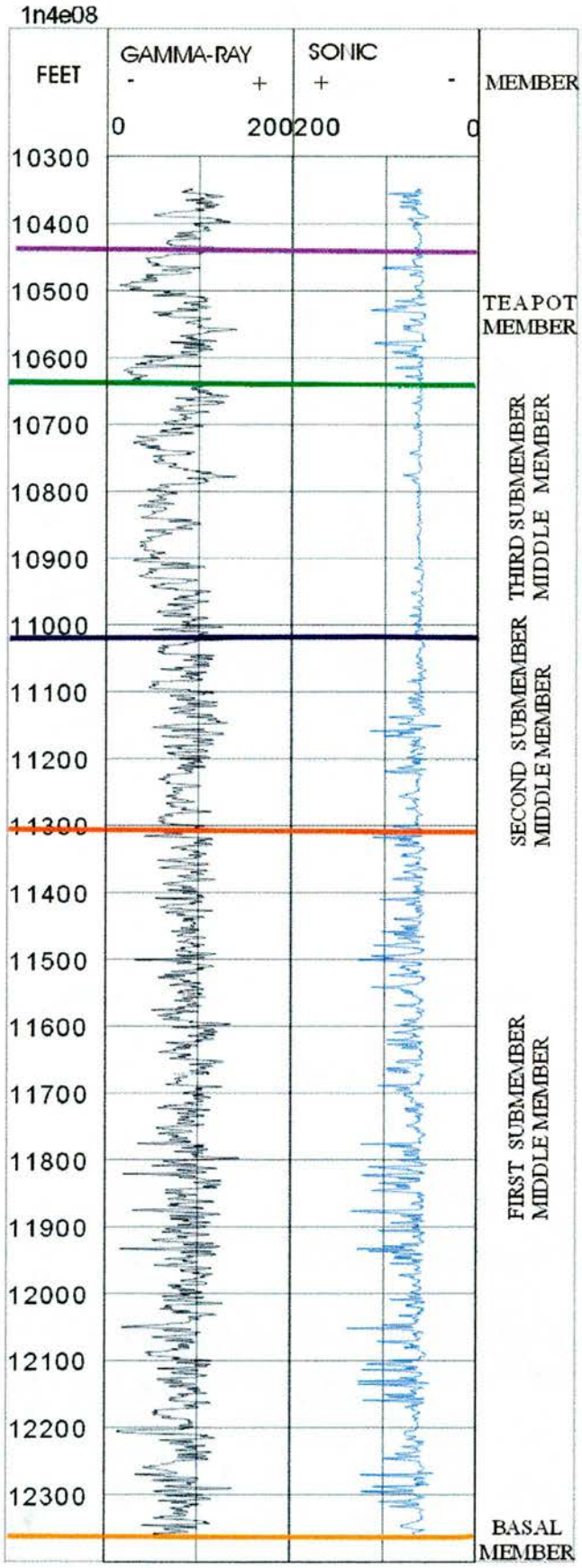

1N4E14U

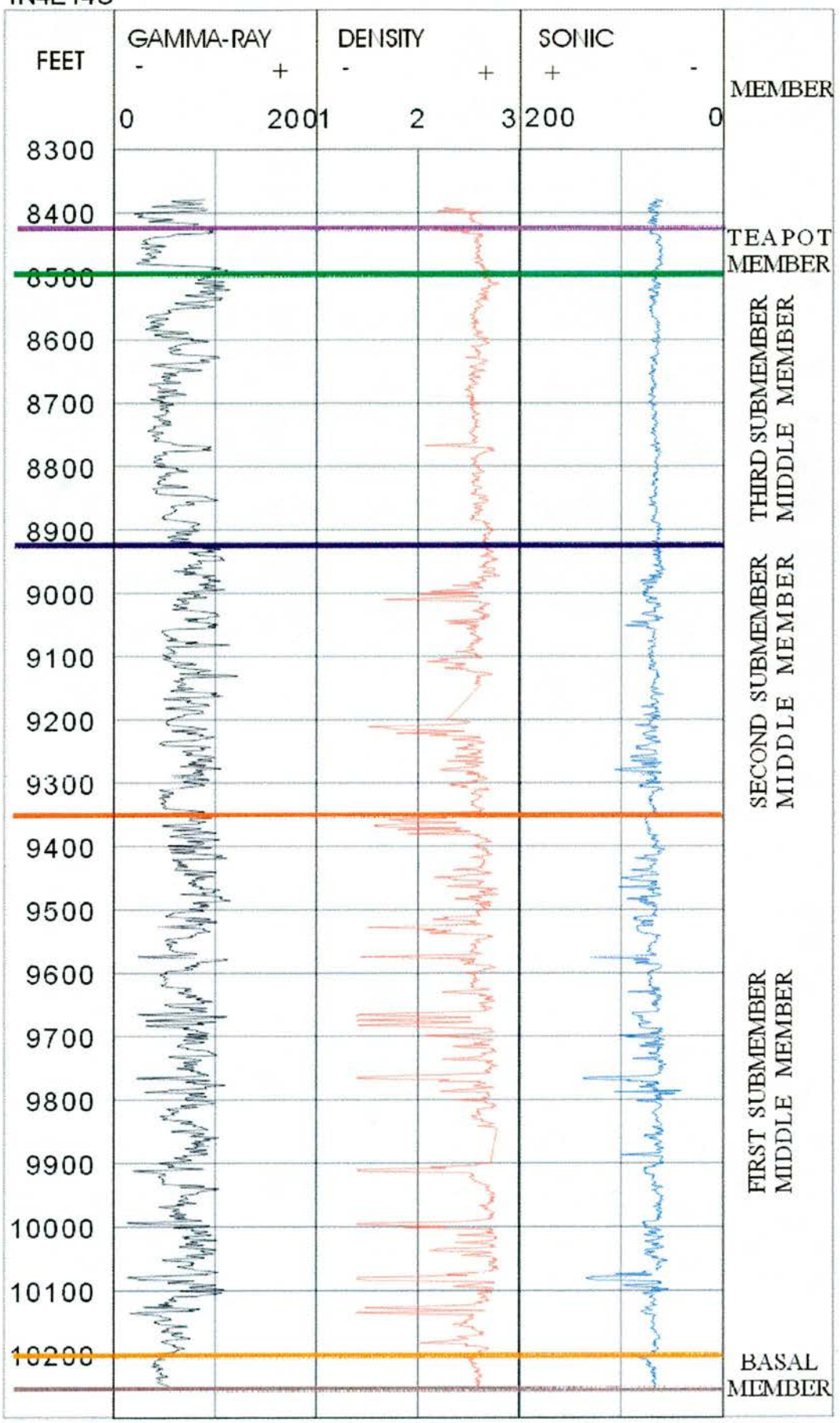
FEET
GAMMA-RAY
- +
0 200
DENSITY
- +
1 2 3
SONIC
+ -
200 0
MEMBER
8300
8400
8500
8600
8700
8800
8900
9000
9100
9200
9300
9400
9500
9600
9700
9800
9900
10000
10100
10200
TEAPOT MEMBER
THIRD SUBMEMBER MIDDLE MEMBER
SECOND SUBMEMBER MIDDLE MEMBER
FIRST SUBMEMBER MIDDLE MEMBER
BASAL MEMBER

1n 4e 26w

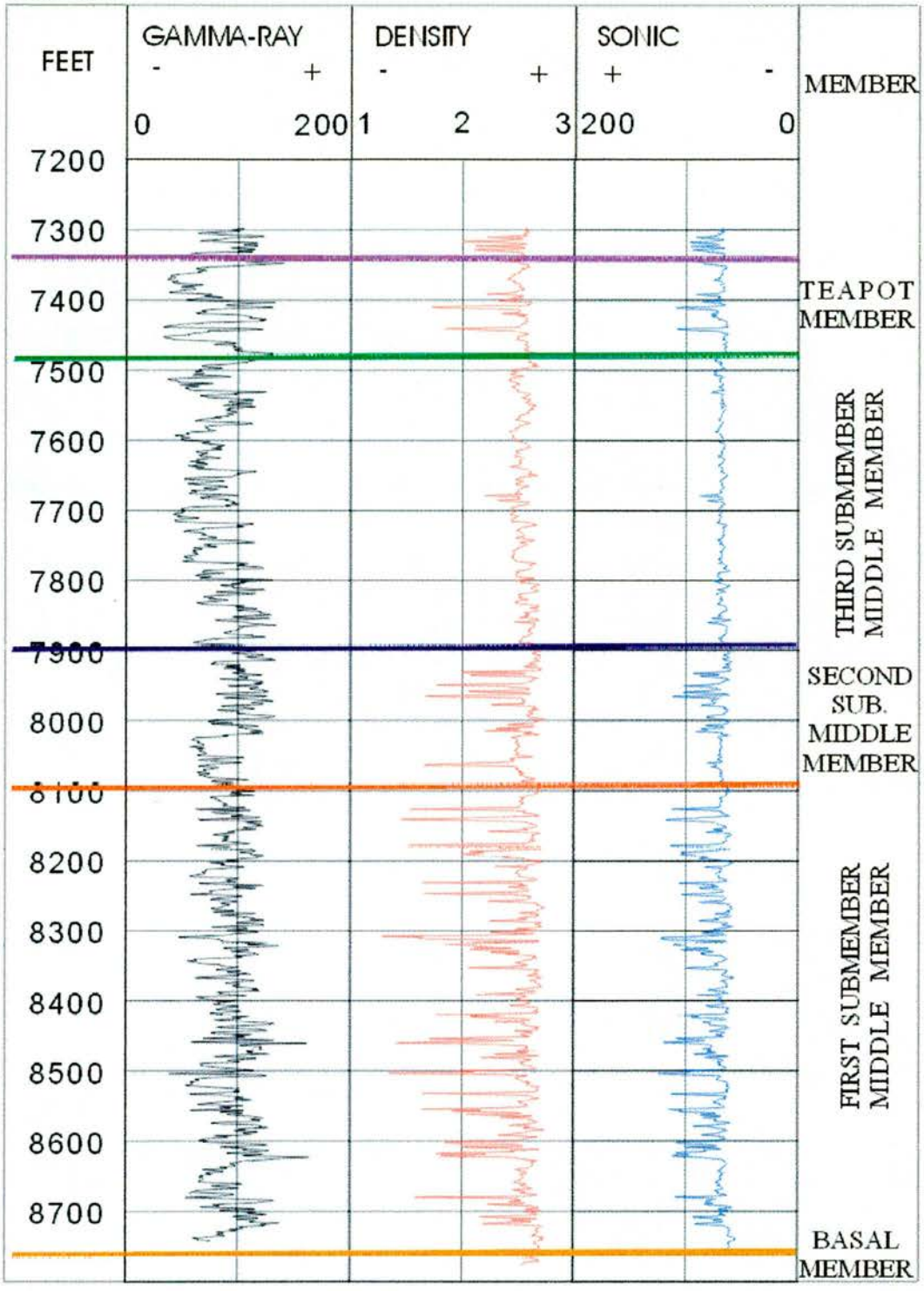
FEET
GAMMA-RAY
- +
0 200
DENSITY
- +
1 2 3
SONIC
+ -
200 0
MEMBER
7200
7300
7400
7500
7600
7700
7800
7900
8000
8100
8200
8300
8400
8500
8600
8700
TEAPOT MEMBER
THIRD SUBMEMBER MIDDLE MEMBER
SECOND SUB. MIDDLE MEMBER
FIRST SUBMEMBER MIDDLE MEMBER
BASAL MEMBER

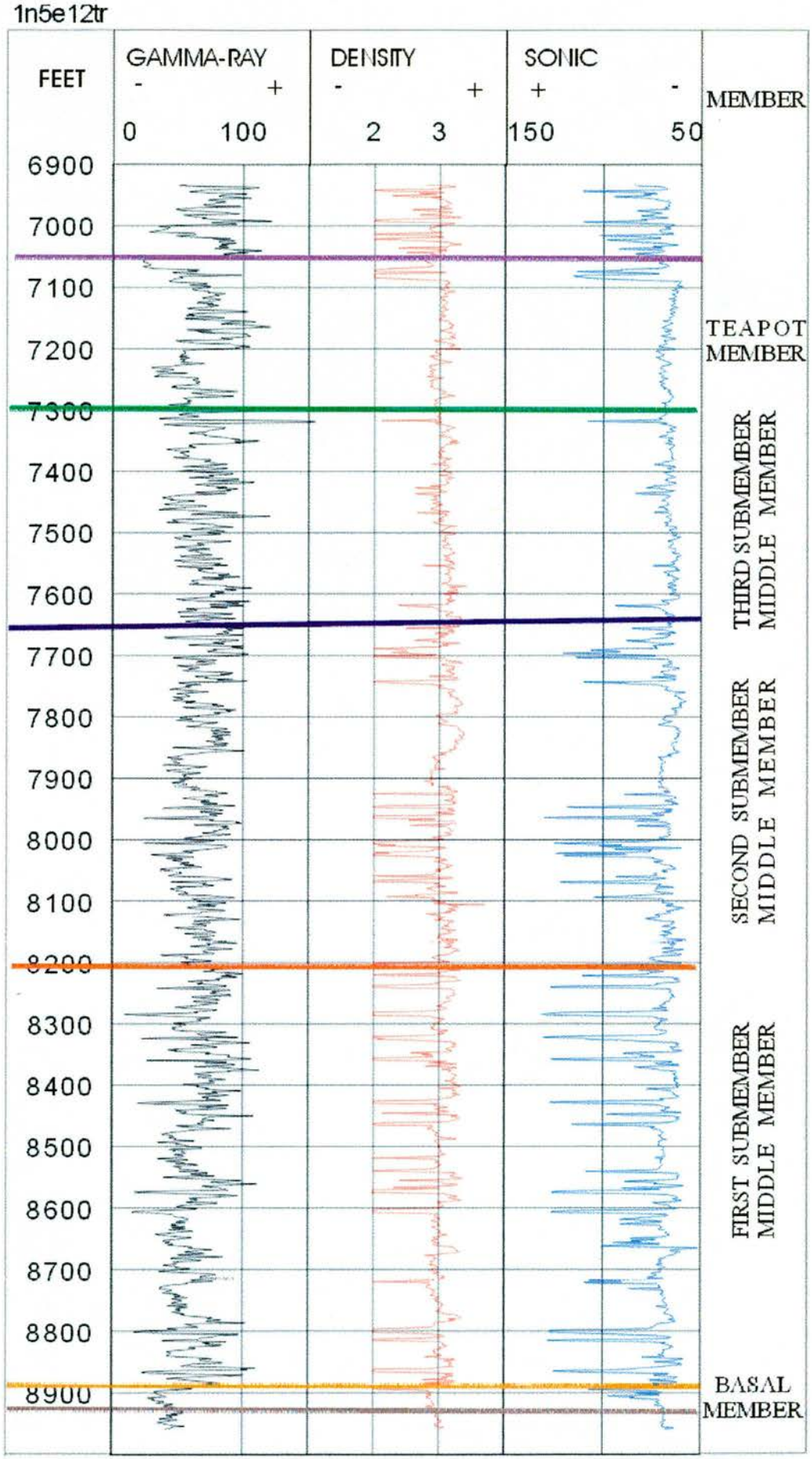
1n5e12tr
FEET
GAMMA-RAY
- +
0 100
DENSITY
- +
2 3
SONIC
+ -
150 50
MEMBER
6900
7000
7100
7200
7300
7400
7500
7600
7700
7800
7900
8000
8100
8200
8300
8400
8500
8600
8700
8800
8900
TEAPOT MEMBER
THIRD SUBMEMBER MIDDLE MEMBER
SECOND SUBMEMBER MIDDLE MEMBER
FIRST SUBMEMBER MIDDLE MEMBER
BASAL MEMBER

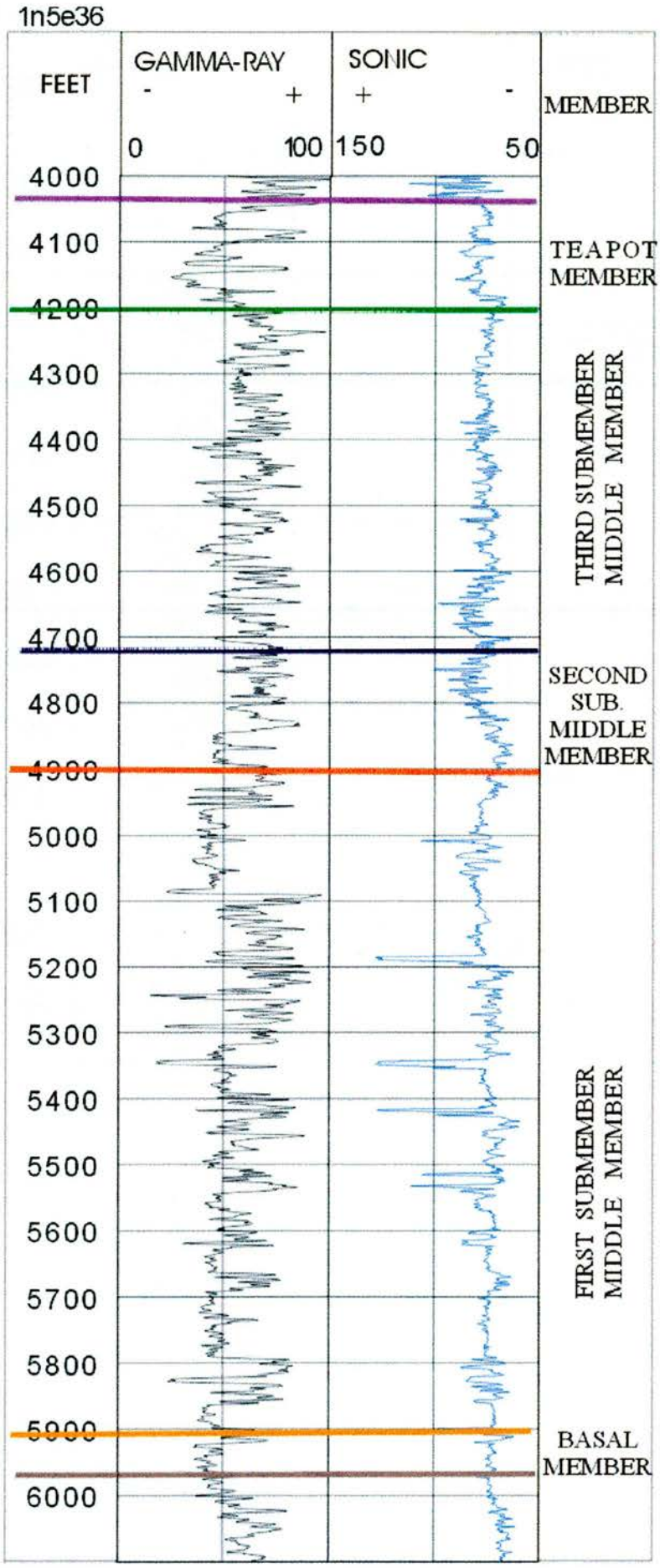
1n5e36
FEET
GAMMA-RAY
-
+
0
100
SONIC
+
-
150
50
MEMBER
4000
4100
4200
4300
4400
4500
4600
4700
4800
4900
5000
5100
5200
5300
5400
5500
5600
5700
5800
5900
6000
TEAPOT MEMBER
THIRD SUBMEMBER MIDDLE MEMBER
SECOND SUB. MIDDLE MEMBER
FIRST SUBMEMBER MIDDLE MEMBER
BASAL MEMBER

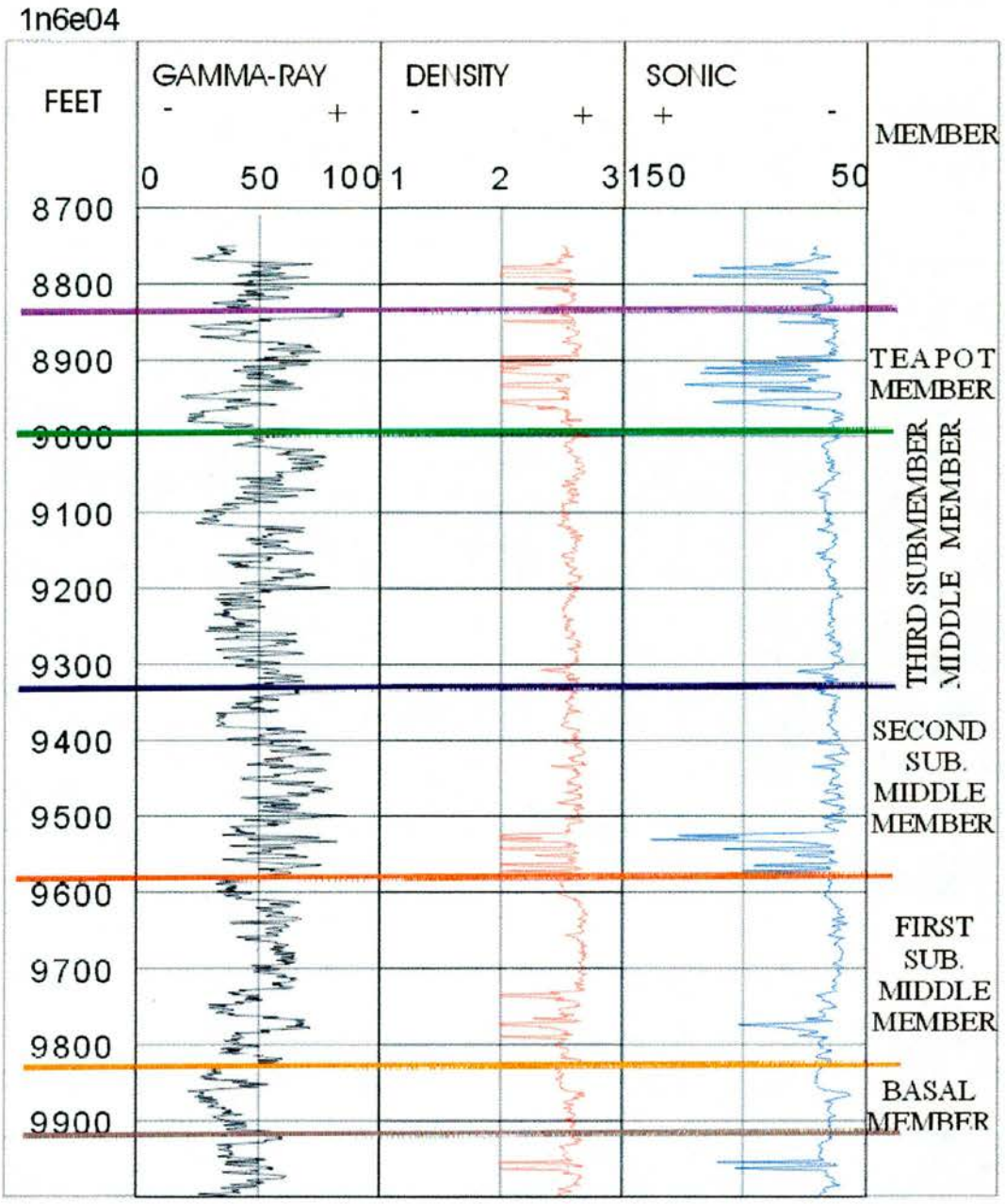
1n6e04
FEET
GAMMA-RAY
- +
0 50 100
DENSITY
- +
1 2 3
SONIC
+ -
150 50
MEMBER
8700
8800
8900
9000
9100
9200
9300
9400
9500
9600
9700
9800
9900
TEAPOT MEMBER
THIRD SUBMEMBER
MIDDLE MEMBER
SECOND SUB. MIDDLE MEMBER
FIRST SUB. MIDDLE MEMBER
BASAL MEMBER

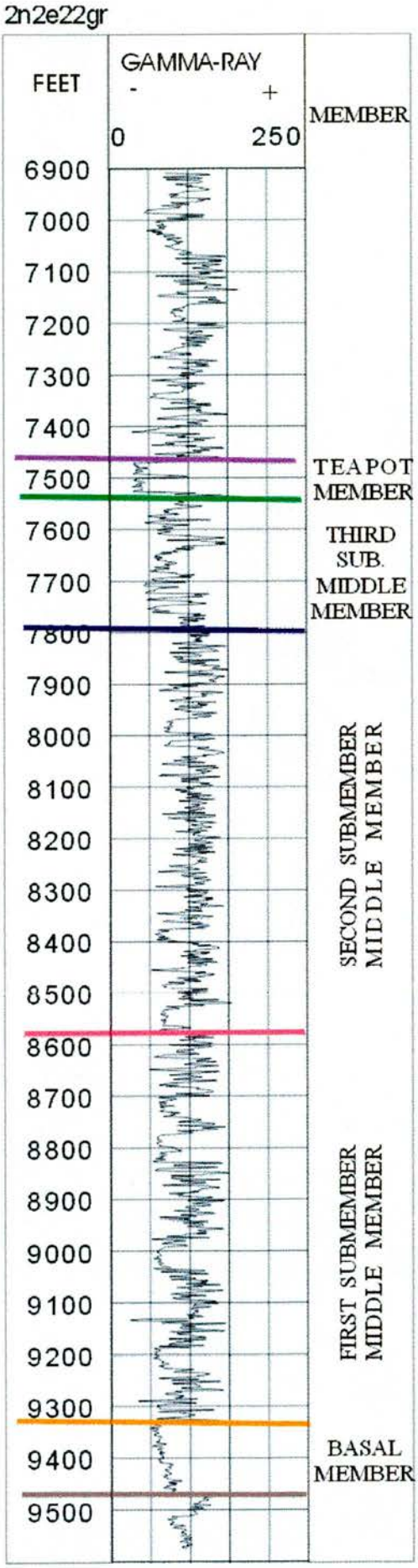
2n2e22gr
FEET
GAMMA-RAY
-
+
0
250
MEMBER
6900
7000
7100
7200
7300
7400
7500
7600
7700
7800
7900
8000
8100
8200
8300
8400
8500
8600
8700
8800
8900
9000
9100
9200
9300
9400
9500
TEAPOT MEMBER
THIRD SUB. MIDDLE MEMBER
SECOND SUBMEMBER MIDDLE MEMBER
FIRST SUBMEMBER MIDDLE MEMBER
BASAL MEMBER

APPENDIX 3 WIRELINE LOGS

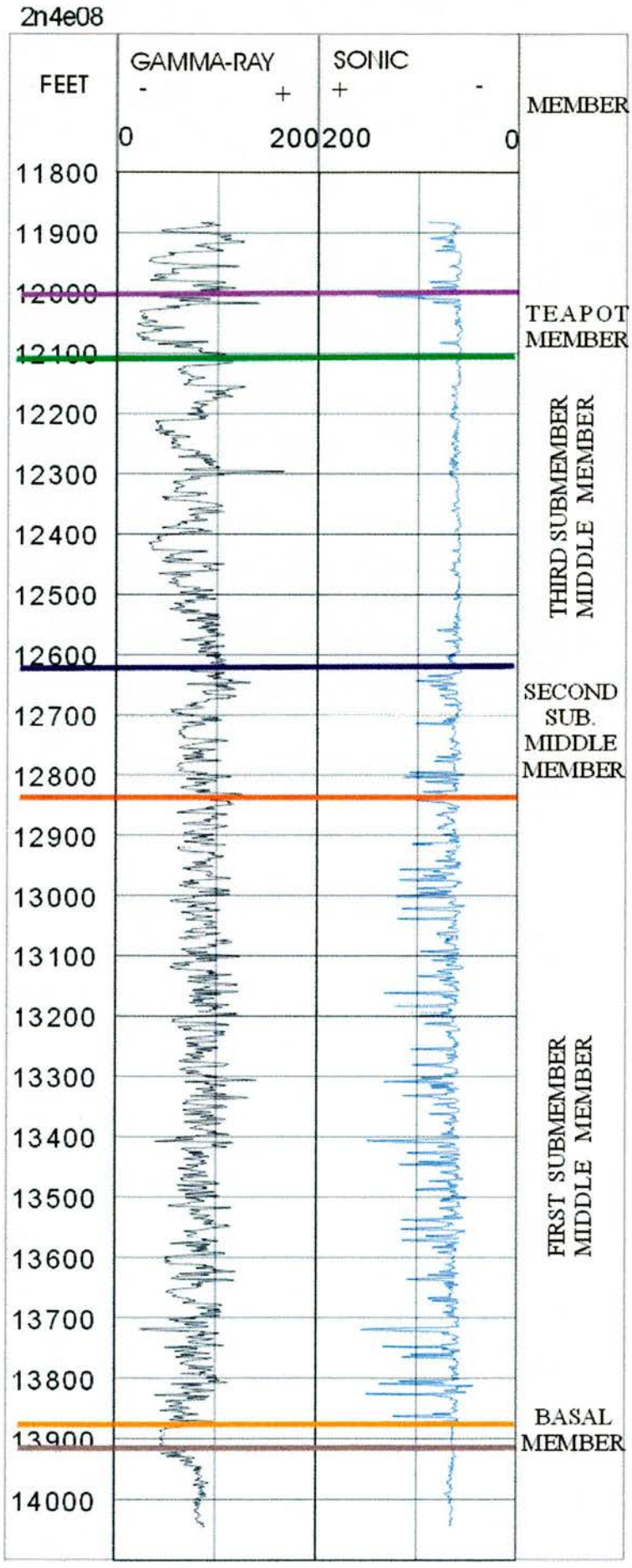

APPENDIX 3 WIRELINE LOGS

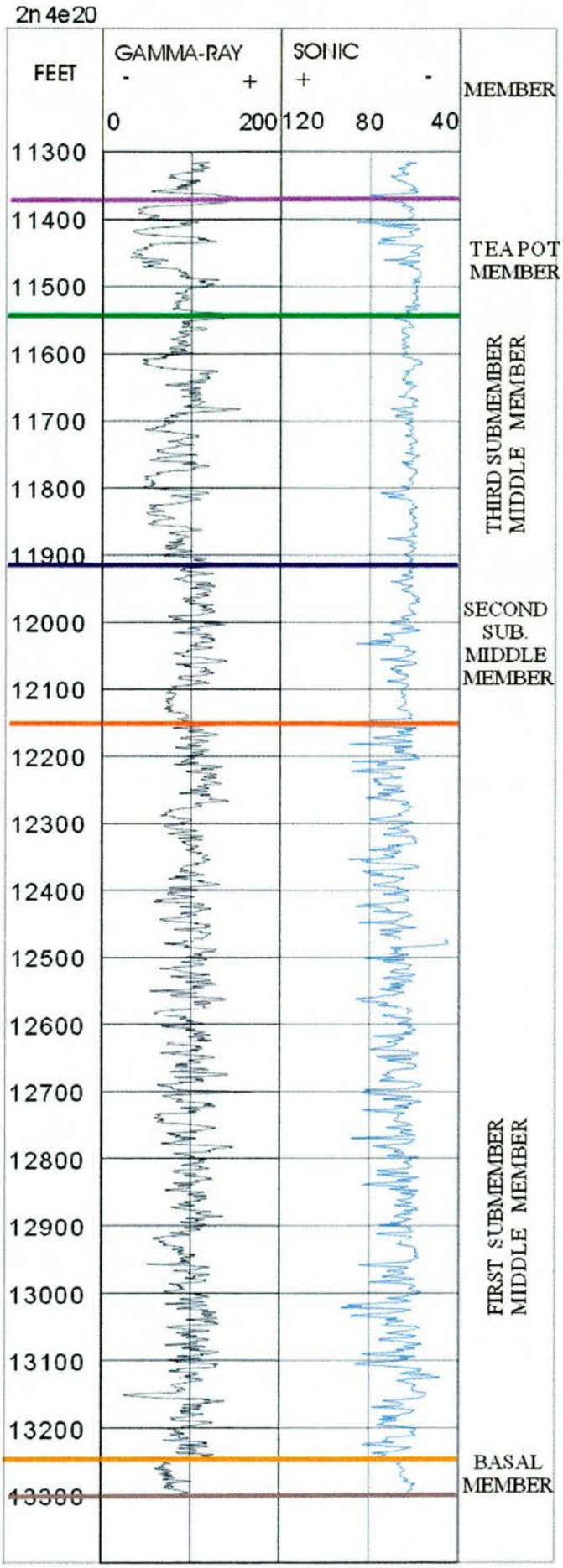

3n2e1521

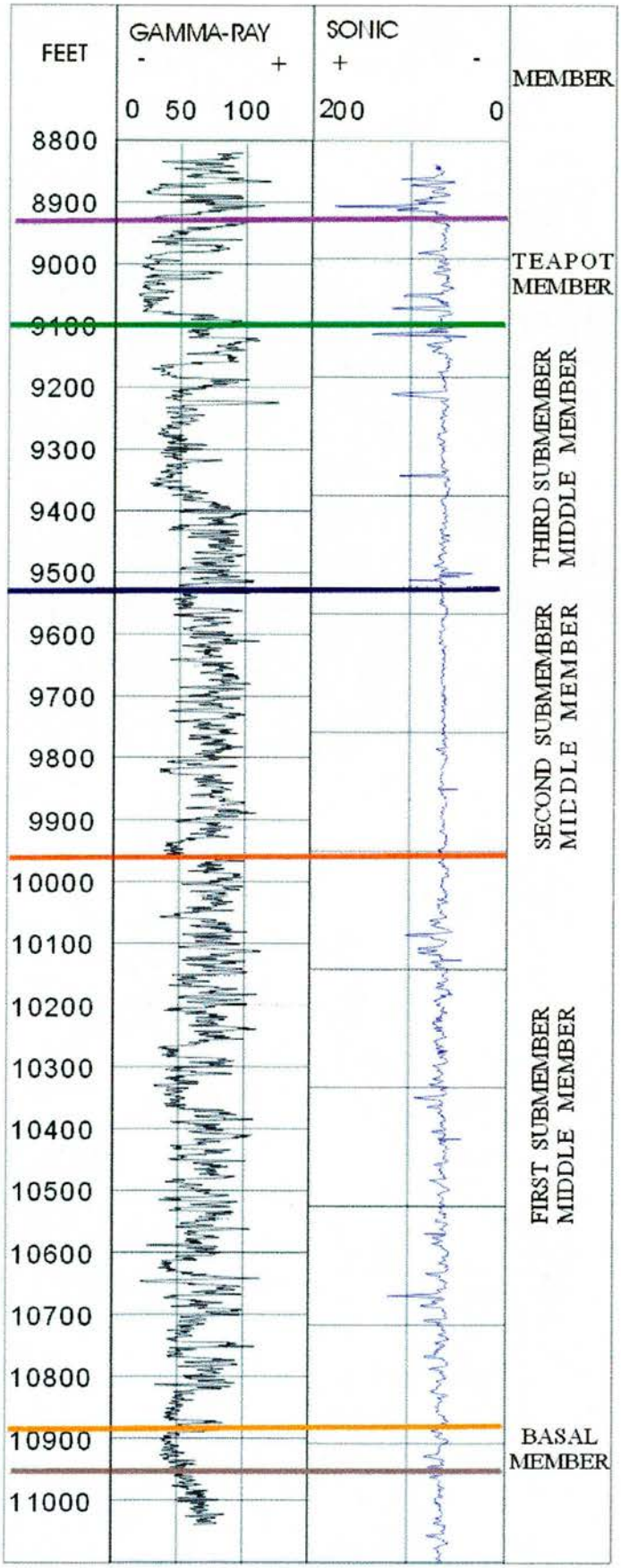
FEET
GAMMA-RAY
-
+
0 50 100
SONIC
+
-
200 0
MEMBER
8800
8900
9000
9100
9200
9300
9400
9500
9600
9700
9800
9900
10000
10100
10200
10300
10400
10500
10600
10700
10800
10900
11000
TEAPOT MEMBER
THIRD SUBMEMBER MIDDLE MEMBER
SECOND SUBMEMBER MIDDLE MEMBER
FIRST SUBMEMBER MIDDLE MEMBER
BASAL MEMBER

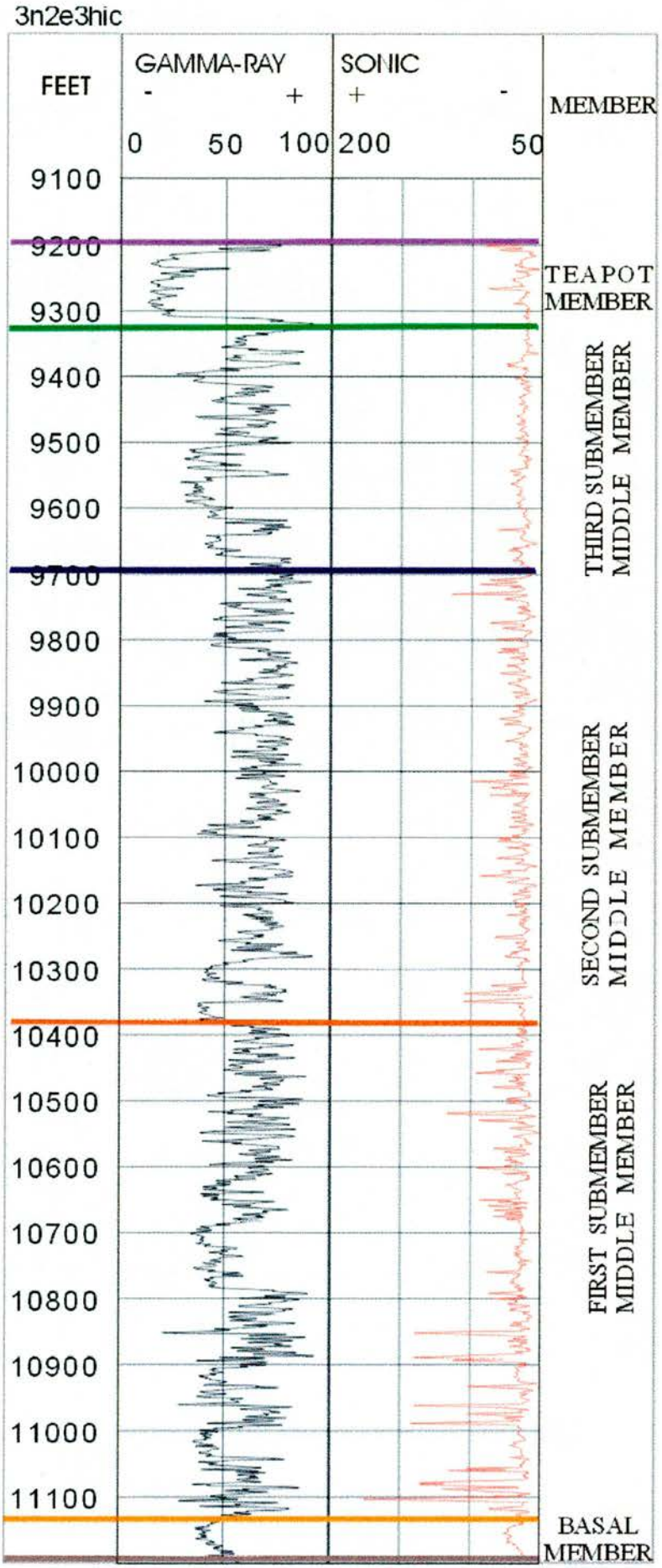
3n2e3hic
FEET
GAMMA-RAY
-
+
0
50
100
SONIC
+
-
200
50
MEMBER
9100
9200
9300
9400
9500
9600
9700
9800
9900
10000
10100
10200
10300
10400
10500
10600
10700
10800
10900
11000
11100
TEAPOT MEMBER
THIRD SUBMEMBER MIDDLE MEMBER
SECOND SUBMEMBER MIDDLE MEMBER
FIRST SUBMEMBER MIDDLE MEMBER
BASAL MEMBER

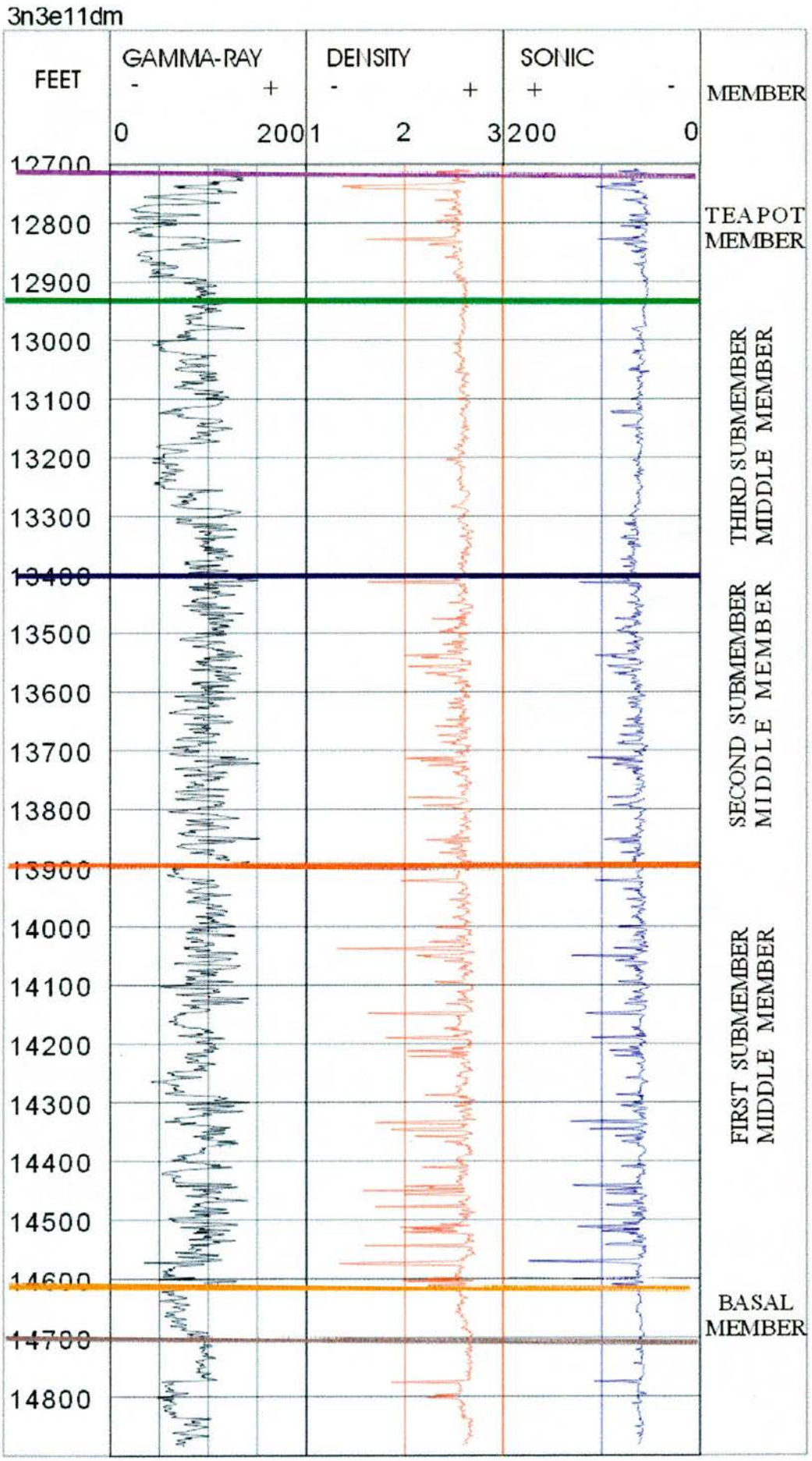
3n3e11dm
FEET
GAMMA-RAY
- +
0 200
DENSITY
- +
1 2 3
SONIC
+ -
200 0
MEMBER
12700
12800
12900
13000
13100
13200
13300
13400
13500
13600
13700
13800
13900
14000
14100
14200
14300
14400
14500
14600
14700
14800
TEAPOT MEMBER
THIRD SUBMEMBER MIDDLE MEMBER
SECOND SUBMEMBER MIDDLE MEMBER
FIRST SUBMEMBER MIDDLE MEMBER
BASAL MEMBER

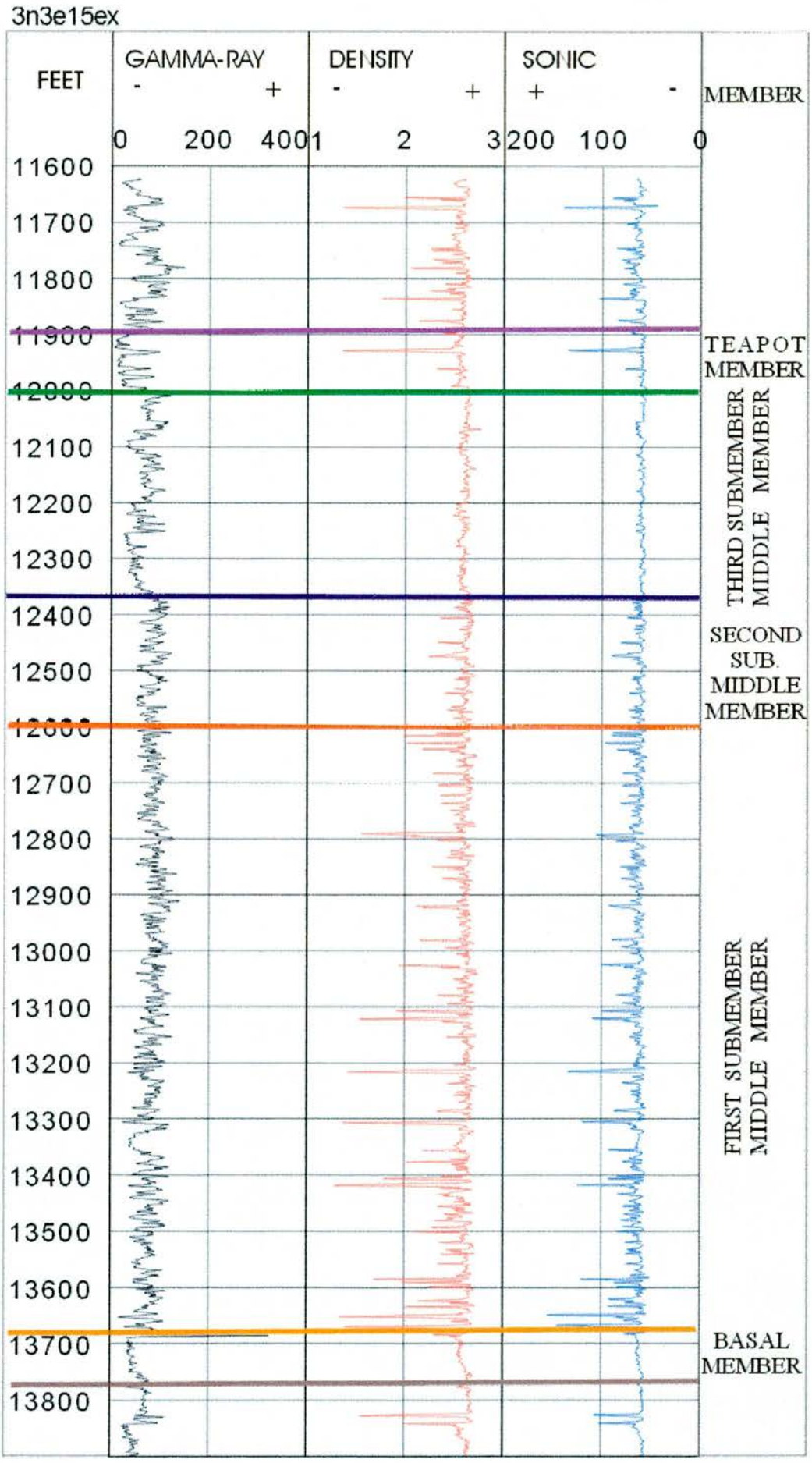
3n3e15ex
FEET
GAMMA-RAY
- +
0 200 400
DENSITY
- +
1 2 3
SONIC
+ -
200 100 0
MEMBER
11600
11700
11800
11900
12000
12100
12200
12300
12400
12500
12600
12700
12800
12900
13000
13100
13200
13300
13400
13500
13600
13700
13800
TEAPOT MEMBER
THIRD SUBMEMBER MIDDLE MEMBER
SECOND SUB. MIDDLE MEMBER
FIRST SUBMEMBER MIDDLE MEMBER
BASAL MEMBER

4n2e2211

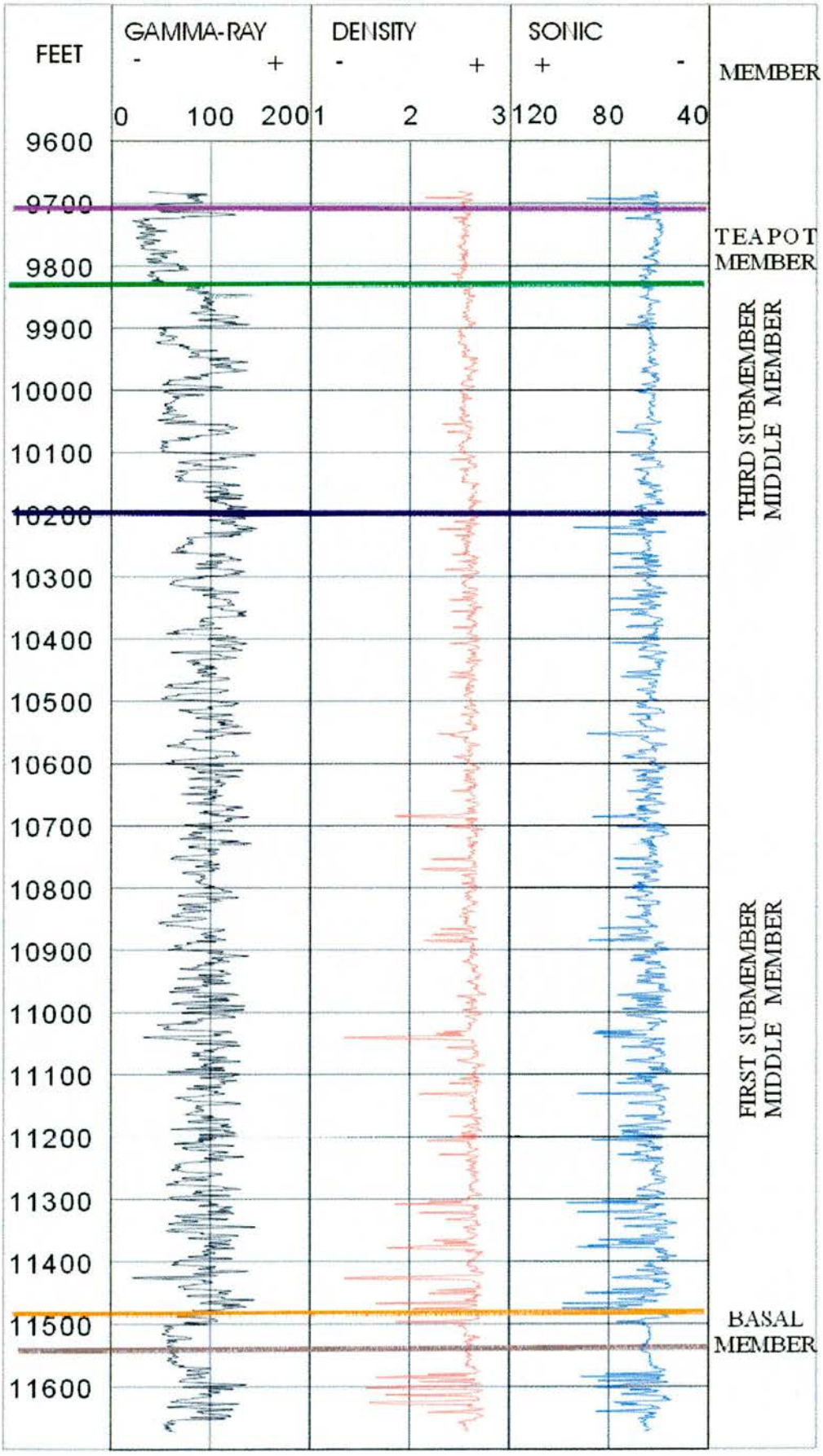
FEET
GAMMA-RAY
- +
0 100 200
DENSITY
- +
1 2 3
SONIC
+ -
120 80 40
MEMBER
9600
9700
9800
9900
10000
10100
10200
10300
10400
10500
10600
10700
10800
10900
11000
11100
11200
11300
11400
11500
11600
TEAPOT MEMBER
THIRD SUBMEMBER MIDDLE MEMBER
FIRST SUBMEMBER MIDDLE MEMBER
BASAL MEMBER

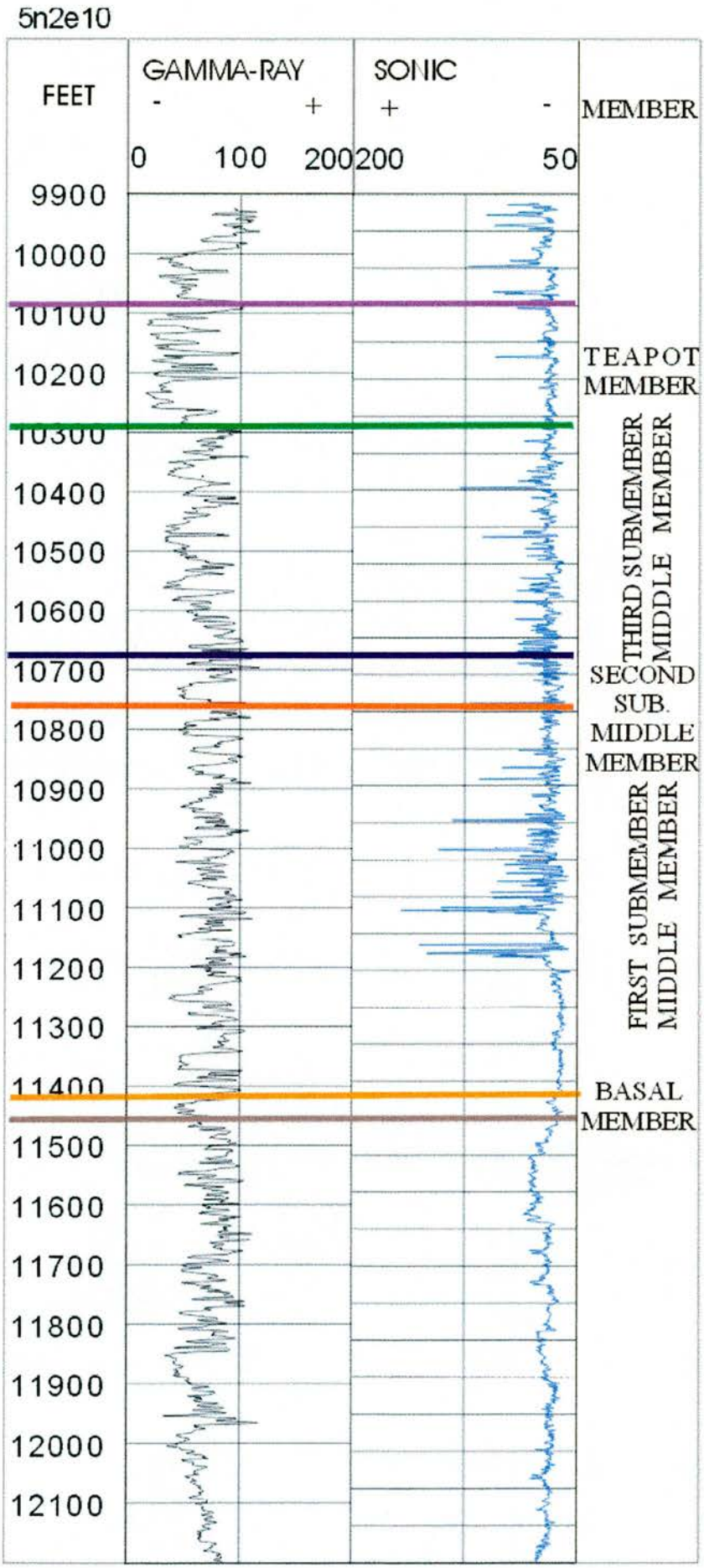
5n2e10
FEET
GAMMA-RAY
-
+
0
100
200
SONIC
+
-
200
50
MEMBER
9900
10000
10100
10200
10300
10400
10500
10600
10700
10800
10900
11000
11100
11200
11300
11400
11500
11600
11700
11800
11900
12000
12100
TEAPOT MEMBER
THIRD SUBMEMBER MIDDLE MEMBER
SECOND SUB. MIDDLE MEMBER
FIRST SUBMEMBER MIDDLE MEMBER
BASAL MEMBER

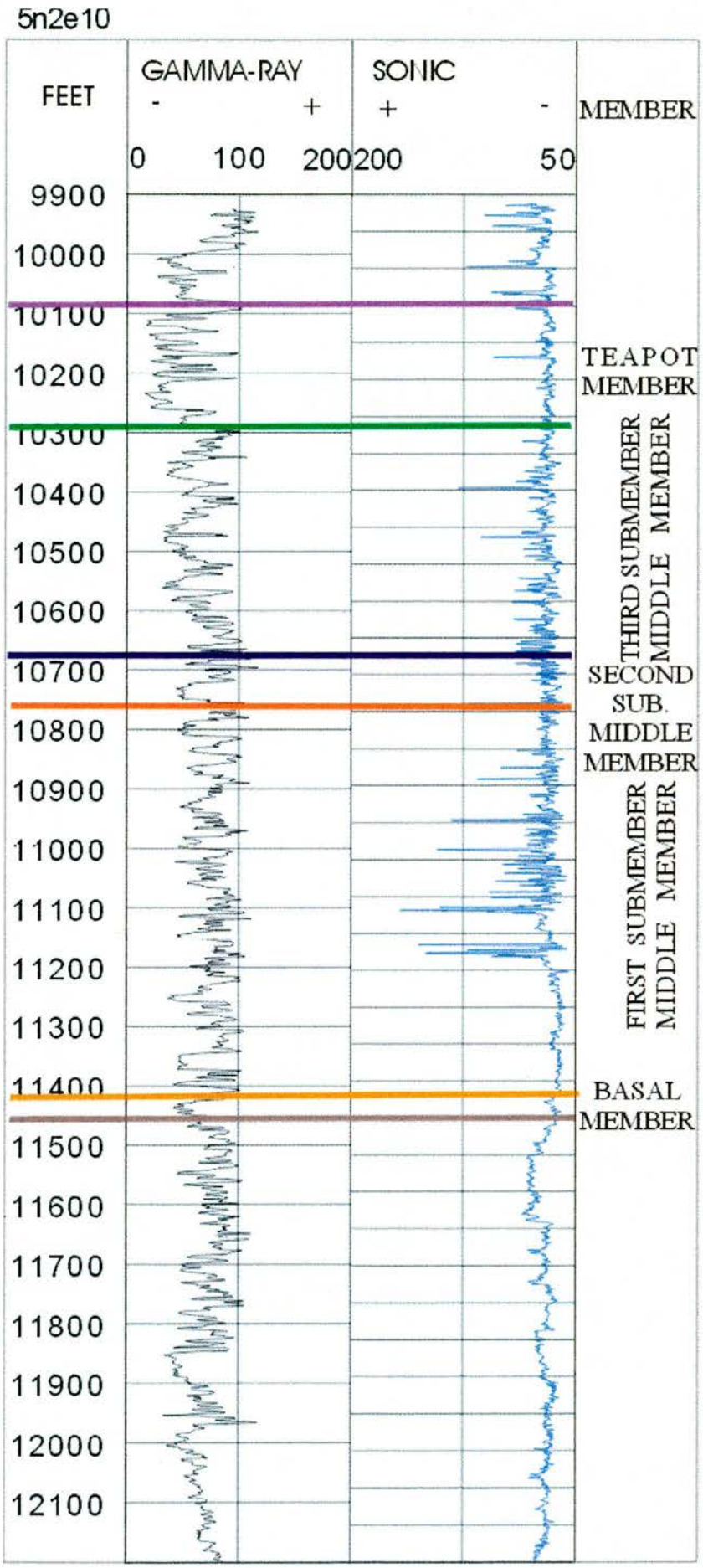
5n2e10
FEET
GAMMA-RAY
-
+
0
100
200
SONIC
+
-
200
50
MEMBER
9900
10000
10100
10200
10300
10400
10500
10600
10700
10800
10900
11000
11100
11200
11300
11400
11500
11600
11700
11800
11900
12000
12100
TEAPOT MEMBER
THIRD SUBMEMBER MIDDLE MEMBER
SECOND SUB. MIDDLE MEMBER
FIRST SUBMEMBER MIDDLE MEMBER
BASAL MEMBER

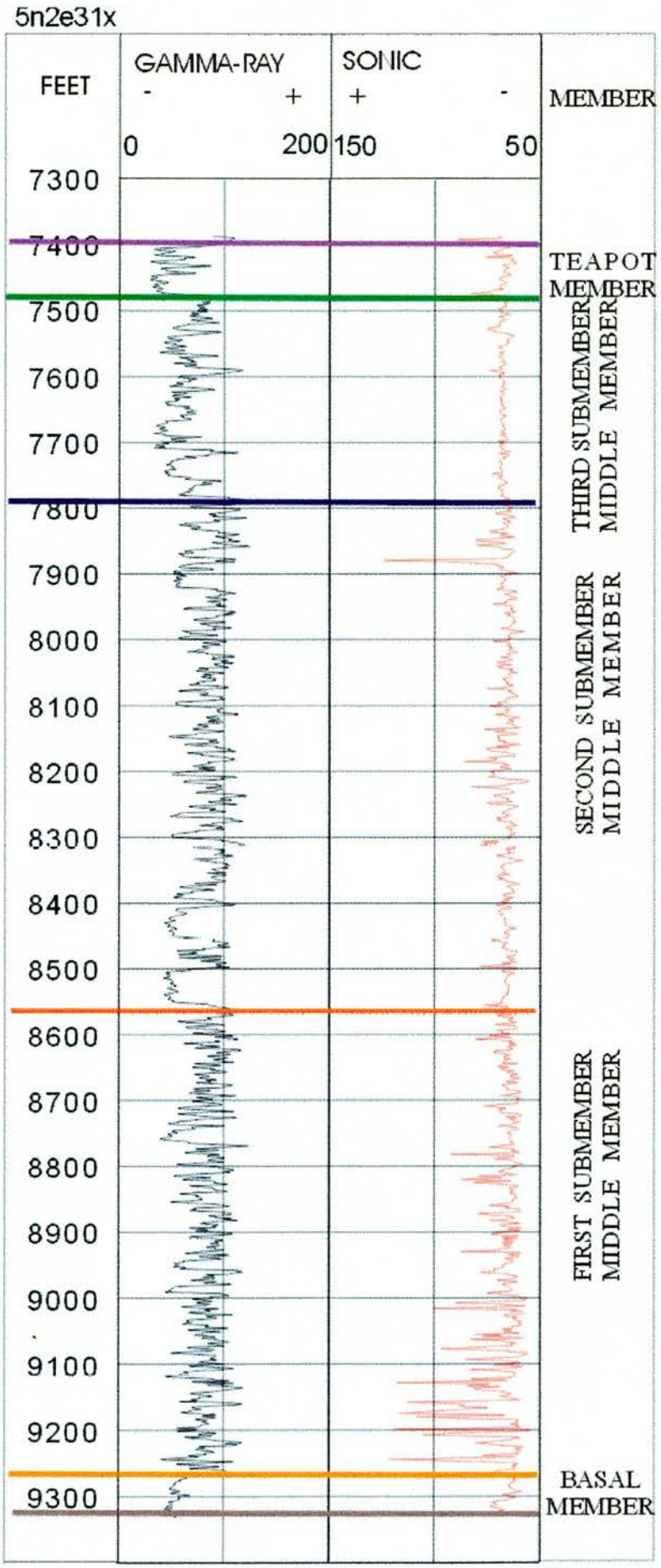
5n2e31x
FEET
GAMMA-RAY
-
+
0
200
SONIC
+
-
150
50
MEMBER
7300
7400
7500
7600
7700
7800
7900
8000
8100
8200
8300
8400
8500
8600
8700
8800
8900
9000
9100
9200
9300
TEAPOT MEMBER
THIRD SUBMEMBER MIDDLE MEMBER
SECOND SUBMEMBER MIDDLE MEMBER
FIRST SUBMEMBER MIDDLE MEMBER
BASAL MEMBER

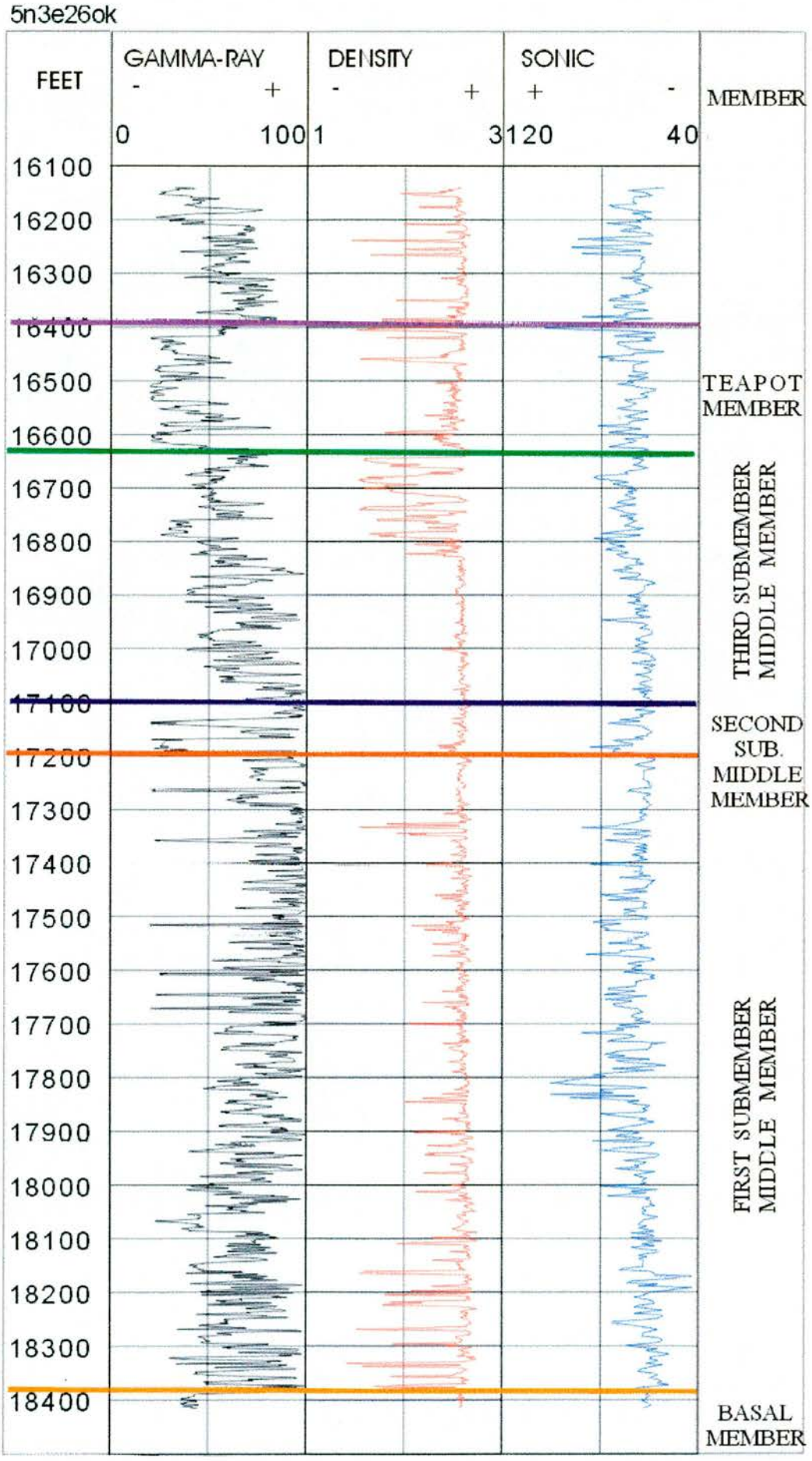
5n3e26ok
FEET
GAMMA-RAY
- +
0 100
DENSITY
- +
1 3
SONIC
+ -
120 40
MEMBER
16100
16200
16300
16400
16500
16600
16700
16800
16900
17000
17100
17200
17300
17400
17500
17600
17700
17800
17900
18000
18100
18200
18300
18400
TEAPOT MEMBER
THIRD SUBMEMBER MIDDLE MEMBER
SECOND SUB. MIDDLE MEMBER
FIRST SUBMEMBER MIDDLE MEMBER
BASAL MEMBER

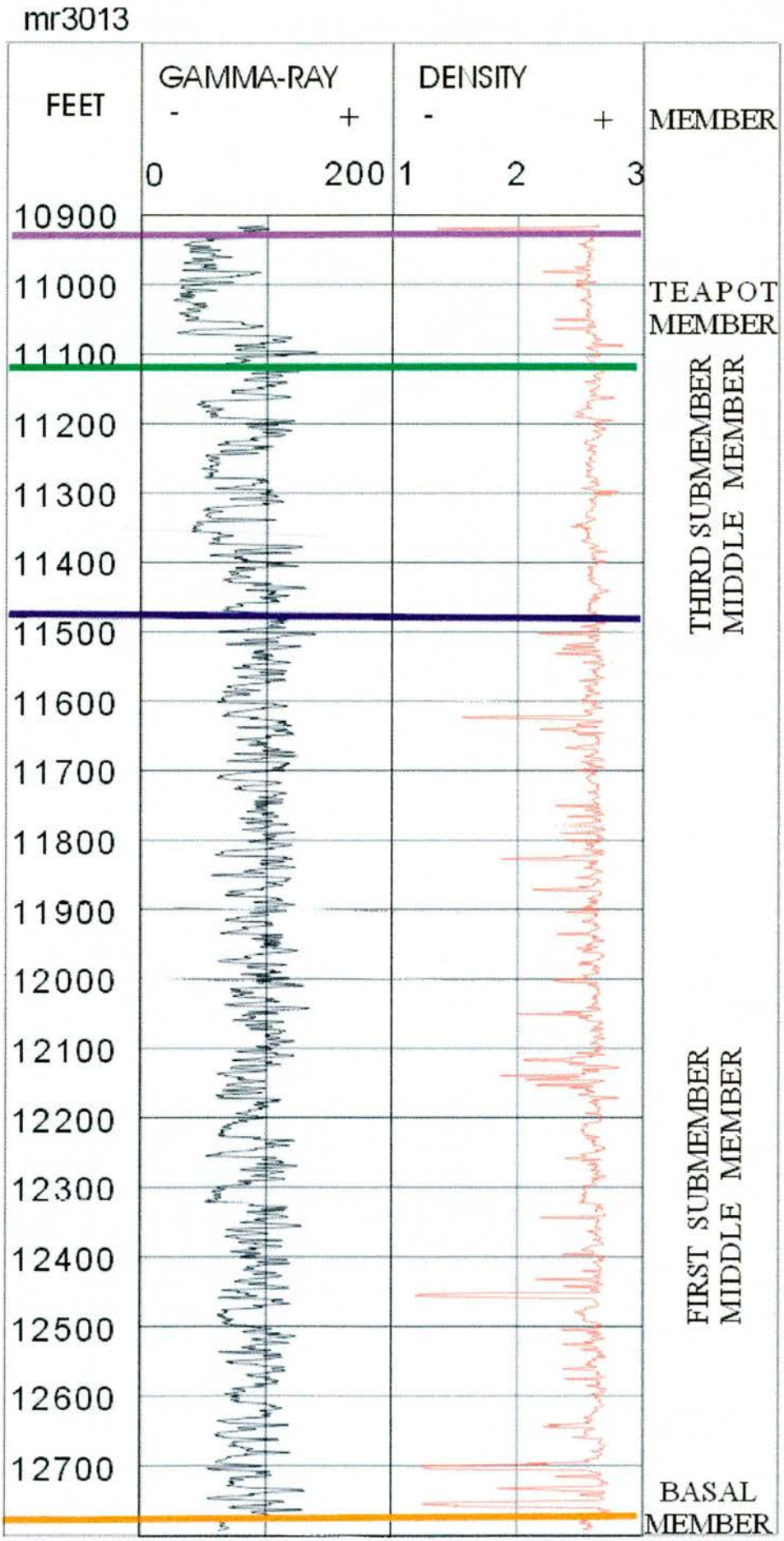
mr3013
FEET
GAMMA-RAY
-
+
0
200
DENSITY
-
+
1
2
3
MEMBER
10900
11000
11100
11200
11300
11400
11500
11600
11700
11800
11900
12000
12100
12200
12300
12400
12500
12600
12700
TEAPOT MEMBER
THIRD SUBMEMBER MIDDLE MEMBER
FIRST SUBMEMBER MIDDLE MEMBER
BASAL MEMBER

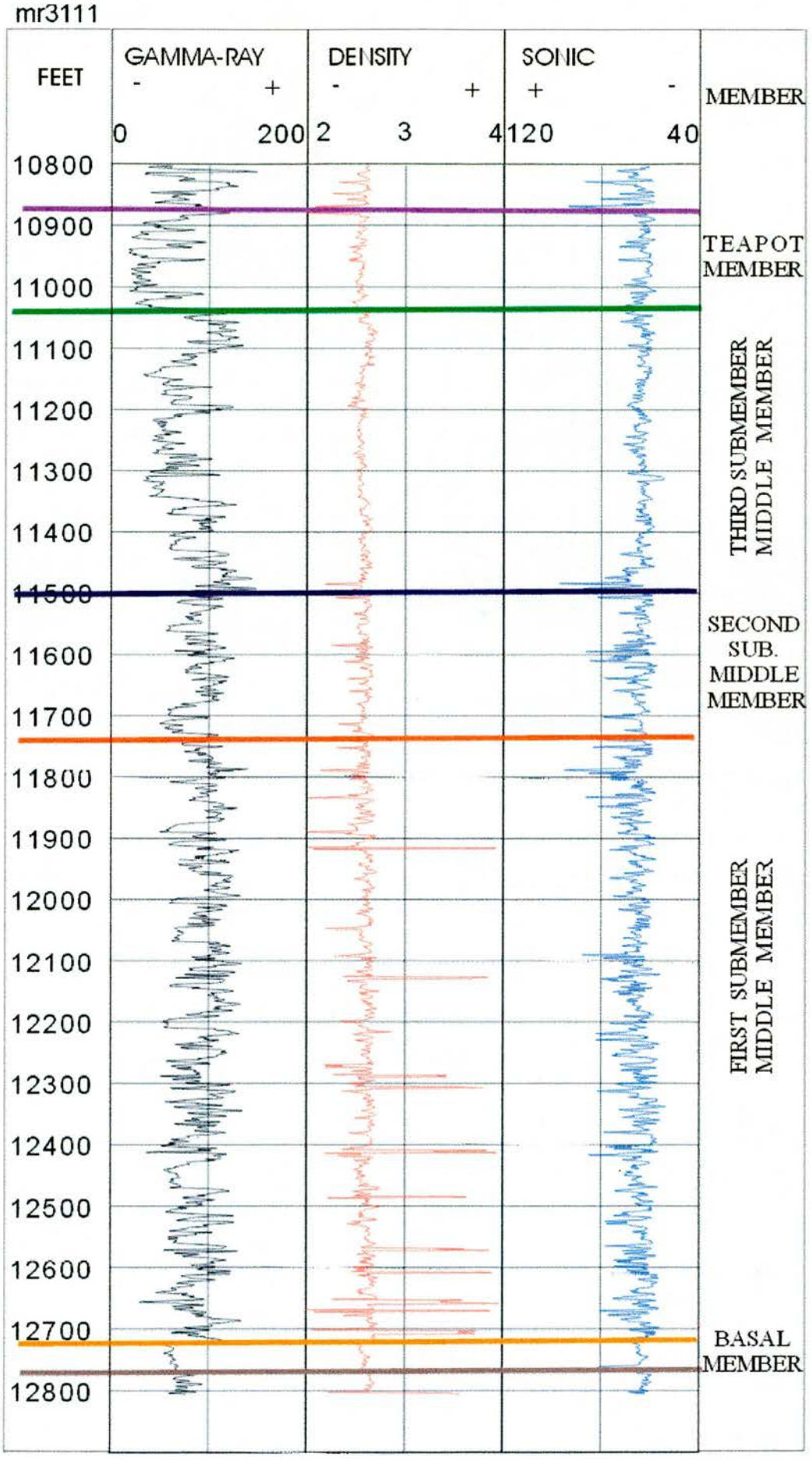
mr3111
FEET
GAMMA-RAY
- +
0 200
DENSITY
- +
2 3 4
SONIC
+ -
120 40
MEMBER
10800
10900
11000
11100
11200
11300
11400
11500
11600
11700
11800
11900
12000
12100
12200
12300
12400
12500
12600
12700
12800
TEAPOT MEMBER
THIRD SUBMEMBER MIDDLE MEMBER
SECOND SUB. MIDDLE MEMBER
FIRST SUBMEMBER MIDDLE MEMBER
BASAL MEMBER

tbi1923gr

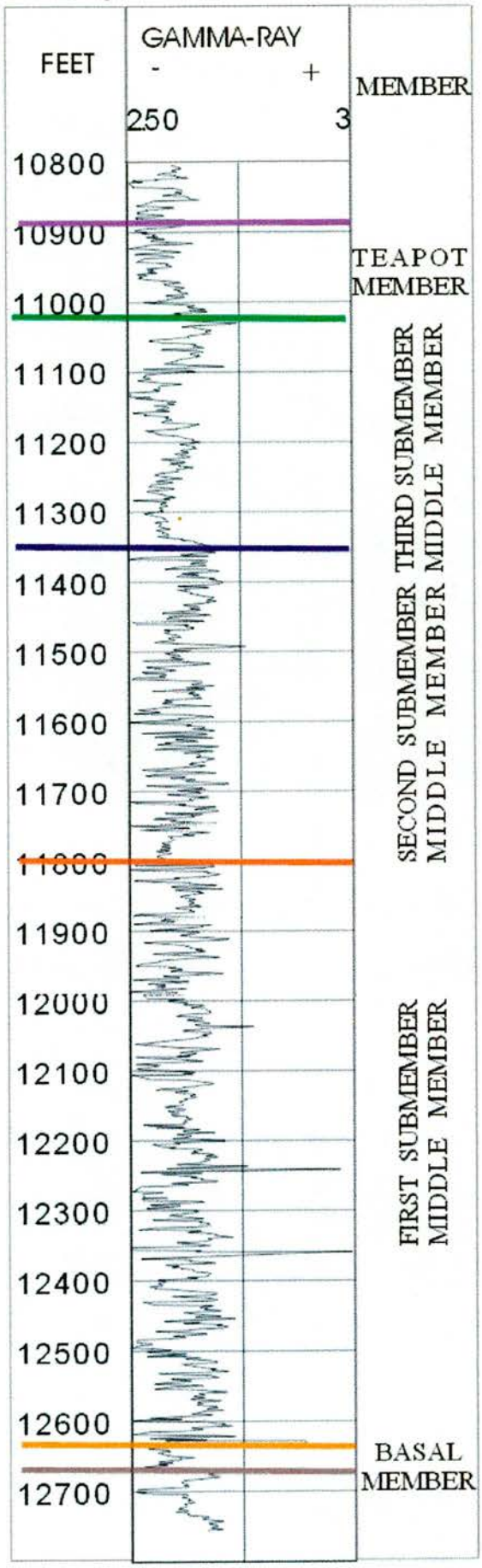
FEET
GAMMA-RAY
-
+
250
3
MEMBER
10800
10900
11000
11100
11200
11300
11400
11500
11600
11700
11800
11900
12000
12100
12200
12300
12400
12500
12600
12700
TEAPOT MEMBER
SECOND SUBMEMBER THIRD SUBMEMBER
MIDDLE MEMBER MIDDLE MEMBER
FIRST SUBMEMBER
MIDDLE MEMBER
BASAL MEMBER

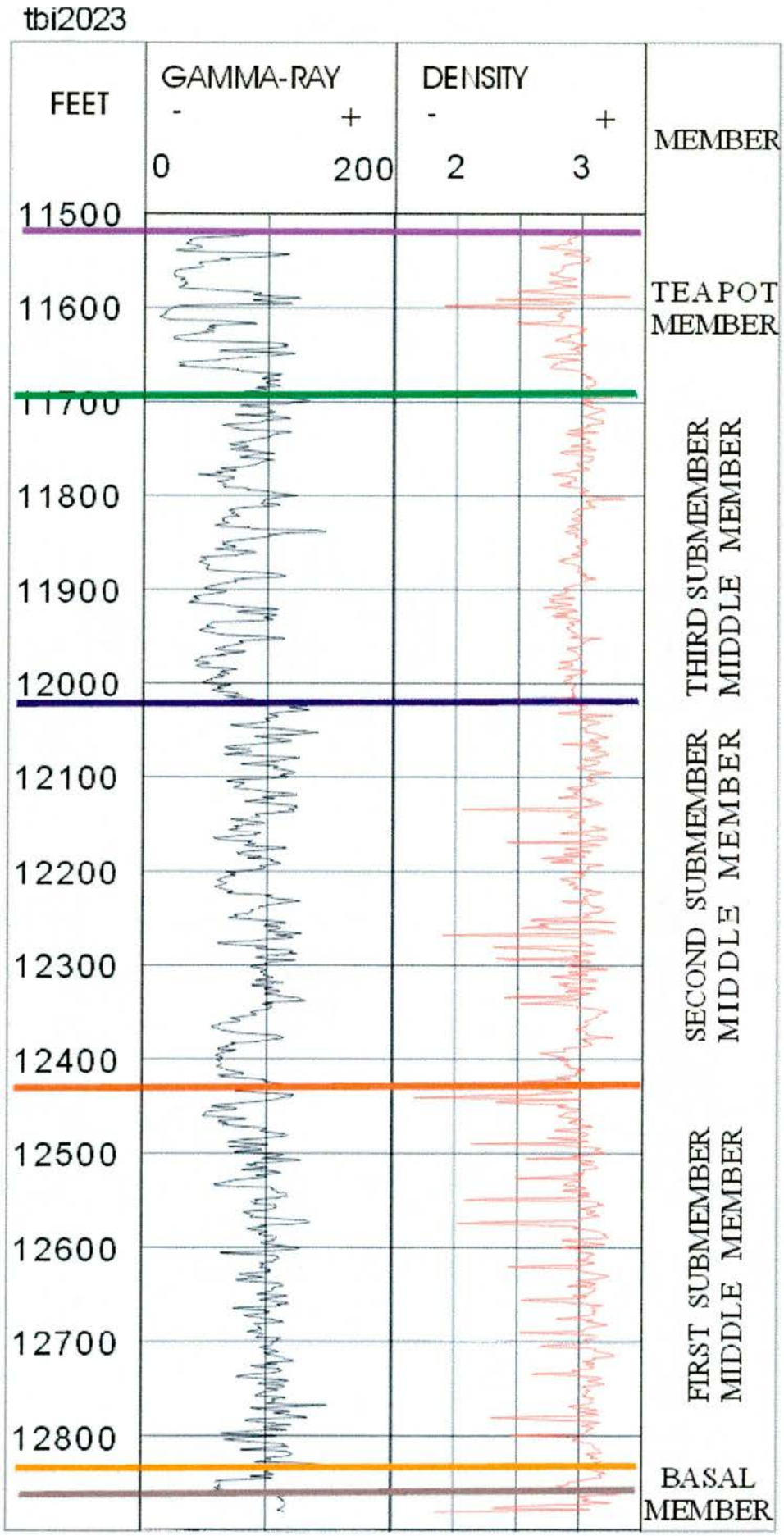
tbi2023
FEET
GAMMA-RAY
-
+
0
200
DENSITY
-
+
2
3
MEMBER
11500
11600
11700
11800
11900
12000
12100
12200
12300
12400
12500
12600
12700
12800
TEAPOT MEMBER
THIRD SUBMEMBER MIDDLE MEMBER
SECOND SUBMEMBER MIDDLE MEMBER
FIRST SUBMEMBER MIDDLE MEMBER
BASAL MEMBER

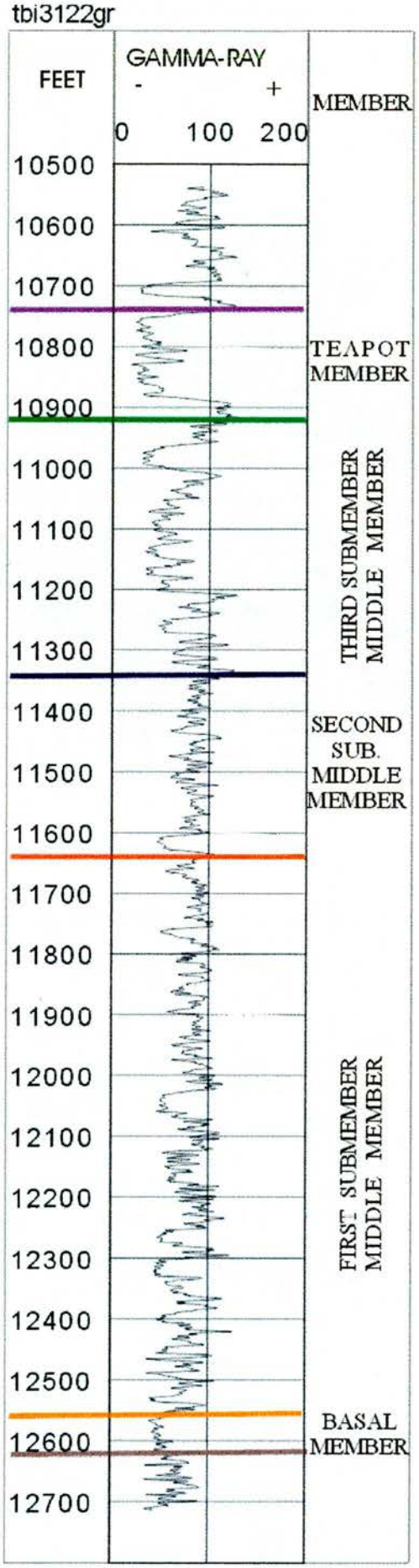
tbi3122gr
FEET
GAMMA-RAY
-
+
0
100
200
MEMBER
10500
10600
10700
10800
10900
11000
11100
11200
11300
11400
11500
11600
11700
11800
11900
12000
12100
12200
12300
12400
12500
12600
12700
TEAPOT MEMBER
THIRD SUBMEMBER MIDDLE MEMBER
SECOND SUB. MIDDLE MEMBER
FIRST SUBMEMBER MIDDLE MEMBER
BASAL MEMBER

ANALYSED WIRELINE LOGS

WIRELINE LOGS	LOCATION
1n4e08	T1NR4E08
1n4e14u	T1NR4E26
1n4e26w	T1NR4E36
1N5E1	T1NR5E12
1n5e12tr	T1NR5E12
1n5e12tr	T1NR5E12
1n5e36	T1NR5E22
1n6e32	T1NR6E32
1s5e1	T1SR5E13
1s5e13	T1SR5E13
1s5e31	T1SR5E31
2n1e21	T2NR1E21
2n2e22gr	T2NR2E22
2n4e08	T2NR4E08
2n4e20	T2NR4E20
2n4e8	T2NR4E8
34n90w23	T34NR90W23
35n87w28	T35NR87W28
35n92w26	T35NR92W26
35n92w31	T35NR94W31
36n94w25	T36NR92W25
37n92w16 21-16	T37NR92W18
39n92w18	T39R93W18
39n93w12	T39NR93W12
39n93w23	T39NR93W23
39n94w4	T39NR94W4
3n2e15-21	T3NR2E15
3n2ehic	T3NR2E
3n3e11	T3NR3E11
3n3e15ex	T3NR3E15
4n2e2211	T4NR2E22
4n2e2443	T4NR2E24
5n2e10	T5NR2E10
5n2e31x	T5NR2E31
5n3e26ok	T5NR3E26
mr3013	T4NR3E30
mr3111	T4NR3E31
tbi 19-23	T4NR3E19
tbi20-23	T4NR2E20
tbi31-22	T4NR3E31-22

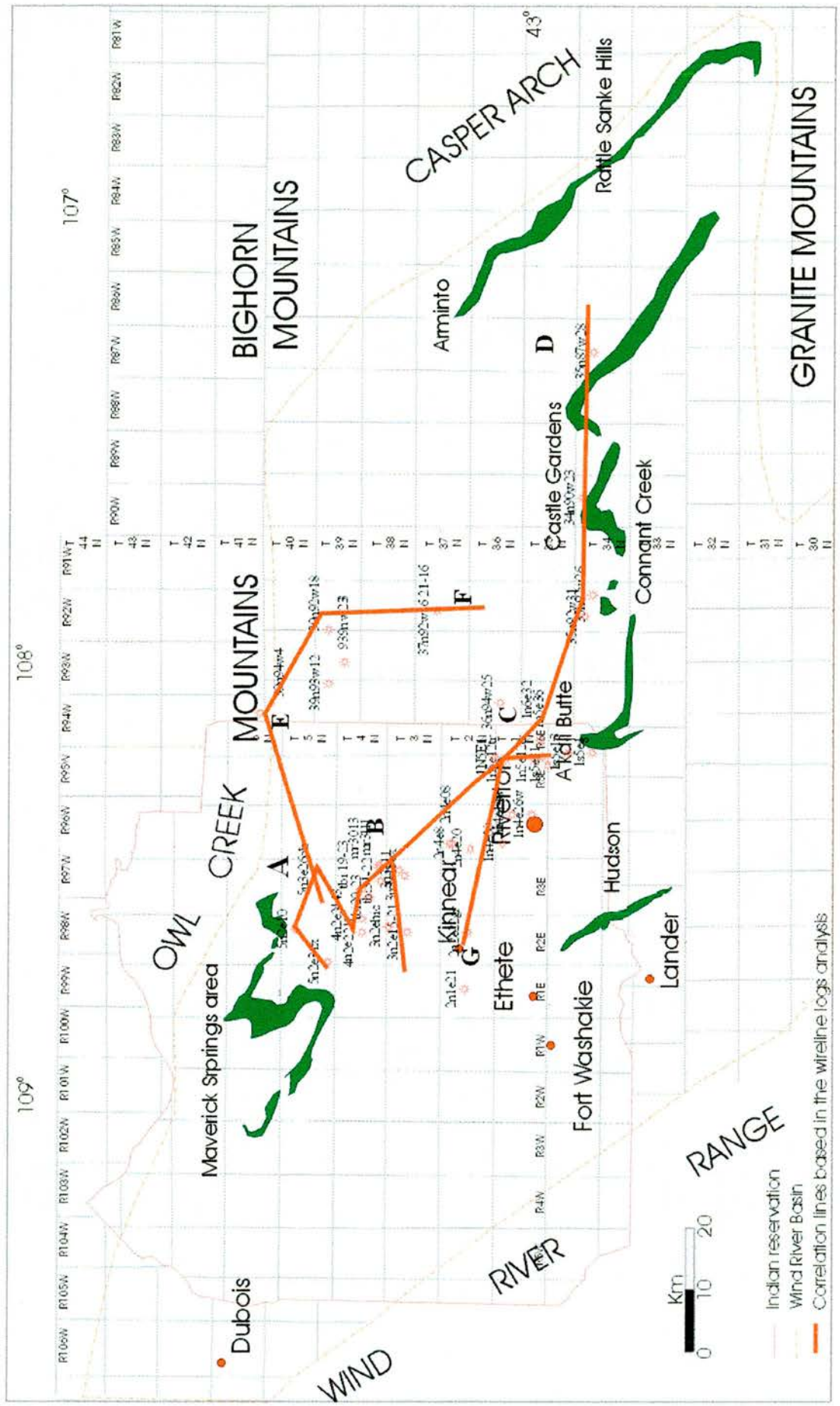

Location of wireline-logs

LINE 1

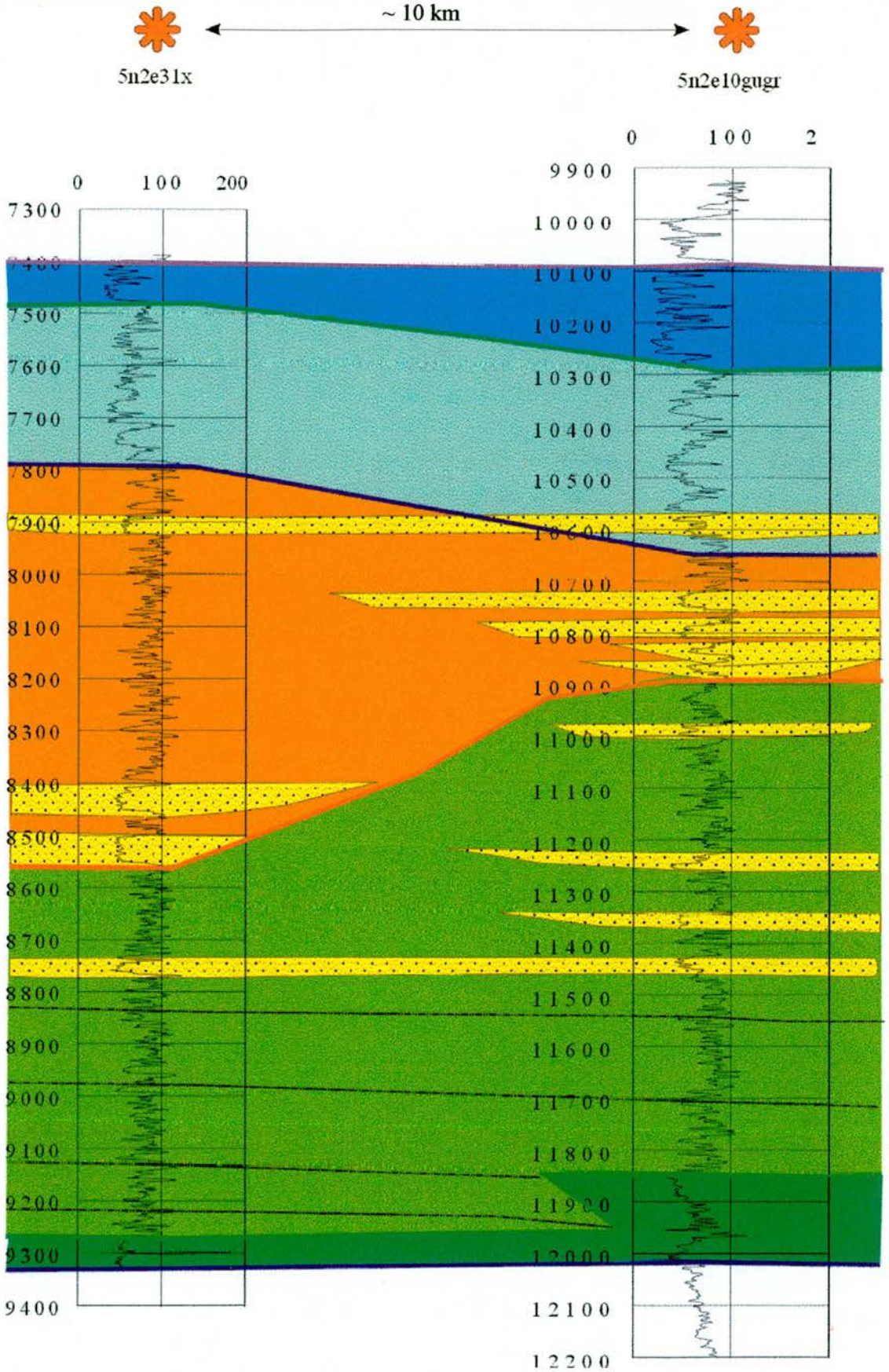
~ 10 km
5n2e31x
5n2e10gugr
0
100
200
7300
7400
7500
7600
7700
7800
7900
8000
8100
8200
8300
8400
8500
8600
8700
8800
8900
9000
9100
9200
9300
9400
0
100
2
9900
10000
10100
10200
10300
10400
10500
10600
10700
10800
10900
11000
11100
11200
11300
11400
11500
11600
11700
11800
11900
12000
12100
12200

LINE 2

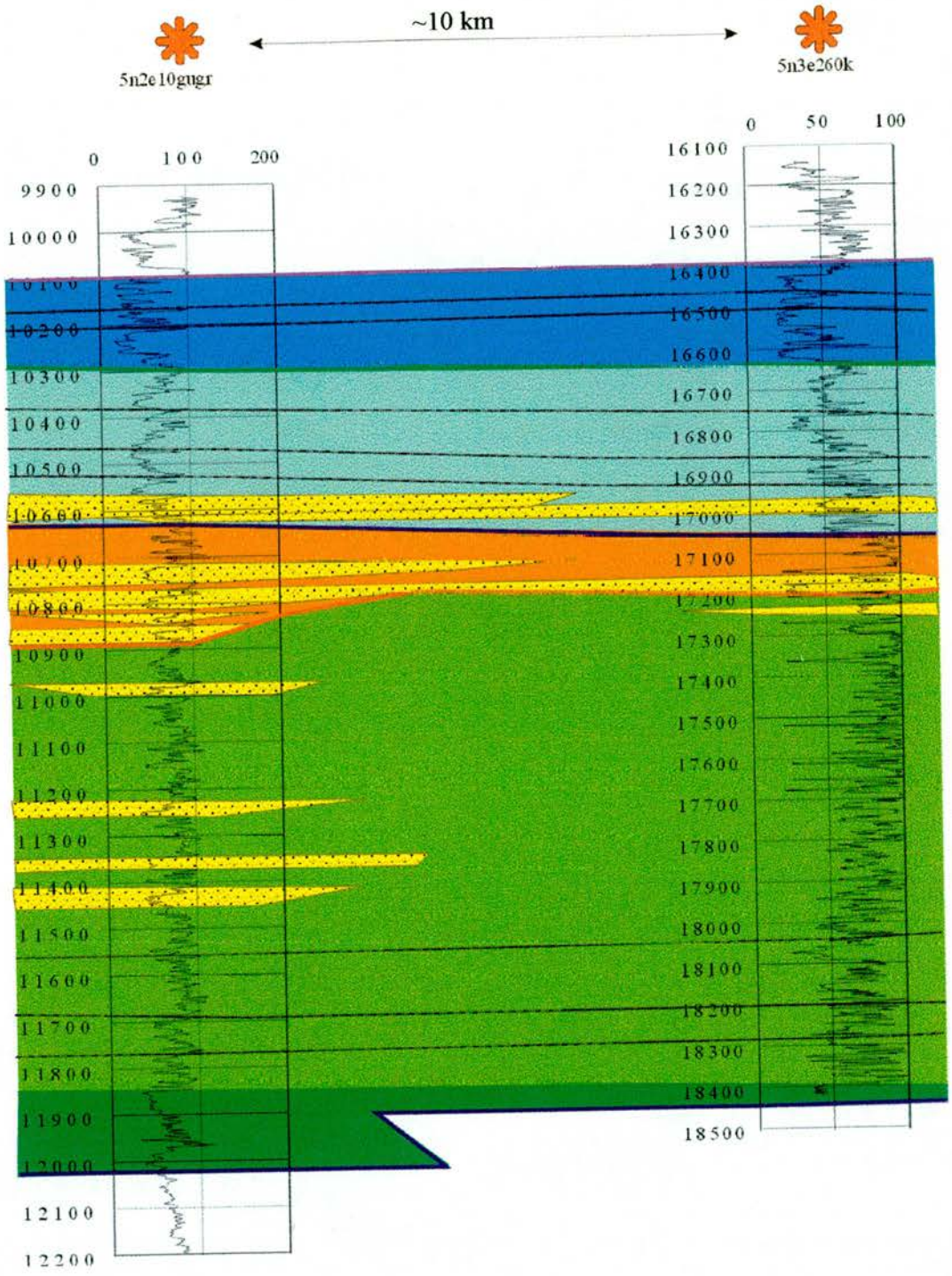
~10 km
5n2e10gugr
5n3e260k
0
100
200
0
50
100
9900
10000
10100
10200
10300
10400
10500
10600
10700
10800
10900
11000
11100
11200
11300
11400
11500
11600
11700
11800
11900
12000
12100
12200
16100
16200
16300
16400
16500
16600
16700
16800
16900
17000
17100
17200
17300
17400
17500
17600
17700
17800
17900
18000
18100
18200
18300
18400
18500

LINE 3

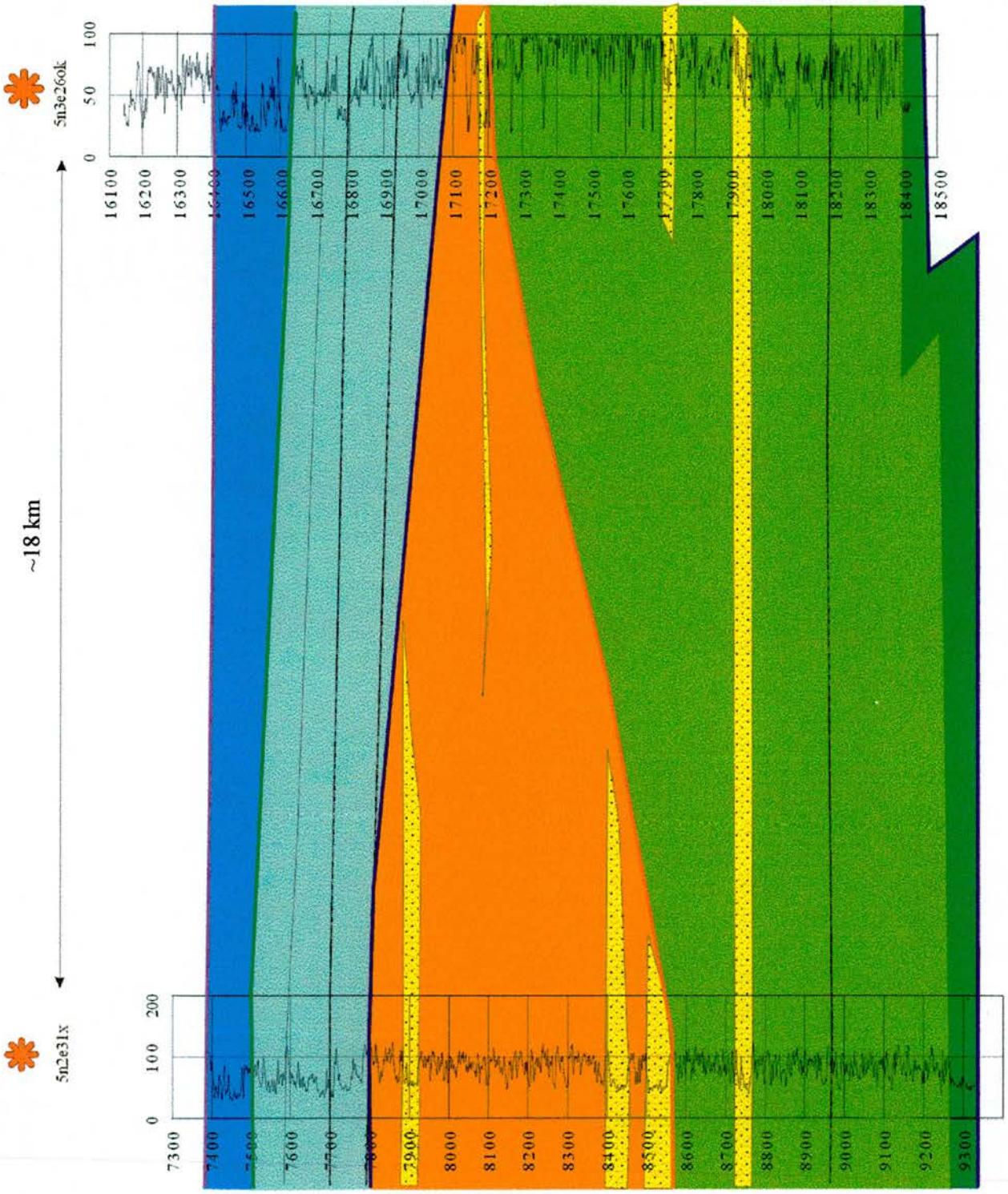
5n3e26ok
5n2e31x
~18 km
0
50
100
0
100
200
16100
16200
16300
16400
16500
16600
16700
16800
16900
17000
17100
17200
17300
17400
17500
17600
17700
17800
17900
18000
18100
18200
18300
18400
18500
7300
7400
7500
7600
7700
7800
7900
8000
8100
8200
8300
8400
8500
8600
8700
8800
8900
9000
9100
9200
9300

LINE 4

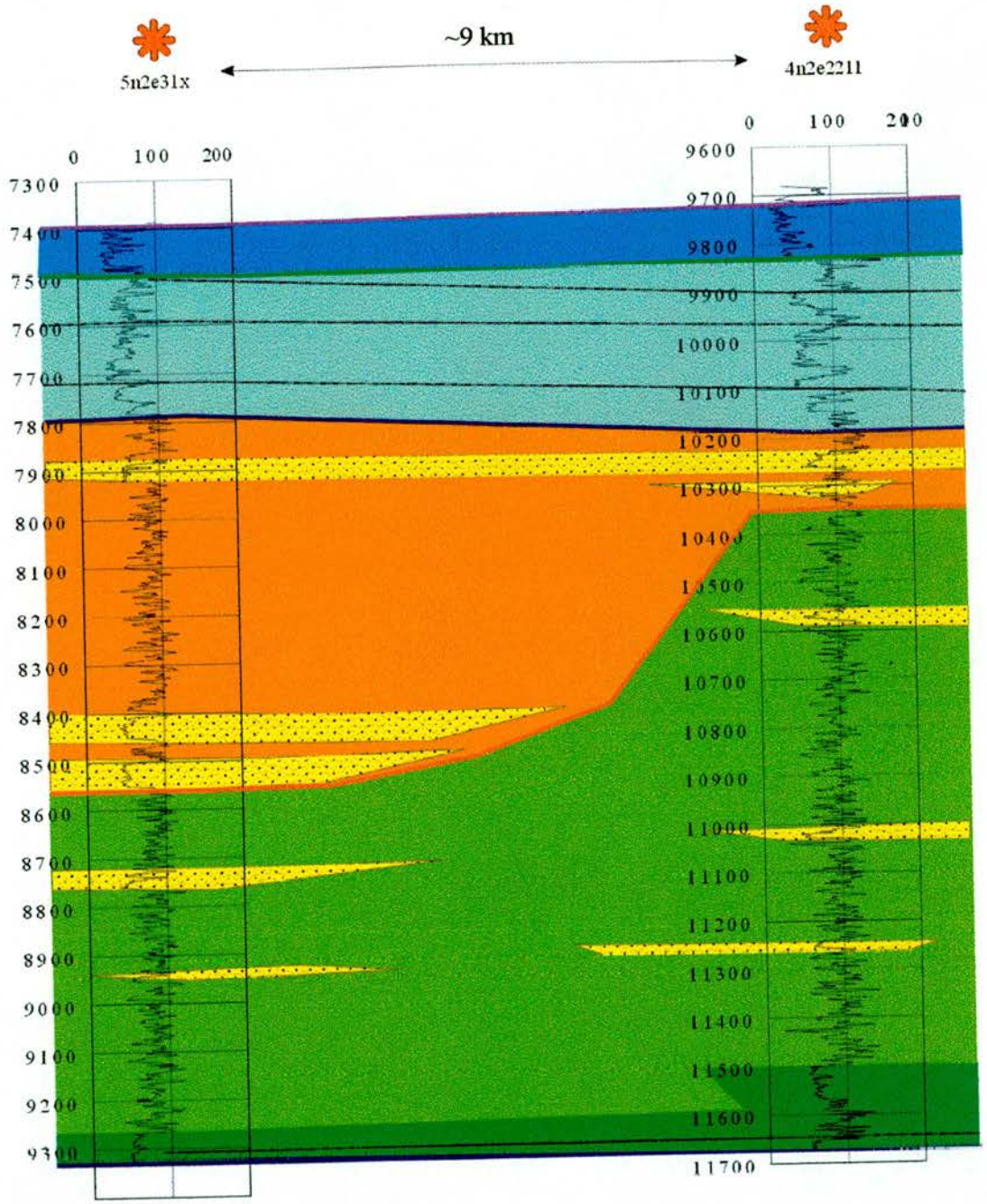
~9 km
5n2e31x
4n2e2211
0
100
200
7300
7400
7500
7600
7700
7800
7900
8000
8100
8200
8300
8400
8500
8600
8700
8800
8900
9000
9100
9200
9300
9600
9700
9800
9900
10000
10100
10200
10300
10400
10500
10600
10700
10800
10900
11000
11100
11200
11300
11400
11500
11600
11700

LINE 5

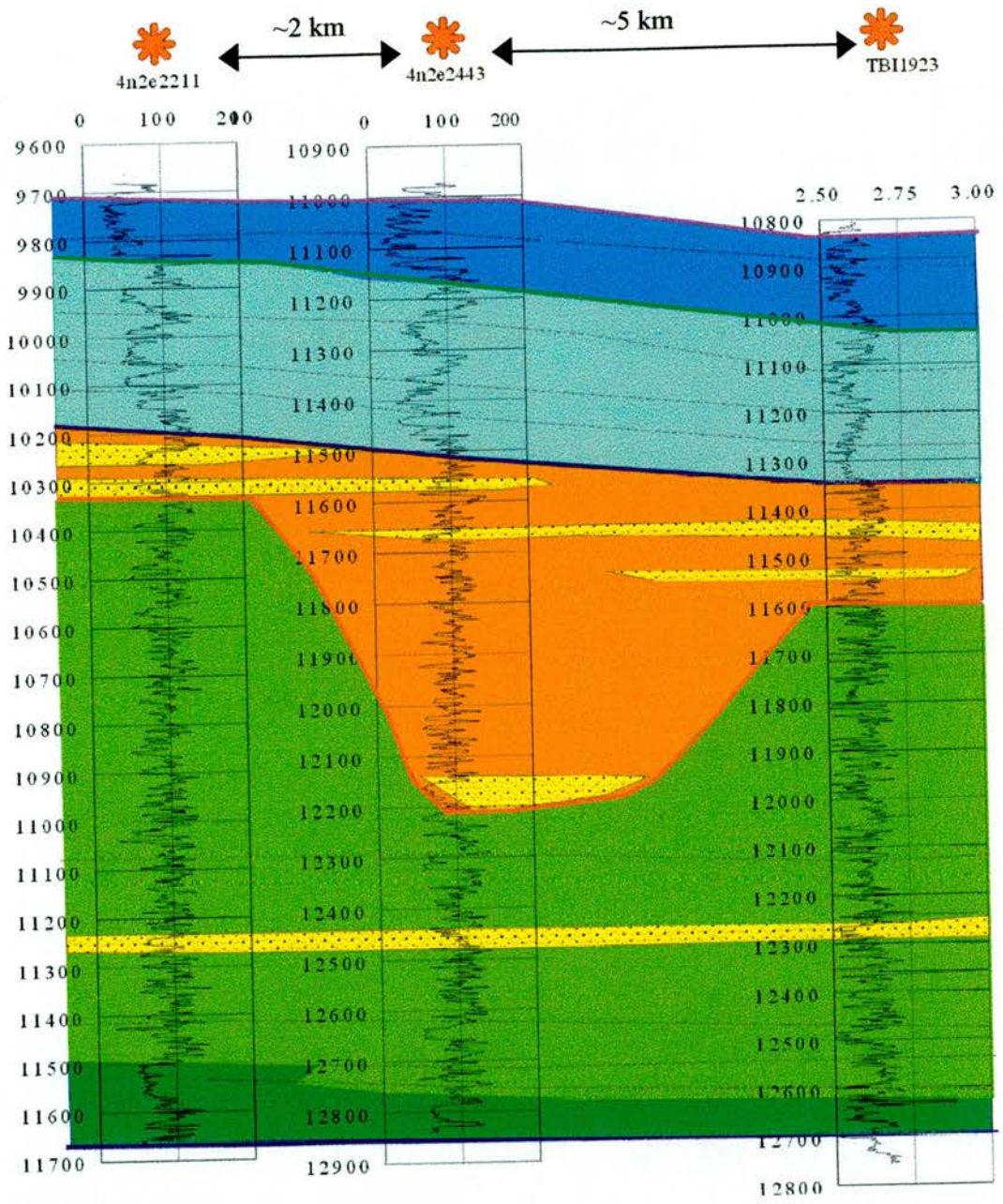
~2 km
~5 km
4n2e2211
4n2e2443
TBI1923
0
100
200
2.50
2.75
3.00
9600
9700
9800
9900
10000
10100
10200
10300
10400
10500
10600
10700
10800
10900
11000
11100
11200
11300
11400
11500
11600
11700
10900
11000
11100
11200
11300
11400
11500
11600
11700
11800
11900
12000
12100
12200
12300
12400
12500
12600
12700
12800
12900
10800
10900
11000
11100
11200
11300
11400
11500
11600
11700
11800
11900
12000
12100
12200
12300
12400
12500
12600
12700
12800

LINE 6

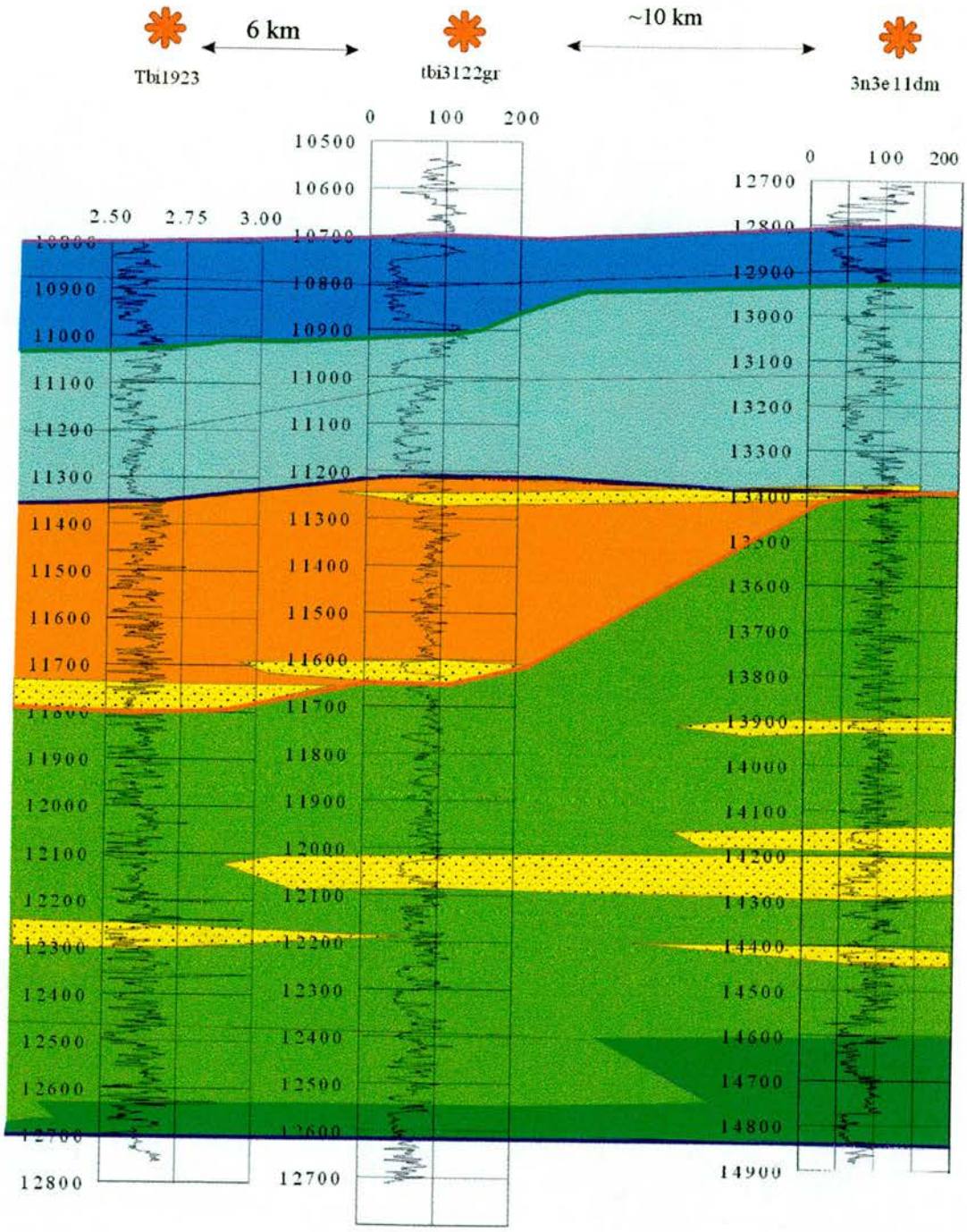
6 km
~10 km
Tbi1923
tbi3122gr
3n3e11dm
0
100
200
2.50
2.75
3.00
10500
10600
10700
10800
10900
11000
11100
11200
11300
11400
11500
11600
11700
11800
11900
12000
12100
12200
12300
12400
12500
12600
12700
12800
12700
12800
12900
13000
13100
13200
13300
13400
13500
13600
13700
13800
13900
14000
14100
14200
14300
14400
14500
14600
14700
14800
14900

LINE 7

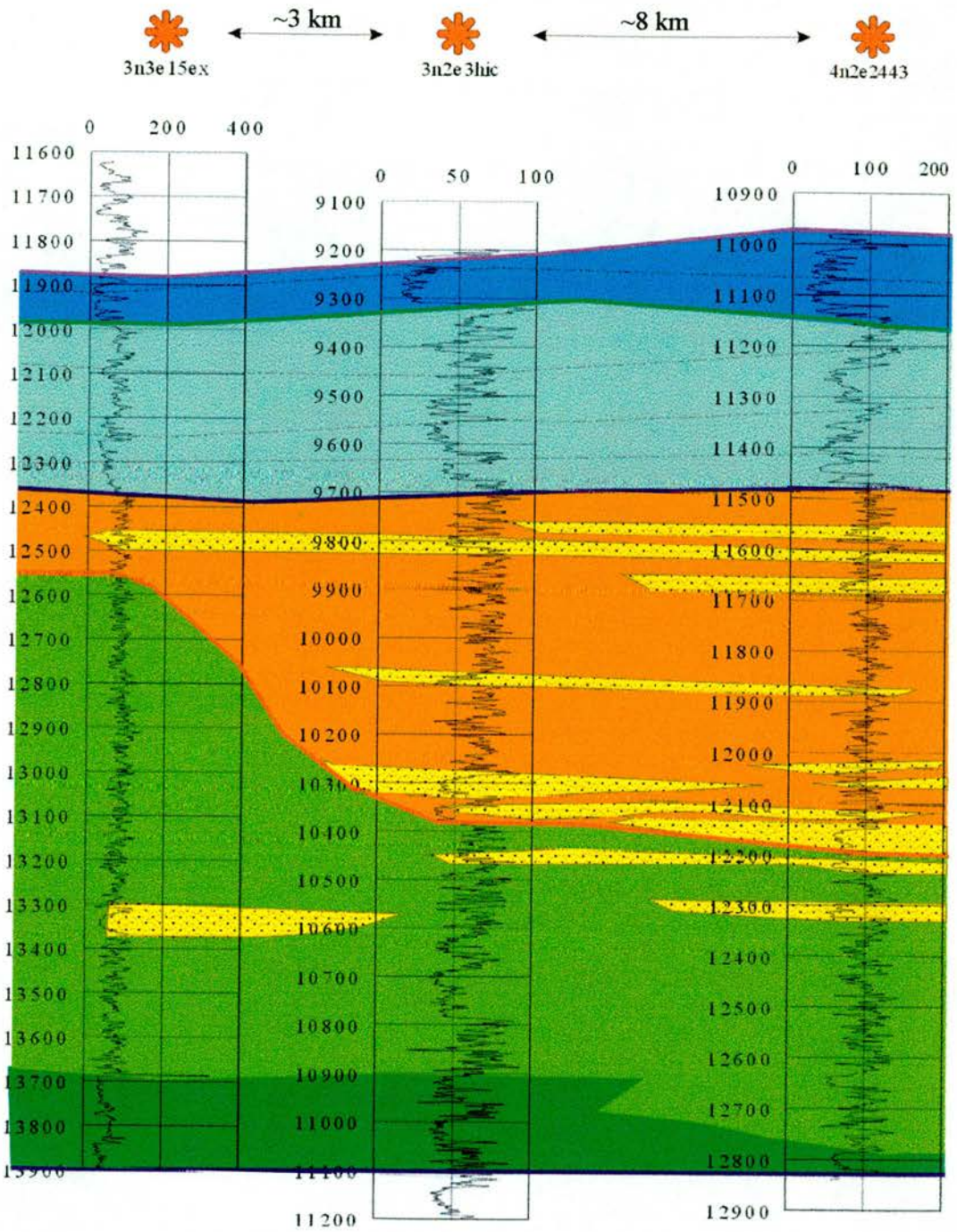
~3 km
~8 km
3n3e 15ex
3n2e 3hic
4n2e2443
0 200 400
0 50 100
0 100 200
11600
11700
11800
11900
12000
12100
12200
12300
12400
12500
12600
12700
12800
12900
13000
13100
13200
13300
13400
13500
13600
13700
13800
9100
9200
9300
9400
9500
9600
9700
9800
9900
10000
10100
10200
10300
10400
10500
10600
10700
10800
10900
11000
11100
11200
10900
11000
11100
11200
11300
11400
11500
11600
11700
11800
11900
12000
12100
12200
12300
12400
12500
12600
12700
12800
12900

LINE 8

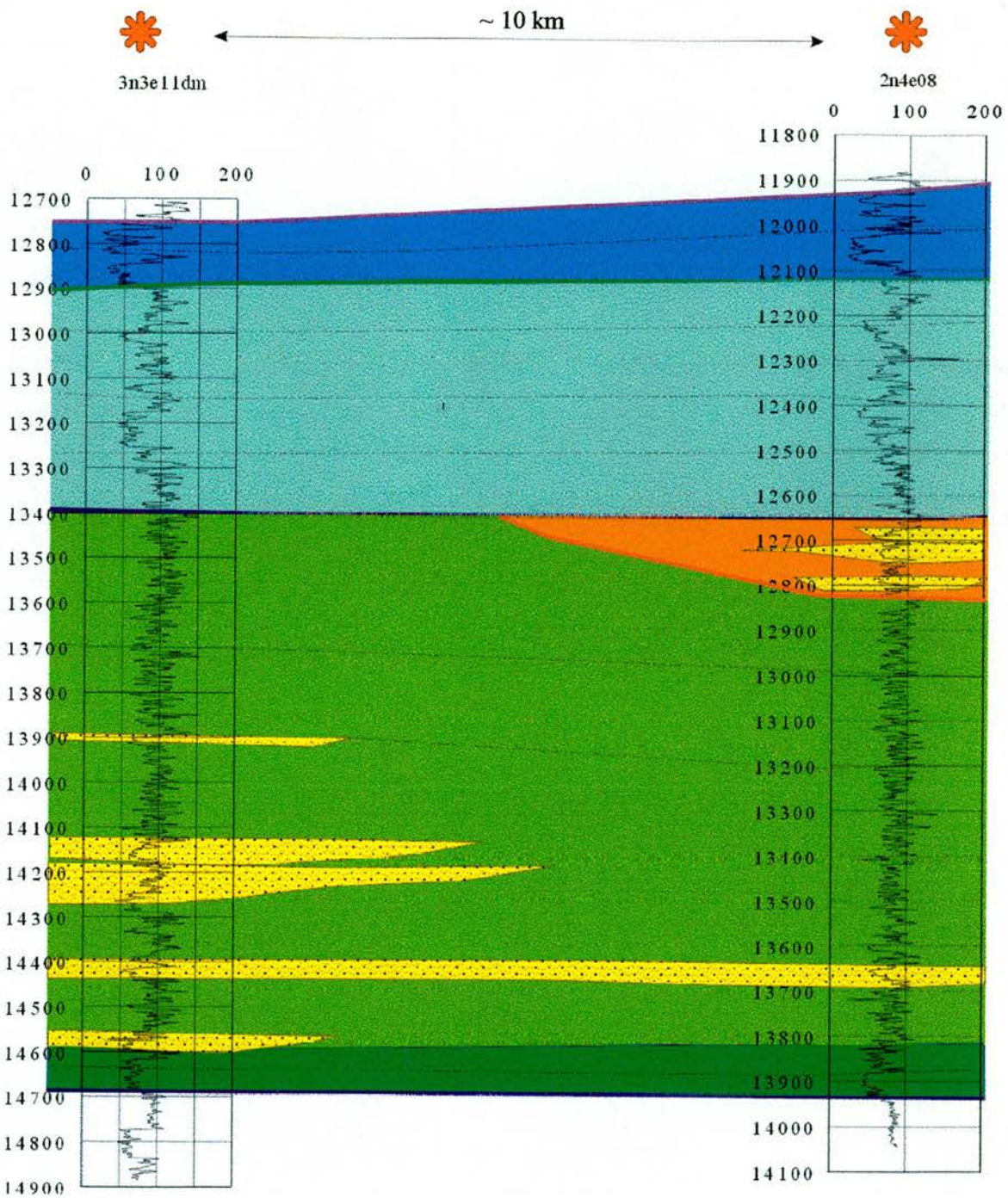
~ 10 km
3n3e11dm
2n4e08
0
100
200
12700
12800
12900
13000
13100
13200
13300
13400
13500
13600
13700
13800
13900
14000
14100
14200
14300
14400
14500
14600
14700
14800
14900
11800
11900
12000
12100
12200
12300
12400
12500
12600
12700
12800
12900
13000
13100
13200
13300
13400
13500
13600
13700
13800
13900
14000
14100

LINE 9

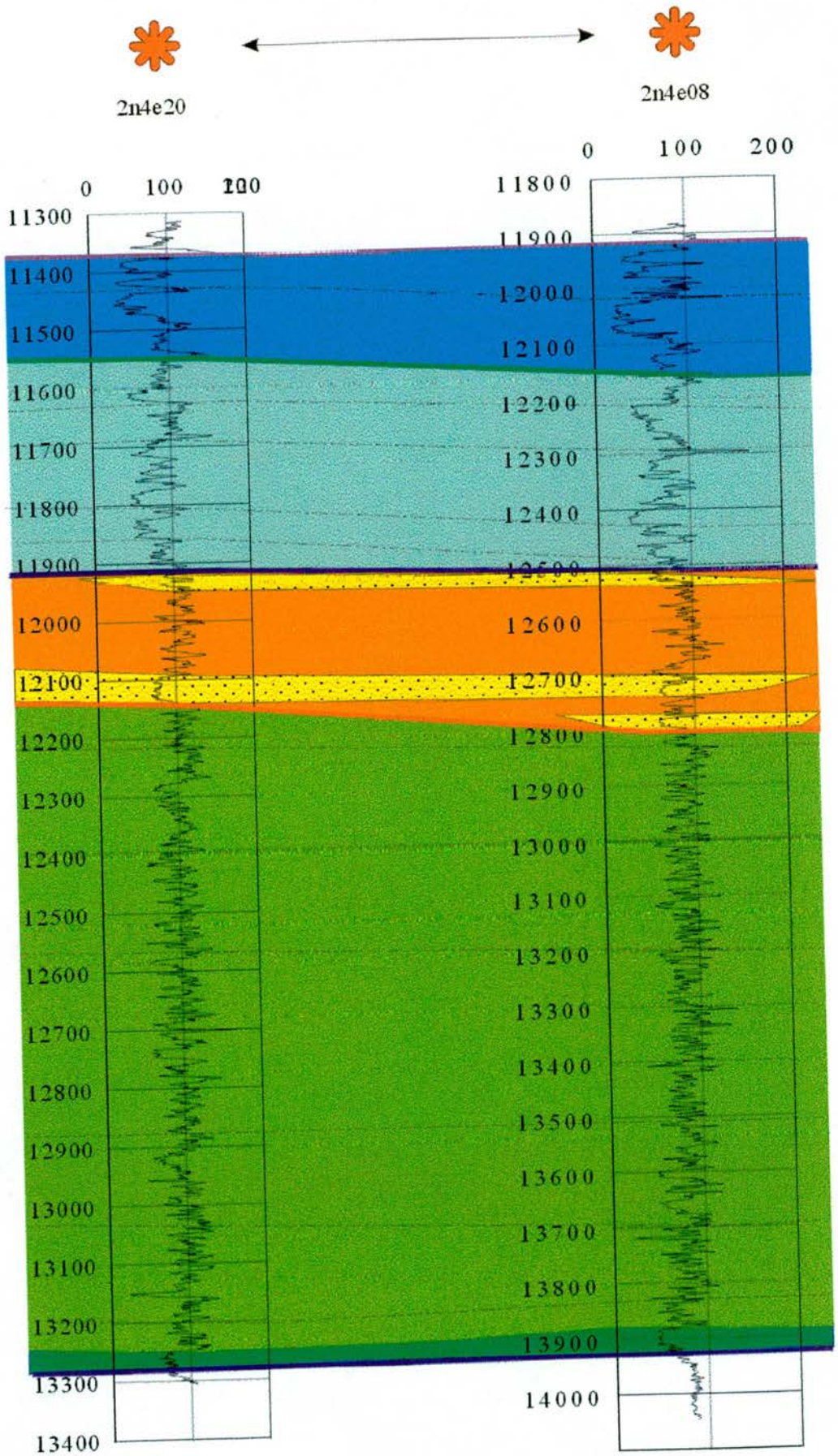
2n4e20
2n4e08
0
100
200
11300
11400
11500
11600
11700
11800
11900
12000
12100
12200
12300
12400
12500
12600
12700
12800
12900
13000
13100
13200
13300
13400
11800
11900
12000
12100
12200
12300
12400
12600
12700
12800
12900
13000
13100
13200
13300
13400
13500
13600
13700
13800
13900
14000

Line 10

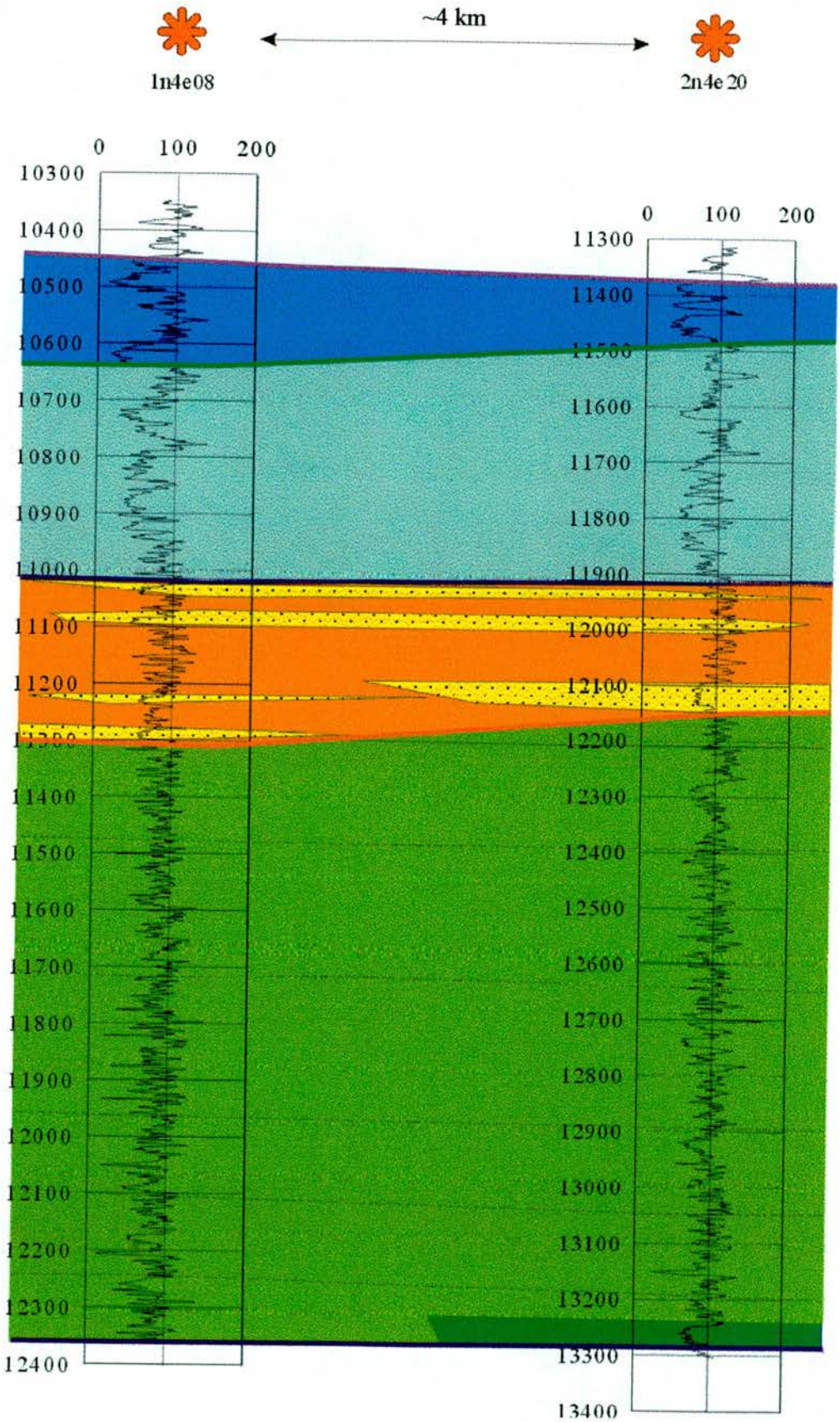
~4 km
1n4e08
2n4e 20
0
100
200
10300
10400
10500
10600
10700
10800
10900
11000
11100
11200
11300
11400
11500
11600
11700
11800
11900
12000
12100
12200
12300
12400
0
100
200
11300
11400
11500
11600
11700
11800
11900
12000
12100
12200
12300
12400
12500
12600
12700
12800
12900
13000
13100
13200
13300
13400

LINE 11

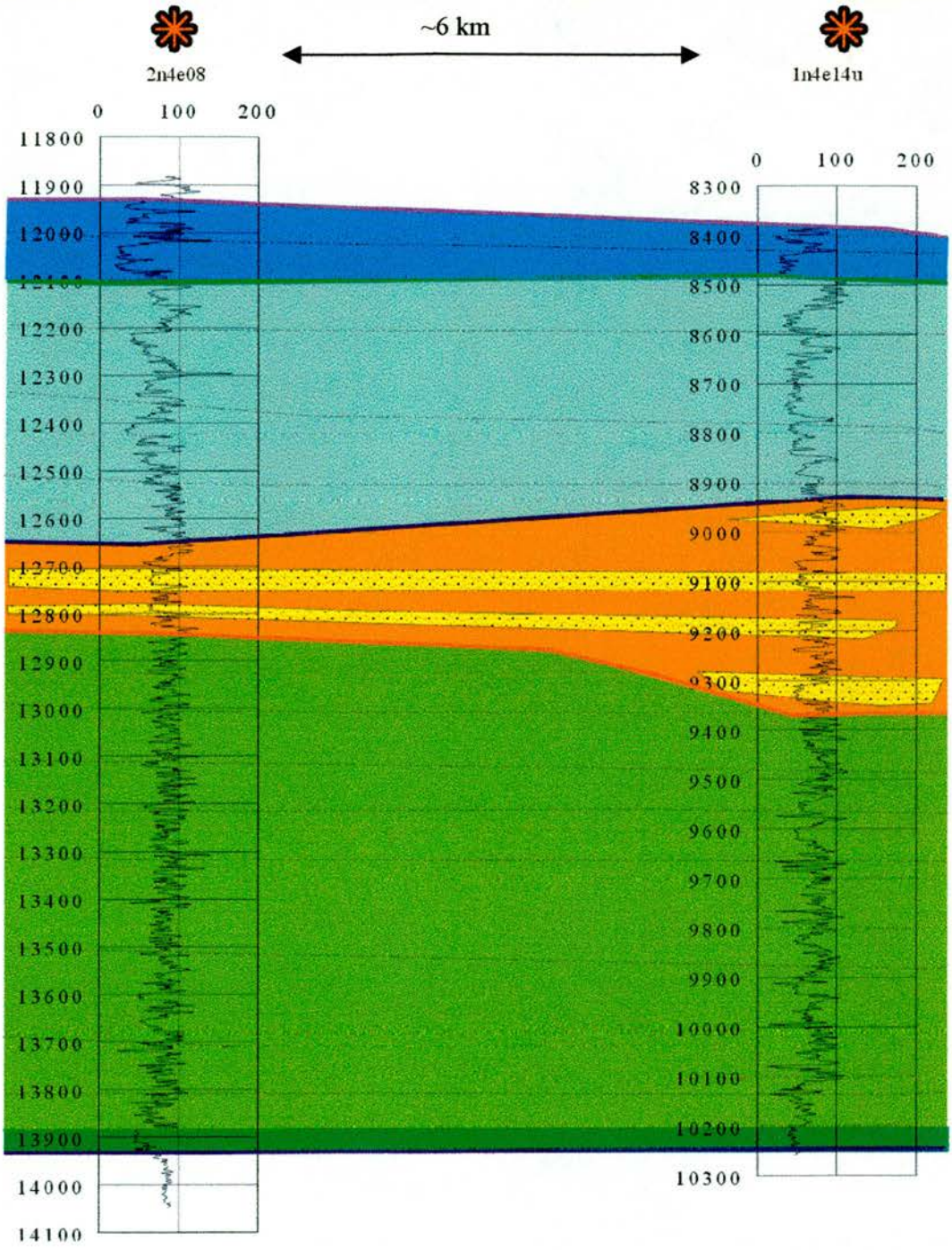
~6 km
2n4e08
1n4e14u
0
100
200
11800
11900
12000
12100
12200
12300
12400
12500
12600
12700
12800
12900
13000
13100
13200
13300
13400
13500
13600
13700
13800
13900
14000
14100
0
100
200
8300
8400
8500
8600
8700
8800
8900
9000
9100
9200
9300
9400
9500
9600
9700
9800
9900
10000
10100
10200
10300

CORRELATION LINE 12

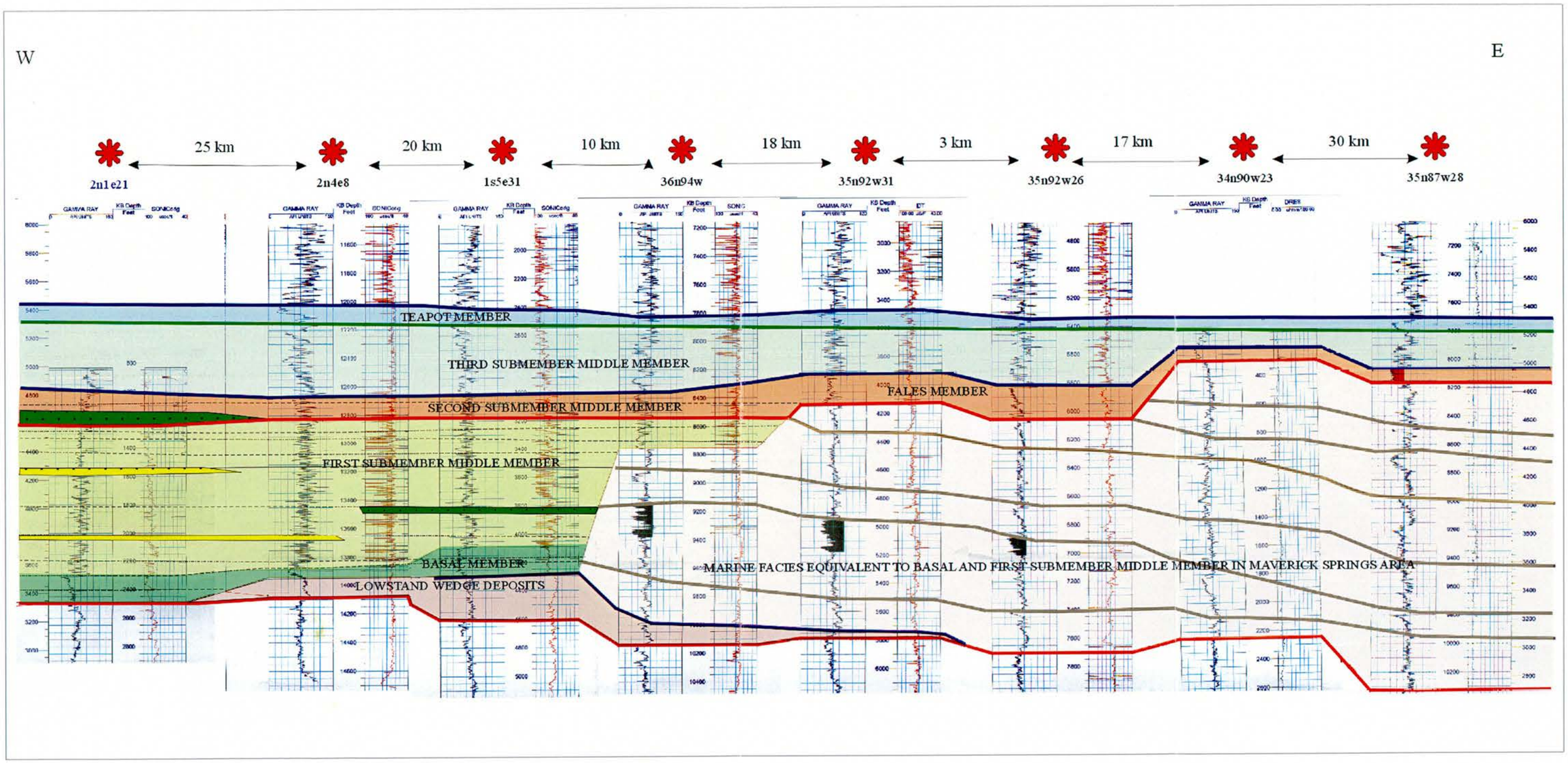

CORRELATION LINE 13

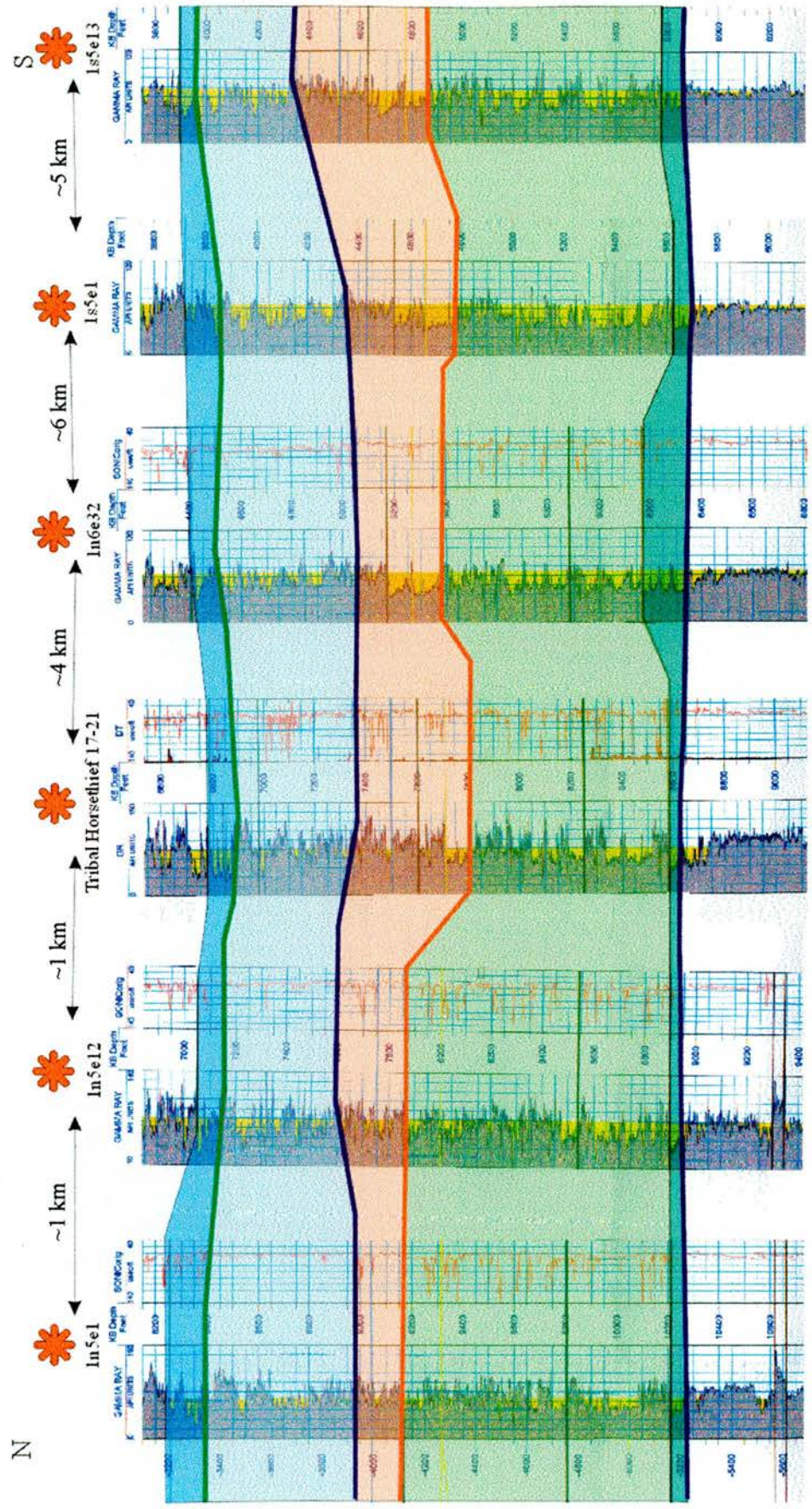

APPENDIX 4 WIRELINE-LOG CORERELATIONS

LINE 14

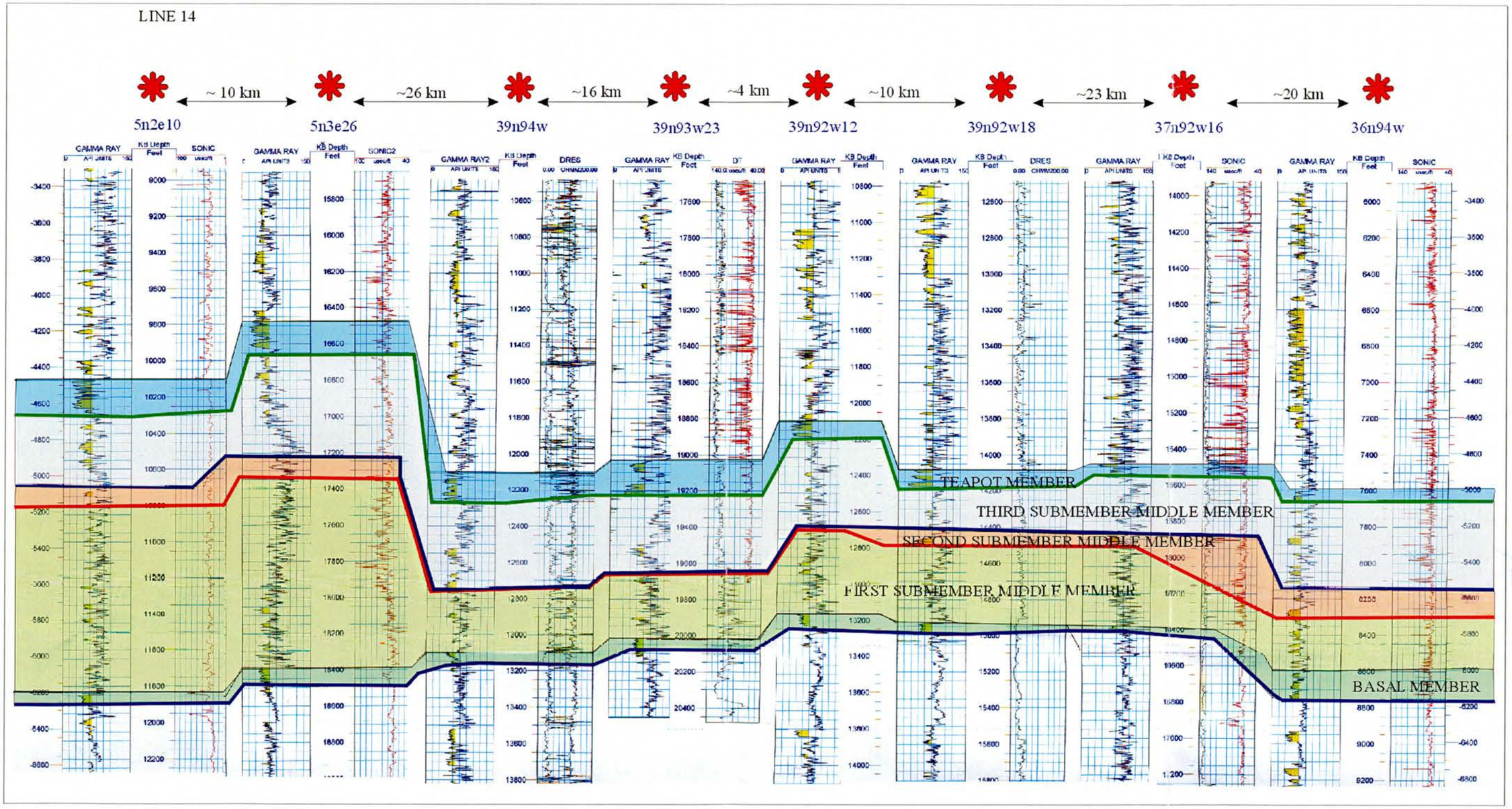

BASINWIDE CORRELATIONS OBTAINED FROM THE ANALYSIS OF THE WIRELINE LOGS (LOCATIONS A-F IN APPENDIX 4-1)

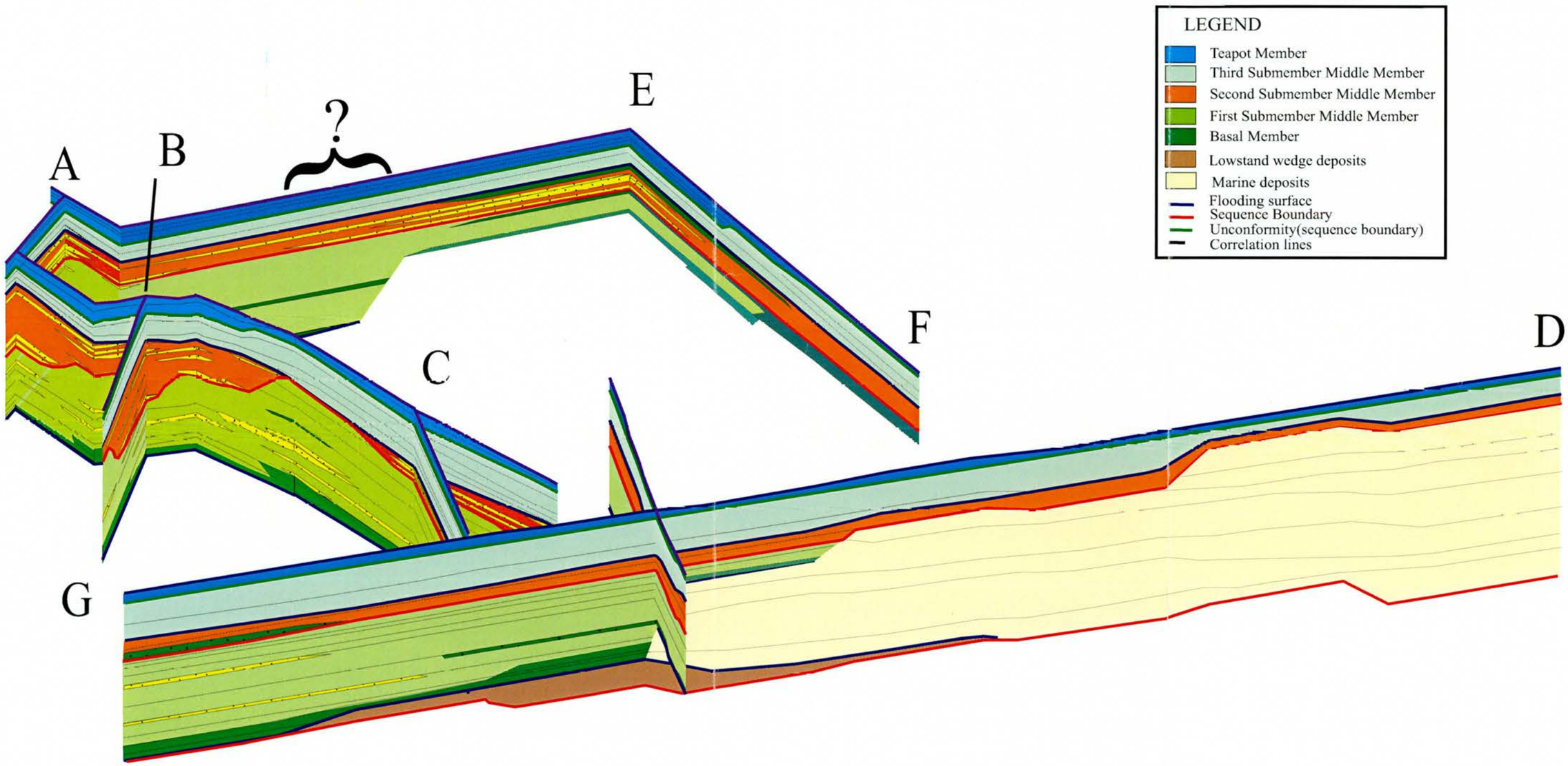

APPENDIX 6 CORRELATION OF MEASURED SECTIONS WITH WIRELINE-LOGS

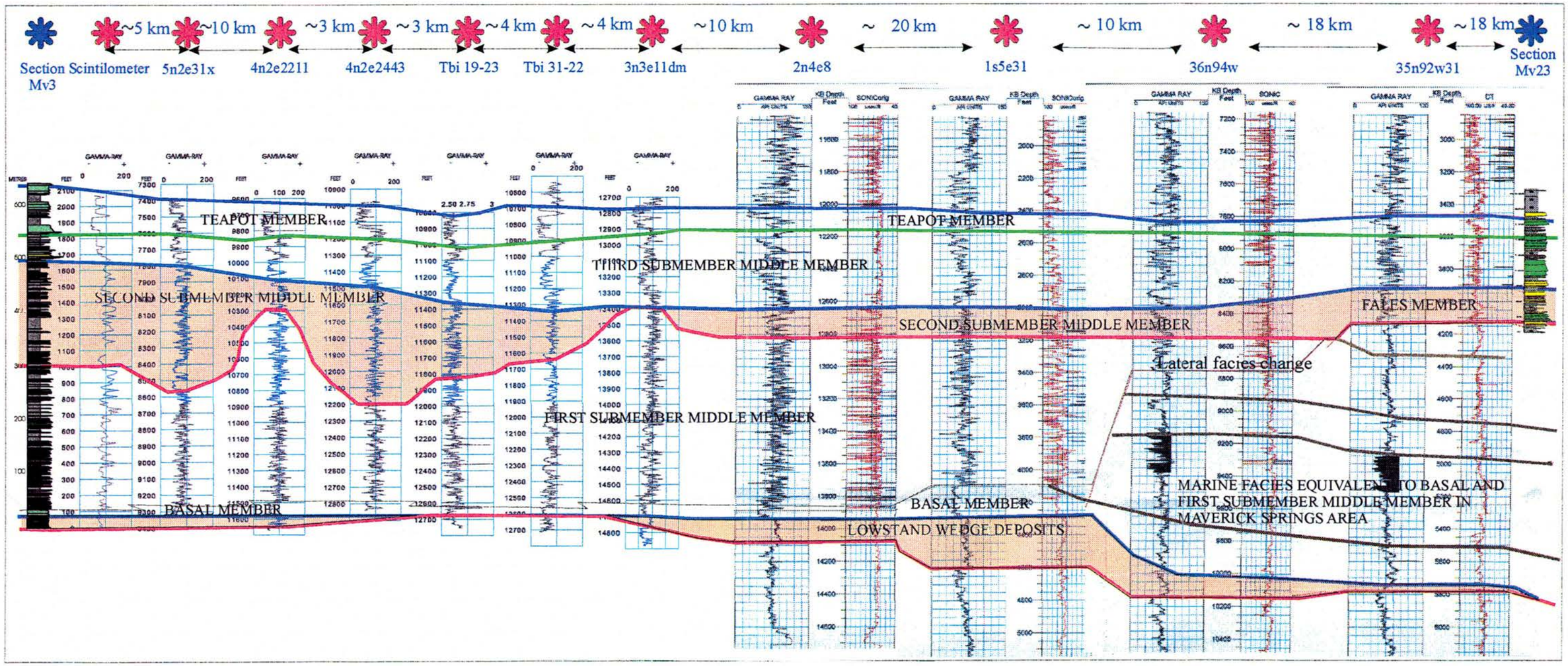

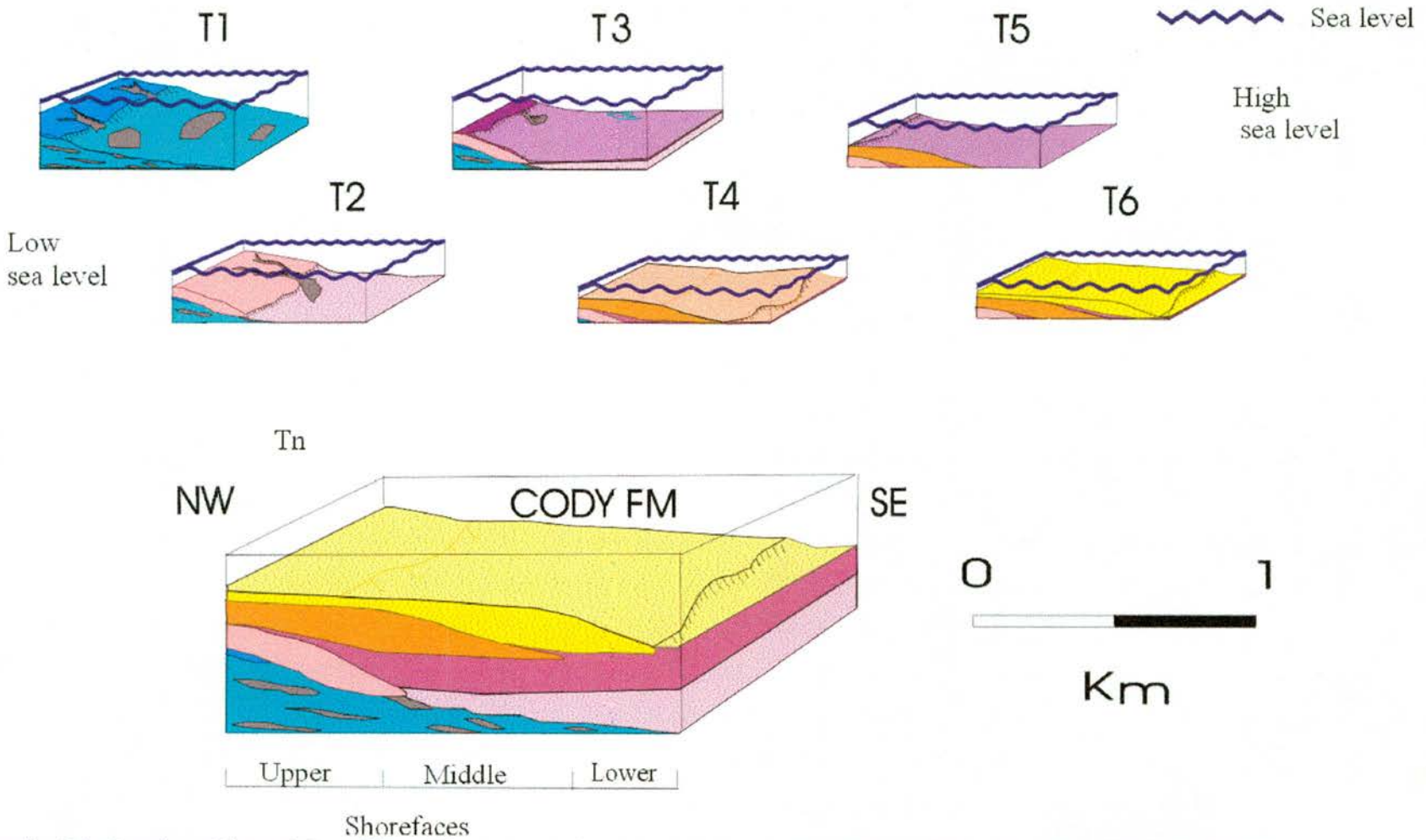

Appendix 7-1: Stratigraphic and depositional Framework for the upper part of the Cody Formation. In this diagram, it can be observed how the clinofroms form the upper part of the Cody Formation were formed by alternation of progradational and local transgressive events that eroded the topmost part of the individual shoreface deposits, with the progradation of the next one located on top of the local flooding surface below. The flooding surfaces can be followed into shelf deposits towards the southeast of the basin.

APPENDIX 7

Appendix 7-2: Stratigraphic and depositional framework for the upper part of the Cody Formation. At this time, a regional fall of relative sea level caused the incision of the middle and lower shoreface deposits from appendix 7-1, the generation of a lowstand wedge deposit in the southern part of the basin, and filling the space by transgressive deposits generated as the sea level increased in the following transgressive period, with the formation of incise valley deposits at the top of the Cody Formation

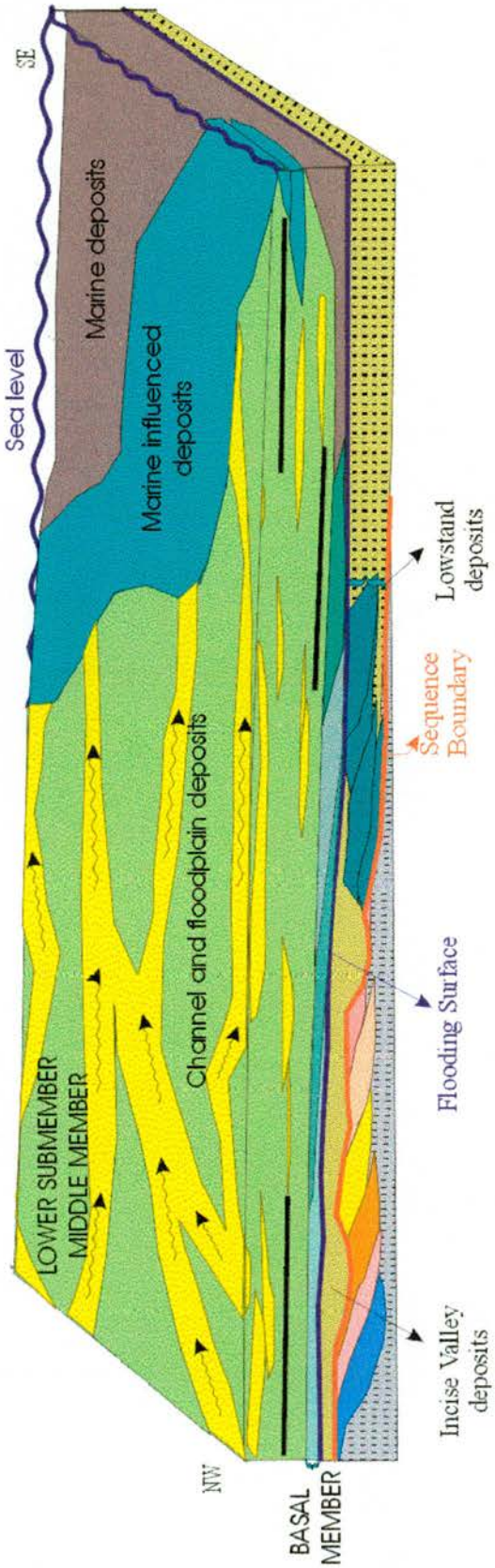

Appendix 7-3: Stratigraphic and depositional framework for the Basal and lower submember of the Middle Member of the Mesaverde Formation. The contact between the Mesaverde and Cody Formation is located at a flooding surface at top of the Cody Formation. Above this, a Highstand system tract composed of the Basal (shoreface deposits) and lower submember of the Middle Member (delta plain deposits) prograded towards the southeast of the Basin.

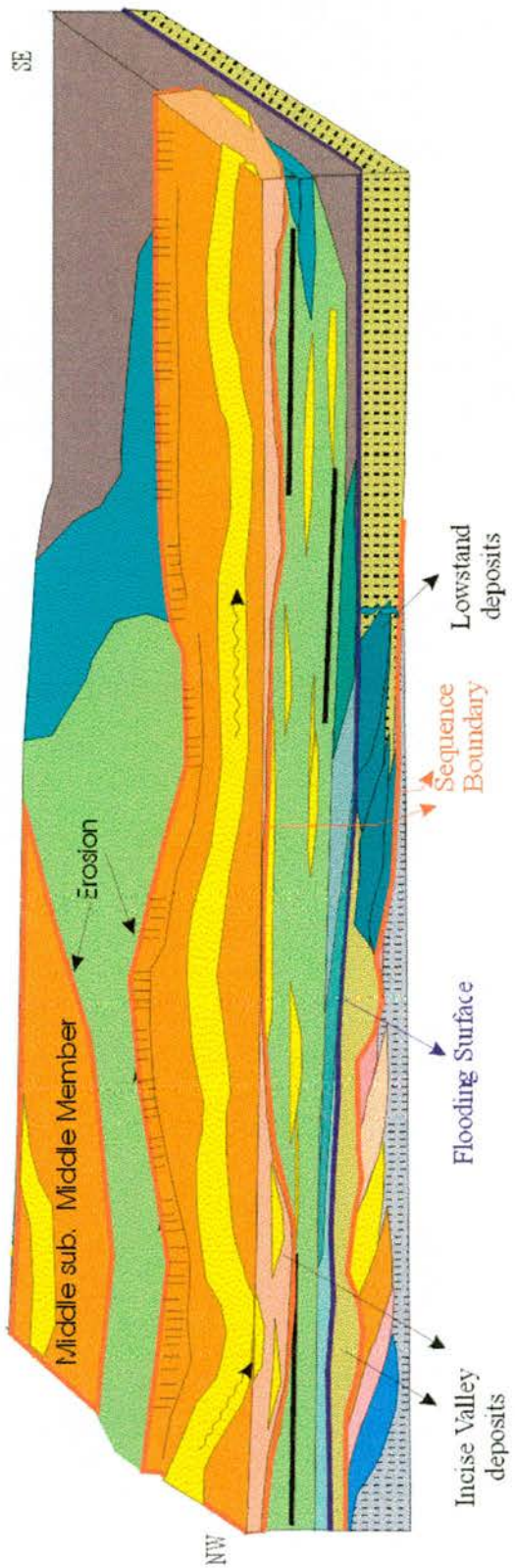

Appendix 7-4: Stratigraphic and depositional framework for the middle submember of the Middle Member of the Mesaverde Formation. A new regional fall in sea level generates an incision over the deposits of the unit below, and the generation of a new sequence boundary, with the generation of a lowstand wedge called the Fales Member in the souteastern part of the basin. The middle submember of the Middle Member is represented by a meandering fluvial system formed during a period of increasing relative sea level.

Appendix 7-5: The base of this submember is represented by a flooding period, which was followed by the progradation of a fluvial system towards the southeast. the thickness of this submember increases in the same direction. The top of this submember is a new sequence boundary, represented by an angular unconformity.

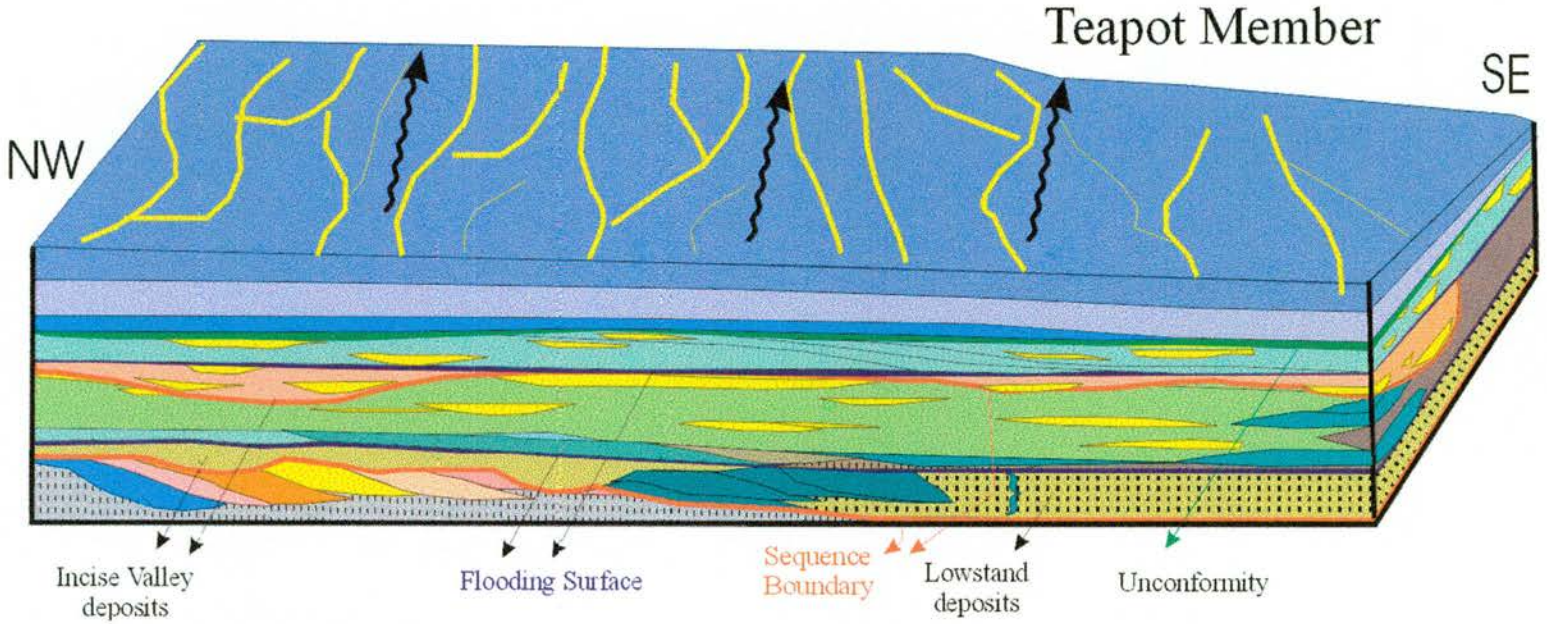

Appendix 7-6: Stratigraphic and depositional Framework for the Teapot Member of the Mesaverde Formation. In this diagram, it can be observed the basal unconformity at the base of the Teapot Member, which scours down in a northwestern direction. The Teapot member is composed of three subunits, a lower and upper one characterised by braided fluvial deposits and a middle one characterised by meandering in character fluvial deposits. The depositional dip of these subunits is slightly oblique to the ones from below.